

Improved Nonparametric Control Charts for Location Based on Runs-Rules

by

Pierre Kritzing

Submitted in partial fulfillment of
the requirements for the degree

MSc (Mathematical Statistics)

In the
Faculty of Natural & Agricultural Sciences
University of Pretoria
Pretoria

April 2011

Declaration

I, Pierre Kritzinger declare that the dissertation, which I hereby submit for the degree MSc (Mathematical Statistics) at the University of Pretoria, is my own work and has not previously been submitted by me for degree at this or any other tertiary institution.

Signature _____

Date _____

Acknowledgements

Thanks to the many for their support throughout the years.

I would like to sincerely thank my supervisor Prof S. Chakraborti for his guidance. To my co supervisor Dr S.W. Human I am grateful for your support, continuous encouragement and the assistance in securing a NRF bursary.

I would also like to express gratitude towards Ms M.A. Graham, Mr S.M. Millard and Dr D. Nolan for their significant contributions towards my studies.

I am indebted to Dr D. Nolan for his unconditional trust in granting me permission to take study leave. Many thanks STATOMET, the University of Pretoria, Standard Bank and the NRF for supporting me financially.

Special thanks to my parents Pierre (Snr) and Nicky, and sister Louise for your love, support and encouragement. Without you my studies would not have been possible.

Finally I would like to thank God for the talents bestowed upon me, and for blessing me so much.

Summary

Numerous nonparametric or distribution-free control charts have been proposed and studied in recent years; see, for example, the overview articles by Chakraborti et al. (2001), Chakraborti and Graham (2007) and Chakraborti et al. (2010). Among the various nonparametric charts, the basic Shewhart-type sign chart for case K (i.e. when the process parameters are known) proposed by Amin et al. (1995) and the basic Shewhart-type precedence chart for case U (i.e. when the process parameters are unknown) proposed by Chakraborti et al. (2004) have received a lot of attention. For example, Human et al. (2010) and Chakraborti et al. (2009a) extended the basic Shewhart-type sign and precedence charts (which signals when the first plotting statistic plots on or outside the control limits), respectively by incorporating runs-rules.

In this dissertation the focus is specifically on the nonparametric Shewhart-type sign and precedence control charts. The goal is to further generalize these two charts by introducing *improved* runs-rules in an attempt to enhance the out-of-control performance of these charts; specifically for large (or larger) shifts. To evaluate the benefits of these new *improved* runs-rules sign and precedence charts, their in-control and out-of-control run-length distributions are evaluated and studied; this is done predominantly by using a Markov chain approach (for both case K and case U) coupled with the idea of conditioning by expectation and the unconditioning (for case U, see, for example the work of Chakraborti et al. (2009a), Chakraborti et al. (2004) and Chakraborti (2000)).

The dissertation consists of five chapters, a brief description of the contents is provided below:

Chapter 1 provides a brief introduction to Statistical Process Control. This will aid in familiarizing the reader with concepts and terminology that are helpful to the following chapters.

Chapter 2 is dedicated to a discussion on the different methods to calculate the run-length distribution of a control chart. The focus is on the Markov chain approach, since the Markov chain approach is used in this dissertation to calculate the run-length distribution of the sign and precedence charts with *improved* runs-rules incorporated.

Chapter 3 provides signalling rules and graphical illustrations of the signalling rules. The transition probability matrices are constructed and explained that are used in the formulas that are used to calculate run-length distribution and the characteristics of the run-length distribution.

Chapter 4 introduces the sign control chart with the *improved* runs-rules incorporated. All the results and transition probability matrices derived and constructed in Chapters 2 and 3 are used to calculate the run-length distribution and properties of the run-length distribution of the new charts.

Chapter 5 introduces the precedence control chart with *improved* runs-rules incorporated. Similarly, all the results and transition probability matrices derived and constructed in Chapters 2 and 3 are used to calculate the run-length distribution and properties of the run-length distribution of the new charts.

Finally **Chapter 6** provides some conclusions and recommendations for future research.

Table of contents

Chapter 1: Brief introduction to Statistical Process Control

1.0 Chapter 1 overview and objective.....	12
1.1 Statistical Process Control.....	13
1.2 Types of variation.....	13
1.3 The control chart.....	14
1.4 Types of control charts.....	15
1.5 Rational subgroups, plotting statistic, control limits and decision rules.....	16
1.5.1 Rational subgroup.....	16
1.5.2 Plotting statistic.....	17
1.5.3 Control limits and the center line.....	18
1.5.4 Signaling rule and signaling event.....	18
1.6 Three important distributions.....	19
1.6.1 The process distribution.....	19
1.6.2 Distribution of the plotting statistic.....	20
1.6.3 The run-length distribution.....	20
1.7 The Shewhart, the CUSUM and the EWMA control charts.....	22
1.7.1 Shewhart chart.....	22
1.7.2 EWMA chart.....	23
1.7.3 CUSUM charts.....	24
1.8 Strengths and weaknesses of the Shewhart, the EWMA and the CUSUM charts..	32
1.9 Phase I and Phase II charts.....	32
1.10 Nonparametric or Distribution-free control charts.....	33
1.11 Variables and Attributes control charts.....	34

1.12 Performance of a control chart.....	35
1.12.1 Operating characteristic.....	35
1.12.2 Run-length distribution.....	36
1.13 Summary of Chapter 1.....	37
1.14 Following chapter.....	38

Chapter 2: Methods to calculate the run-length distribution

2.0 Chapter 2 overview and objective.....	39
2.1 The Markov chain approach.....	42
2.1.1 Introduction.....	42
2.1.2 Definitions.....	43
2.1.3 The run-length distribution.....	47
2.1.4 Transition probability matrix of a finite Markov chain.....	49
2.1.5 Results.....	50
2.1.6 Theorems.....	52
2.1.7 Summary of the Markov chain approach.....	55
2.2 Computer simulations or Monte Carlo simulations.....	59
2.3 Exact approach or Integral equation approach.....	60
2.4 Summary of Chapter 2.....	60
2.5 Following chapter.....	61

Chapter 3: Runs-rules, *improved* runs-rules and transition probability matrices

3.0 Chapter 3 overview and objective.....	62
3.1 Introduction.....	63
3.2 Runs-rules and signalling events.....	67
3.2.1 The <i>1-of-1</i> control charts.....	68
3.2.1.1 The upper one-sided <i>1-of-1</i> control chart.....	68

3.2.1.2	The lower one-sided <i>1-of-1</i> control chart.....	69
3.2.1.3	The two-sided <i>1-of-1</i> control chart.....	70
3.2.2	The <i>2-of-2</i> control charts.....	71
3.2.2.1	The upper one-sided <i>2-of-2</i> control chart.....	71
3.2.2.2	The lower one-sided <i>2-of-2</i> control chart.....	72
3.2.2.3	The two-sided <i>2-of-2</i> control chart.....	73
3.2.3	The <i>2-of-3</i> control charts.....	75
3.2.3.1	The upper one-sided <i>2-of-3</i> control chart.....	75
3.2.3.2	The lower one-sided <i>2-of-3</i> control chart.....	77
3.2.3.3	The two-sided <i>2-of-3</i> control chart.....	79
3.2.4	The <i>improved 2-of-2</i> control charts.....	84
3.2.4.1	The upper one-sided <i>improved 2-of-2</i> control chart.....	84
3.2.4.2	The lower one-sided <i>improved 2-of-2</i> control chart.....	85
3.2.4.3	The two-sided <i>improved 2-of-2</i> control chart.....	87
3.2.5	The <i>improved 2-of-3</i> control charts.....	89
3.2.5.1	The upper one-sided <i>improved 2-of-3</i> control chart.....	89
3.2.5.2	The lower one-sided <i>improved 2-of-3</i> control chart.....	93
3.2.5.3	The two-sided <i>improved 2-of-3</i> control chart.....	96
3.2.6	Summary of the signalling events.....	101
3.3	Transition probability matrices.....	105
3.3.1	The <i>1-of-1</i> control charts.....	108
3.3.1.1	The upper one-sided <i>1-of-1</i> control chart.....	108
3.3.1.2	The lower one-sided <i>1-of-1</i> control chart.....	108
3.3.1.3	The two-sided <i>1-of-1</i> control chart.....	109
3.3.2	The <i>2-of-2</i> control charts.....	110
3.3.2.1	The upper one-sided <i>2-of-2</i> control chart.....	110
3.3.2.2	The lower one-sided <i>2-of-2</i> control chart.....	110
3.3.2.3	The two-sided <i>2-of-2</i> control chart.....	111
3.3.3	The <i>2-of-3</i> control charts.....	112

3.3.3.1	The upper one-sided <i>2-of-3</i> control chart.....	112
3.3.3.2	The lower one-sided <i>2-of-3</i> control chart.....	113
3.3.3.3	The two-sided <i>2-of-3</i> control chart.....	114
3.3.4	The <i>improved 2-of-2</i> control charts.....	117
3.3.4.1	The upper one-sided <i>improved 2-of-2</i> control chart.....	117
3.3.4.2	The lower one-sided <i>improved 2-of-2</i> control chart.....	117
3.3.4.3	The two-sided <i>improved 2-of-2</i> control chart.....	118
3.3.5	The <i>improved 2-of-3</i> control charts.....	119
3.3.5.1	The upper one-sided <i>improved 2-of-3</i> control chart.....	119
3.3.5.2	The lower one-sided <i>improved 2-of-3</i> control chart.....	120
3.3.5.3	The two-sided <i>improved 2-of-3</i> control chart.....	121
3.4	Control limits.....	123
3.4.1	Upper one-sided control charts.....	123
3.4.2	Lower one-sided control charts.....	125
3.4.3	Two-sided control charts.....	125
3.5	Summary of Chapter 3.....	128
3.6	Following two chapters.....	128

Chapter 4: Sign control charts (Case K)

4.0	Chapter 4 overview and objective.....	129
4.1	Introduction.....	130
4.2	Assumptions.....	131
4.3	Applications and general information on the sign chart.....	131
4.4	Plotting statistic.....	132
4.5	Control limits.....	133
4.6	Run-length distribution of the sign charts.....	134
4.6.1	Transition probabilities.....	134

4.6.2	Essential transition probability matrices.....	135
4.6.2.1	The <i>1-of-1</i> sign charts.....	135
4.6.2.2	The <i>2-of-2</i> sign charts.....	136
4.6.2.3	The <i>2-of-3</i> sign charts.....	136
4.6.2.4	The <i>improved 2-of-2</i> sign charts.....	137
4.6.2.5	The <i>improved 2-of-3</i> sign charts.....	138
4.6.3	Run-length distribution and associated characteristics of the charts.....	139
4.7	False alarm rates.....	140
4.8	Design of the <i>improved</i> runs-rules sign charts.....	143
4.8.1	Tables presenting the IC characteristics of the <i>improved</i> runs-rules sign charts.....	145
4.8.2	The use of Tables 4.2, 4.3, 4.4 and 4.5.....	146
4.8.3	Discussion on Tables 4.2, 4.3, 4.4 and 4.5.....	147
4.9	Performance of the <i>improved</i> runs-rules sign charts.....	154
4.9.1	Discussion on the performance analysis tables.....	155
4.9.2	Discussion on the performance analysis results.....	157
4.10	Final comments regarding the <i>improved</i> runs-rules sign charts.....	172
4.11	Summary of Chapter 4.....	173
4.12	Following chapter.....	173

Chapter 5: Precedence control charts (Case U)

5.0	Chapter 5 overview and objective.....	174
5.1	Introduction.....	175
5.2	Assumptions.....	176
5.3	Plotting statistic and control limits.....	177

5.4 The run-length distribution and some characteristics of the precedence charts.....	180
5.4.1 The <i>1-of-1</i> precedence charts.....	180
5.4.1.1 The upper one-sided <i>1-of-1</i> precedence chart.....	180
5.4.1.2 The lower one-sided <i>1-of-1</i> precedence chart.....	181
5.4.1.3 The two-sided <i>1-of-1</i> precedence chart.....	182
5.4.2 The <i>2-of-2</i> precedence charts.....	183
5.4.2.1 The upper one-sided <i>2-of-2</i> precedence chart.....	183
5.4.2.2 The lower one-sided <i>2-of-2</i> precedence chart.....	183
5.4.2.3 The two-sided <i>2-of-2</i> precedence chart.....	184
5.4.3 The <i>2-of-3</i> precedence charts.....	185
5.4.3.1 The upper one-sided <i>2-of-3</i> precedence chart.....	185
5.4.3.2 The lower one-sided <i>2-of-3</i> precedence chart.....	185
5.4.3.3 The two-sided <i>2-of-3</i> precedence chart.....	186
5.4.4 The <i>improved 2-of-2</i> precedence charts.....	187
5.4.4.1 The upper one-sided <i>improved 2-of-2</i> precedence chart.....	187
5.4.4.2 The lower one-sided <i>improved 2-of-2</i> precedence chart.....	187
5.4.4.3 The two-sided <i>improved 2-of-2</i> precedence chart.....	188
5.4.5 The <i>improved 2-of-3</i> precedence charts.....	189
5.4.5.1 The upper one-sided <i>improved 2-of-3</i> precedence chart.....	189
5.4.5.2 The lower one-sided <i>improved 2-of-3</i> precedence chart.....	190
5.4.5.3 The two-sided <i>improved 2-of-3</i> precedence chart.....	191
5.5 Design of the <i>improved</i> runs-rules precedence charts.....	192
5.6 Performance of the <i>improved</i> runs-rules precedence charts.....	199
5.6.1 Discussion on the performance analysis Tables.....	200
5.6.2 Discussion on the performance analysis results.....	201
5.7 Final comments regarding the <i>improved</i> runs-rules precedence charts.....	206

5.8 Summary of Chapter 5.....	207
5.9 Following chapter.....	207
Chapter 6: Concluding remarks.....	208
Appendix 1	
Appendix of Chapter 1's theorems and proofs.....	209
Appendix 2	
Appendix of Chapter 2's theorems and proofs.....	211
Appendix 5	
Appendix of Chapter 3's theorems and proofs.....	221
SAS and Mathcad Appendix	
Appendix of Chapter 4 and Chapter 5's SAS and Mathcad programs.....	265
References.....	300

Chapter 1

Brief introduction to Statistical Process Control

1.0 Chapter 1 overview and objective

Chapter 1 provides a basic yet broad introduction to Statistical Process Control (SPC). In particular, general notation, terminology, definitions and key concepts are introduced that are essential for the developments in Chapters 2, 3, 4 and 5.

After reading this chapter the reader should be familiar with:

- The different types of variation in a process,
- The concept of the control chart,
- The different types of control charts,
- The concept of a rational subgroup,
- What a plotting statistic is and what the function of the control limits is,
- What a signaling event is,
- The three distributions that are of interest in SPC,
- The strengths and weaknesses of the Shewhart, the Exponentially Weighted Moving Average (EWMA) and the Cumulative Sum (CUSUM) control charts,
- The differences and/or similarities between Phase I and Phase II control charts,
- The difference and/or similarities between a parametric and nonparametric control chart, and
- How the average run length and the operating characteristic are used as performance measures for a control chart.

1.1 Statistical Process Control

SPC is a collection of statistical procedures and problem-solving tools that are used to control, monitor and improve the quality of the output of a production process, including the output of services, through the reduction of variability within a process to the extent that is economically feasible (Montgomery (2005), p.148 and Kotz et al. (2006) p.6678).

A process, from a SPC point of view, essentially refers to any repetitive procedure where the same action or the same task is performed over-and-over with the intention to obtain identical “outcomes” or similar “results” on each trial. Examples of processes where SPC plays a key role, range from a typical high-volume manufacturing process (e.g. the production of engine valves) to the service industry where the quality characteristics are less tangible and not easily quantified numerically (e.g. monitoring the time it takes a call centre operator to answer an incoming call).

1.2 Types of variation

The type of variation in a process plays a major role in SPC seeing that not all types of variation can be detected and reduced (or eliminated) to the same extent. There are two major types of variation that are pointed out.

The first type is inherent or natural variation. This type of variation is also labeled chance or common causes of variation and always forms part of the “background noise” in a process, no matter how well the process is maintained and controlled. When a process is operating with only inherent or natural variation at, or around some acceptable target, it is said to be in statistical control, or just in-control (hereafter denoted IC) (Montgomery (2005), p.148).

The second important type of variation does not form part of the natural variation of a process and is thought to be caused by assignable (special) causes of variation; these are typically triggered by external factors that can be controlled, minimized or removed by taking the necessary corrective action. When a process is operating in the presence of an assignable cause, the process is said to be out-of-control (hereafter abbreviated OOC) (Montgomery (2005), p.149).

Ideally a process should operate without any assignable causes of variation; this ensures, for example that the maximum number of items that conform to the specified standards. To ensure the accomplishment of this goal a tool is needed that is able to detect assignable causes as quickly as

possible, and at the same time, not be influenced by the natural variation within the process. The best tool for the job is a control chart. In the next few paragraphs a description of a control chart is given and its application is illustrated.

1.3 The control chart

A typical Shewhart control chart (Walter. A. Shewhart developed the statistical control-chart concept in 1924) is shown in Figure 1.1. This is probably the simplest and most well-known of the different types of control charts. Consequently, the Shewhart chart is chosen to introduce the reader to the basic concepts and then discuss more advanced types of control charts in the next section.

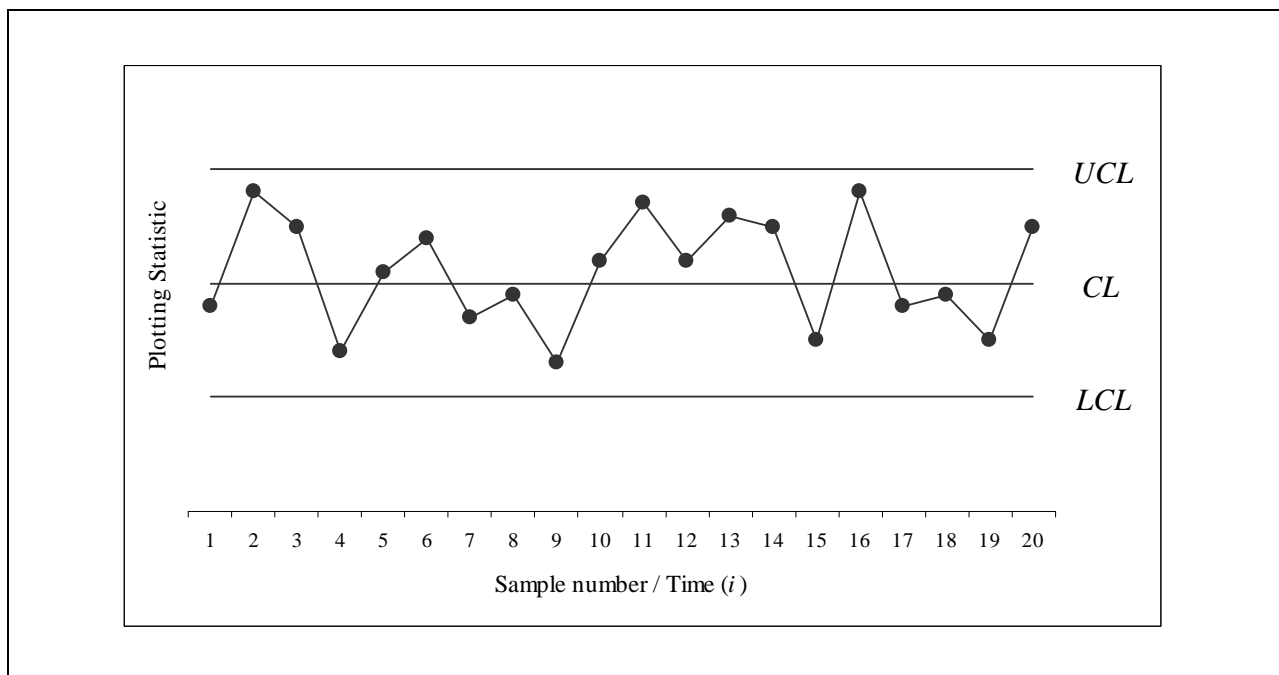


Figure 1.1: A graphical illustration of a typical Shewhart control chart.

A control chart is a display of a statistic corresponding to a parameter of interest (a quality characteristic) of a process output on the vertical axis versus the sample number or time plotted on the horizontal axis. A quality characteristic corresponds to a parameter of interest of the process output, which is some measure of quality of the process output (Montgomery (2005), p.6). A quality characteristic is a statistic calculated from a sample of observations obtained from the process output. The point that is plotted on the chart is typically referred to as a plotting statistic or charting statistic. Examples of plotting statistics are the sample mean, the sample variance and the fraction of

nonconforming items (i.e. the fraction of items not conforming to the specified standards within a sample). A set of control limits and a center line (CL) are typically added to the control chart and provide easy checks on the stability of the process (i.e. whether any special causes are present). The center line represents the typical or average value of the charting statistic corresponding to the in-control state. The upper and the lower control limits are placed on both sides of the center line. The line above the center line is called the upper control limit (UCL) and the line below the center line is labeled the lower control limit (LCL). The control limits define a control chart and, as mentioned earlier, help the user to make an informed and objective decision regarding the state of the process. Typically the decision whether the process is IC or OOC is based on the pattern of the points on the control chart and/or the position of the plotting statistics with respect to the control limits. For example, in the usual operation of a Shewhart control chart, when a single plotting statistic plots between the control limits the process is said to be IC and if the plotting statistic plots on or above the UCL or on or below the LCL , the process is said to be OOC; in the latter case a search for assignable causes should be initiated to eliminate the root cause of the problem. It is customary to join successive points on the control chart with a line so that it is easier to visualize the status of the process over time. A control chart with both upper and lower control limits is called a two-sided control chart. When the detection of only an upward (downward) shift in the process is of interest, a control chart with only an upper (lower) control limit is needed. A control chart with only an upper or only a lower control limit is called an upper or a lower one-sided control chart, respectively.

1.4 Types of control charts

There are three main types of control charts and these are: (i) the Shewhart charts, (ii) the exponentially weighted moving average (EWMA) charts and (iii) the cumulative sum (CUSUM) charts. The Shewhart chart typically utilizes only the information at the last time point i.e. the most recent plotting statistic (calculated from a sample of observations obtained from the process output) to determine if the process is IC or OOC (Montgomery (2005), p.153). Technically more sophisticated control charts are also available and widely used in practice. The EWMA (Montgomery (2005), p.406) and the CUSUM (Montgomery (2005), p.390) control charts are two such charts. The EWMA and CUSUM charts are “memory-based” control charts in the sense that they combine historical information from past plotting statistics with the information from the latest (most recent) sample in the decision making process.

Another type of control chart that has received lots of attention in the SPC literature is the so-called Q -chart. Q -charts use the classical probability integral transformation and the inverse probability integral transformation to transform the sample statistic to a unit less real number (that retains the information from the original sample statistic) but has the advantage that the points may all be plotted on “standardized” Shewhart charts. For more details on Q -charts see, for example, the papers by Quesenberry (1991a), Quesenberry (1991b), Quesenberry (1991c), Quesenberry (1995a), Quesenberry (1995b), Quesenberry (1995c) and Quesenberry (1995d).

1.5 Rational subgroups, plotting statistic, control limits and decision rules

The construction of the various types of control charts differs considerably. Hence, a brief discussion regarding the “building blocks” and the assumptions underlying the Shewhart, the EWMA and the CUSUM charts is given next. The building blocks of a control chart are: (i) the rational subgroups (or the random samples), (ii) the plotting statistics or the charting statistics, (iii) the control limits, (iv) the center line, and (v) the decision rule or the signaling rule.

1.5.1 Rational subgroup

A rational subgroup consists of individual process units from the process output. From each unit a “measurement” is typically obtained; this measurement can be, for example, in the form of a numerical measurement on a continuous numerical scale such as length, width, diameter, volume etc. or a classification such as “conforming” (i.e. the items meet the requirements or specification) or “nonconforming” (i.e. the items do not meet the requirements or specification). The exact nature of the measurement depends on the type of process or the type of quality characteristic that is monitored, or a combination of the process and the quality characteristic of interest.

The method of obtaining rational subgroups is critical, since it is desired to obtain the rational subgroups in such a way, as to be able to effectively detect if an assignable cause is present in the process. Usually, the requirement is that the rational subgroups should be selected in such a way as to maximize the chance of detecting any assignable causes between subgroups, while the likelihood that there are any differences within any of the rational subgroups should be minimized (see e.g. Montgomery (2005), p.245 and Farnum (1994), p.165). This requirement implies that a rational subgroup is not a random sample, as it is typically used in the statistical literature (see e.g. Montgomery (2005), p.87). However, for the developments in this dissertation both terms i.e. rational

subgroup and random sample, are used interchangeably and it is assumed (for the purposes of this dissertation) that they mean the same. For more information on the different methods of obtaining rational subgroups and the recommended size of rational subgroups see e.g. Montgomery (2005), p.162, Farnum (1994), p.165 and Kotz et al. (2006), p.6678.

1.5.2 Plotting statistic

Let $X_{i1}, X_{i2}, \dots, X_{in}$ denote a random sample of size $n \geq 1$ from the output of some process at time $i = 1, 2, 3, \dots$ and let T_i denote the statistic calculated from it. The statistic T_i is typically referred to as the plotting statistic or the charting statistic and is plotted on the vertical axis of a control chart versus the sample number or time on the horizontal axis.

Typical plotting statistics that are used to monitor the location of a process include the sample mean (\bar{X}), the sample median, the sign statistic and the Wilcoxon signed-rank (SR) statistic etc. The sample mean is used to monitor the average of the process, the SR statistic is used to monitor the 50th percentile (the median) and the sign statistic can be used to monitor any process percentile of interest; all of these statistics are used to monitor the location of the process. The sample range, sample standard deviation and the sample variance, on the other hand, are statistics used to monitor the variation of a process (see e.g. Montgomery (2005), p.106).

When the quality characteristic of the process output is not measurable or easily measurable on a numerical scale the p , np , c or u control charts are typically used to monitor the process (see e.g. Chapter 6 of Montgomery (2005)). The p and np charts measure the proportion and number of items in a random sample or rational subgroup respectively that are nonconforming to the specified standards. Where the c and u charts measure the count of non-conformances in the random sample and count of non-conformances per observation unit respectively.

Control charts based on statistics such as the mean, the range, the standard deviation and the variance are called parametric control charts and are typically designed with a specific underlying process distribution in mind. However, when the underlying distribution deviates from the conditions under which it was designed, the properties and/or the performance of the chart may be adversely affected, which could mean loss of time and resources (see e.g. Chakraborti et al. (2004)). Thus, when monitoring, for example the location of a process where the underlying process distribution is unknown the conventional parametric control charts should not be used blindly; in these cases

nonparametric control charts may be used, which are not developed with a specific underlying distribution in mind. Examples of nonparametric charts include the Shewhart-type sign and signed-rank charts which are based on the well-known nonparametric sign and Wilcoxon signed-rank statistics, respectively.

1.5.3 Control limits and the center line

The control limits are placed on the control chart to aid the user in making an objective and informed decision regarding the state of a process i.e. whether the process is IC or OOC. The exact placement of the control limits depends on a number of key elements. These elements are for example: (i) the distribution of the individual observations (the distribution of the individual observations influences the distribution of the plotting statistic, since the plotting statistic is a function of the individual observation); (ii) the natural variability in the process (see e.g. Montgomery (2005), p.206), (iii) the distribution of the plotting statistic T_i , (iv) the type of control chart (since, for instance, the EWMA and the Shewhart charts have varying and constant control limits over time, respectively) and (v) the specified performance criteria of the control chart (narrower control limits are required to detect smaller shifts), to name but a few.

1.5.4 Signaling rule and signaling event

A control chart signals following a sequence (or pattern) of plotting statistics on the control chart that correspond to a signaling rule, this event is known as a signaling event. Thus a signaling rule describes a specific event on a control chart and once the event occurs it is labeled as a signaling event. At each point in time, the signaling rule(s) is (are) used to determine whether the process is declared IC or OOC. The simplest signaling rule is based only on the last plotting statistic i.e. if the last plotting statistic plots on or outside one of the control limits the process is declared OOC otherwise the process is deemed IC.

Because the simplest or basic signaling rule uses information only from the last sample to decide if the process is IC or OOC (known as the *1-of-1* signaling rule), the *1-of-1* signaling rule is relatively insensitive to small shifts in the process and consequently other signaling rules were developed. These rules include, for example, the rule that declares the process OOC if the last two plotting statistics plot on or outside the control limits (i.e. the *2-of-2* signaling rule) and the rule that declares the process OOC if two of the last three plotting statistics plot on or outside the control limits (i.e. the *2-of-3*

signaling rule). The *2-of-2* and the *2-of-3* signaling rules are also known as runs-rules. Note that, in general, *k-of-w* runs-rules can be defined (where $1 \leq k \leq w$); however, for simplicity the focus is on the *2-of-2* and the *2-of-3* signaling rules.

By incorporating runs-rules into a Shewhart-type control chart, not only the last plotting statistic but also some historic information about the process is used in determining the IC or OOC state of the process. This is similar in spirit (but not exactly the same) as the EWMA and the CUSUM control charts in that they are memory-based control charts. For example, by incorporating signaling rules in the operation of a Shewhart-type control chart the last two or three plotting statistics (which are the sample statistics) are considered in determining the state of the process, whereas the EWMA and CUSUM control charts only consider the last plotting statistic (but, which is a function of all the sample statistics from start-up) in determining the state of the process.

1.6 Three important distributions

In SPC there are three distributions of interest and these are: (i) the underlying process distribution, (ii) the distribution of the plotting statistic (which is affected by the process distribution), (iii) the distribution of the run-length (which is in turn affected by both the distribution of the process and the distribution of the plotting statistic). These three distributions and their associated notations are introduced and discussed in the next section.

1.6.1 The process distribution

The sample of measurements taken from the process output is a set of random variables denoted by X_{ij} where $i = 1, 2, 3, \dots$ and $j = 1, 2, \dots, n$ and X is labeled the process random variable. Note that, the X_{ij} 's are, for example, typically obtained from some key quality characteristic of the manufactured product.

The probability density function (pdf) and the cumulative distribution function (cdf) of X are denoted by f_X and F_X , respectively where the subscript X indicates that the functions are related to the random variable X ; similar notation is used for other random variables. The mean and variance of the process is denoted by μ_X and σ_X^2 respectively.

1.6.2 Distribution of the plotting statistic

The plotting statistic or charting statistic is denoted by T_i for $i = 1, 2, 3, \dots$ and is calculated from the corresponding sample measurements X_{ij} . Because each T_i is a function of the X_{ij} 's (which are random variables) it follows that T_i is a random variable. The distribution of the plotting statistic, especially its mean and variance, is crucial in the determination of the control limits of the control chart (see e.g. Section 1.5.3), because the control limits are typically functions of the characteristics of the distribution of the plotting statistic.

The pdf and cdf of T_i are denoted by f_T and F_T , whereas the mean and the variance of T_i are denoted by μ_T and σ_T^2 , respectively. Note that, as long as the distribution of the X_{ij} 's remain unchanged (process is IC) the distribution of all the T_i 's are exactly the same; hence, the pdf and cdf of T_i is not indexed by an “ i ”.

1.6.3 The run-length distribution

“The number of rational subgroups to be collected or the number of charting statistics to be plotted on a control chart before the first OOC signal is observed is the run-length of a chart” Human and Graham (2007), which is denoted by N . The distribution of the run-length is of particular interest because it conveys information regarding the properties and/or the performance of a control chart. The pdf and cdf of the run-length random variable are denoted by f_N and F_N , respectively. The mean, variance and standard deviation of N are known as the average run-length (denoted ARL), the variance of the run-length (denoted VRL) and the standard deviation of the run-length (denoted $SDRL$).

Table 1.1 summarizes the notation used for the pdf, cdf, mean and variance of the process distribution, the distribution of the plotting statistic and the run-length distribution, respectively. Note that arrows are added to Table 1.1 to emphasize that the run-length distribution is influenced/affected by the distribution of the plotting statistic, which in turn is influenced by the underlying process distribution.

Since the focus in this dissertation is on nonparametric charts, it is worth noting that the distribution of a nonparametric statistic (plotting statistic of a nonparametric chart) is unaffected by the underlying distribution of the process (f_X). Consequently the IC run-length distribution of a

nonparametric control chart does not depend on the underlying process distribution (f_X) (Chakraborti et al. (2004)).

Table 1.1: Summary of the notation of the Process distribution, Plotting statistic and Run-length random variable.

Process distribution	
$f_X(x), x \in \mathfrak{R}$	pdf
$F_X(x) = P(X \leq x)$	cdf
$\mu_X = E(X)$	mean
$\text{var}(X) = \sigma_X^2$	variance

↓

Distribution of the plotting statistic	
$f_T(t)$	pdf
$F_T(t) = P(T \leq t)$	cdf
$\mu_T = E(T_i)$	mean
$\text{var}(T_i) = \sigma_T^2$	variance

↓

Run-length distribution	
$f_N(j) = P(N = j) \quad j = 1, 2, 3, \dots$	pdf
$F_N(j) = P(N \leq j) \quad j = 1, 2, 3, \dots$	cdf
$ARL = E(N)$	Mean: labeled average run-length (<i>ARL</i>)
$VRL = \text{var}(N) = \sigma_N^2$	Variance: labeled the variance of the run-length (<i>VRL</i>)

- 1: In this dissertation the underlying process distribution $f_X(x)$ is assumed to be continuous,
- 2: Accordingly $f_T(t)$ is also continuous, and
- 3: The run-length random variable N is discrete.

In the following chapter the Markov chain technique is described, which is used to calculate the run-length distribution and some associated characteristics of the run-length distribution as is done in this dissertation. Formulas are derived and these are used to calculate the run-length distribution and some associated characteristics of the run-length distribution in specific cases.

1.7 The Shewhart, the CUSUM and the EWMA control charts

The control limits are one of the key building blocks/elements of any control chart and their position on the chart directly influences the chart's performance (see e.g. Montgomery (2005), p.156). In this section, the control limits of the Shewhart, the EWMA and the CUSUM charts are discussed.

1.7.1 Shewhart chart

The founding father of the Shewhart control chart is Walter. A. Shewhart who developed the statistical control chart concept in 1924 while working at Bell Telephone Laboratories (see e.g. Montgomery (2005), p.8)

To describe the Shewhart chart in more detail, assume that $X_{i1}, X_{i2}, \dots, X_{in}$ denote a random sample (i.e. measurements from some quality characteristic) of size $n \geq 1$ from process at time $i = 1, 2, 3, \dots$, with known process mean μ_0 and known process standard deviation σ_0 .

Let T_i $i = 1, 2, 3, \dots$ denote the plotting statistics (calculated from each random sample i.e. the X_{ij} 's) and suppose that the mean and standard deviation of the plotting statistic, as mentioned in Table 1.1, are denoted by μ_T and σ_T , respectively. Then, the center line (CL), the upper control limit (UCL) and the lower control limit (LCL) are given by:

$$\begin{aligned}
 UCL &= \mu_T + L\sigma_T \\
 CL &= \mu_T \\
 LCL &= \mu_T - L\sigma_T
 \end{aligned}
 \tag{1.1}$$

where the constant $L > 0$ is the charting constant which is a design parameter that determines the width of the control limits expressed in standard deviation units (Montgomery (2005), p.153). The plotting statistic T_i is plotted on the vertical axis versus the sample number or time on the horizontal axis of the control chart. Once a point plots on or outside the control limits, the process is declared to be OOC and the charting procedure stops (*1-of-1* signaling rule). Typically, a search for assignable

causes is then started. In this dissertation, a sequence of the plotting statistics is considered and not only a single plotting statistic when determining the state of the process (i.e. IC or OOC).

1.7.2 EWMA chart

The Exponentially Weighted Moving Average (EWMA) chart was introduced by Roberts (1959) and is more effective than the *I-of-I* Shewhart-type chart in detecting small process shifts (Montgomery (2005), p.386). For a more in-depth discussion on the EWMA chart than what is given below, the reader may refer to Montgomery (2005), p.406-p.419, Crowder (1987, 1989) and Lucas and Saccucci (1990).

To describe the EWMA chart in more detail, assume that X_1, X_2, X_3, \dots denote independent and identically distributed observations from a process (distribution) with a known mean μ_0 and a known standard deviation σ_0 . The plotting statistic of the EWMA control chart for individual observations is defined as:

$$T_i = \lambda X_i + (1 - \lambda)T_{i-1} \quad \text{for } i = 1, 2, 3, \dots \quad (1.2)$$

where X_i is the current observation and the constant $0 < \lambda \leq 1$ is the smoothing parameter. The starting value of the plotting statistic (which is required for the first observation at time $i = 1$) is typically taken to be the process mean so that $T_0 = \mu_0$.

The expected value and the variance of T_i in (1.2) are:

$$\mu_{T_i} = E(T_i) = \mu_0 \text{ and } \sigma_{T_i}^2 = \text{Var}(T_i) = \sigma^2 \left(\frac{\lambda}{2 - \lambda} \right) [1 - (1 - \lambda)^{2i}] \quad (\text{see Appendix 1 for the derivation}) \quad (1.3)$$

The exact upper and lower control limits and the center line of the EWMA chart are:

$$UCL/LCL = \mu_0 \pm L\sigma_0 \sqrt{\frac{\lambda}{2 - \lambda} (1 - (1 - \lambda)^{2i})} \quad (1.4)$$

$$CL = \mu_0$$

where $L > 0$ and λ are suitably chosen constants. For large values of i the term $[1 - (1 - \lambda)^{2i}]$ approaches unity so that the exact control limits approach their so-called steady-state values. The steady-state EWMA control limits are:

$$UCL/LCL = \mu_0 \pm L\sigma_0 \sqrt{\frac{\lambda}{2-\lambda}} \quad (1.5)$$

The EWMA plotting statistics are plotted on the vertical axis of the control chart versus the sample number or time (i) on the horizontal axis with the UCL and LCL in either (1.4) or (1.5) (Montgomery (2005), p.407). Once a point exceeds (i.e. plots on or outside) the control limits, the process is declared to be OOC and the charting procedure stops. Typically, a search for assignable causes is then initiated.

The two constants L and λ are known as the design parameters of the EWMA chart. The constant $0 < \lambda \leq 1$ is the smoothing parameter. “A rule of thumb is to use smaller values of λ to detect smaller shifts” (Montgomery (2005), p.411). The constant L determines the width of the control limits i.e. for larger (smaller) values of L the wider (narrower) the control limits are and the longer (sooner) it will be before the chart signals. Montgomery (2005), p.411-p.412 gives a discussion on the design of the EWMA control chart i.e. the choice of L and λ .

The preceding discussion focused on the EWMA chart for individual observations. The EWMA chart can be adapted or extended for the case where rational subgroups of size $n \geq 1$ are considered (see e.g. Montgomery (2005), p.413).

1.7.3 CUSUM charts

The cumulative sum (CUSUM) chart is similar in spirit to the EWMA chart in that it is memory-based and is able to detect small process shifts better than the *I-of-I* Shewhart control chart (Montgomery (2005), p.386). The CUSUM chart was first proposed by Page (1954) and subsequently studied in detail by numerous researchers. For an in-depth coverage of the CUSUM chart the books by Hawkins and Olwell (1998) and Montgomery (2005) may be consulted. Below a brief introduction is given on the CUSUM chart.

The tabular CUSUM chart uses two plotting statistics to monitor the process: One plotting statistic is sensitive to upward shifts and is used to detect upward shifts in the process, and the second plotting statistic is sensitive to downward shifts and is thus used to detect downward shifts in the process.

To describe the tabular CUSUM chart in more detail, assume that X_1, X_2, X_3, \dots denote independent and identically distributed observations from a process with a known process mean μ_0 and a known process standard deviation σ_0 .

Let C^+ be the statistic that is calculated by accumulating the deviations from μ_0 that are above μ_0 and let C^- be the statistic that is calculated by accumulating the deviations from μ_0 that are below μ_0 ; these statistics are defined (calculated) as:

$$\begin{aligned} C_i^+ &= \max[0, X_i - (\mu_0 + K) + C_{i-1}^+] \\ C_i^- &= \max[0, (\mu_0 - K) - X_i + C_{i-1}^-] \end{aligned} \quad (1.6)$$

where C^+ and C^- are known as the one-sided upper and one-sided lower CUSUMs respectively, the starting values are $C_0^+ = C_0^- = 0$ and K is the reference value; the value of K is usually chosen to be the value halfway between μ_1 and μ_0 i.e.

$$K = \frac{|\mu_1 - \mu_0|}{2} \quad (1.7)$$

where μ_1 is that value of the process mean that is of interest to be detected quickly (Montgomery (2005), p.390).

The process is declared to be OOC if either C^+ or C^- exceed the decision interval H i.e. the control limit of a tabular CUSUM chart, which is usually chosen to be five times the process standard deviation σ_0 (Montgomery (2005), p.391).

Note that, the tabular CUSUM defined above is for individual observations but can be extended and used in settings where rational subgroups of size $n \geq 1$ are obtained from the process (Montgomery (2005), p.402)

Note that, for a one-sided Shewhart, EWMA and CUSUM chart (where only an upward or only a downward shift is of interest) the control limit that is not of interest is simply discarded, and the remaining control limit is adjusted appropriately so that the control chart has desirable properties (Montgomery (2005), p.400).

Example 1.1

A Shewhart, two EWMA and a CUSUM control chart is created from the dataset given in Table 1.2 and are displayed in Figures 1.2, 1.3, 1.4 and 1.5, respectively.

Consider the example from the book by Farnum (1994) p.185 where the groove dimensions of keys (which are important quality characteristics in the manufacturing of keys) are monitored. Table 1.2 displays the groove dimensions of 20 rational subgroups each of size 5. The mean (μ_0 is unknown) of the groove dimensions are monitored by calculating the average of the groove dimension measurements in each subgroup of keys. A Shewhart, two EWMA and a CUSUM control chart is constructed with these subgroup averages as plotting statistics.

Note that in Table 1.2 the second row, columns two, three, four, five and six x_{i1} , x_{i2} , x_{i3} , x_{i4} and x_{i5} refer to the groove dimension measurements. The first value of the subscript of these five measurements (i) indicate the number of the subgroup, where the second value of the subscript indicate the number of the measurement of the subgroup in consideration.

Table 1.2 Groove dimension measurements from the manufacturing of keys.

Subgroup	Measurements					Subgroup Mean
<i>i</i>	<i>X(i,1)</i>	<i>X(i,2)</i>	<i>X(i,3)</i>	<i>X(i,4)</i>	<i>X(i,5)</i>	<i>X-bar(i)</i>
1	0.0061	0.0084	0.0076	0.0076	0.0044	0.00682
2	0.0088	0.0083	0.0076	0.0074	0.0059	0.0076
3	0.008	0.008	0.0094	0.0075	0.007	0.00798
4	0.0067	0.0076	0.0064	0.0071	0.0088	0.00732
5	0.0087	0.0084	0.0088	0.0094	0.0086	0.00878
6	0.0071	0.0052	0.0072	0.0088	0.0052	0.0067
7	0.0078	0.0089	0.0087	0.0065	0.0068	0.00774
8	0.0087	0.0094	0.0086	0.0073	0.0071	0.00822
9	0.0074	0.0081	0.0086	0.0083	0.0087	0.00822
10	0.0081	0.0065	0.0075	0.0089	0.0097	0.00814
11	0.0078	0.0098	0.0081	0.0062	0.0084	0.00806
12	0.0089	0.009	0.0079	0.0087	0.009	0.0087
13	0.0087	0.0075	0.0089	0.0076	0.0081	0.00816
14	0.0084	0.0083	0.0072	0.01	0.0069	0.00816
15	0.0074	0.0091	0.0083	0.0078	0.0077	0.00806
16	0.0069	0.0093	0.0064	0.006	0.0064	0.007
17	0.0077	0.0089	0.0091	0.0068	0.0094	0.00838
18	0.0089	0.0081	0.0073	0.0091	0.0079	0.00826
19	0.0081	0.009	0.0086	0.0087	0.008	0.00848
20	0.0074	0.0084	0.0092	0.0074	0.0103	0.00854

In Figure 1.2 the Shewhart control chart for the sample mean or \bar{x} (\bar{X}) is created by choosing the design parameter $L = 3$; these are the well-known 3σ control limits. Given that the process has an underlying Normal distribution the ARL will be 370 (Montgomery (2005), p.237). The control limits are constructed using equations (1.1). The plotting statistic T_i in this case is the subgroup mean. The \bar{x} -bar control chart is a chart that monitors the location of a process. Note that the process is IC since none of the plotting statistics plotted on or outside the control limits. Therefore it can be concluded that there is no shift in the location of the process.

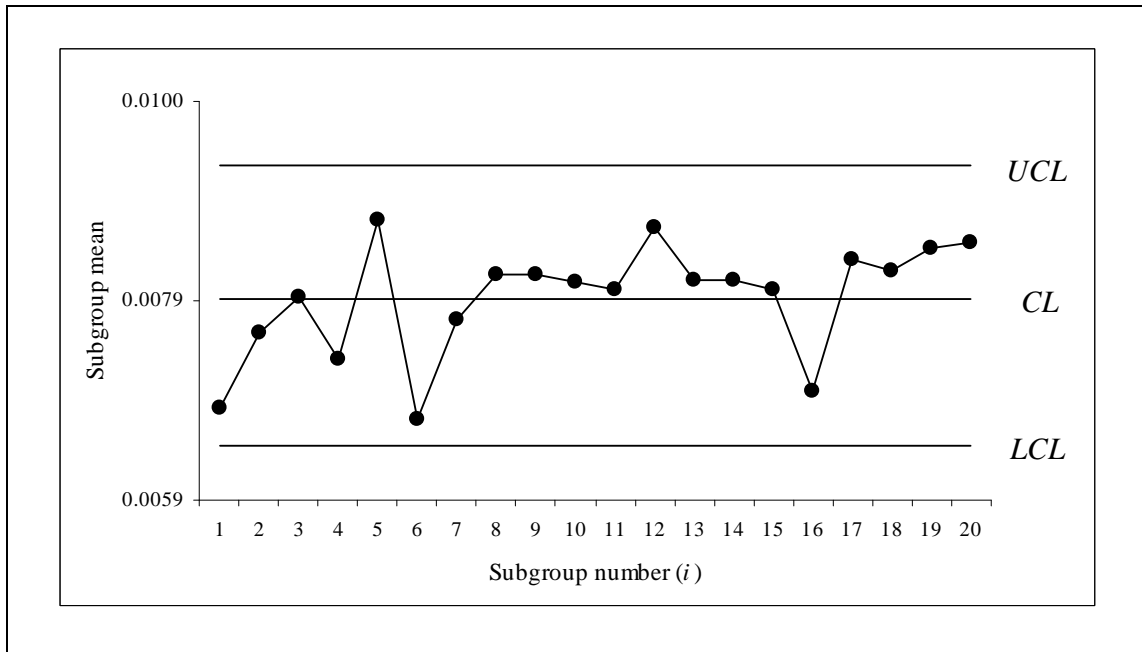


Figure 1.2: Shewhart \bar{X} -bar control chart.

The EWMA control chart in Figure 1.3 for \bar{x} is created by choosing the design parameters as follows: $L = 2.703$ and $\lambda = 0.1$; given these parameters and a Normal underlying process distribution the ARL is 370 (Montgomery (2005), p.413). The exact control limits are constructed using equations (1.4). Note that equations (1.4) are for individual observations and in this case they are applied to rational subgroups (refer to the end of Section 1.7.2 for a brief discussion on rational subgroups). The plotting statistic plotted on the chart is given in equation (1.2), again equation (1.2) is for individual observations. Appropriate adjustments are made since rational subgroups are considered in this case. The \bar{x} -bar EWMA control chart is also a chart that monitors the location of the process and is more sensitive to small shifts compared to the Shewhart control chart. Note that the process is IC since none of the plotting statistics plotted on or outside the control limits.

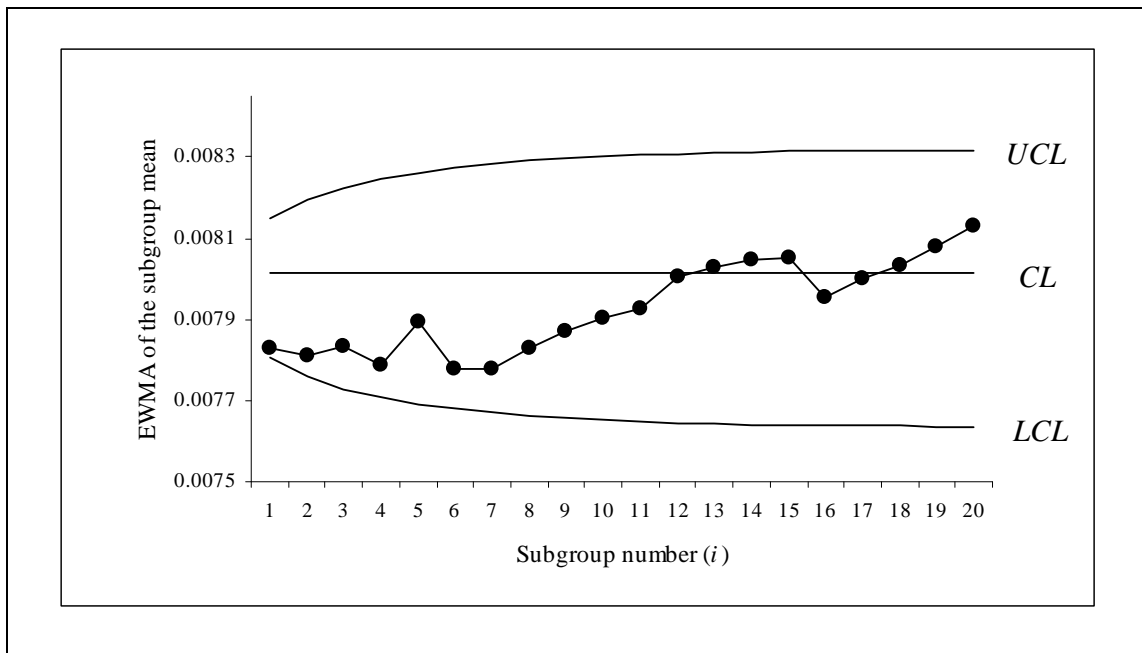


Figure 1.3 EWMA control chart with exact control limits.

Note that the EWMA control chart in Figure 1.4 has steady-state control limits. The design parameters are chosen as follows: $L = 2.703$ and $\lambda = 0.1$. Since the control limits in this case are wider at start-up than the EWMA control chart with exact control limits, the ARL will be greater than 370. The steady-state control limits are constructed using equations (1.5). The plotting statistic plotted on the chart is given in equation (1.2). Note that since rational subgroups are considered, equations (1.5) and (1.2) are adjusted accordingly. None of the plotting statistics plot on or outside the control limits therefore it can be concluded that the process is IC.

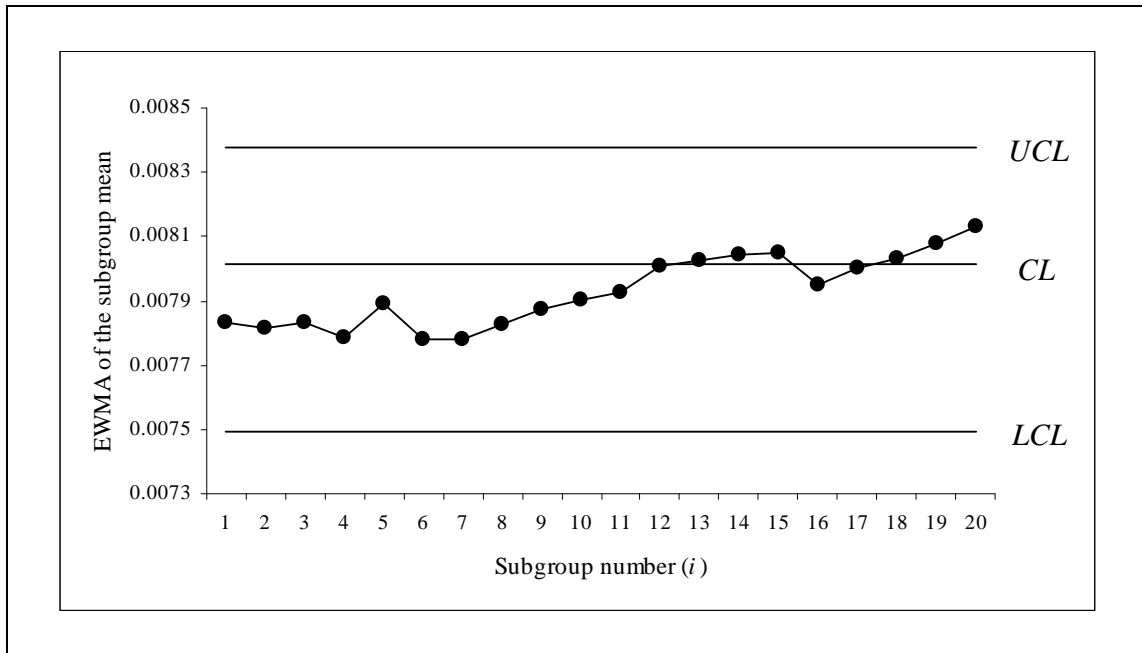


Figure 1.4: EWMA control chart with steady-state control limits.

A CUSUM control chart that monitors \bar{x} is illustrated in Figure 1.5. This chart is constructed for illustration purposes by choosing the design parameters as follows: $H = 0.002449947$ and $K = 0.0002$. H is chosen to be five times the standard deviation of the process mean where the process mean is estimated by $\bar{\bar{X}}$. For illustration purposes the out-of-control mean to be detected is chosen to be $u_1 = 0.000889989$. Consequently from equation (1.7) it follows that $K = 0.0002$. Note that the process is IC since none of the plotting statistics plotted on or outside the decision interval H . The plotting statistics are defined in equations (1.6). Since rational subgroups are considered, equations (1.6) are adjusted accordingly.

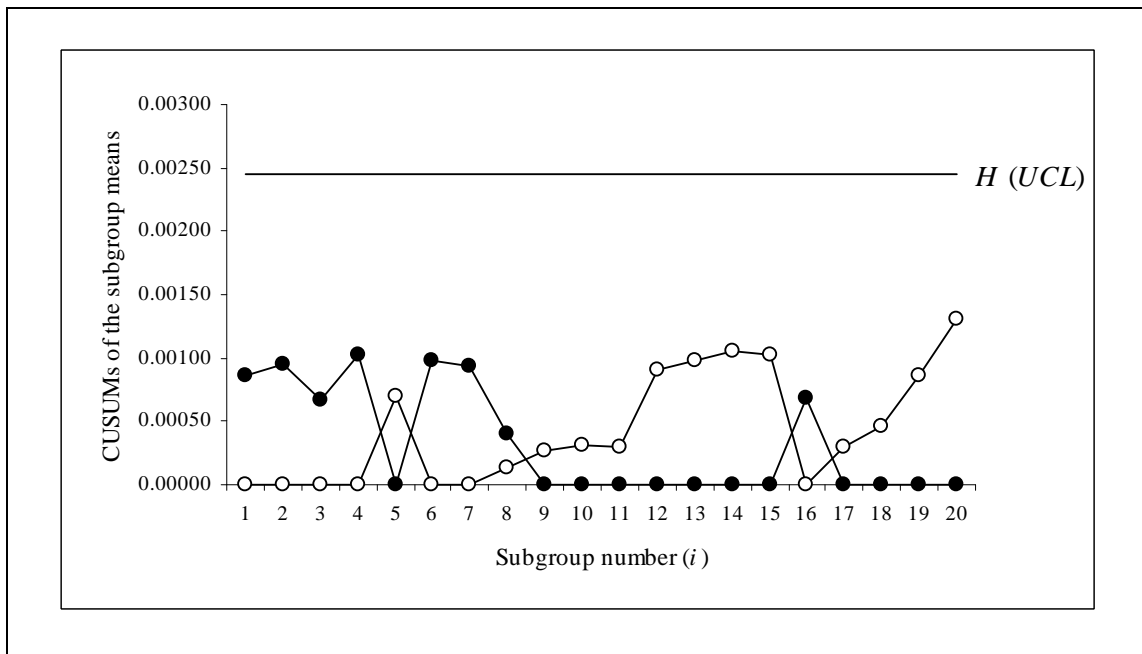


Figure 1.5: CUSUM control chart.

1.8 Strengths and weaknesses of the Shewhart, the EWMA and the CUSUM charts

The plotting statistics of the Shewhart chart are calculated using only the last (i.e. latest) random sample or rational subgroup, which causes the chart to be relatively insensitive to small process shifts i.e. shift of order $1.5\sigma_0$ units or less (Montgomery (2005), p.388). However, the CUSUM and EWMA charts consider historic values of the plotting statistic, and are consequently more effective in detecting small process shifts (Montgomery (2005), p.386).

The traditional Shewhart, EWMA and CUSUM charts are parametric control charts; this means that they are typically designed with a specific distribution in mind (such as the Normal distribution). Hence, their run-length distribution is affected by the underlying process distribution (see e.g. Human et al. (accepted) regarding the effect of non-Normality of the underlying process distribution on the EWMA chart's performance). This can be a drawback in some practical situations since these charts will be less useful when the underlying process does not follow a specific distribution.

1.9 Phase I and Phase II charts

There are two distinct phases in the application of a control chart, these are: Phase I and Phase II, respectively (see e.g. Woodall (2000), Woodall et al. (2004) and Chakraborti et al. (2009b) for a discussion of Phase I and Phase II control charts). As stated by Chakraborti et al. (2009b), in "Phase I, the primary interest is to better understand the process and assess process stability" whereas in Phase II, the process is assumed to be IC and needs to be monitored for the possible occurrence of an assignable cause(s).

In order to apply a Phase II chart some knowledge is needed concerning the location and variability of the underlying process distribution to determine the control limits. If this knowledge is unavailable a Phase I analysis needs to be done to find an IC reference sample from which the control limits can be estimated. The general methodology of a Phase I analysis can be described as follows:

In Phase I the process is assumed to be OOC. Typically 20 to 25 samples of size 5 each are obtained from which trial control limits are estimated/calculated. Note that the control limits in Phase I are referred to as trial limits since they may change as the Phase I analysis progresses. The Plotting statistics and trial control limits are calculated from the same values of the process output, these plotting statistics are then plotted on the control chart with the trial control limits. All the plotting statistics plotting on or outside the control limits are investigated for potential assignable causes. If an

assignable cause is found in the process, the output values associated with the presence of an assignable cause is discarded. New revised trial control limits are then calculated with the remaining process values that are associated with the plotting statistics that have all plotted IC. This *trial and error* process is repeated until all plotting statistics plot inside the control limits or until there are no more assignable causes present in the process. Eventually, the remaining set of values is assumed to be from an IC process. The ultimate goal in Phase I is to familiarize oneself with the process, to stabilize the process and to obtain a set of IC process samples.

In Phase I the shifts in the process could be large since the process is assumed to be OOC (Montgomery (2005), p168) i.e. in the presence of assignable causes. Shewhart-type control charts are popular Phase I control charts since they are affective in detecting large shifts in the process (Montgomery (2005), p168). In Phase II the process shifts are expected to be smaller compared to Phase I since the process is already brought into control. CUSUM and EWMA control charts are popular Phase II control charts since they are effective in detecting small process shifts (Montgomery (2005), p.386). Note that it is not implied that Shewhart charts can only be applied in a Phase I analysis; similarly it is not implied that CUSUM and EWMA charts can only be applied in a Phase II analysis.

There are different objectives in the design and operation of Phase I and Phase II control charts. In Phase II a control chart with a large in-control average run length (IC *ARL*) and a small out-of-control average run length (OOC *ARL*) is desirable. Whereas in Phase I the *ARL* is not a reasonable performance measure, since “the problem of simultaneous comparison of a number of (charting) statistics to the same set of control limits is similar to that encountered in the ‘multiple testing’ literature. Under these motivations, the false alarm probability (*FAP*), which is the (overall) probability of at least one false alarm, is used to construct (design) and evaluate Phase I control charts in the literature” (Chakraborti et al. (2009b)).

1.10 Nonparametric or Distribution-free control charts

A nonparametric control chart is defined in terms of its in-control run-length distribution i.e. if the in-control run-length distribution of the control chart is the same for every continuous distribution, the chart is said to be nonparametric or distribution-free (see Chakraborti et al. (2004)). Note that the terms nonparametric and distribution-free are used interchangeably, as for the purpose in this dissertation they mean the same. Since non-Normal process distributions are frequently encountered in practice,

there exists a demand for control charts that do not depend on the underlying process distribution i.e. nonparametric charts.

The performance (as reported in the literature) of the Shewhart, the EWMA and the CUSUM control charts are typically for the Normal distribution and can be misleading to the unsuspected and ill-informed quality practitioner. Non-normal distributions can markedly affect a parametric control chart's performance and can lead to an increase in false alarms, which in turn, will lead to a loss of time and resources (see e.g. Chakraborti et al. (2004)). When a process follows a Normal distribution, the traditional Shewhart, EWMA and CUSUM charts (which are all developed with the Normal distribution in mind) will perform very well compared to nonparametric control charts. Conversely, when the process follows a skew or heavy tailed distribution, nonparametric control charts will most likely outperform their parametric counterparts (see e.g. the performance comparisons of Human et al. (2009)). A thorough review of the literature on nonparametric charts can be found in Chakraborti et al. (2001), Chakraborti and Graham (2007) and Chakraborti et al. (2010).

1.11 Variables and Attributes control charts

Control charts can be classified into two general categories i.e. variables and attributes charts (see e.g. Montgomery (2005), p.156).

Variables charts are used when the quality characteristic of a process is measurable on a numerical or some continuous scale. Some examples of variables charts that are often used are: (i) the \bar{X} control chart which measures/monitors the central tendency or location of a process, and (ii) the S chart, which is based on the standard deviation (S), and used to monitor the variation or spread of a process. For more details, see Chapter 5 of Montgomery (2005) which gives a discussion on variables control charts.

Sometimes a process quality characteristic is not measurable on a continuous or even a quantitative scale. If this is the case, a unit of product is usually classified as conforming or nonconforming, based on whether it possesses certain attributes, or sometimes it is possible to count the number of nonconformities in a unit of production. Control charts that are used to monitor such quality characteristics are called attribute control charts. Examples of attribute control charts are: the p charts, u charts and c charts. Chapter 6 of Montgomery (2005) gives a discussion on attribute control charts.

1.12 Performance of a control chart

The performance of a control chart is affected by the design of the chart. The design of the chart consists of a number of “building blocks” (refer, for example, to Section 1.5 and Montgomery (2005), p.156).

The most popular performance measures of a control chart include the IC and the OOC *ARL*, and the operating characteristic (OC) curve (see e.g. Montgomery (2005), p.110 and p.160). Both the *ARL* and the OC effectively measure how quickly the control chart signals following a shift in the process. So, these performance measures can be used when comparing different control charts.

When implementing a control chart, it is desired that the number of plotting statistics, plotting on or outside the control limits when the process is IC, to be a minimum (so that the *FAR* is small) and the control chart has the ability to detect a shift in the process as quickly as possible (i.e. small OOC *ARL*). A control chart with these properties is said to have good performance. Note that there is a sacrifice that has to be made between the *FAR* and the OOC *ARL*. In order to obtain a small *FAR* the OOC *ARL* deteriorates (OOO *ARL* increase), conversely when obtaining a small OOC *ARL* the *FAR* deteriorates (*FAR* increase). Consequently a balance needs to be found between a small OOC *ARL* and a small *FAR*.

Note that in this dissertation the OOC *ARL* is used in performance comparisons. The OC curve is also a performance comparisons measure and is briefly discussed, as it is well-known and widely used in the literature.

1.12.1 Operating characteristic

The OC curve is a tool used to measure the performance of a control chart, for a discussion on OC curves consider Human and Graham (2007). The OC curve is the probability that no signal will be given by the chart on the first subsequent sample following a shift in the process i.e. the chart failed to detect the shift. Let β denote the probability of a non-signaling event, this probability is also referred to as the β -risk. The β -risk can be calculated given a shift in the process i.e. the probability of a non-signaling event given the process is OOC. An OC curve has the β -risk on the y-axis and the shift in a process parameter on the x-axis.

When comparing control charts using OC curves, the design parameters of the charts are chosen such that their no signal probabilities (given the process is IC) are equal. The control chart with the “lower” OC curve is declared to be the better chart i.e. the chart has superior performance. To declare a control chart superior over a competing control chart could be more ambiguous; for instance for a certain range of shifts one chart’s OC curve can be lower while at a different range of shifts another chart’s OC curve can be lower. In this case it is not always clear which control chart is the best. “For a detailed discussion on the use of operating-characteristic curves, refer to Montgomery and Runger (2003)” (Montgomery (2005), p111).

1.12.2 Run-length distribution

“The number of rational subgroups to be collected or the number of charting statistics to be plotted on a control chart before the first OOC signal is observed is the run-length of a chart.” Human and Graham (2007). The run-length random variable is denoted by N . The distribution of the run-length random variable is denoted by f_N and called the run-length distribution. Characteristics of the run-length distribution that are typically calculated and used as measures of a control chart’s performance are:

- Average Run Length (ARL),
- Standard deviation of the run-length ($SDRL$),
- Variance of the run-length (VRL),
- Median of the run-length (MRL),
- The quartiles (Q_1, Q_2, Q_3),
- The percentiles, and
- Inter quartile range (IQR)

All of these run-length distribution characteristics give the user more insight into the performance of the chart. For example, the ARL , Q_1 , Q_2 , Q_3 and MRL are measures of the run-length’s location, where as the $SDRL$ and IQR is a measure of the run-length’s variation.

When there is no shift in the process i.e. there are no assignable causes present in the process, it is said that N follows an IC run-length distribution. If assignable causes are present in the process, N has an OOC run-length distribution.

As stated previously, the characteristics of the run-length distribution can be used as performance measures. The *ARL* is a measure of central tendency of the run length distribution. A control chart with good performance has a large in-control average run length (*IC ARL*) i.e. given there are no assignable causes present in the process the chart has a low *FAR*. It is also desirable for a control chart to have a small out-of-control average run length (*OOA ARL*) i.e. the chart signals quickly in the presence of an assignable cause or in the presence of a shift in the process.

When performing performance comparisons between two competing control charts, their in-control average run-length (*IC ARL*) is usually fixed at an acceptable high level. Then, the chart with the smallest out-of-control average run-length (*OOA ARL*) is declared to be the better chart.

1.13 Summary of Chapter 1

A brief introduction to SPC is presented in this chapter. A solid foundation regarding general notation, terminology, definitions and key concepts in SPC is laid down, namely:

- The different types of variation in a process,
- The concept of the control chart,
- The different types of control charts,
- The concept of a rational subgroup,
- What a plotting statistic is and what the function of the control limits is,
- What a signaling event is,
- The three distributions that are of interest in SPC,
- The strengths and weaknesses of the Shewhart, the Exponentially Weighted Moving Average (EWMA) and the Cumulative Sum (CUSUM) control charts,
- The differences and/or similarities between Phase I and Phase II control charts,
- The difference and/or similarities between a parametric and nonparametric control chart, and
- How the average run length and the operating characteristic are used as performance measures for a control chart.

This will aid the reader in comprehending the means and goals in the following chapters.

1.14 Following chapter

Chapter 2 focuses on the three methods to calculate the run-length distribution and the characteristics of the run-length distribution. The three methods are: (i) computer simulations or Monte Carlo simulations, (ii) the Markov chain approach, and (iii) the exact or integral equation approach. The emphasis falls on the Markov chain approach to calculate the run-length distribution and the characteristics of the run-length distribution, since it is the approach used in this dissertation to calculate the run-length distribution of the sign and precedence charts.

Chapter 2

Methods to calculate the run-length distribution

2.0 Chapter 2 overview and objective

There are three methods to calculate (or at least approximate) a control chart's run-length distribution. These methods are: (i) computer simulations or Monte Carlo simulations, (ii) the Markov chain approach, and (iii) the exact or integral equation approach. The objective in Chapter 2 is to provide a discussion on the Markov chain approach, as this is the approach used in this dissertation to calculate the run-length distribution of the sign and precedence charts. For completeness, a brief discussion is given on the Monte Carlo simulation and the exact approach.

After reading this chapter the reader should be familiar with:

- The three different approaches that can be used to calculate the run-length distribution and some of the characteristics of the run-length distribution, and
- The formulas, when using the Markov chain approach to calculate the run-length distribution and some of the characteristics of the run-length distribution.

Example 2.1

This example is provided to aid in illustrating the key concepts of the Markov chain approach. Throughout Chapter 2 references are made to Example 2.1.

The weights of 1kg (1000g) packets of sweets are monitored for quality purposes. Suppose that the standard deviation of the weight of a packet of sweets is 20g and that the distribution of the weight of a packet of sweets is Normally distributed. A Shewhart-type chart is used to monitor the process where the UCL and LCL are three standard deviation units above and below the center line respectively i.e. $UCL = \mu_0 + 3 \times \sigma_0 = 1000 + 3 \times 20 = 1060g$ and the $LCL = \mu_0 - 3 \times \sigma_0 = 1000 - 3 \times 20 = 940g$. Note that individual units (packets of sweets) are monitored and not rational subgroups.

From the information above the following probabilities can be calculated:

$$\begin{aligned}
 p^+ &= P(T_i \geq UCL) \\
 &= P(T_i \geq 1060g) \\
 &= P\left(\frac{T_i - 1000g}{20g} \geq \frac{1060g - 1000g}{20g}\right) \\
 &= P(z \geq 3) \\
 &= 0.001349898
 \end{aligned}$$

$$\begin{aligned}
 p^- &= P(T_i \leq LCL) \\
 &= P(T_i \leq 940g) \\
 &= P\left(\frac{T_i - 1000g}{20g} \leq \frac{940g - 1000g}{20g}\right) \\
 &= P(z \leq -3) \\
 &= 0.001349898
 \end{aligned}$$

$$\begin{aligned}
 p^+ + p^- &= P(T_i \geq UCL) + P(T_i \leq LCL) \\
 &= 0.001349898 + 0.001349898 \\
 &= 0.002699796
 \end{aligned}$$

$$\begin{aligned}
 1 - (p^+ + p^-) &= P(LCL \leq T_i \leq UCL) \\
 &= 1 - (P(T_i \geq UCL) + P(T_i \leq LCL)) \\
 &= 1 - 0.002699796 \\
 &= 0.997300204
 \end{aligned}$$

$$FAR = p^+ + p^- = 0.00266796$$

The run-length of this (traditional) Shewhart-type control chart has a Geometric distribution (see Montgomery (2005), p.218) with parameter equal to the probability of a point plotting OOC i.e.

$$p^+ + p^- = 0.00266796.$$

Therefore:

$$f_N(n) = P(N = n) = (p^+ + p^-) \left(1 - (p^+ + p^-)\right)^{n-1} = 0.002699796 \times (0.997300204)^{n-1}$$

$$ARL = \frac{1}{FAR} = \frac{1}{p^+ + p^-} = \frac{1}{0.00266796} = 370.3983473$$

$$VRL = \frac{1 - (p^+ + p^-)}{(p^+ + p^-)^2} = \frac{1 - 0.00266796}{0.00266796^2} = 136824.5438$$

$$SDRL = \sqrt{\frac{1 - (p^+ + p^-)}{(p^+ + p^-)^2}} = \sqrt{\frac{1 - 0.00266796}{0.00266796^2}} = 369.8980181$$

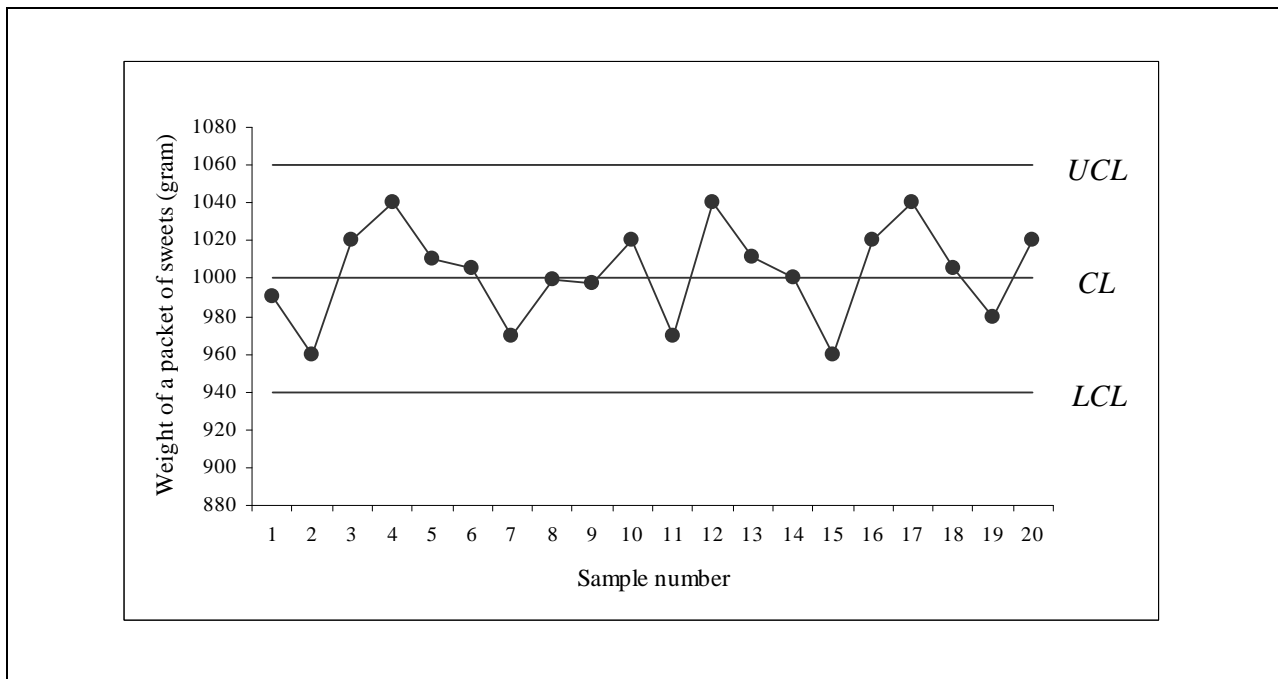


Figure 2.1: Graphical illustration of the chart that monitors the weights of the packets of sweets.

In the following section (Section 2.1) the Markov chain technique that is used to calculate the run-length distribution and the characteristics of the run-length distribution is introduced and discussed. Section 2.1 is concluded by calculating the run-length distribution and the characteristics of the run-length distribution of Example 2.1, using the Markov chain approach. This illustrates, firstly how to apply the Markov chain approach in a practical example, and secondly to illustrate that the results are consistent with what was calculated here.

2.1 The Markov chain approach

2.1.1 Introduction

A simple and unified method, which is based on a finite Markov chain, can be used to calculate the run-length distribution and the characteristics of the run-length distribution of various types of control charts; hence these include the Shewhart-type chart (see e.g. Human et al. (2009), Klein(2000), Antzoulakos and Rakitzis (2008), Khoo (2003) and Koo and Ariffin (2006)), the EWMA-type chart (see e.g. Borror et al. (1998), Borror et al. (1999), Saccucci and Lucas (1990) and Graham et al. (2009)) and the CUSUM-type chart (see e.g. Brook and Evans (1972), Woodall (1984) and Crosier (1986)). In this chapter definitions, results and theorems are provided that give the necessary background to lay a solid foundation, that ultimately leads to the derivation of the run-length distribution and formulas, that are used to calculate the characteristics of the run-length distribution via the Markov chain approach. The theorems and results are critical to the following chapters, in calculating the run-length distribution and the associated characteristics of the run-length distribution, of the sign and precedence control charts.

Brook and Evans (1972) were of the first to make use of a Markov chain approach to calculate the run-length distribution of a CUSUM control chart. Since then there were numerous applications of the Markov chain approach in analyzing the run-length distribution of other control charts (see e.g. Borror et al. (1999), Koo and Ariffin (2006) and Human et al. (2009)). The manner in which the Markov chain approach is used in this dissertation to calculate the run-length distribution differs from the way the Markov chain approach was used by Brook and Evens (1972). This is due to the advances in the area of distribution theory of runs and patterns, its application and the dissemination of the results by especially Fu and Lou (2003) and Fu, Spiring and Xie (2002); their research is mainly used here, since it fits neatly into the spectrum of this dissertation.

2.1.2 Definitions

First, the focus falls on some basic definitions to assist in deriving the run-length distribution and characteristics of the run-length distribution in the following sections; these definitions are given in a Markov chain context.

Definition 2.1

A **stochastic process** is a collection of random variables $\{Y_t : t \in T\}$.

All possible values that can be attained by $\{Y_t, t \in T\}$, are called the **states** of the stochastic process and the set of all possible states is called the **state space**, denoted by Ω . The set of all indexing parameters T is called the **parameter space**. If the parameter t is time, the value of $\{Y_t\}$ is called the state the process is in at time t (Ross (1997), p.77).

Definition 2.2

The sequence $\{Y_t\}$ is called a **Markov chain** if, for any sequence

$$\{Y_0 = \omega_0, Y_1 = \omega_1, \dots, Y_{t-1} = \omega_{t-1}, Y_t = \omega_t\}, \quad t = 1, 2, 3, \dots,$$

it follows that

$$P(Y_t = \omega_t | Y_{t-1} = \omega_{t-1}, \dots, Y_0 = \omega_0) = P(Y_t = \omega_t | Y_{t-1} = \omega_{t-1})$$

where $\{\omega_0, \omega_1, \omega_2, \dots, \omega_t\} \in \Omega$

Thus, the sequence $\{Y_t\}$ is a Markov chain if the probability that the system enters the state ω_t at time t , depends only on the immediately preceding state ω_{t-1} at time $t-1$ (Fu and Lou (2003), p.5).

In a SPC context the sequence $\{Y_t\}$ is a Markov chain if the probability that the process enters the state ω_t at time t , depends only on where the process was at time $t-1$.

For the purposes in this dissertation, only finite Markov chains are considered, i.e. the Markov chain $\{Y_t\}$ has a finite state space Ω , since it is shown later in this chapter and in the next chapter that the control chart is divided into a finite number of “zones” (the control limits divide the chart into the zones). The zones and combinations of multiple zones are associated with the states of the Markov

chain. Let Ω be a finite state space with m states ($m < \infty$), and let $\{Y_t\} = \{Y_0, Y_1, Y_2, \dots\}$ be a sequence of random variables defined on Ω , i.e. the stochastic process $\{Y_t\}$ is a finite Markov chain (Fu and Lou (2003), p.5).

One of the challenges in calculating the run-length distribution is to create or define the state space Ω for the Markov chain $\{Y_t\}$ (with finite state space). In the following chapter, illustrations are provided on how to create or choose the state spaces of the Markov chains for the charts considered.

Definition 2.3

At each step (i.e. point in time) the process $\{Y_t, t = 1, 2, 3, \dots\}$ may remain in the current state or move to another state according to some probability distribution. The state changes are called **transitions** and the probabilities associated with these transitions are called **transition probabilities** and denoted by:

$$P(Y_t = \omega_j | Y_{t-1} = \omega_i) = p_{i,j}(t), \text{ where } \omega_j, \omega_i \in \Omega$$

at time t . The **transition probabilities** $p_{i,j}(t), 1 \leq i, j \leq m$, may be represented as an $m \times m$ matrix

$$\mathbf{M}_t = [p_{i,j}(t)] = \begin{bmatrix} p_{1,1}(t) & p_{1,2}(t) & \dots & p_{1,m}(t) \\ p_{2,1}(t) & \dots & \dots & \dots \\ \dots & \dots & \dots & \dots \\ p_{m,1}(t) & p_{m,2}(t) & \dots & p_{m,m}(t) \end{bmatrix}_{m \times m}$$

$\mathbf{M}_t, t = 1, 2, 3, \dots$, are the **one-step transition probability matrices**. Note that this transition probability matrix depends on time; this implies that $p_{i,j}(t)$ is not necessarily equal to $p_{i,j}(w)$ for $t \neq w$. However, if $p_{i,j}(t) = p_{i,j}(w)$ for all $t \neq w$ then a major simplification occurs; this is looked at next (Fu and Lou (2003), p.5).

Definition 2.4

A Markov chain $\{Y_0, Y_1, Y_2, \dots\}$ is **homogeneous** if the transition probabilities are constant over time (i.e. independent of time), i.e. $P(Y_t = \omega_j | Y_{t-1} = \omega_i) = p_{i,j}$ for any $\omega_i, \omega_j \in \Omega$, and all $t = 1, 2, 3, \dots$, where the transition probabilities $p_{i,j}$ are independent of the time index t (Fu and Lou (2003), p.6).

Definition 2.5

State $\omega_i \in \Omega$ of a Markov chain is called an **absorbing state** if, once the system enters state ω_i , it can never leave state ω_i ; i.e. $p_{\omega_i, \omega_i} \equiv 1$ and $p_{\omega_i, \omega_j} \equiv 0$ for any $i \neq j$ (Fu and Lou (2003), p.18).

Definition 2.6

State $\omega_j \in \Omega$ of a Markov chain is called a **transient state** if, given the process is in state ω_j , there is a positive probability that the process will never return to state ω_j (Fu and Lou (2003), p.18).

Interpreting absorbing and transient states on the control chart

The Markov chain's transitions between the transient state(s) are associated with the plotting statistic moving in a stochastic manner on the control chart without causing the chart to signal; this indicates that the process is IC and the state(s) associated with the process being IC are the transient state(s). There is a positive probability of the plotting statistic plotting OOC at any point in time, with the result that the chart signals. This is equivalent to the stochastic process $\{Y_t\}$ moving to an absorbing state (the process can then not move back to any of the transient states).

Remark 2.1

Zones are created on a chart as illustrated in Figure 2.2 (for the two-sided *1-of-1* chart). Note that zones are simply used as an indicator variable, in other words to indicate in which area/zone the plotting statistic T_i plotted on the control chart. The states of the Markov chain $\{Y_t\}$ consist of the zones and can also consist of a combination of multiple zones, for instance a two-sided *2-of-2* chart has the absorbing state $\{88\}$ i.e. the absorbing state consists of a combination of zones. Zones are simply tools to aid in applying the Markov chain approach that is used to calculate the run-length distribution and the characteristics of the run-length distribution.

To better understand the previous discussion, Example 2.1 is revisited. The control chart in Figure 2.1 can be divided into 3 zones, as illustrated in Figure 2.2. The zone numbers may seem illogical; for clarity on the choice of zones numbers refer to Chapter 3.

Let $Z_i, i=1,2,3,\dots$ be a sequence of random variables that keeps track of the classification of the plotting statistics T_i 's, $i=1,2,3,\dots$ in the different zones on the chart.

Table 2.1: Defining the $Z_i, i=1,2,3,\dots$ random variables for the *1-of-1* Shewhart chart.

The Z_i 's are defined as follows:
$Z_i = 8$ if $T_i \geq UCL$
$Z_i = 9$ if $T_i \leq LCL$
$Z_i = 3$ if $LCL < T_i < UCL$

Table 2.2: Defining the probabilities for the *1-of-1* Shewhart chart.

The probabilities that the plotting statistics T_i 's, $i = 1,2,3,\dots$ plot inside the zones are denoted by:
$p_8 = P(Z_i = 8) = P(T_i \geq UCL) = p^+$
$p_9 = P(Z_i = 9) = P(T_i \leq LCL) = p^-$
$p_3 = P(Z_i = 3) = P(LCL < T_i < UCL) = 1 - (p^+ + p^-)$

The Markov chain $\{Y_t\}$ has the following three states namely state 8, state 3 and state 9.

If the plotting statistic moves (plots) in a stochastic manner between the UCL and LCL , it is equivalent to transitions of the Markov chain between state 3 and state 3 (since there is only a single transient state).

When the plotting statistic plots above (below) the UCL (LCL) the control chart signals which is equivalent to the Markov chain entering state 8 (9) which is an absorbing state.

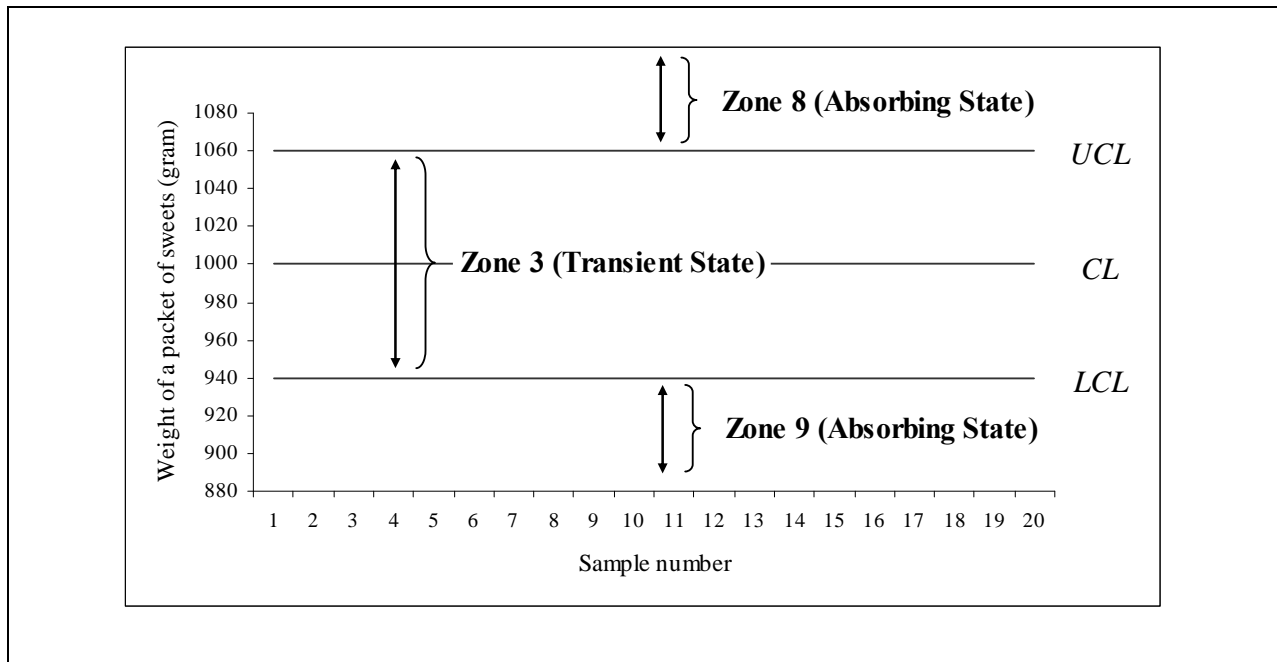


Figure 2.2: Illustration of the “zones” on the control chart.

2.1.3 The run-length distribution

The run-length is the number of points (plotting statistics) that plot on the chart until the chart signals (Montgomery (2005), p.160). In SPC one of the main goals is to calculate the run-length distribution, since the run-length distribution and its characteristics (such as the average run-length (*ARL*), standard deviation of the run-length (*SDRL*), median (*MDRL*) etc.) provide important information regarding the performance of the chart (see e.g. Human and Graham (2007)). In the Markov chain setting the run-length is the number of transitions until the Markov chain enters an absorbing state for the first time, i.e. the chart signals (which would typically occur/happen when the first plotting statistic plots on or outside the control limits).

The Markov chain technique is used to calculate the run-length distribution, or, the distribution of the waiting time until a certain pattern or sequence of plotting statistics T_i , $i = 1, 2, 3, \dots$ (on the control chart) occur. The pattern in the T_i 's, $i = 1, 2, 3, \dots$ could be the first occurrence of a single plotting statistic plotting on or outside a control limit, or it could be the first occurrence where the last two plotting statistics plot on or outside the control limits etc. Each plotting statistic T_i can be classified into a zone, where a zone is defined as an area on the control chart divided by horizontal lines (control limits). A new sequence of random variables Z_1, Z_2, Z_3, \dots is created that keeps track of the

classification of the T_i 's in the different zones on the control chart. The Z_i 's are then used to aid in applying the Markov chain approach to calculate the run-length distribution.

An approach is followed to properly imbed (fit together or fit inside) the run-length random variable $\{N\}$ into a finite Markov chain $\{Y_j\}$, so that the probability of $\Lambda = \{Z_i, Z_{i+1}, \dots, Z_{i+d}\}$ (where d is the sequence or pattern length of interest or number of plotting statistics that is kept track of), can be expressed in terms of the probability that the Markov chain outcome $\{Y_j\}$ resides in a subset Λ of the state space Ω , i.e. $P(\{Z_i, Z_{i+1}, \dots, Z_{i+d}\} = \Lambda) = P(Y_j \in \Omega_\Lambda)$ (where $i + d = j$). Note that $\Lambda = \Omega_\Lambda$; the notation is used interchangeably where Ω_Λ is used to indicate Λ is an element or subset of elements of the state space Ω , where $P(Y_j \in \Omega_\Lambda)$ can be computed with relative ease using the Markov chain transition probability matrices (Fu and Lou (2003), p.2). The run-length distribution is of interest, i.e. the waiting time of the event $\Lambda = \{Z_i, Z_{i+1}, \dots, Z_{i+d}\}$ or $\{Y_j \in \Omega_\Lambda\}$, where Ω_Λ in this case would be an absorbing state. Note that in more general terms Λ may be a collection of patterns or sequences, i.e. $\Lambda = \Lambda_1 \cup \Lambda_2 \cup \dots \cup \Lambda_w$, where w is the number of patterns or sequences of the plotting statistic that cause the chart to signal. The run-length of the control chart then becomes the waiting time until the first occurrence of one of the patterns $\Lambda_1, \Lambda_2, \dots, \Lambda_w$. Note that $\Lambda_1, \Lambda_2, \dots, \Lambda_w$ are the absorbing states of the Markov chain $\{Y_j\}$. Using the Markov chain approach, the representation of the run-length distribution, or the waiting time distribution of the event $\{Z_j, Z_{j+1}, \dots, Z_{j+d}\} \in \Lambda$, or $\{Y_j \in \Omega_\Lambda\}$ is compact, easy to compute, and amenable to further analysis (Fu and Lou (2003), p.3). The method is largely dependent on being able to construct a proper Markov chain associated with the random variables Z_i 's. Once the Markov chain is constructed, the linearity of the Markov chain reduces the computational complexity of the run-length distribution and its properties, often associated with combinatorial and generating-function techniques for computing the exact run-length distribution of the control chart (Fu and Lou (2003), p.3). For this reason the application of the Markov chain approach in SPC to calculate the run-length distribution and its characteristics, are utilized in this dissertation.

Remark 2.2

To be noted is that there is a difference between the run-length in an SPC environment and in the Markov chain setting. The states of the Markov chain are associated with plotting statistics, or sequences of plotting statistics plotting in associated zones on the control chart. The run-length in a Markov chain setting are the number of transitions between the states until an absorbing state is entered into for the first time, and not the number of times that states are visited until an absorbing state is entered into for the first time. More discussions will follow regarding this point in Chapter 3 Section 3.3.

2.1.4 Transition probability matrix of a finite Markov chain

Let $\Lambda = \{\omega_1, \omega_2, \dots, \omega_{m-h}\}$ be the subset of Ω containing all absorbing states of a Markov chain $\{Y_t\}$ with transition probability matrix denoted by \mathbf{M} . A dummy state “ ϕ ” is added in the state space Ω . The initial distribution of the Markov chain $\{Y_t\}$ is: $P(Y_0 = \phi) = 1$. The reason for the inclusion of the dummy state “ ϕ ” in the state space Ω , is so that the process starts IC with certainty and that the difference between the run-length in an SPC and Markov chain setting is overcome; more detail can be found in Chapter 3 Section 3.3. The transition probability matrix \mathbf{M} can always be written in the following form:

$$\mathbf{M}_{m \times m} = \left[\begin{array}{c|c} \mathbf{Q}_{h \times h} & \mathbf{C}_{h \times (m-h)} \\ \hline \mathbf{0}_{(m-h) \times h} & \mathbf{I}_{(m-h) \times (m-h)} \end{array} \right] \quad (2.1)$$

where m and $(m-h)$ are the number of states in Ω and Λ respectively, i.e. the Markov chain $\{Y_j\}$ has a total of m states in its state space Ω , where $(m-h)$ of the states are absorbing states; h is the number of transient states and one of the transient states is the dummy state “ ϕ ” (Fu and Lou (2003), p.18). The matrix \mathbf{Q} is referred to as the essential transition probability submatrix of the Markov chain (Fu and Lou (2003), p.18). Let ξ be the initial distribution, where $\xi_{1 \times h} = (1, 0, 0, \dots, 0)$ i.e. the process always start in the dummy state “ ϕ ” with probability one. Note that it must always be true that

$$\sum_{i=1}^h \xi_i = 1, \text{ which is the case here.}$$

2.1.5 Results

In this section the results are provided that are used to derive the run-length distribution and the associated characteristics of the run-length distribution; the proofs of the results are provided in Appendix 2.

Assume that the states of the Markov chain can be ordered, i.e.

$$\Omega = \{\omega_1 < \omega_2 < \omega_3 < \dots < \omega_h < \omega_{h+1} < \dots < \omega_m\},$$

where $\omega_1 = \phi$ is the dummy state, $\{\omega_1, \omega_2, \dots, \omega_h\}$ are the transient states and $\{\omega_{h+1}, \omega_{h+2}, \dots, \omega_m\}$ are the absorbing states respectively. Then some general results are as follows:

Result 2.1

If the transition probability matrix \mathbf{M} has the form given in equation (2.1) and $(\mathbf{I} - \mathbf{Q})^{-1}$ exists, then:

$$\text{i) } \mathbf{M}^j = \begin{bmatrix} \mathbf{Q}^j & \mathbf{W}_j \mathbf{C} \\ \mathbf{0} & \mathbf{I} \end{bmatrix}, \quad \forall j = 1, 2, 3, \dots \quad (2.2)$$

$$\text{where } \mathbf{W}_j = \mathbf{I} + \mathbf{Q} + \mathbf{Q}^2 + \mathbf{Q}^3 + \dots + \mathbf{Q}^{j-1}$$

$$\text{ii) } \lim_{j \rightarrow \infty} \mathbf{W}_j = (\mathbf{I} - \mathbf{Q})^{-1} \quad (2.3)$$

(Fu et al. (2002))

The proofs of Result 2.1(i) and Result 2.1 (ii) are given in Appendix 2 as Proof 2.1 and Proof 2.2 respectively.

Result 2.2

Given that the Markov chain $\{Y_j\}$ starts in the dummy state “ ϕ ”, i.e. $\{Y_0 = \phi\}$, and the transition probability matrix is of the form given in equation (2.2), then:

$$\begin{aligned} P(Y_j < \omega_{h+1} | Y_0 = \phi) &= P(N > j | Y_0 = \phi) \\ &= \xi \mathbf{Q}^j \mathbf{1}, \quad \forall j = 1, 2, 3, \dots \\ \therefore P(Y_j < \omega_{h+1} | Y_0 = \phi) &= \xi \mathbf{Q}^j \mathbf{1}, \quad \forall j = 1, 2, 3, \dots \end{aligned} \quad (2.4)$$

where $\mathbf{1}_{h \times 1} = (1, 1, 1, \dots, 1)^T$ and $\xi_{1 \times h} = (1, 0, 0, \dots, 0)$

Note that since h and m are the number of transient and absorbing states respectively, it follows from the definitions of $\{Y_j\}$ and $\{N\}$ that

$$\{Y_j < \omega_{h+1}\} \Leftrightarrow \{N > j\}$$

(Fu et al. (2002))

In order to interpret $\{Y_j < \omega_{h+1}\} \Leftrightarrow \{N > j\}$, recall that $\{Y_j\}$ and $\{N\}$ are the Markov chain and run-length random variable, respectively. It simply means that the run-length is greater than j (i.e. the chart has not yet signalled at time j) if and only if the Markov chain at time j has not yet entered an absorbing state.

The proof of Result 2.2 is given in Appendix 2 as Proof 2.3.

2.1.6 Theorems

The run-length distribution and some of its characteristics are presented in this section. This includes the moment generating function, and the factorial moment generating function (or the probability generating function), which are both used to derive some characteristics of the run-length distribution. Only the results are presented in this section, the proofs are provided in Appendix 2.

Theorem 2.1

Let $\{Y_j\}$ be the finite Markov chain with state space Ω and transition probability matrix given in equation (2.1), initial distribution given by $\xi_{1 \times h} = (1, 0, 0, \dots, 0)$ and where $\mathbf{1}_{h \times 1} = (1, 1, 1, \dots, 1)^T$ is the unit vector, then:

$$\text{i) } P(N = j | Y_0 = \phi) = \xi \mathbf{Q}^{j-1} (\mathbf{I} - \mathbf{Q}) \mathbf{1}, \text{ for } j=1, 2, 3, \dots, \text{ with } \mathbf{Q}^0 = \mathbf{I} \quad (2.5)$$

ii) The moment generating function is given by:

$$M_N(t) = 1 + (e^t - 1) \xi (\mathbf{I} - e^t \mathbf{Q})^{-1} \mathbf{1} \quad (2.6)$$

$$\text{iii) } E(N) = \xi (\mathbf{I} - \mathbf{Q})^{-1} \mathbf{1} \quad (2.7)$$

$$E(N^2) = \xi (\mathbf{I} + \mathbf{Q}) (\mathbf{I} - \mathbf{Q})^{-2} \mathbf{1} \quad (2.8)$$

$$\text{var}(N) = \xi (\mathbf{I} + \mathbf{Q}) (\mathbf{I} - \mathbf{Q})^{-2} \mathbf{1} - (\xi (\mathbf{I} - \mathbf{Q})^{-1} \mathbf{1})^2 \quad (2.9)$$

$$\text{Stdv}(N) = \sqrt{\xi (\mathbf{I} + \mathbf{Q}) (\mathbf{I} - \mathbf{Q})^{-2} \mathbf{1} - (\xi (\mathbf{I} - \mathbf{Q})^{-1} \mathbf{1})^2} \quad (2.10)$$

(Fu et al. (2002))

The proofs of Theorem 2.1(i), (ii) and (iii) are given in Appendix 2 as Proofs 2.4, 2.5 and 2.6 respectively.

Theorem 2.2

Let $\{Y_j\}$ be the finite Markov chain, having state space Ω and transition probability matrix given in equation (2.1), initial distribution $\xi_{1 \times h} = (1, 0, 0, \dots, 0)$ and where $\mathbf{1}_{h \times 1} = (1, 1, 1, \dots, 1)^T$ is the unit vector. The same results as found in Theorem 2.1 can be obtained by considering the probability generating function or the factorial moment generating function:

- i) The probability generating function is given by:

$$G_N(t) = (t-1)\xi(\mathbf{I} - t\mathbf{Q})^{-1}\mathbf{1} + 1 \quad (2.11)$$

ii) $E(N) = \xi(\mathbf{I} - \mathbf{Q})^{-1}\mathbf{1} \quad (2.12)$

$$E(N^2) = \xi(\mathbf{I} + \mathbf{Q})(\mathbf{I} - \mathbf{Q})^{-2}\mathbf{1} \quad (2.13)$$

$$\text{var}(N) = \xi(\mathbf{I} + \mathbf{Q})(\mathbf{I} - \mathbf{Q})^{-2}\mathbf{1} - (\xi(\mathbf{I} - \mathbf{Q})^{-1}\mathbf{1})^2 \quad (2.14)$$

$$\text{stdv}(N) = \sqrt{\xi(\mathbf{I} + \mathbf{Q})(\mathbf{I} - \mathbf{Q})^{-2}\mathbf{1} - (\xi(\mathbf{I} - \mathbf{Q})^{-1}\mathbf{1})^2} \quad (2.15)$$

(Fu and Lou (2003), p.73)

The proofs of Theorem 2.2 (i) and (ii) are given in Appendix 2 as Proofs 2.7 and 2.8 respectively.

Theorem 2.3

The cumulative distribution function of the run-length distribution is given by:

$$\begin{aligned} \text{i)} \quad P(N \leq j | Y_0 = \phi) &= \sum_{i=1}^j P(N = i | Y_0 = \phi) \\ &= \sum_{i=1}^j \xi \mathbf{Q}^{i-1} (\mathbf{I} - \mathbf{Q}) \mathbf{1}, \quad \text{for } j=1,2,3,\dots, \text{ with } \mathbf{Q}^0 = \mathbf{I} \end{aligned} \quad (2.16)$$

$$\text{ii)} \quad P(N \leq j | Y_0 = \phi) = 1 - \xi \mathbf{Q}^j \mathbf{1}, \quad j = 1,2,3,\dots \quad (2.17)$$

iii) From the definition of a percentile it follows that the $100\pi^{\text{th}}$ percentile of the run-length distribution is the smallest integer j so that:

$$P(N \leq j | Y_0 = \phi) \geq \pi \quad (2.18)$$

Stated differently, the $100\pi^{\text{th}}$ percentile of the run-length distribution is the integer j so that:

$$\inf \left\{ j : \sum_{i=1}^j \xi \mathbf{Q}^{i-1} (\mathbf{I} - \mathbf{Q}) \mathbf{1} \geq \pi \right\} \quad (2.19)$$

or

$$\inf \left\{ j : 1 - \xi \mathbf{Q}^j \mathbf{1} \geq \pi \right\} \quad (2.20)$$

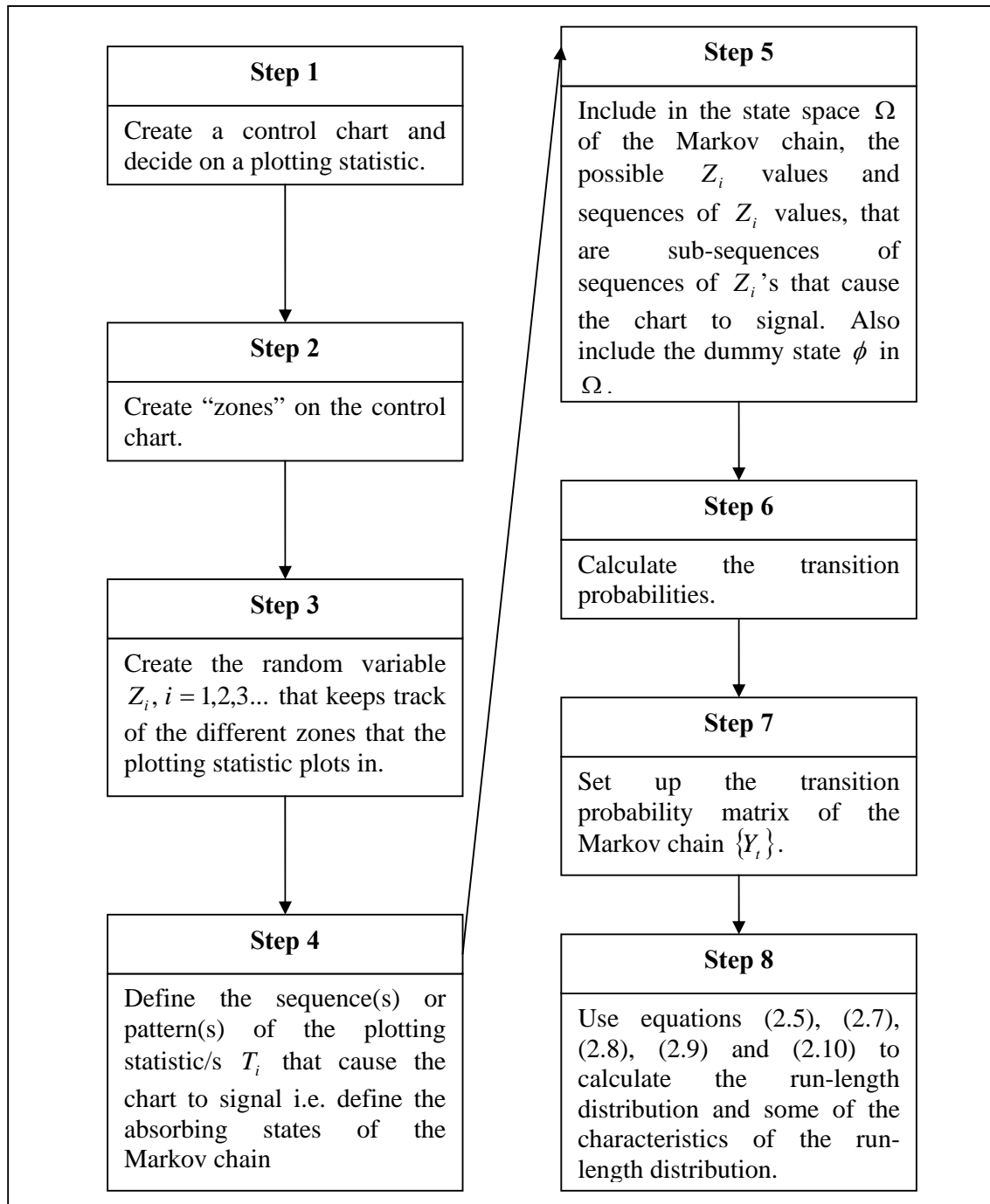
The proof of Theorem 2.3 (ii) is given in Appendix 2 as Proof 2.9.

The necessary results and formulas are now established which is used in Chapters 4 and 5 to calculate the run length distribution and some of the characteristics of the run-length distribution of the sign and precedence charts.

2.1.7 Summary of the Markov chain approach

A brief summary is presented to recapitulate and illustrate the Markov chain approach to calculate the run-length distribution and some of the characteristics of the run-length distribution.

Table 2.3: Summary of the Markov chain approach.



Remark 2.2

The steps illustrated in Table 2.3 present clear stepwise instructions to apply the Markov chain approach. However, note that the run-length random variable $\{N\}$ is imbedded (fit together or fit inside) into a finite Markov chain $\{Y_j\}$, so that the run-length distribution and the characteristics of the run-length distribution can be calculated.

To illustrate the application of Table 2.3 Example 2.1 is revisited.

Step 1: The control chart is created and illustrated in Figure 2.1; the plotting statistic that is decided on is the individual measurements of the weights (gram) of the packets of sweets.

Step 2: Zones 1, 2 and 3 are created as illustrated in Figure 2.2.

Step 3: The random variable $Z_i, i = 1, 2, 3, \dots$ is created in Table 2.1.

Step 4: The chart signal following either one of the following two patterns of plotting statistics: $\{Z_i = 8, i = 1, 2, 3, \dots\}$ or $\{Z_i = 9, i = 1, 2, 3, \dots\}$.

Step 5: The state space of the Markov chain Y_i is $\Omega = \{\phi, 3, 8, 9\}$ (in this case the absorbing states have no sub-sequences).

Step 6: The transition probabilities are calculated at the start of Example 2.1, given as follows:

$$p_8 = p^+ = P(T_i \geq UCL) = 0.001349898$$

$$p_9 = p^- = P(T_i \leq UCL) = 0.001349898$$

$$p_3 = P(LCL < T_i < UCL) = 1 - p^+ - p^- = 0.997300204$$

Step 7: The transition matrix of the Markov chain Y_t is as follows:

$$\begin{aligned}
 \mathbf{M}_{4 \times 4} &= \left[\begin{array}{c|c} \mathbf{Q}_{2 \times 2} & \mathbf{C}_{2 \times 2} \\ \hline \mathbf{0}_{2 \times 2} & \mathbf{I}_{2 \times 2} \end{array} \right] = \left[\begin{array}{cc|cc} p_{\phi,\phi} & p_{\phi,3} & p_{\phi,8} & p_{\phi,9} \\ p_{3,\phi} & p_{3,3} & p_{3,8} & p_{3,9} \\ \hline p_{8,\phi} & p_{8,3} & p_{8,8} & p_{8,9} \\ p_{9,\phi} & p_{9,3} & p_{9,8} & p_{9,9} \end{array} \right] = \left[\begin{array}{cc|cc} 0 & p_3 & p_8 & p_9 \\ 0 & p_3 & p_8 & p_9 \\ \hline 0 & 0 & 1 & 0 \\ 0 & 0 & 0 & 1 \end{array} \right] \\
 &= \left[\begin{array}{cc|cc} 0 & 0.997300204 & 0.001349898 & 0.001349898 \\ 0 & 0.997300204 & 0.001349898 & 0.001349898 \\ \hline 0 & 0 & 1 & 0 \\ 0 & 0 & 0 & 1 \end{array} \right] \\
 \therefore \mathbf{Q}_{2 \times 2} &= \begin{bmatrix} 0 & p_3 \\ 0 & p_3 \end{bmatrix} \\
 &= \begin{bmatrix} 0 & 0.997300204 \\ 0 & 0.997300204 \end{bmatrix}
 \end{aligned}$$

Step 8: Using equations 2.5, 2.7, 2.8, 2.9 and 2.10 where $\xi_{1 \times 2} = (1,0)$, $\mathbf{1}_{h \times 1} = (1,1)^T$ and

$\mathbf{I} = \begin{bmatrix} 1 & 0 \\ 0 & 1 \end{bmatrix}$ the following is obtained:

$$\begin{aligned}
 P(N = j | Y_0 = \phi) &= \xi \mathbf{Q}^{j-1} (\mathbf{I} - \mathbf{Q}) \mathbf{1} \\
 &= (1,0) \begin{bmatrix} 0 & p_3 \\ 0 & p_3 \end{bmatrix}^{j-1} \left(\begin{bmatrix} 1 & 0 \\ 0 & 1 \end{bmatrix} - \begin{bmatrix} 0 & p_3 \\ 0 & p_3 \end{bmatrix} \right) \begin{pmatrix} 1 \\ 1 \end{pmatrix} \\
 &= (1,0) \begin{bmatrix} 0 & 0.997300204 \\ 0 & 0.997300204 \end{bmatrix}^{j-1} \left(\begin{bmatrix} 1 & 0 \\ 0 & 1 \end{bmatrix} - \begin{bmatrix} 0 & 0.997300204 \\ 0 & 0.997300204 \end{bmatrix} \right) \begin{pmatrix} 1 \\ 1 \end{pmatrix}
 \end{aligned}$$

$$\begin{aligned}
 E(N) &= ARL = \xi (\mathbf{I} - \mathbf{Q})^{-1} \mathbf{1} \\
 &= (1 \ 0) \left(\begin{pmatrix} 1 & 0 \\ 0 & 1 \end{pmatrix} - \begin{pmatrix} 0 & p_3 \\ 0 & p_3 \end{pmatrix} \right)^{-1} \begin{pmatrix} 1 \\ 1 \end{pmatrix} \\
 &= \frac{1}{1 - p_3} \\
 &= \frac{1}{p^+ + p^-} \\
 &= 370.3983560
 \end{aligned}$$

$$\begin{aligned}
 \text{var}(N) &= \xi(\mathbf{I} + \mathbf{Q})(\mathbf{I} - \mathbf{Q})^{-2}\mathbf{1} - (\xi(\mathbf{I} - \mathbf{Q})^{-1}\mathbf{1})^2 \\
 &= (\mathbf{1} \ 0) \left(\begin{pmatrix} 1 & 0 \\ 0 & 1 \end{pmatrix} + \begin{pmatrix} 0 & p_3 \\ 0 & p_3 \end{pmatrix} \right) \left(\begin{pmatrix} 1 & 0 \\ 0 & 1 \end{pmatrix} - \begin{pmatrix} 0 & p_3 \\ 0 & p_3 \end{pmatrix} \right)^{-2} \begin{pmatrix} 1 \\ 1 \end{pmatrix} - \left((\mathbf{1} \ 0) \left(\begin{pmatrix} 1 & 0 \\ 0 & 1 \end{pmatrix} - \begin{pmatrix} 0 & p_3 \\ 0 & p_3 \end{pmatrix} \right)^{-1} \begin{pmatrix} 1 \\ 1 \end{pmatrix} \right)^2 \\
 &= \frac{p_3}{(1 - p_3)^2} \\
 &= \frac{1 - p^+ - p^-}{(p^+ + p^-)^2} \\
 &= 136824.5438
 \end{aligned}$$

$$\begin{aligned}
 \text{stdv}(N) &= \sqrt{\text{var}(N)} \\
 &= \sqrt{136824.5438} \\
 &= 369.8980181
 \end{aligned}$$

From the above, exactly the same results are obtained as at the start of the chapter by making use of the Geometric distribution characteristics.

It may seem that the density functions differ, but when calculating numerical values it is seen that they are in fact the same. Consider the following illustration:

$$f_N(n) = P(N = n) = (p^+ + p^-) \left(1 - (p^+ + p^-) \right)^{n-1} = 0.002699796 \times (0.997300204)^{n-1}$$

$$f_N(200) = P(N = 200) = 0.002699796 \times (0.997300204)^{200-1} = 0.001576473$$

$$\begin{aligned}
 P(N = j | Y_0 = \phi) &= \xi \mathbf{Q}^{j-1} (\mathbf{I} - \mathbf{Q}) \mathbf{1} \\
 &= (\mathbf{1}, 0) \begin{bmatrix} 0 & p_3 \\ 0 & p_3 \end{bmatrix}^{j-1} \left(\begin{bmatrix} 1 & 0 \\ 0 & 1 \end{bmatrix} - \begin{bmatrix} 0 & p_3 \\ 0 & p_3 \end{bmatrix} \right) \begin{pmatrix} 1 \\ 1 \end{pmatrix} \\
 &= (\mathbf{1}, 0) \begin{bmatrix} 0 & 0.997300204 \\ 0 & 0.997300204 \end{bmatrix}^{j-1} \left(\begin{bmatrix} 1 & 0 \\ 0 & 1 \end{bmatrix} - \begin{bmatrix} 0 & 0.997300204 \\ 0 & 0.997300204 \end{bmatrix} \right) \begin{pmatrix} 1 \\ 1 \end{pmatrix}
 \end{aligned}$$

$$\begin{aligned}
 P(N = 200 | Y_0 = \phi) &= \xi \mathbf{Q}^{200-1} (\mathbf{I} - \mathbf{Q}) \mathbf{1} \\
 &= (\mathbf{1}, 0) \begin{bmatrix} 0 & 0.997300204 \\ 0 & 0.997300204 \end{bmatrix}^{199} \left(\begin{bmatrix} 1 & 0 \\ 0 & 1 \end{bmatrix} - \begin{bmatrix} 0 & 0.997300204 \\ 0 & 0.997300204 \end{bmatrix} \right) \begin{pmatrix} 1 \\ 1 \end{pmatrix} \\
 &= 0.001576473
 \end{aligned}$$

2.2 Computer simulations or Monte Carlo simulations

Computer simulations or Monte Carlo simulations are often used to estimate the run length distribution of a control chart. The popularity of this method stems from the fact that no matter how complicated the analytical form of the run-length distribution is, computer simulations can almost always be used with relative ease to estimate the run-length distribution and its associated characteristics fairly accurately, provided the simulation size is big enough. Unfortunately the size of the simulation is very ambiguous; there is no “magical” number of simulations which always results in accurate results. However, the standard error of a run-length characteristic can be bounded by increasing the simulation size sufficiently. The two main drawbacks of this method are: (i) in order to find accurate values of the run-length distribution a large number of simulation iterations must be performed, which can be very time consuming and (ii) this method does not provide the exact (or theoretical) values, but only approximate values.

A stepwise computer simulation procedure to calculate the run-length distribution for a two sided control chart, where the plotting statistic is calculated from a random sample, is given as follows:

- Step 1:** Calculate the control limits. (Prior knowledge is required regarding the process and design parameters in order to calculate the control limits.)
- Step 2:** Create a counting variable namely *count* and set the variable *count* equal to zero ($count = 0$).
- Step 3:** Simulate a random sample from an assumed underlying process distribution, for example from the standard Normal distribution ($N(0,1)$).
- Step 4:** Calculate the plotting statistic from the simulated sample.
- Step 5:** Determine if the control chart has signalled by comparing the plotting statistic(s) to the control limits.
- Step 6:** If a signalling event has not realized, then $count = count + 1$.
- Step 7:** If a signalling event has realized; store the value of the *count* random variable and reset *count* i.e. $count = 0$.
- Step 8:** Repeat steps 1 to 7 many times (number of simulations).
- Step 9:** All the stored *count* values are values from the run-length distribution. From these a frequency distribution can be obtained.
- Step 10:** From these stored run-length values, any unknown statistic or characteristic of the unknown run-length distribution can be calculated and estimated.

By increasing the number of simulations, the accuracy of the estimated run-length distribution and characteristics of the run-length distribution can be improved.

The IC run-length distribution characteristics are found by evaluating the run-length values that were obtained by simulating the random samples from an IC process distribution. Similarly the OOC run-length characteristics are found by evaluating the run-length values that were obtained by simulating the random samples from an OOC process distribution.

Examples of where the run-length distribution or some characteristics of the run-length distribution are found through computer simulations can be found in, e.g., Khoo (2005), Khoo and Ariffin (2006), Graham et al. (2009) and de Vargas et al. (2004).

2.3 Exact approach or Integral equation approach

The exact approach utilizes mathematics and combinatorics to find a closed form expression of the run-length distribution. This approach is sometimes challenging, in that the expression obtained is typically complex or difficult to be evaluated numerically. Often the exact expression of the run-length distribution can be found, but simulations are used instead, since that is easier. Papers where the exact approach was used to calculate the run-length distribution include Jones et al. (2001) (for the EWMA control chart), Jones et al. (2004) (for the CUSUM control chart) and Human et al. (2009) (for the nonparametric Shewhart-type control charts).

2.4 Summary of Chapter 2

The reader should now be familiar with the three different methods that can be used to calculate the run-length distribution and some characteristics of interest of the run-length distribution. In particular the theoretical background and the application of the Markov chain approach to calculate the run-length distribution should be clear.

2.5 Following chapter

The following chapter (Chapter 3) gives a discussion on the runs-rules that are applied to the nonparametric charts in Chapters 4 and 5. The transition probability matrices that are required in the Markov chain formulas are constructed in Chapter 3.

Chapter 3

Runs-rules, improved runs-rules and transition probability matrices

3.0 Chapter 3 overview and objective

The *improved 2-of-2* and the *improved 2-of-3* runs-rules (Shewhart-type) nonparametric charts are considered in this dissertation. These *improved* runs-rules charts are extensions of the original *2-of-2* and *2-of-3* charts (see Human et al. (2009)), which in turn are extensions of the original *1-of-1* charts (see Amin et al. (1995) and Chakraborti et al. (2004)).

The *improved 2-of-2* charts are a combination of the *1-of-1* and *2-of-2* runs-rules based charts, whereas the *improved 2-of-3* charts are a combination of the *1-of-1* and *2-of-3* runs-rules based charts.

The objective in Chapter 3 is to clearly explain and graphically illustrate the signalling rules of the *1-of-1*, the *2-of-2*, the *2-of-3*, the *improved 2-of-2* and the *improved 2-of-3* charts. The transition probability matrices are also constructed for all these charts. Note that, both one-sided and two-sided charts are considered.

After reading this chapter the reader should be familiar with:

- How the control limits divide the control chart decision region into “zones”,
- The signaling rules,
- The transition probability matrices, and
- How to use the general results in Chapter 2 for the charts in this chapter.

3.1 Introduction

When monitoring a process an appropriate plotting statistic is used, for example when monitoring the location, the sample mean (\bar{X}) is typically used as the plotting statistic. The plotting statistics are plotted on the control chart until a particular plotting statistic or a sequence of plotting statistics leads to a signal, then the process is declared to be OOC and a search for an assignable cause is started. Since Shewhart-type control charts use only the last plotting statistic (calculated only from the last sample) in determining the state of the process, i.e. whether the process is IC or OOC, only large shifts in the process are efficiently detected (see Klein (2000)). Sensitizing rules have been proposed to address the lack of sensitivity of the Shewhart-type chart for small process shifts (see e.g. Page (1955), the Western Electric Handbook (1956), Roberts (1958), Bissell (1978) and Wheeler (1983), among others). Sensitizing rules are signalling rules designed to detect some improbable and/or non-random pattern of the plotting statistics on the control chart (Montgomery (2005), p.166).

Runs-rules, which are specific/special signalling rules, are the types of sensitizing rules discussed in this chapter; these rules are used to improve the Shewhart chart's sensitivity in detecting small process shifts. The original Shewhart chart considers only the last plotting statistic (calculated from the last sample) in determining the state of the process; this chart is also known as the *1-of-1* chart. Two of the most popular signalling rules are the *2-of-2* and the *2-of-3* runs-rules suggested by Klein (2000) and the corresponding charts are thus labelled the *2-of-2* and the *2-of-3* charts.

Note that the *k-of-k* ($k \geq 2$) runs-rules chart is the general case. The *k-of-k* runs-rules chart signals when k consecutive charting statistics all plot on or outside the control limit(s). A generalization of the *k-of-k* runs-rules chart is the *k-of-w* ($1 \leq k \leq w$) runs-rules chart which signals when k of the last w charting statistics plot on or outside the control limit(s).

The *2-of-2* and *2-of-3* charts have a drawback, namely the lack of being able to immediately detect a large process shift i.e. the *2-of-2* and the *2-of-3* charts require at least the last two or three plotting statistics to signal, respectively. This dilemma can potentially be costly to the practitioner in the sense that the chart's ability to detect a large shift in the process is delayed; the proposed *improved* runs-rules offer a possible solution in this case.

The control limits of the runs-rules and the *improved* runs-rules charts divide the chart area into so called "zones". Figure 3.1 is a graphical illustration of all the zones that are created when using the runs-rules and the *improved* runs-rules charts.

Note that referring to Figure 3.1, the UCL_B and LCL_B are known as the *outer* control limits or the so called *B* control limits. Similarly UCL_A and LCL_A are known as the *inner* control limits or the so called *A* control limits.

In Figure 3.1 the set of *inner* control limits is labelled UCL_A (or UCL) and LCL_A (or LCL). Note that, when the usual runs-rules charts are used the upper and lower control limits referred to as the UCL and LCL respectively, are used. When the *improved* runs-rules are used the *inner* upper and *inner* lower control limits, referred to as UCL_A and LCL_A , respectively, and UCL_B and LCL_B referred to as the *outer* control limits or the so called *B* control limits, respectively, are all used.

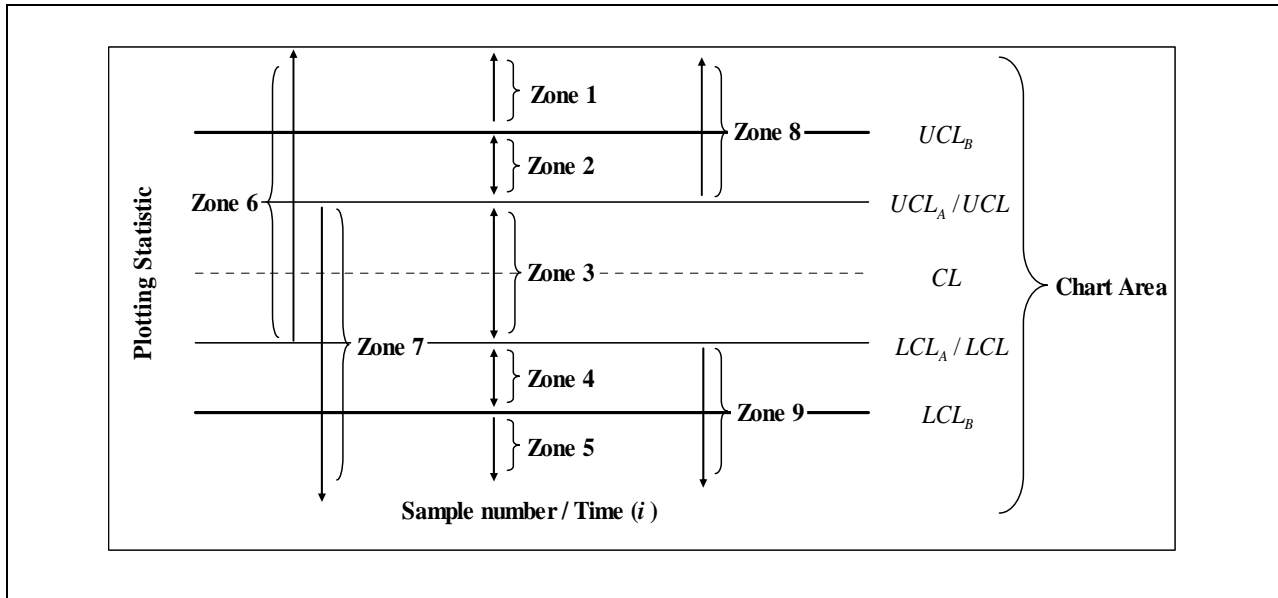


Figure 3.1: Illustration of the different “zones” on the runs-rules and *improved* runs-rules control charts.

Remark 3.1:

Note that throughout this dissertation the *inner* lower control limit of the *improved* runs-rules charts will be denoted by LCL_A and the lower control limit of the runs-rules charts will be denoted by LCL . The LCL_A and LCL are taken to be the same in this dissertation, this is denoted by LCL_A/LCL on the graphical illustrations as is shown in Figure 3.1. The same is implied for the outer upper control limit denoted by UCL_A/UCL .

Note that not all the zones and/or control limits are relevant to a particular control chart. For instance, when considering an upper one-sided *1-of-1* Shewhart-type control chart, the UCL_B , LCL_A/LCL and LCL_B are not applicable (not used), only the UCL_A/UCL are used. Thus only zones 7 and 8 are used (and zones 1, 2, 3, 4, 5, 6 and 9 are not used) as illustrated in panel (a) of Figure 3.2.

In Figure 3.2, panels (a) through (f), the various cases that arise out of Figure 3.1 are shown:

- Panel (a) of Figure 3.2 illustrates how Figure 3.1 reduces for the upper one-sided *1-of-1*, the upper one-sided *2-of-2* and the upper one-sided *2-of-3* charts.
- Panel (c) of Figure 3.2 illustrates how Figure 3.1 reduces for the lower one-sided *1-of-1*, the lower one-sided *2-of-2* and the lower one-sided *2-of-3* charts.
- Panel (e) of Figure 3.2 illustrates how Figure 3.1 reduces for the two-sided *1-of-1*, the two-sided *2-of-2* and the two-sided *2-of-3* charts.
- Panel (b) of Figure 3.2 illustrates how Figure 3.1 reduces for the upper one-sided *improved 2-of-2* and the upper one-sided *improved 2-of-3* charts.
- Panel (d) of Figure 3.2 illustrates how Figure 3.1 reduces for the lower one-sided *improved 2-of-2* and the lower one-sided *improved 2-of-3* charts.
- Panel (f) Figure 3.2 illustrates how Figure 3.1 reduces for the two-sided *improved 2-of-2* and the two-sided *improved 2-of-3* charts.

Note that the panels are not discussed in sequence (a) to (f) since in Figure 3.2 the first row consists of the upper one-sided charts, the second row consists of the lower one-sided charts and the third row consists of two-sided charts. The discussion above is presented by first considering the first column of Figure 3.2 and then the second column of Figure 3.2.

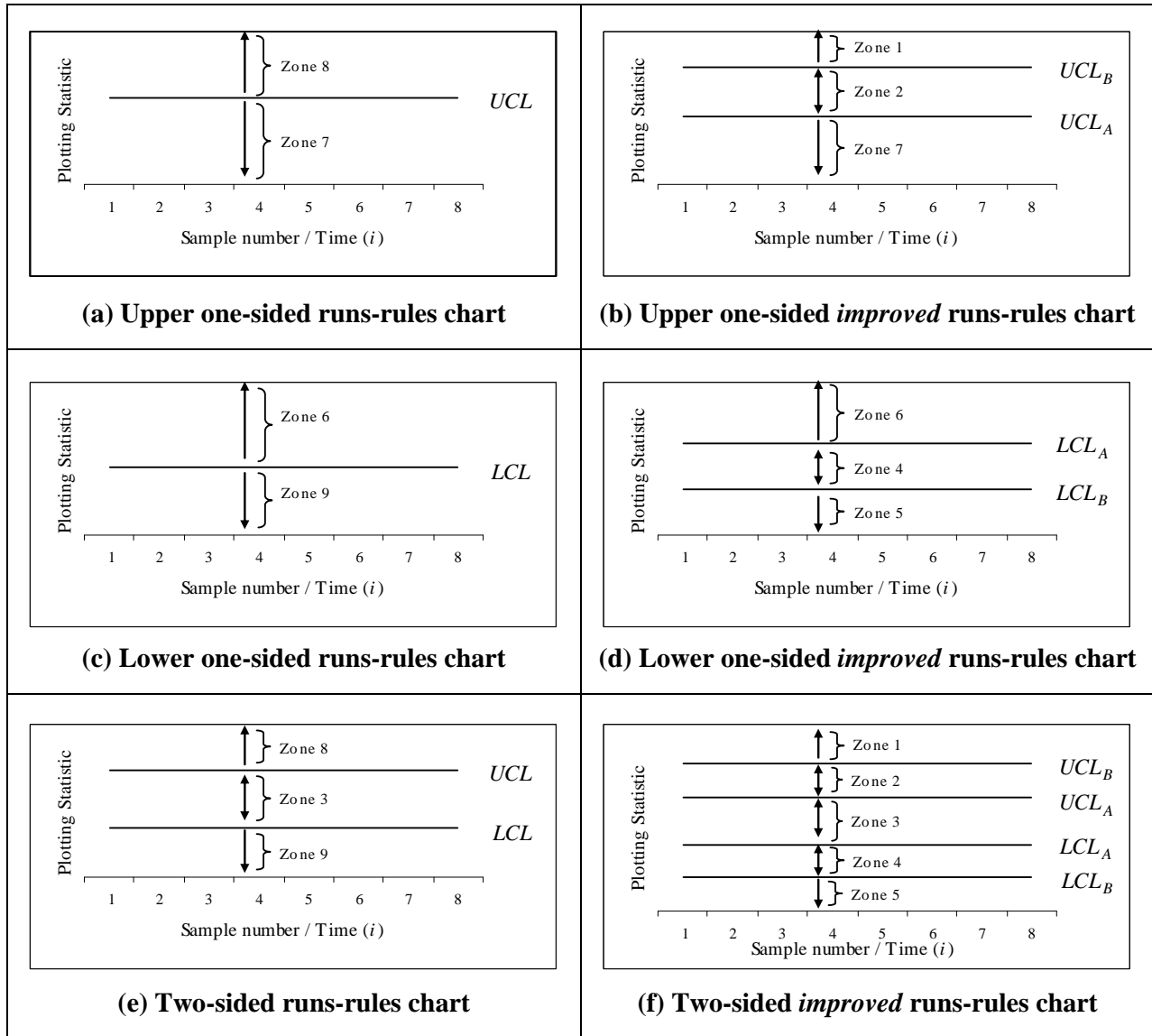


Figure 3.2: Figure 3.1 reduces to these Figures for specific charts.

3.2 Runs-rules and signalling events

Let $Z_i, i = 1, 2, 3, \dots$, be a sequence of random variables that keeps track of the classification of the plotting statistics $T_i, i = 1, 2, 3, \dots$, in the zones on the control chart. Thus, for example, $Z_i = 2$ if the i^{th} plotting statistic lies in zone 2, i.e., it falls between UCL_A and UCL_B . These cases are summarized in Table 3.1.

Table 3.1: Defining the Z_i 's and the corresponding probabilities.

The Z_i 's are defined as follows:	The probabilities that the plotting statistics T_i 's, $i = 1, 2, 3, \dots$, plot inside the zones are denoted by:
$Z_i = 1$ if $UCL_B \leq T_i$	$p_1 = P(Z_i = 1)$
$Z_i = 2$ if $UCL_A \leq T_i < UCL_B$	$p_2 = P(Z_i = 2)$
$Z_i = 3$ if $LCL_A / LCL < T_i < UCL_A / UCL$	$p_3 = P(Z_i = 3)$
$Z_i = 4$ if $LCL_B < T_i \leq LCL_A$	$p_4 = P(Z_i = 4)$
$Z_i = 5$ if $T_i \leq LCL_B$	$p_5 = P(Z_i = 5)$
$Z_i = 6$ if $T_i > LCL_A / LCL$	$p_6 = P(Z_i = 6)$
$Z_i = 7$ if $T_i < UCL_A / UCL$	$p_7 = P(Z_i = 7)$
$Z_i = 8$ if $T_i \geq UCL$	$p_8 = P(Z_i = 8)$
$Z_i = 9$ if $T_i \leq LCL$	$p_9 = P(Z_i = 9)$

Note that in Table 3.1, Z_i can only equal 1, 2, 4 or 5 when *improved* runs-rules are considered, therefore mention is only made to the control limits UCL_B , UCL_A , LCL_A and LCL_B when $Z_i = 1, 2, 4$ or 5 (see e.g. panels (b), (d) and (f) of Figure 3.2). Similarly Z_i can only equal 8 or 9 when runs-rules are considered, therefore mention is only made to the control limits LCL and UCL when $Z_i = 8$ or 9 (see e.g. panels (a), (c) and (e) of Figure 3.2). But Z_i can equal 3, 6 or 7 in both runs-rules and *improved* runs-rules charts, therefore mention is made to the control limits LCL_A / LCL and UCL_A / UCL when $Z_i = 3, 6$ or 7 (see e.g. panels (a), (c), (e) and (f) of Figure 3.2).

3.2.1 The *1-of-1* control charts

The *1-of-1* Shewhart chart signals when a single plotting statistic T_i plots on or outside a control limit. The upper one-sided, lower one-sided and two-sided *1-of-1* charts are discussed next.

3.2.1.1 The upper one-sided *1-of-1* control chart

The upper one-sided *1-of-1* chart is used to detect an upward shift in the process and only has an upper control limit. Studying panel (a) of Figure 3.2, the upper one-sided *1-of-1* control chart is divided by the UCL into zones 7 and 8.

The upper one-sided *1-of-1* chart signals when a plotting statistic T_i plots on or above the upper control limit UCL (or when T_i plots in zone 8). Hence, the signalling event of the upper one-sided *1-of-1* chart is:

$$E_{1-of-1(U)}^1 = \{Z_i = 8\}.$$

The E represents an *event*, the subscript indicates which chart is considered i.e. the *1-of-1*, *improved 2-of-2* etc. and whether it is an upper, lower or two-sided chart, indicated by U , L or T , respectively. In this case the signalling event of an upper one-sided *1-of-1* chart is considered.

The superscript represents the signalling event number; this is necessary because a control chart can have multiple signalling events. In this case the chart has only a single signalling event denoted by 1.

Consider the following two examples: (i) the event $E_{2-of-2(T)}^2$ is the second signalling event of the two-sided *2-of-2* chart and (ii) the event $E_{12-of-3(L)}^3$ is the third signalling event of the lower one-sided *improved 2-of-3* chart.

Examples of the signalling event of the upper one-sided *1-of-1* chart are graphically illustrated in Figure 3.3. In panel (a) of Figure 3.3 there is no signal and in panel (b) there is a signal at the eighth sample (without loss of generality).

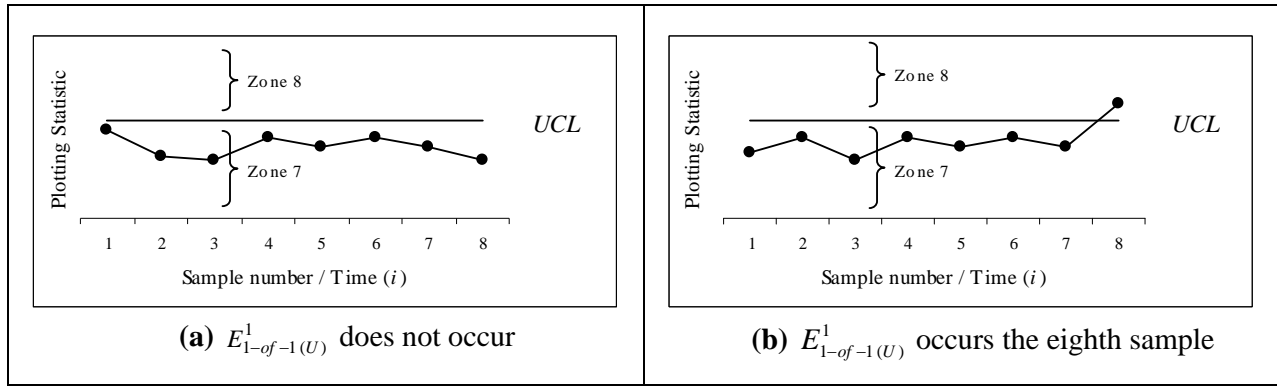


Figure 3.3: Illustrations of the signalling event of the upper one-sided *I-of-1* control chart.

3.2.1.2 The lower one-sided *I-of-1* control chart

The lower one-sided *I-of-1* chart is used to detect a downward shift in the process and thus only has a lower control limit. Studying panel (c) of Figure 3.2, the lower one-sided *I-of-1* chart is divided by the *LCL* into zones 6 and 9.

The lower one-sided *I-of-1* chart signals when the first plotting statistic T_i plots on or below the *LCL* (or when T_i plots in zone 9). Hence, the signalling event of the lower one-sided *I-of-1* control chart is:

$$E_{1-of-1(L)}^1 = \{Z_i = 9\}.$$

Examples of the signalling event of the lower one-sided *I-of-1* chart are graphically illustrated in Figure 3.4. In panel (a) of Figure 3.4 there is no signal, whereas in panel (b) there is a signal at the eighth sample.

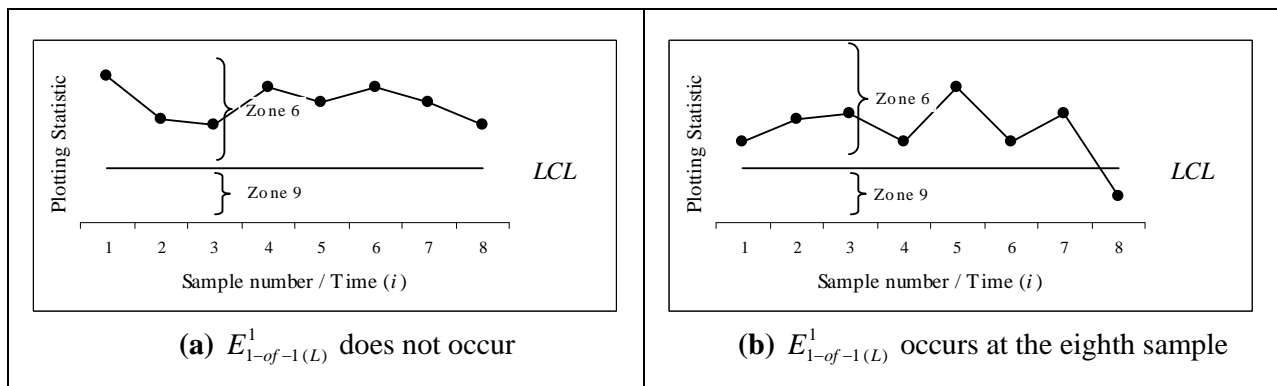


Figure 3.4: Illustrations of the signalling event of the lower one-sided *I-of-1* control chart.

3.2.1.3 The two-sided I -of- I control chart

The two-sided I -of- I chart is used to detect upward and downward shifts in the process and thus has an upper and lower control limit. Studying panel (e) of Figure 3.2, the two-sided I -of- I chart is divided by the UCL and LCL into zones 3, 8 and 9.

The two-sided I -of- I chart signals when the plotting statistic T_i plots on or above (below) the UCL (LCL) (or when T_i plots in zone 8 (9)). Hence the signalling events of the two-sided I -of- I control chart are:

$$E_{1-of-1(T)}^1 = \{Z_i = 8\}$$

$$\text{and } E_{1-of-1(T)}^2 = \{Z_i = 9\}.$$

Examples of the signalling events of the two-sided I -of- I chart are graphically illustrated in Figure 3.5. In panels (a) and (b) there is a signal at the first sample, and in panels (c) and (d) there is a signal at the eighth sample.

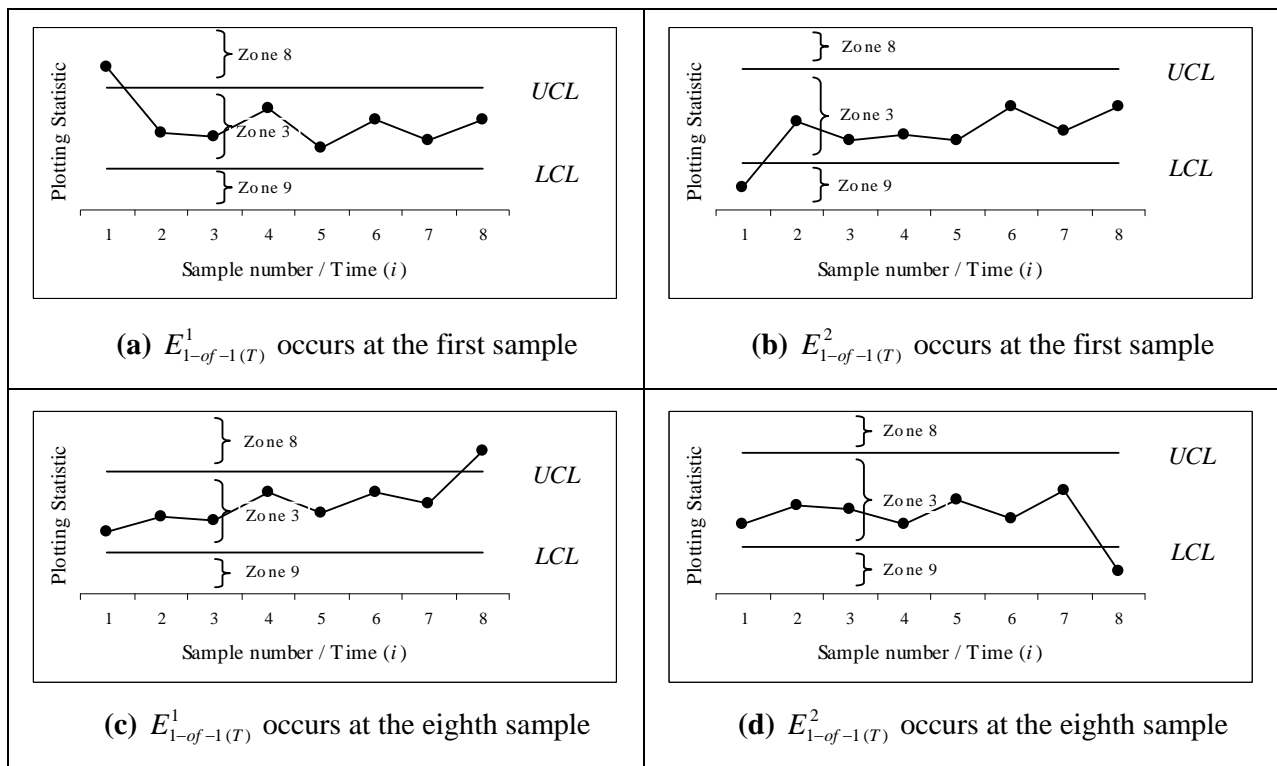


Figure 3.5: Illustrations of the signalling events of the two-sided I -of- I control chart.

3.2.2 The 2-of-2 control charts

The 2-of-2 control charts signal when two consecutive plotting statistics T_{i-1} and T_i plot on or outside the same control limit.

3.2.2.1 The upper one-sided 2-of-2 control chart

The upper one-sided 2-of-2 chart is used to detect an upward shift in the process and consequently has an upper control limit. Studying panel (a) of Figure 3.2 the upper one-sided 2-of-2 chart is divided by the UCL into two zones namely zones 7 and 8.

The upper one-sided 2-of-2 chart signals when two consecutive plotting statistics, T_{i-1} and T_i , plot on or above the UCL (or when two consecutive plotting statistics, T_{i-1} and T_i , plot in zone 8). Hence, the signalling event of the upper one-sided 2-of-2 chart is:

$$E_{2-of-2(U)}^1 = \{Z_{i-1} = 8, Z_i = 8\}.$$

Examples of the signalling event of the upper one-sided 2-of-2 chart are graphically illustrated in Figure 3.6. In panel (a) of Figure 3.6 there is no signal and in panel (b) there is a signal at the eighth sample.

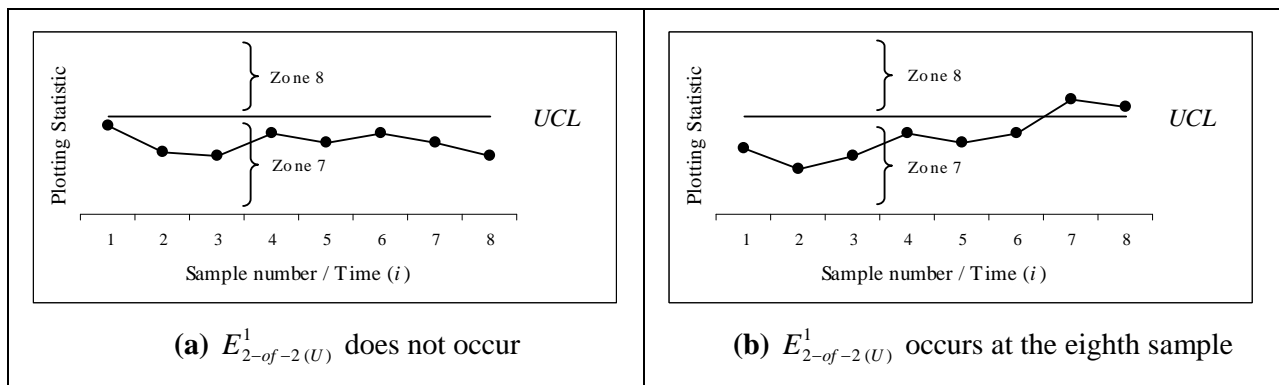


Figure 3.6: Illustrations of the signalling event of the upper one-sided 2-of-2 control chart.

3.2.2.2 The lower one-sided 2-of-2 control chart

The lower one-sided 2-of-2 chart is used to detect a downward shift in the process and consequently has a lower control limit. Studying panel (c) of Figure 3.2 the lower one-sided 2-of-2 chart is divided by the *LCL* into zones 6 and 9.

The lower one-sided 2-of-2 chart signals when two consecutive plotting statistics, T_{i-1} and T_i , plot on or below the *LCL* (or when two consecutive plotting statistics, T_{i-1} and T_i , plot in zone 9). Hence the signalling event of the lower one-sided 2-of-2 chart is:

$$E_{2-of-2(L)}^1 = \{Z_{i-1} = 9, Z_i = 9\}.$$

Examples of the signalling event of the lower one-sided 2-of-2 chart are graphically illustrated in Figure 3.7. In panel (a) of Figure 3.7 there is no signal and in panel (b) there is a signal at the eighth sample.

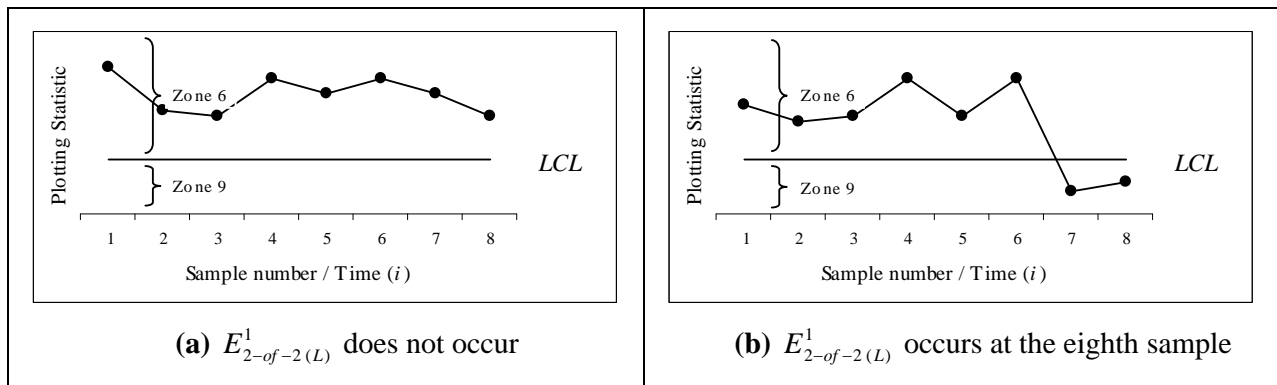


Figure 3.7: Illustrations of the signalling event of the lower one-sided 2-of-2 control chart.

3.2.2.3 The two-sided 2-of-2 control chart

The two-sided 2-of-2 chart is used to detect an upward or downward shift in the process and consequently has an upper and lower control limit. Studying panel (e) of Figure 3.2 the two-sided 2-of-2 chart is divided by the UCL and LCL into three zones namely zones 3, 8 and 9.

The two-sided 2-of-2 chart signals when two consecutive plotting statistics, T_{i-1} and T_i , plot on or above (below) the UCL (LCL) (or when two consecutive plotting statistics, T_{i-1} and T_i , plot in zone 8 (9)). Hence the signalling events of the two-sided 2-of-2 chart are:

$$E_{2-of-2(T)}^1 = \{Z_{i-1} = 8, Z_i = 8\}$$

and $E_{2-of-2(T)}^2 = \{Z_{i-1} = 9, Z_i = 9\}$.

Note that Human et al. (2009) also referred to this chart as the 2-of-2 KL chart since Klein (2000) considered these signalling rules in the context of the Shewhart \bar{X} chart.

Examples of the signalling events of the two-sided 2-of-2 chart are graphically illustrated in Figure 3.8. In panels (a) and (b) of Figure 3.8 there is no signal, whereas in panel (c), (d) there is a signal at the eighth sample.

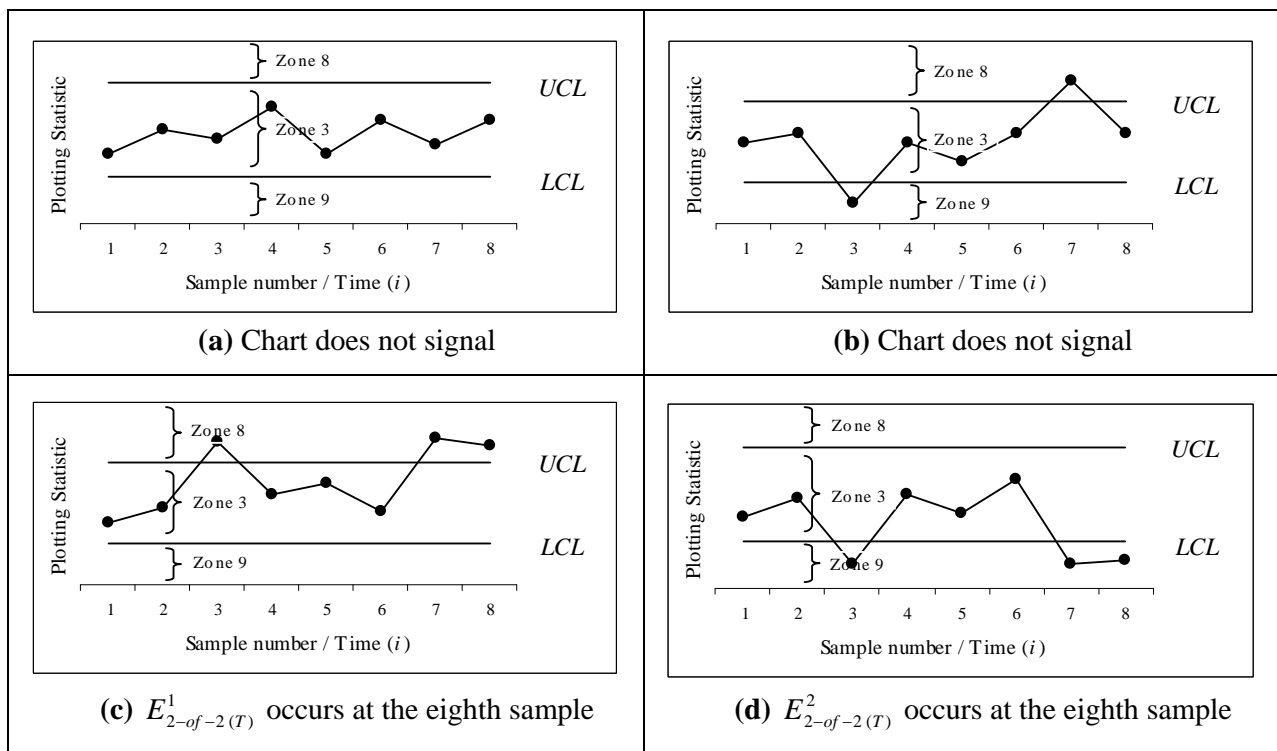


Figure 3.8: Illustrations of the signalling events of the two-sided 2-of-2 control chart.

Remark 3.2:

Note that there are combinations where the last two plotting statistics plot on or outside the control limits, where it is defined/chosen that the chart does not signal. These events are graphically illustrated in Figure 3.9.

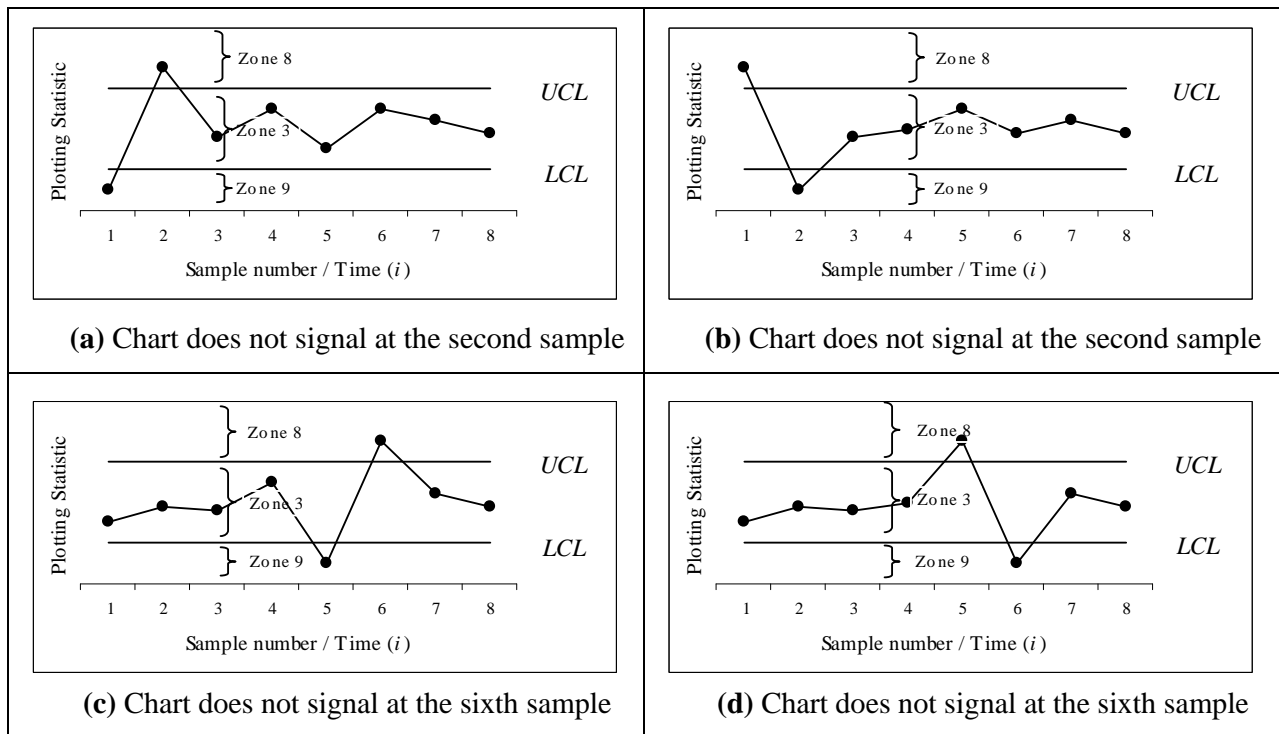


Figure 3.9: Illustrations of combinations of the last two plotting statistics plotting on or outside the control limits, where the chart does not signal.

Figure 3.9 illustrates four possible patterns of the plotting statistics, where two consecutive plotting statistics plot on or outside the control limits, but not outside the same control limit. These events are excluded as signalling events in the two-sided *2-of-2* control charts, since only upward or downward shifts in the process are of interest here. These patterns could indicate a possible swing in the process, the aim here is not to detect a swing in the process, and therefore these events are excluded as signalling events. Human et al. (2009) developed a two-sided *2-of-2* control chart that can detect upward shifts, downward shifts and swings in the process and named this chart the *2-of-2* DR chart, since these signalling rules were proposed by Derman and Ross (1997).

Therefore the following events are excluded as signalling events of the two-sided *2-of-2* control chart:

$$E = \{Z_{i-1} = 8, Z_i = 9\}$$

and $E = \{Z_{i-1} = 9, Z_i = 8\}$.

3.2.3 The 2-of-3 control charts

The 2-of-3 control charts signal when two of the last three plotting statistics, T_{i-2} , T_{i-1} and T_i , plot on or above (below) the UCL (LCL).

3.2.3.1 The upper one-sided 2-of-3 control chart

The upper one-sided 2-of-3 chart is used to detect an upward shift in the process and thus only has an upper control limit. Studying panel (a) of Figure 3.2 the upper one-sided 2-of-3 chart is divided by the UCL into zones 7 and 8.

The upper one-sided 2-of-3 chart signals when two of the last three plotting statistics, namely T_{i-2} , T_{i-1} and T_i , plot on or above the UCL (or when two of the last three plotting statistics plot in zone 8). Hence the signalling events of the upper one-sided 2-of-3 control chart are:

$$E_{2-of-3(U)}^1 = \{Z_{i-2} = 7, Z_{i-1} = 8, Z_i = 8\}$$

and $E_{2-of-3(U)}^2 = \{Z_{i-2} = 8, Z_{i-1} = 7, Z_i = 8\}$.

Examples of the signalling events of the upper one-sided 2-of-3 chart are graphically illustrated in Figure 3.10. In panels (a) and (b) of Figure 3.10 there is a signal at the eighth sample.

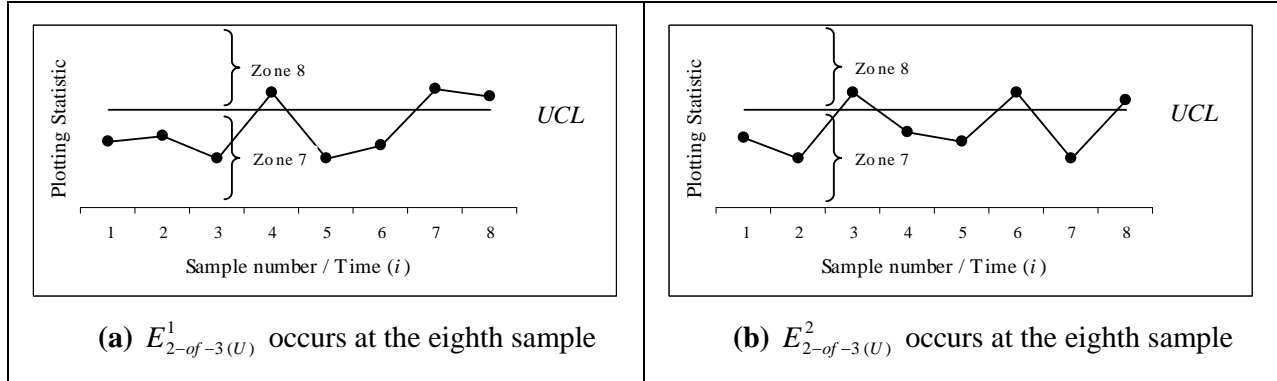


Figure 3.10: Illustrations of the signalling events of the upper one-sided 2-of-3 control chart.

Remark 3.3:

Panel (d) of Figure 3.11 illustrates a combination of plotting statistics where two of the last three plotting statistics plot on or above the UCL which is not included as a signalling event, namely where the first two plotting statistics, T_{i-2} and T_{i-1} , plot on or above the UCL (zone 8), and the third plotting statistic, T_i , plots below the UCL (zone 7). This event is excluded as a signalling event since it is undesirable in practice to have a chart that signals when the last plotting statistic, T_i , plots IC ($T_i < UCL$). Hence the following event is excluded as a signalling event:

$$E = \{Z_{i-2} = 8, Z_{i-1} = 8, Z_i = 7\}.$$

Remark 3.4:

Panels (b) and (c) of Figure 3.11 illustrates sequences of plotting statistics where the chart does not signal since these events are not included in the signalling events $E_{2-of-3(U)}^1$ and $E_{2-of-3(U)}^2$ which is undesirable since there are clearly assignable causes present in the process. To address this issue the following event is included as a signalling event:

$$E_{2-of-3(U)}^3 = \{Z_1 = 8, Z_2 = 8\}.$$

With these three signalling events $E_{2-of-3(U)}^1$, $E_{2-of-3(U)}^2$ and $E_{2-of-3(U)}^3$ the chart will signal at the second sample following the sequence of plotting statistics illustrated in Figure 3.11 panels (a), (b), (c) and (d).

Note that in Figure 3.11 panel (d) it is said that it is undesirable for the chart to signal where the last, in this case the third plotting statistic plots below the UCL (zone 7). However, $E_{2-of-3(U)}^3$ occurs at the second plotting statistic i.e. the chart signals where the last plotting statistic plots on or above the UCL (zone 8).

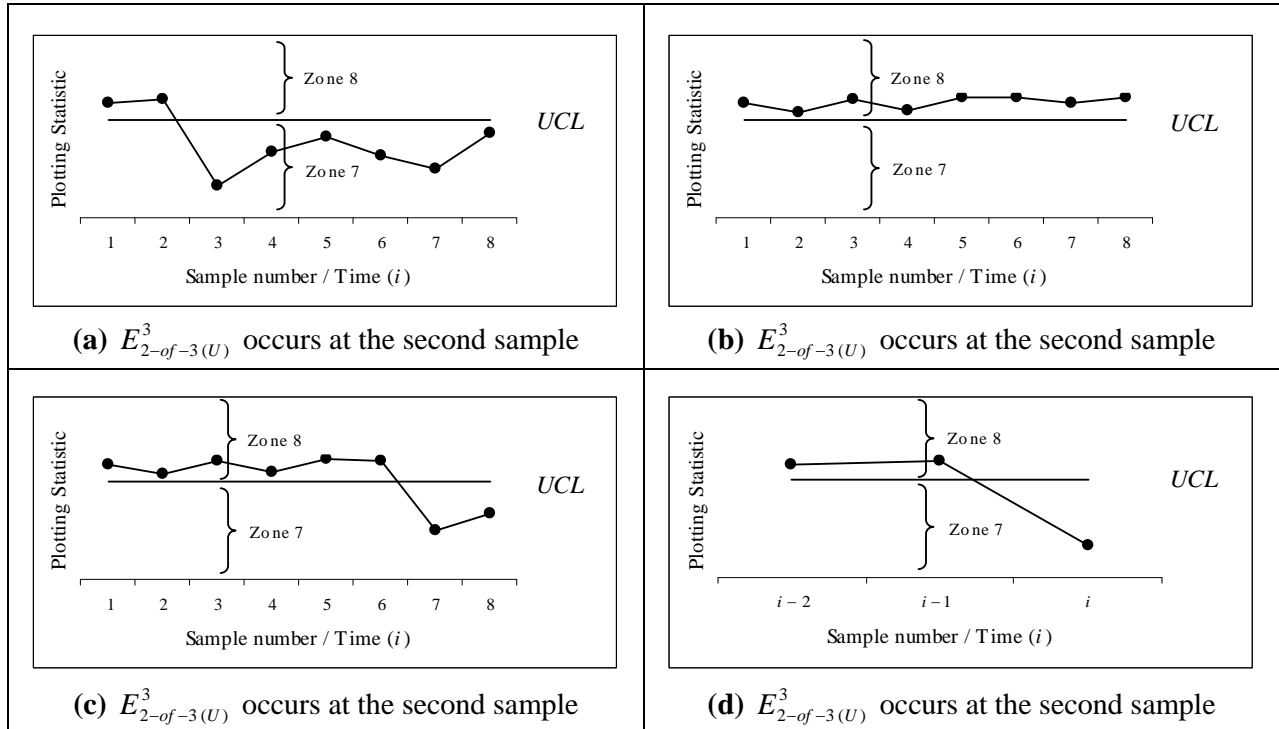


Figure 3.11: Illustrations of signalling events of the upper one-sided 2-of-3 control chart.

3.2.3.2 The lower one-sided 2-of-3 control chart

The lower one-sided 2-of-3 chart is used to detect a downward shift in the process and thus only has a lower control limit. Studying panel (c) of Figure 3.2 the lower one-sided 2-of-3 chart is divided by the LCL into zones 6 and 9.

The lower one-sided 2-of-3 chart signals when two of the last three plotting statistics namely, T_{i-2} , T_{i-1} and T_i , plot on or below the LCL (or when two consecutive plotting statistics plot in zone 9). Hence the signalling events of the lower one-sided 2-of-3 control chart are:

$$E_{2-of-3(L)}^1 = \{Z_{i-2} = 6, Z_{i-1} = 9, Z_i = 9\}$$

and

$$E_{2-of-3(L)}^2 = \{Z_{i-2} = 9, Z_{i-1} = 6, Z_i = 9\}.$$

The signalling events of the lower one-sided 2-of-3 chart are graphically illustrated in Figure 3.12. In panels (a) and (b) of Figure 3.12 the chart signals at the eighth sample.

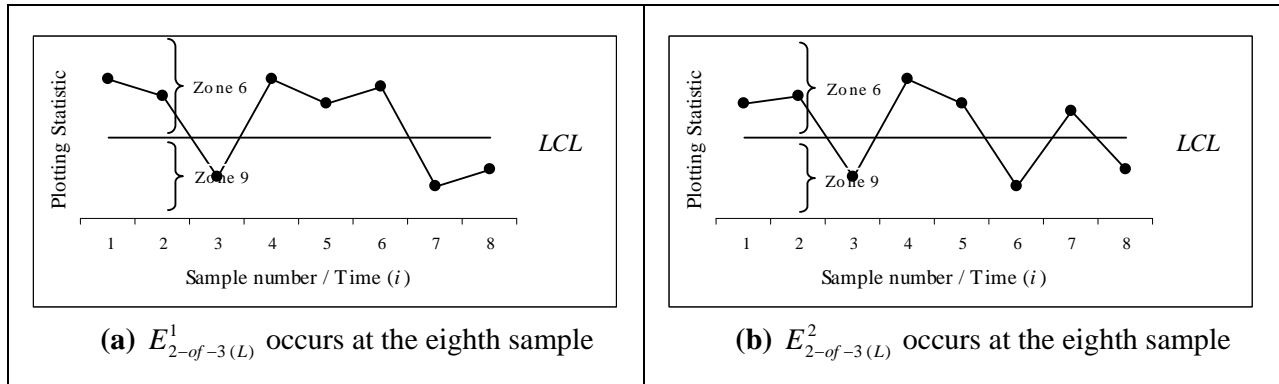


Figure 3.12: Illustrations of signalling events of the lower one-sided 2-of-3 control chart.

Remark 3.5:

Panel (d) of Figure 3.13 illustrates a combination of plotting statistics where two of the last three plotting statistics plot on or below the LCL (zone 9) which is not included as a signalling event, namely where the first two plotting statistics, T_{i-2} and T_{i-1} , plot on or below the LCL (zone 9), and the third plotting statistic, T_i , plots above the LCL (zone 6). This event is excluded as a signalling event since it is undesirable in practice to have the chart signal where the most recent plotting statistic, T_i , plots IC ($T_i > LCL$). Hence the following event is excluded as a signalling event:

$$E = \{Z_{i-2} = 9, Z_{i-1} = 9, Z_i = 6\}.$$

Remark 3.6:

Panels (b) and (c) of Figure 3.13 illustrate sequences of plotting statistics where the chart does not signal, since these events are not included in the signalling events $E_{2-of-3(L)}^1$ and $E_{2-of-3(L)}^2$. This is undesirable, since there are clearly assignable causes present in the process. To address this issue the following event is included as a signalling event:

$$E_{2-of-3(L)}^3 = \{Z_1 = 9, Z_2 = 9\}$$

With these three signalling events $E_{2-of-3(L)}^1$, $E_{2-of-3(L)}^2$ and $E_{2-of-3(L)}^3$ the chart will signal at the second sample following the sequence of plotting statistics illustrated in panels (a), (b), (c) and (d) of Figure 3.13.

Note that in panel (d) of Figure 3.13 it is said that it is undesirable for the chart to signal where the last, in this case the third plotting statistic, plots above the LCL (zone 6). However, $E_{2-of-3(L)}^3$ occurs at the second plotting statistic i.e. the chart signals when the last plotting statistic plots OOC ($T_{i-1} < LCL$).

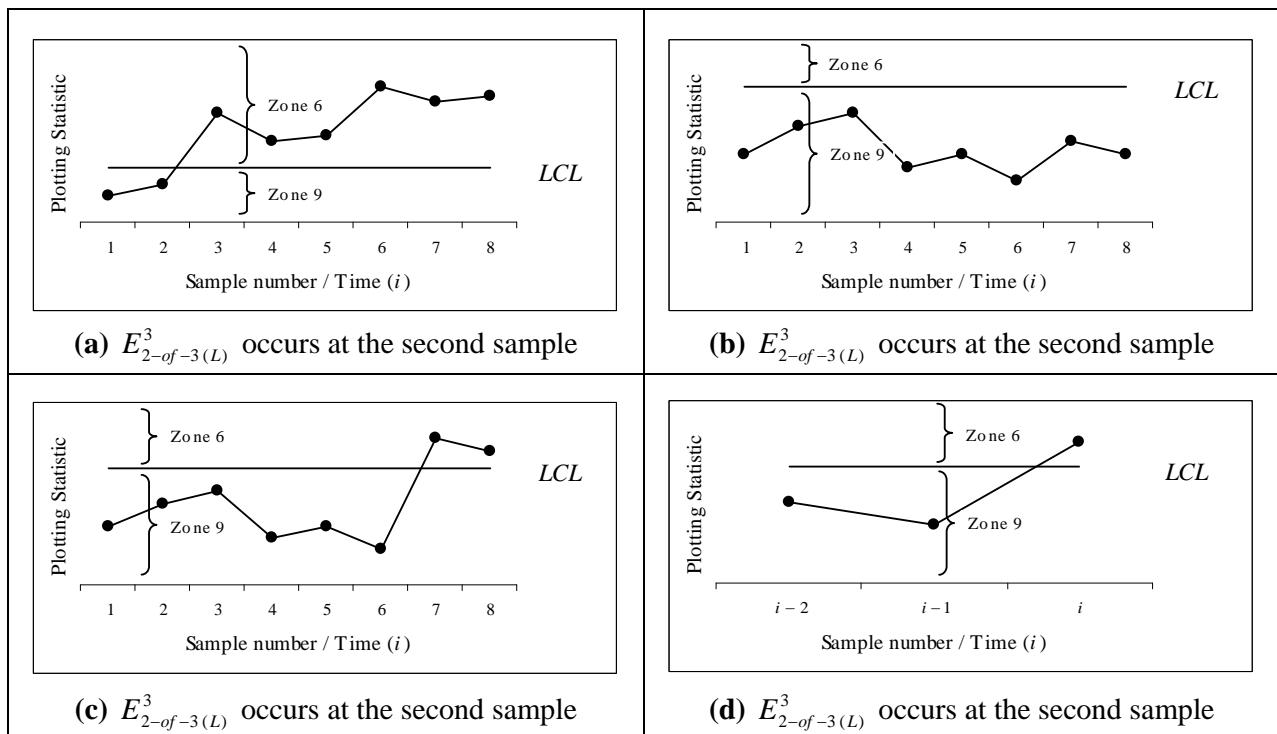


Figure 3.13: Illustrations of signalling events of the lower one-sided 2-of-3 control chart.

3.2.3.3 The two-sided 2-of-3 control chart

The two-sided 2-of-3 chart is used to detect an upward or downward shift in the process and consequently has an upper and lower control limit. Studying panel (e) of Figure 3.2 the two-sided 2-of-3 chart is divided by the UCL and LCL into zones 3, 8 and 9.

The two-sided 2-of-3 chart signals when two of the last three plotting statistics, T_{i-2} , T_{i-1} and T_i , plot on or above (below) the UCL (LCL) (or when two of the last three plotting statistics T_{i-2} , T_{i-1} and T_i , plot in zone 8 (9)). Hence the signalling events of the two-sided 2-of-3 chart are:

$$\begin{aligned}
 E_{2-of-3(T)}^1 &= \{Z_{i-2} = 3, Z_{i-1} = 8, Z_i = 8\}, \\
 E_{2-of-3(T)}^2 &= \{Z_{i-2} = 8, Z_{i-1} = 3, Z_i = 8\}, \\
 E_{2-of-3(T)}^3 &= \{Z_{i-2} = 3, Z_{i-1} = 9, Z_i = 9\} \\
 \text{and } E_{2-of-3(T)}^4 &= \{Z_{i-2} = 9, Z_{i-1} = 3, Z_i = 9\}.
 \end{aligned}$$

Examples of the signalling events of the two-sided 2-of-3 chart are graphically illustrated in Figure 3.14. In panels (a), (b), (c) and (d) of Figure 3.14 there is a signal at the eighth sample.

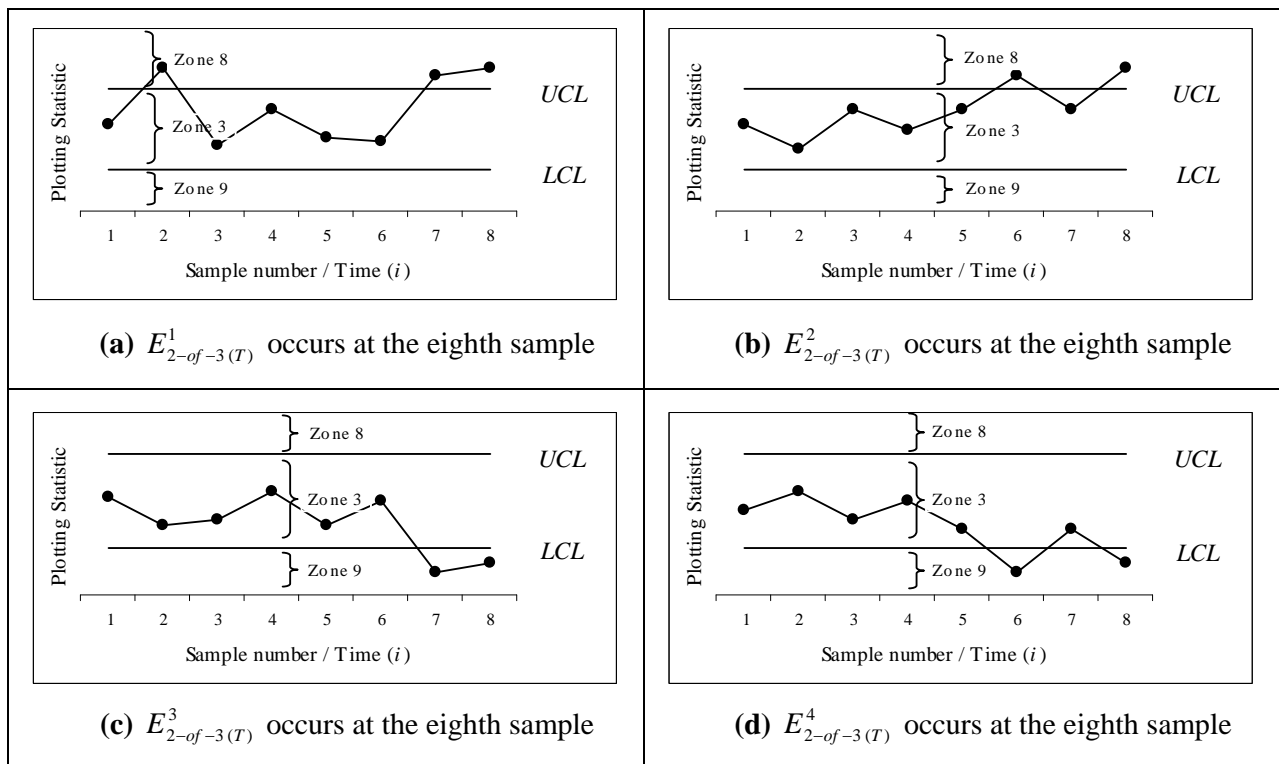


Figure 3.14: Illustrations of the signalling events of the two-sided 2-of-3 control chart.

Remark 3.7:

Two combinations where two of the last three plotting statistics, namely T_{i-2} , T_{i-1} and T_i , plot on or outside the same control limit that is not included as signalling events, are illustrated in panels (c)

and (g) of Figure 3.15, i.e. where the first two plotting statistics, T_{i-2} and T_{i-1} , plot on or above (below) the UCL (zone 8) (LCL (zone 9)), and the third plotting statistic, T_i , plots between the UCL and the LCL (zone 3) respectively. These events are excluded as signalling events since it is undesirable in practice to have the chart signal were the last plotting statistic T_i plots IC i.e. between the upper and lower control limits (zone 3). Therefore the following two events are excluded as signalling events:

$$E = \{Z_{i-2} = 8, Z_{i-1} = 8, Z_i = 3\},$$

$$\text{and } E = \{Z_{i-2} = 9, Z_{i-1} = 9, Z_i = 3\}.$$

The signalling events are defined in such a way that the two-sided 2-of-3 control chart will not signal given the sequence of plotting statistics illustrated in panels (b), (d), (f) and (h) of Figure 3.15. This is undesirable since there are clearly assignable causes present in the process, therefore the following events are included as signalling events:

$$E_{2-of-3(T)}^5 = \{Z_1 = 8, Z_2 = 8\},$$

$$\text{and } E_{2-of-3(T)}^6 = \{Z_1 = 9, Z_2 = 9\}.$$

Remark 3.8:

With these six signalling events $E_{2-of-3(T)}^1$, $E_{2-of-3(T)}^2$, $E_{2-of-3(T)}^3$, $E_{2-of-3(T)}^4$, $E_{2-of-3(T)}^5$ and $E_{2-of-3(T)}^6$ the chart will signal at the second sample following the sequence of plotting statistics illustrated in panels (a), (b), (c), (d), (e), (f), (g) and (h) of Figure 3.15.

Note that in panels (c) and (g) of Figure 3.15 it is said that it is undesirable for the chart to signal where the last, in this case the third plotting statistic, plots above (below) the LCL (UCL). However, $E_{2-of-3(T)}^5$ $E_{2-of-3(T)}^6$ occur at the second plotting statistic i.e. the chart signals when the last plotting statistic (T_{i-1}) plots OOC.

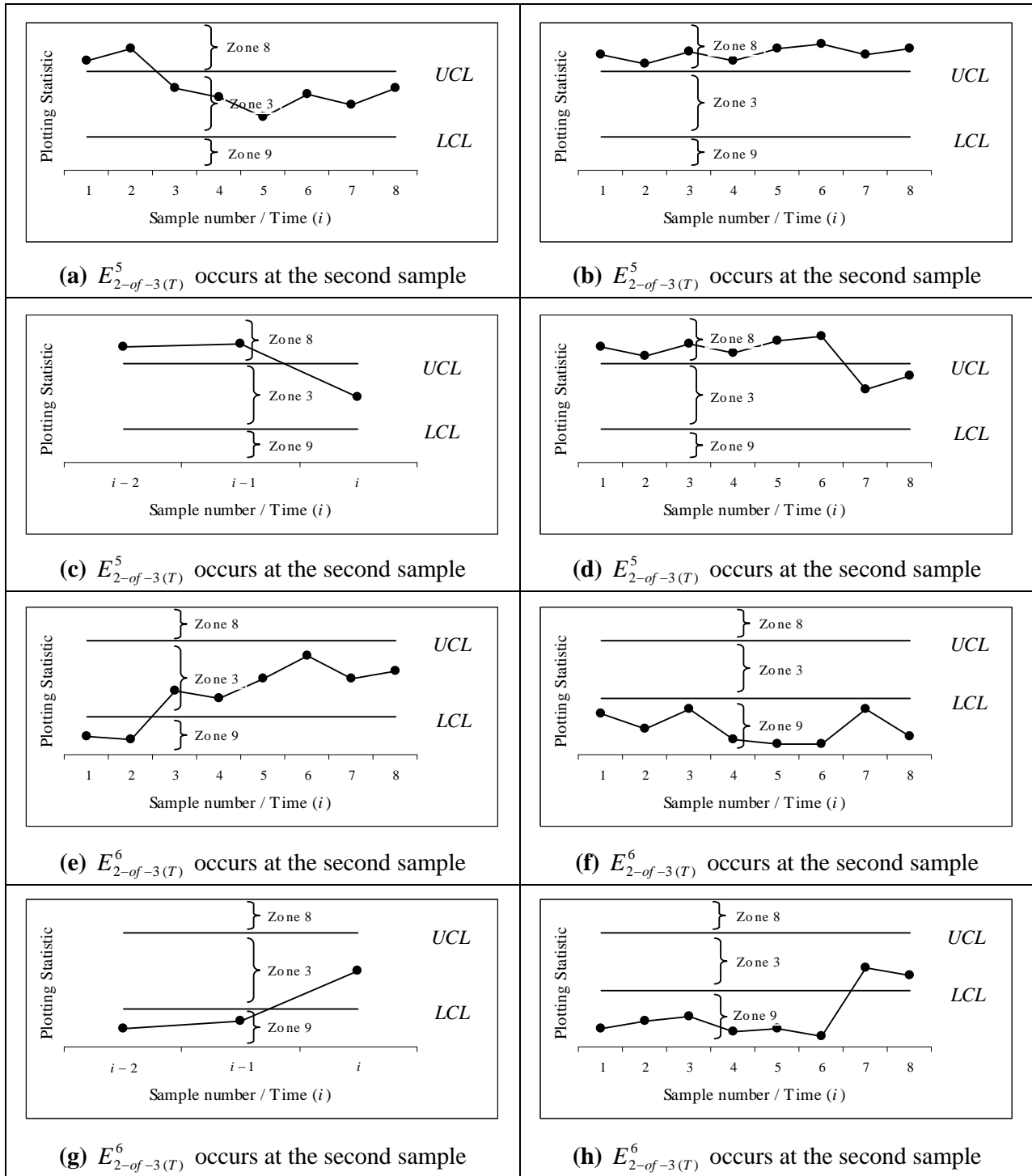


Figure 3.15: Illustrations of signalling events of the two-sided 2-of-3 control chart.

Remark 3.9:

Not all combinations of plotting statistics, where two of the last three plotting statistics plot on or outside the control limits cause the two-sided 2-of-3 chart to signal. The combinations that do not lead to a signal are illustrated in Figure 3.16. When applying the two-sided 2-of-3 control chart only the detection of an upward or downward shift in the process is of interest here. The sequences of plotting statistics namely T_3 , T_4 and T_5 , illustrated in panels (a) and (b) of Figure 3.16 are excluded as signalling events since these indicate a possible swing in the process. The sequence of plotting statistics illustrated in panels (c) and (d) of Figure 3.16 are excluded as signalling events since these indicate a possible drift in the process. Only the detection of upward or downward shifts in the process is of interest in this dissertation and not swings or drifts in the process.

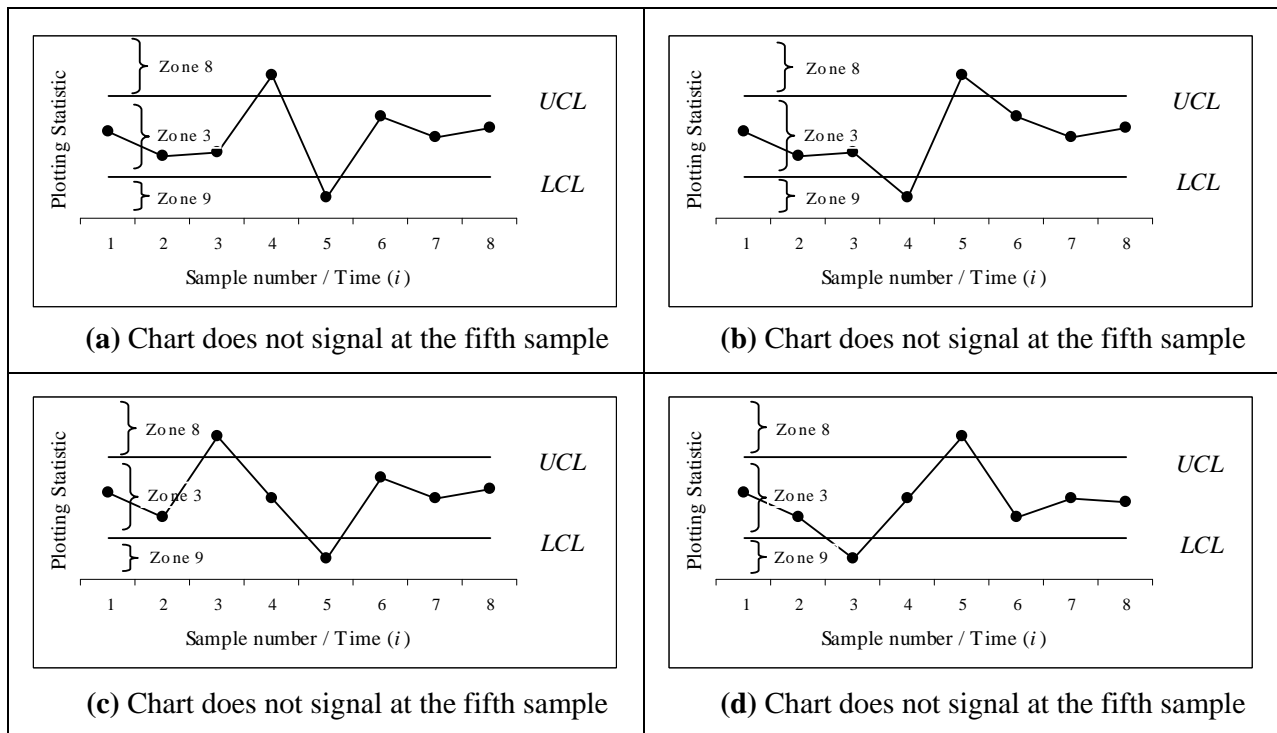


Figure 3.16: Illustrations of drifts and swings of the two-sided 2-of-3 control chart.

Remark 3.10:

Note that Human et al. (2009) incorporated the 2-of-3 runs-rules to the sign and precedence charts, respectfully, and that the events $E_{2-of-3(U)}^3 = \{Z_1 = 8, Z_2 = 8\}$, $E_{2-of-3(L)}^3 = \{Z_1 = 9, Z_2 = 9\}$, $E_{2-of-3(T)}^5 = \{Z_1 = 8, Z_2 = 8\}$ and $E_{2-of-3(T)}^6 = \{Z_1 = 9, Z_2 = 9\}$ were not included as signalling events by them, and, consequently the 2-of-3 control charts given here differ slightly to theirs.

3.2.4 The improved 2-of-2 control charts

The improved 2-of-2 control charts signal when the plotting statistic T_i plots on or above (below) the UCL_B (LCL_B), or when two consecutive plotting statistics plot on or above (below) the UCL_A (LCL_A).

3.2.4.1 The upper one-sided improved 2-of-2 control chart

The upper one-sided improved 2-of-2 chart is used to detect small upward shifts and has the ability to immediately detect large upward shifts in the process and thus has two upper control limits. Studying panel (b) of Figure 3.2 the upper one-sided improved 2-of-2 chart is divided by the UCL_A and UCL_B into zones 1, 2 and 7.

The upper one-sided improved 2-of-2 chart signals when the plotting statistic T_i plots on or above the UCL_B ($T_i \geq UCL_B$) (T_i plots in zone 1), or when two consecutive plotting statistics, T_{i-1} and T_i , plot on or above the UCL_A while plotting below the UCL_B ($UCL_A \leq T_{i-1} < UCL_B$, $UCL_A \leq T_i < UCL_B$) (T_{i-1} and T_i plot in zone 2). Hence the signalling events of the upper one-sided improved 2-of-2 chart are:

$$E_{12-of-2(U)}^1 = \{Z_i = 1\}$$

$$\text{and } E_{12-of-2(U)}^2 = \{Z_{i-1} = 2, Z_i = 2\}.$$

Examples of the signalling events of the upper one-sided improved 2-of-2 control chart are graphically illustrated in Figure 3.17. In panels (a) and (b) of Figure 3.17 there is a signal at the eighth sample. In panels (c) and (d) there is a signal at the seventh and sixth sample, respectively.

Note that panels (c) and (d) of Figure 3.17 include both events $E_{12-of-2(U)}^1$ and $E_{12-of-2(U)}^2$. The chart signals on the first occurrence of either $E_{12-of-2(U)}^1$ or $E_{12-of-2(U)}^2$.

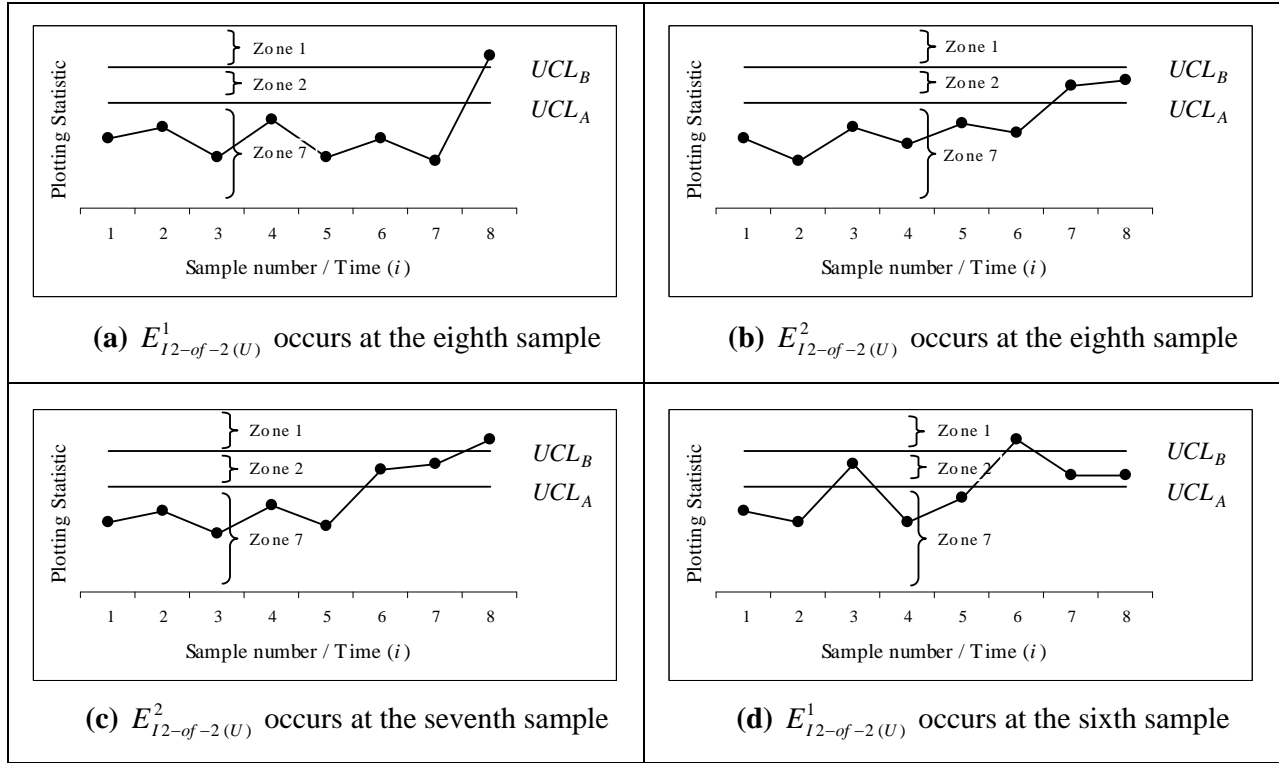


Figure 3.17: Illustrations of the signalling events of the upper one-sided *improved 2-of-2* control chart.

3.2.4.2 The lower one-sided *improved 2-of-2* control chart

The lower one-sided *improved 2-of-2* chart is used to detect a small downward shift in the process and has the ability to immediately detect large downward shifts in the process and thus has two lower control limits. Studying panel (d) of Figure 3.2 the lower one-sided *improved 2-of-2* chart is divided by the LCL_A and LCL_B into zones 4, 5 and 6.

The lower one-sided *improved 2-of-2* chart signals when the plotting statistic, T_i , plots on or below the LCL_B ($T_i \leq LCL_B$) (T_i plots in zone 5), or when two consecutive plotting statistics, T_{i-1} and T_i , plot on or below the LCL_A while plotting above the LCL_B ($LCL_B < T_{i-1} \leq LCL_A, LCL_B < T_i \leq LCL_A$)

(T_{i-1} and T_i plot in zone 4). Hence the signalling events of the lower one-sided *improved 2-of-2* control chart are:

$$E_{I2-of-2(L)}^1 = \{Z_i = 5\}$$

$$\text{and } E_{I2-of-2(L)}^2 = \{Z_{i-1} = 4, Z_i = 4\}.$$

Examples of the signalling events of the lower one-sided *improved 2-of-2* chart are graphically illustrated in Figure 3.18. In panels (a) and (b) of Figure 3.18 there is a signal at the eighth sample and in panels (c) and (d) there is a signal at the seventh and sixth sample, respectively.

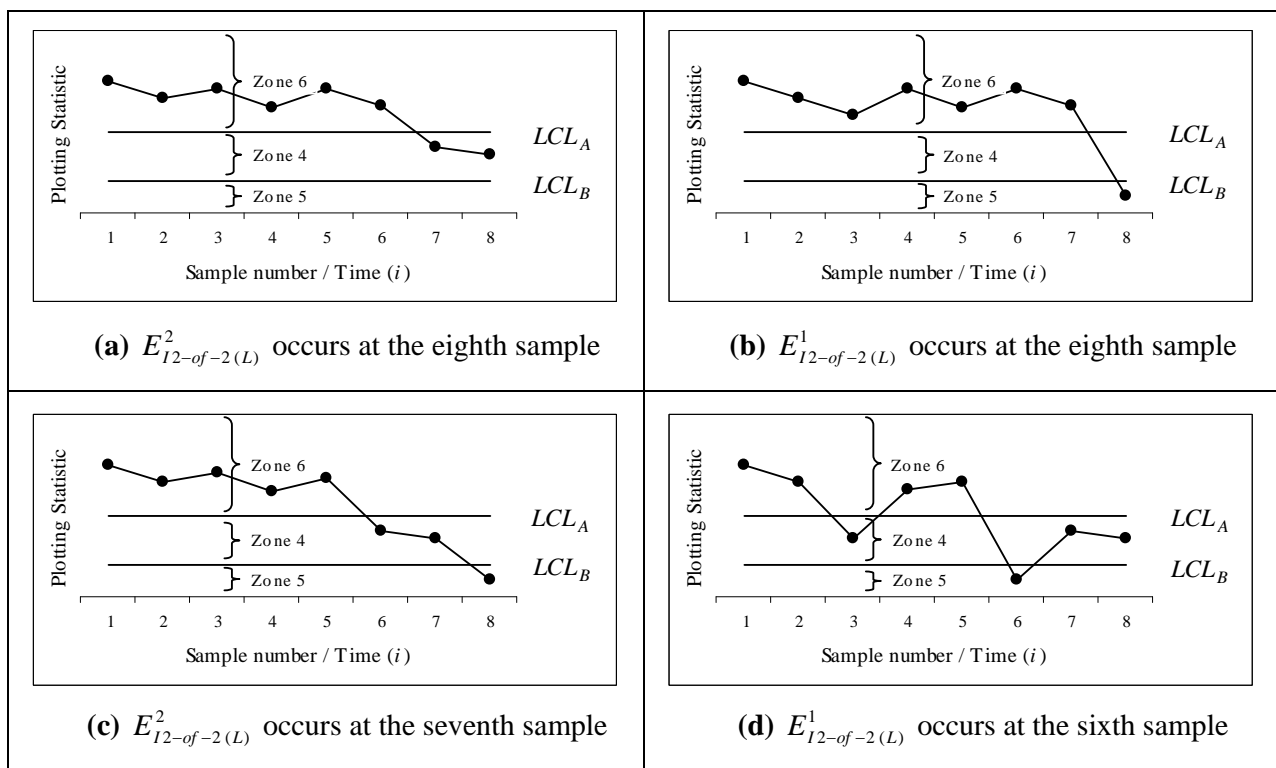


Figure 3.18: Illustrations of the signalling events of the lower one-sided *improved 2-of-2* control chart.

3.2.4.3 The two-sided *improved 2-of-2* control chart

The two-sided *improved 2-of-2* chart is used to detect a small upward or downward shift in the process and has the ability to immediately detect large upward or downward shifts in the process and thus have two upper and two lower control limits. Studying panel (f) of Figure 3.1 the two-sided *improved 2-of-2* chart is divided by the UCL_A , UCL_B , LCL_A and LCL_B into zones 1, 2, 3, 4 and 5.

The two-sided *improved 2-of-2* chart signals when the plotting statistic, T_i , plots on or above (below) the UCL_B (LCL_B) ($T_i \geq UCL_B$ or $T_i \leq LCL_B$) (T_i plots in zones 1 or 5), or when two consecutive plotting statistics, T_{i-1} and T_i , plot on or above (below) the UCL_A (LCL_A) while plotting below (above) the UCL_B (LCL_B) ($UCL_A \leq T_{i-1} < UCL_B$, $UCL_A \leq T_i < UCL_B$ or $LCL_B < T_{i-1} \leq LCL_A$, $LCL_B < T_i \leq LCL_A$) (both T_{i-1} and T_i plot in zone 2 or both T_{i-1} and T_i plot in zone 4). Hence the signalling events of the two-sided *improved 2-of-2* chart are:

$$E_{I2-of-2(T)}^1 = \{Z_i = 1\},$$

$$E_{I2-of-2(T)}^2 = \{Z_{i-1} = 2, Z_i = 2\},$$

$$E_{I2-of-2(T)}^3 = \{Z_i = 5\}$$

and $E_{I2-of-2(T)}^4 = \{Z_{i-1} = 4, Z_i = 4\}$

Examples of the signalling events of the two-sided *improved 2-of-2* chart are graphically illustrated in Figure 3.19. In panels (a), (b), (c) and (d) of Figure 3.19 there is a signal at the eighth sample.

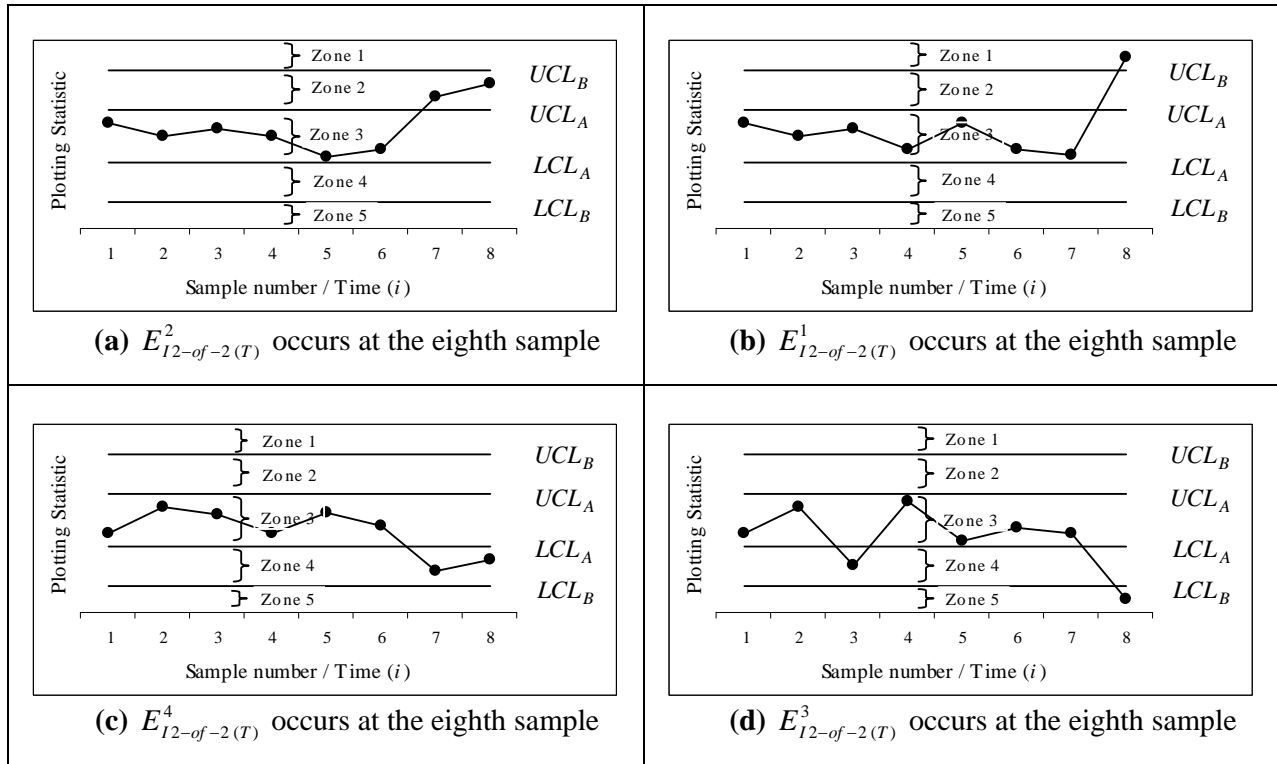


Figure 3.19: Illustrations of the signalling events of the two-sided *improved 2-of-2* control chart.

Remark 3.11:

Panels (a) and (b) of Figure 3.20 illustrate sequences of the plotting statistics that are not included as signalling events of the two-sided *improved 2-of-2* chart. Panels (a) and (b) of Figure 3.20 illustrate sequences of the plotting statistics where two consecutive plotting statistics plot on or outside different *inner* control limits, indicating a possible swing in the process. Since only the detection of an upward or a downward shift in the process is of interest here, these events are excluded as signalling events.

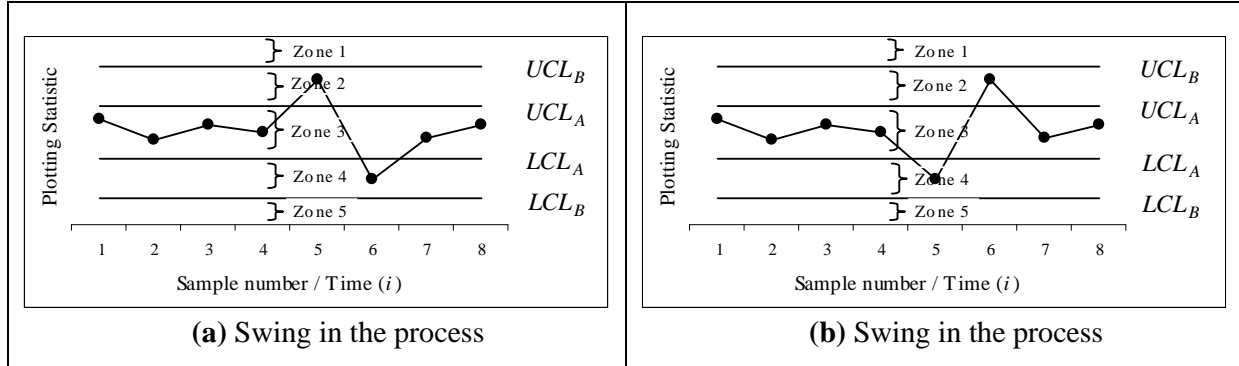


Figure 3.20: Illustrations of swings in the process.

3.2.5 The improved 2-of-3 control charts

The improved 2-of-3 chart signals when the plotting statistic T_i plots on or above (below) the UCL_B (LCL_B), or when two out of three consecutive plotting statistics plot on or above (below) the UCL_A (LCL_A).

3.2.5.1 The upper one-sided improved 2-of-3 control chart

The upper one-sided improved 2-of-3 chart is used to detect a small upward shift and has the ability to immediately detect a large upward shift and thus has two upper control limits. Studying panel (b) of Figure 3.2 the upper one-sided improved 2-of-3 chart is divided by the UCL_A and UCL_B into zones 1, 2 and 7.

The upper one-sided improved 2-of-3 chart signals when the plotting statistic T_i plots on or above the UCL_B ($T_i \geq UCL_B$) (T_i plots in zone 1), or when two out of three consecutive plotting statistics, T_{i-2} , T_{i-1} and T_i , plot on or above the UCL_A while plotting below the UCL_B (two out of three consecutive plotting statistics, T_{i-2} , T_{i-1} and T_i , plot in zone 2). Hence the signalling events of the upper one-sided improved 2-of-3 chart are:

$$\begin{aligned}
 E_{I2-of-3(U)}^1 &= \{Z_i = 1\}, \\
 E_{I2-of-3(U)}^2 &= \{Z_{i-2} = 7, Z_{i-1} = 2, Z_i = 2\} \\
 \text{and } E_{I2-of-3(U)}^3 &= \{Z_{i-2} = 2, Z_{i-1} = 7, Z_i = 2\}
 \end{aligned}$$

Examples of the signalling events of the upper one-sided *improved 2-of-3* chart are graphically illustrated in Figure 3.21. In panels (a), (b), (c) and (d) of Figure 3.21 there is a signal at the eighth sample.

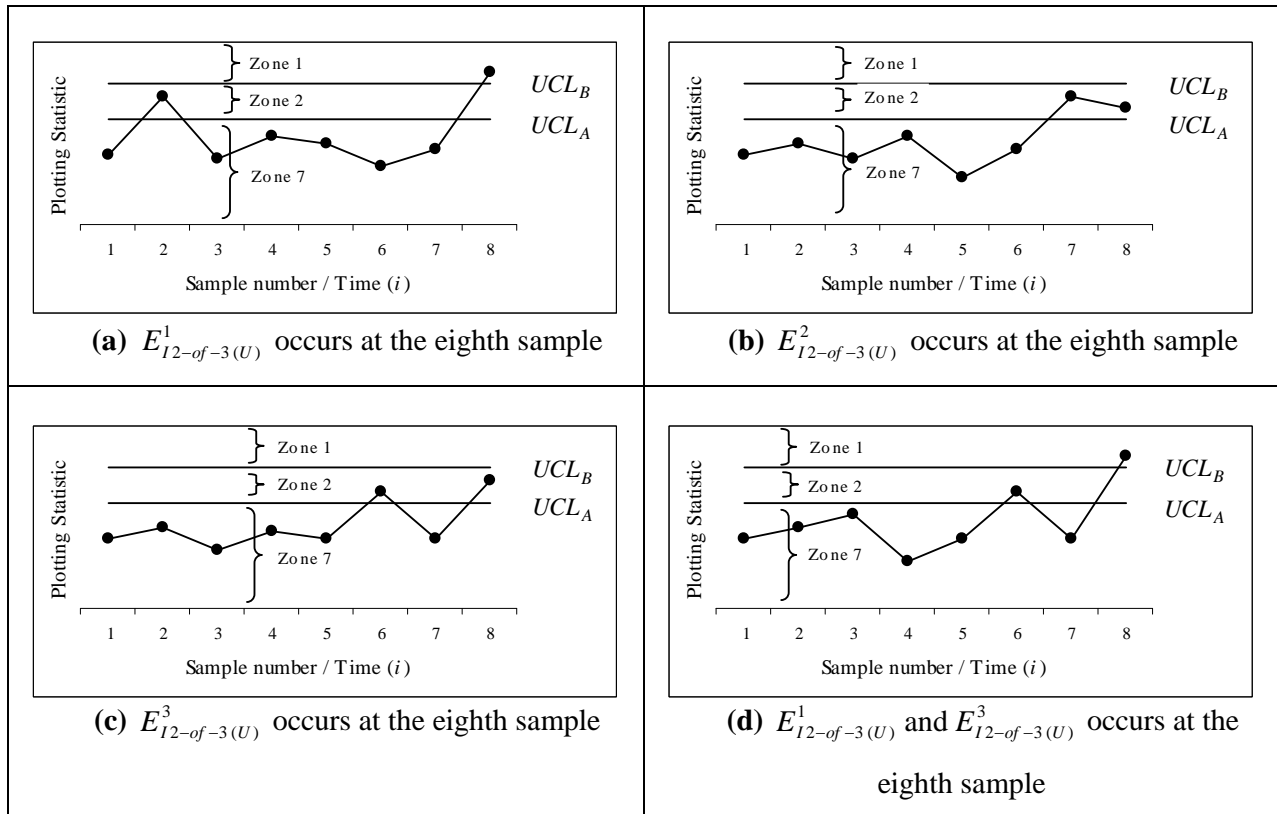


Figure 3.21: Illustrations of the signalling events of the upper one-sided *improved 2-of-3* control chart.

Remark 3.12:

Figure 3.22 panel (d) illustrates a combination of plotting statistics where two of the last three plotting statistics plot on or above the UCL_A (zone 2), i.e. the first two plotting statistics, T_{i-2} and T_{i-1} , plot on or above the UCL_A (zone 2), and the third plotting statistic, T_i , plots below the UCL_A (zone 7). This event is excluded as a signalling event since it is undesirable in practice to have a chart that signals when the last plotting statistic, T_i , plots IC ($T_i < UCL_B$) (T_i plots in zone 7).

Therefore the following event is excluded as a signalling event:

$$E = \{Z_{i-2} = 2, Z_{i-1} = 2, Z_i = 7\}.$$

Remark 3.13:

Panels (b) and (c) of Figure 3.22 illustrates sequences of plotting statistics where the chart does not signal since these events are not included in the signalling events $E_{I2-of-3(U)}^1$, $E_{I2-of-3(U)}^2$ and $E_{I2-of-3(U)}^3$. These events are undesirable since there are clearly assignable causes present in the process. To address this issue the following event is included as a signalling event:

$$E_{I2-of-3(U)}^4 = \{Z_1 = 2, Z_2 = 2\}.$$

With these four signalling events $E_{I2-of-3(U)}^1$, $E_{I2-of-3(U)}^2$, $E_{I2-of-3(U)}^3$ and $E_{I2-of-3(U)}^4$ the upper one-sided *improved 2-of-3* chart signals at the second sample following the sequence of plotting statistics illustrated in panels (a), (b), (c) and (d) of Figure 3.22.

Note that in panel (d) of Figure 3.22 it is said that it is undesirable for the chart to signal where the last, in this case the third plotting statistic, plots below the UCL_A (zone 7). However, $E_{I2-of-3(U)}^4$ occurs at the second plotting statistic i.e. the chart signals where the last plotting statistic plots above the UCL_A ($UCL_A \leq T_{i-1} < UCL_B$) (T_{i-1} plots in zone 2).

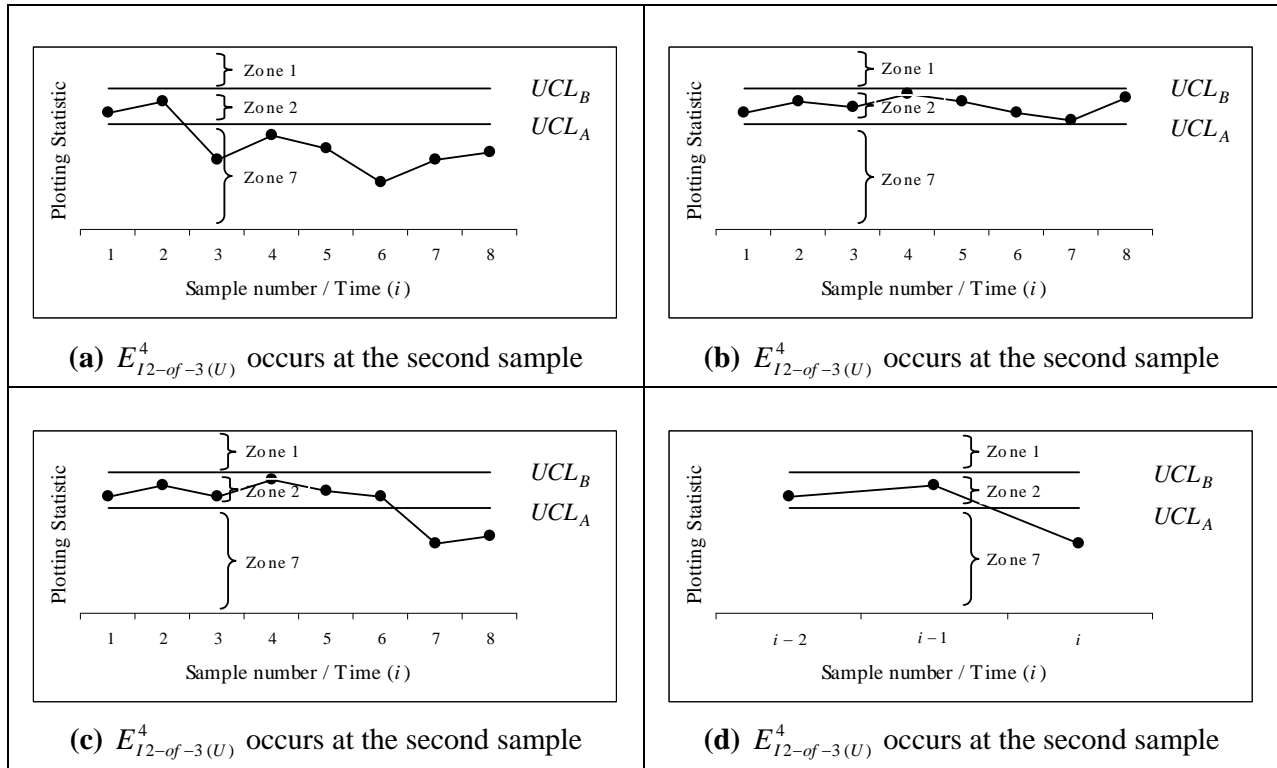


Figure 3.22: Illustrations of signalling events of the upper one-sided *improved 2-of-3* control chart.

3.2.5.2 The lower one-sided *improved 2-of-3* control chart

The lower one-sided *improved 2-of-3* chart is used to detect a small downward shift in the process and has the ability to immediately detect a large downward shift in the process and thus has two lower control limits. Studying panel (d) of Figure 3.2 the lower one-sided *improved 2-of-3* chart is divided by the LCL_A and LCL_B into zones 4, 5 and 6.

The lower one-sided *improved 2-of-3* chart signals when the plotting statistic T_i plots on or below the LCL_B ($T_i \leq LCL_B$) (T_i plots in zone 5), or when two of the last three plotting statistics, T_{i-2} , T_{i-1} and T_i , plot on or below the LCL_A while plotting above the LCL_B (zone 4). Hence the signalling events of the lower one-sided *improved 2-of-3* chart are:

$$E_{I2-of-3(L)}^1 = \{Z_i = 5\},$$

$$E_{I2-of-3(L)}^2 = \{Z_{i-2} = 6, Z_{i-1} = 4, Z_i = 4\}$$

and $E_{I2-of-3(L)}^3 = \{Z_{i-2} = 4, Z_{i-1} = 6, Z_i = 4\}$

Examples of the signalling events of the lower one-sided *improved 2-of-3* chart are graphically illustrated in Figure 3.23. In panels (a), (b), (c) and (d) of Figure 3.23 there is a signal at the eighth sample.

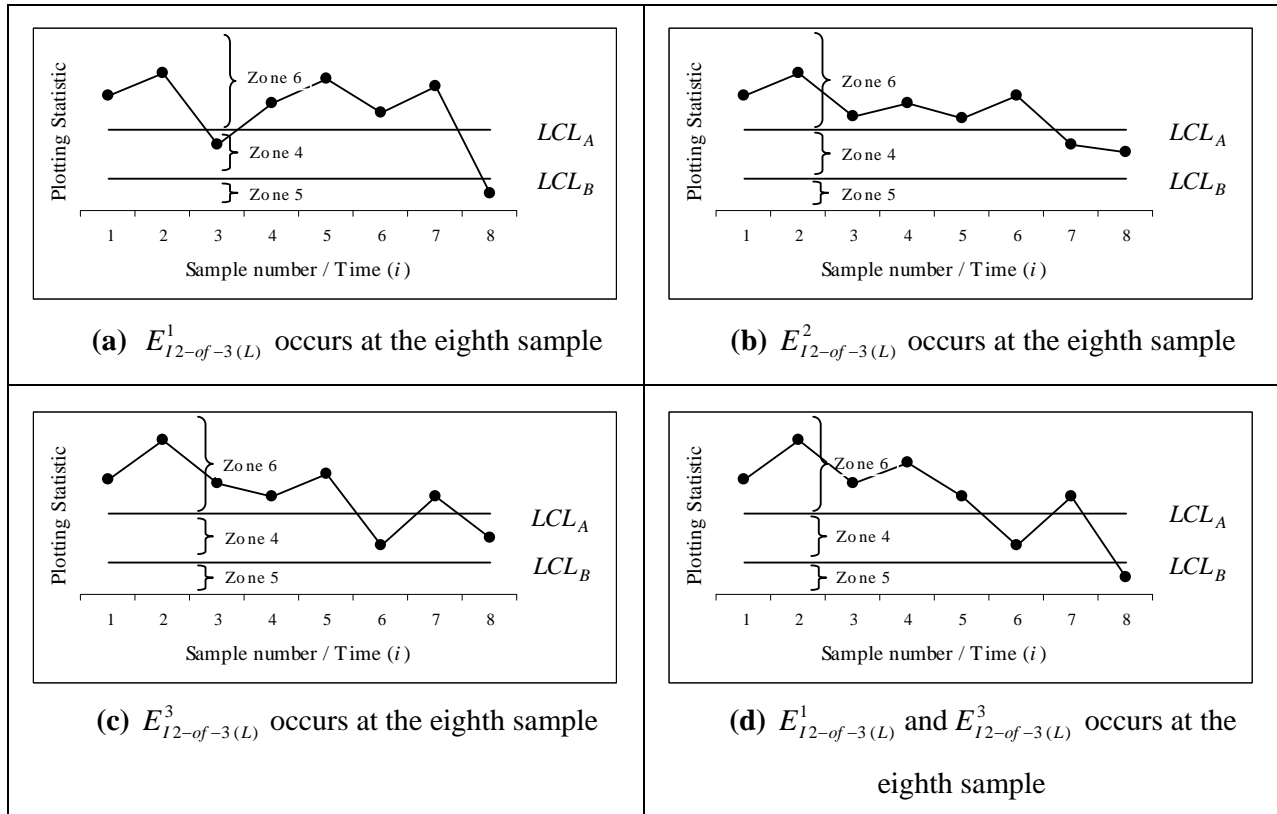


Figure 3.23: Illustrations of the signalling events of the lower one-sided *improved 2-of-3* control chart.

Remark 3.14:

Figure 3.24 panel (d) illustrates a combination of plotting statistics where two of the last three plotting statistics plots on or below the LCL_A , while plotting above the LCL_B (zone 4), i.e. the first two plotting statistics, T_{i-2} and T_{i-1} , plot on or below the LCL_A (zone 4), and the third plotting statistic, T_i , plots above the LCL_A (zone 6). This event is excluded as a signalling event since it is undesirable in practice to have a chart that signals when the last plotting statistic, T_i , plots IC (zone 6).

Therefore the following event is excluded as a signalling event:

$$E = \{Z_{i-2} = 4, Z_{i-1} = 4, Z_i = 6\}.$$

Remark 3.15:

Panels (a) and (c) of Figure 3.24 illustrates sequences of plotting statistics where the chart does not signal since these events are not included in the signalling events $E_{I2-of-3(L)}^1$, $E_{I2-of-3(L)}^2$ and $E_{I2-of-3(L)}^3$. These events are undesirable since there are clearly assignable causes present in the process. To address this issue the following event is included as a signalling event:

$$E_{I2-of-3(L)}^4 = \{Z_1 = 4, Z_2 = 4\}.$$

With these four signalling events the chart signals at the second sample following the sequence of plotting statistics illustrated in panels (a), (b), (c) and (d) of Figure 3.24.

Note that in panel (d) of Figure 3.24 it is said that it is undesirable for the chart to signal where the last, in this case the third plotting statistic, plots above the LCL_A . However, $E_{I2-of-3(L)}^4$ occurs at the second plotting statistic i.e. the chart signals where the last plotting statistic plots below the LCL_A ($LCL_B < T_{i-1} \leq LCL_A$) (T_{i-1} plots in zone 4).

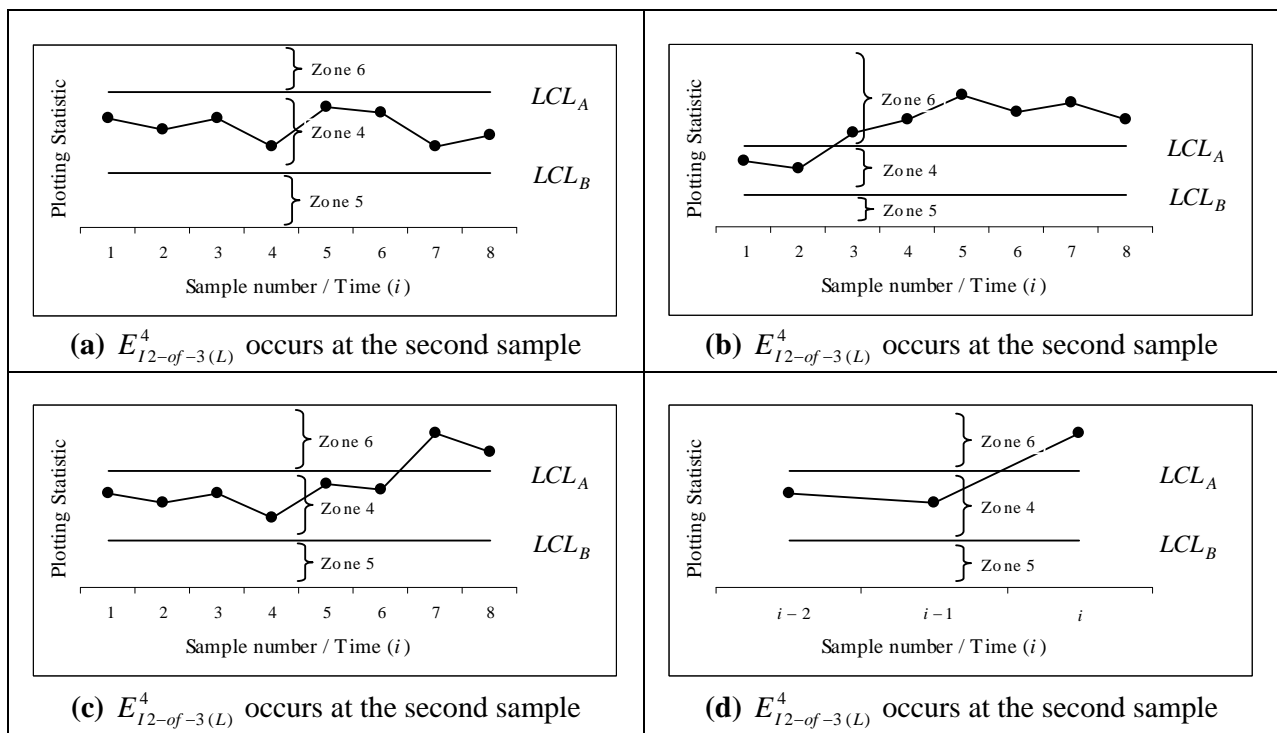


Figure 3.24: Illustrations of the signalling events of the lower one-sided improved 2-of-3 control chart.

3.2.5.3 The two-sided *improved 2-of-3* control chart

The two-sided *improved 2-of-3* chart is used to detect a small upward or downward shift in the process and has the ability to immediately detect large upward or large downward shifts in the process and consequently have two upper and two lower control limits. Referring to panel (f) of Figure 3.2 the two-sided *improved 2-of-3* chart is divided by the UCL_A , UCL_B , LCL_A and LCL_B into zones 1, 2, 3, 4 and 5.

The two-sided *improved 2-of-3* chart signals when the plotting statistic, T_i , plots on or above (below) the UCL_B (LCL_B) (zone 1 (zone 5)), or when two out of three consecutive plotting statistics T_{i-2} , T_{i-1} and T_i , plot on or above (below) the UCL_A (LCL_A) while plotting below (above) the UCL_B (LCL_B) (zone 2 (zone 4)). Hence the signalling events of the two-sided *improved 2-of-3* chart are:

$$\begin{aligned}
 E_{I2-of-3(T)}^1 &= \{Z_i = 1\}, \\
 E_{I2-of-3(T)}^2 &= \{Z_{i-2} = 3, Z_{i-1} = 2, Z_i = 2\}, \\
 E_{I2-of-3(T)}^3 &= \{Z_{i-2} = 2, Z_{i-1} = 3, Z_i = 2\}, \\
 E_{I2-of-3(T)}^4 &= \{Z_i = 5\}, \\
 E_{I2-of-3(T)}^5 &= \{Z_{i-2} = 3, Z_{i-1} = 4, Z_i = 4\} \\
 \text{and } E_{I2-of-3(T)}^6 &= \{Z_{i-2} = 4, Z_{i-1} = 3, Z_i = 4\}
 \end{aligned}$$

Examples of the signalling events of the two-sided *improved 2-of-3* chart are graphically illustrated in Figure 3.25. In panels (a), (b), (c), (d), (e) and (f) of Figure 3.25 there is a signal at the eighth sample.

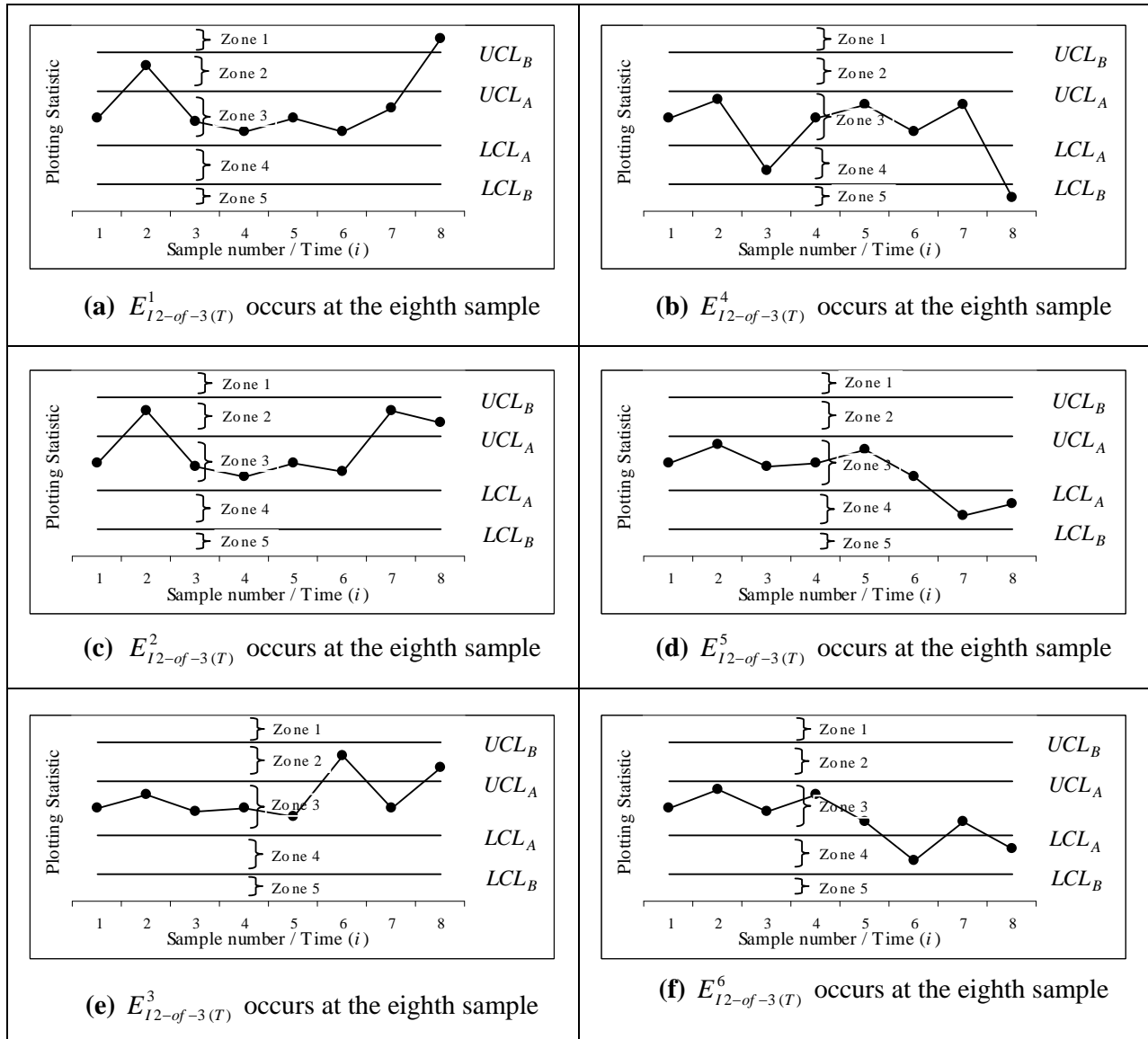


Figure 3.25: Illustrations of the signalling events of the two-sided improved 2-of-3 control chart.

Remark 3.16:

Panel (d) of Figure 3.26 illustrates combinations of plotting statistics where two of the last three plotting statistics plot on or above the UCL_A while plotting below the UCL_B (zone 2), i.e. the first two plotting statistics, T_{i-2} and T_{i-1} , plot on or above the UCL_A (zone 2), and the third plotting statistic, T_i , plots below the UCL_A (zone 3). Similarly panel (h) of Figure 3.26 illustrates a combination of plotting statistics where two of the last three plotting statistics plot on or below the LCL_A while plotting above the LCL_B (zone 4), i.e. the first two plotting statistics, T_{i-2} and T_{i-1} , plot on or below the LCL_A (zone

4), and the third plotting statistic, T_i , plots above the LCL_A (zone 3). These events are excluded as signalling events since it is undesirable in practice to have a chart that signals when the last plotting statistic, T_i , plots IC ($LCL_A < T_i < UCL_A$) (T_i plots in zone 3).

Therefore the following events are excluded as signalling events:

$$E = \{Z_{i-2} = 2, Z_{i-1} = 2, Z_i = 3\}$$

and $E = \{Z_{i-2} = 4, Z_{i-1} = 4, Z_i = 3\}$.

Remark 3.17:

However, panels (a), (c), (e) and (g) of Figure 3.26 illustrates sequences of plotting statistics where the chart does not signal since these events are not included in the signalling events $E^1_{12-of-3(T)}$, $E^2_{12-of-3(T)}$, $E^3_{12-of-3(T)}$, $E^4_{12-of-3(T)}$, $E^5_{12-of-3(T)}$ and $E^6_{12-of-3(T)}$ which is undesirable since there are clearly assignable causes present in the process. To address this issue the following two events are included as signalling events:

$$E^7_{12-of-3(T)} = \{Z_1 = 2, Z_2 = 2\}$$

and $E^8_{12-of-3(T)} = \{Z_1 = 4, Z_2 = 4\}$.

With these eight signalling events the chart signals at the second sample following the sequence of plotting statistics illustrated in panels (a), (b), (c), (d), (e), (f), (g) and (h) of Figure 3.26.

Note that in panels (d) and (h) of Figure 3.26 it is said that it is undesirable for the chart to signal where the last, in this case the third plotting statistic, plots below (above) the UCL_A (LCL_A) (zone 3). However, $E^7_{12-of-3(T)}$ and $E^8_{12-of-3(T)}$ occurs at the second plotting statistic i.e. the chart signals where the last plotting statistic (T_{i-1}) plots below (above) the LCL_A (UCL_A) i.e. plots OOC.

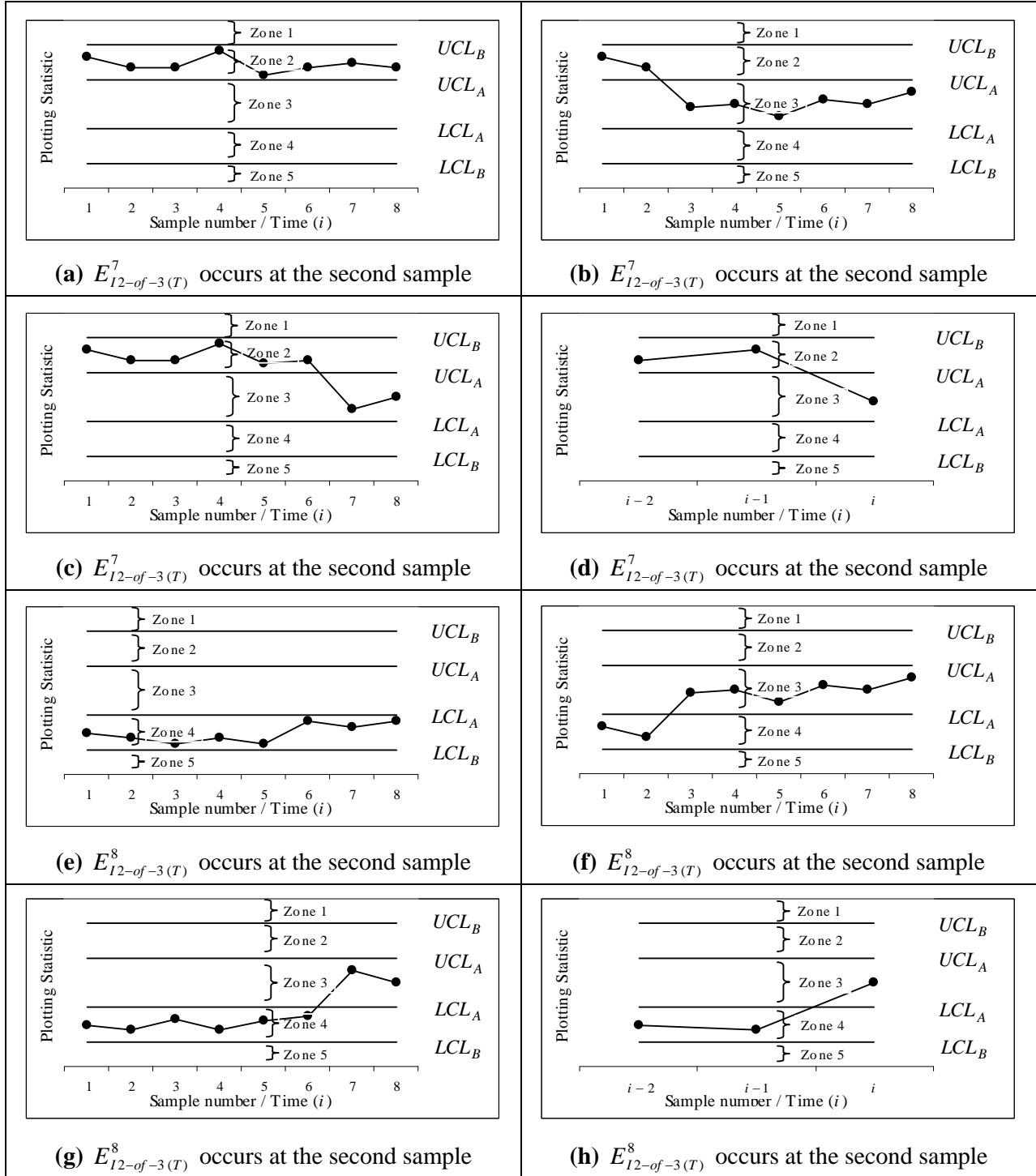


Figure 3.26: Illustrations of the signalling events of the two-sided improved 2-of-3 control chart.

Remark 3.18:

Figure 3.27 illustrates combinations of plotting statistics where two of the last three plotting statistics, T_{i-2} , T_{i-1} and T_i , plot on or above (below) the UCL_A (LCL_A) (zone 2 (zone 4)) that does not cause the two-sided *improved 2-of-3* control chart to signal. Only the detection of an upward or downward shift in the process is of interest here. Panels (a) and (b) of Figure 3.27 indicate a possible swing in the process, where panels (c) and (d) indicate a possible drift in the process. Consequently the events illustrated in panels (a), (b), (c) and (d) of Figure 3.27 are discarded as signalling events since they can not be interpreted as an upward or downward shift in the process.

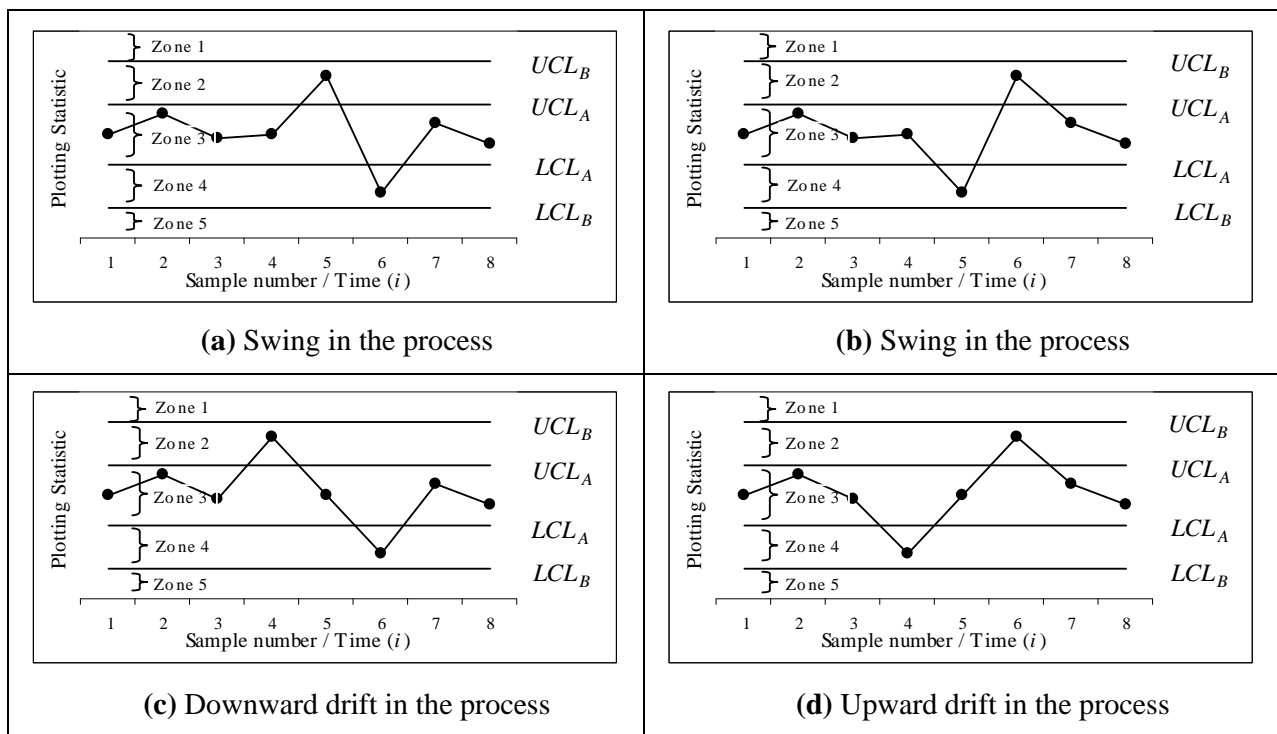


Figure 3.27: Illustrations of plotting statistic combinations that are not included as signalling events for the two-sided *improved 2-of-3* control chart.

3.2.6 Summary of the signalling events

Table 3.1: The 1-of-1 control charts (Signalling events).

The 1-of-1 control charts
Upper one-sided 1-of-1
$E_{1-of-1(U)}^1 = \{Z_i = 8\}$
Lower one-sided 1-of-1
$E_{1-of-1(L)}^1 = \{Z_i = 9\}$
Two-sided 1-of-1
$E_{1-of-1(T)}^1 = \{Z_i = 8\}$
$E_{1-of-1(T)}^2 = \{Z_i = 9\}$

Table 3.2: The 2-of-2 control charts (Signalling events).

The 2-of-2 control charts
Upper one-sided 2-of-2
$E_{2-of-2(U)}^1 = \{Z_{i-1} = 8, Z_i = 8\}$
Lower one-sided 2-of-2
$E_{2-of-2(L)}^1 = \{Z_{i-1} = 9, Z_i = 9\}$
Two-sided 2-of-2
$E_{2-of-2(T)}^1 = \{Z_{i-1} = 8, Z_i = 8\}$
$E_{2-of-2(T)}^2 = \{Z_{i-1} = 9, Z_i = 9\}$

Table 3.3: The 2-of-3 control charts (Signalling events).

The 2-of-3 control charts
Upper one-sided 2-of-3
$E_{2-of-3(U)}^1 = \{Z_{i-2} = 7, Z_{i-1} = 8, Z_i = 8\}$ $E_{2-of-3(U)}^2 = \{Z_{i-2} = 8, Z_{i-1} = 7, Z_i = 8\}$ $E_{2-of-3(U)}^3 = \{Z_1 = 8, Z_2 = 8\}$
Lower one-sided 2-of-3
$E_{2-of-3(L)}^1 = \{Z_{i-2} = 6, Z_{i-1} = 9, Z_i = 9\}$ $E_{2-of-3(L)}^2 = \{Z_{i-2} = 9, Z_{i-1} = 6, Z_i = 9\}$ $E_{2-of-3(L)}^3 = \{Z_1 = 9, Z_2 = 9\}$
Two-sided 2-of-3
$E_{2-of-3(T)}^1 = \{Z_{i-2} = 7, Z_{i-1} = 8, Z_i = 8\}$ $E_{2-of-3(T)}^2 = \{Z_{i-2} = 8, Z_{i-1} = 7, Z_i = 8\}$ $E_{2-of-3(T)}^3 = \{Z_{i-2} = 6, Z_{i-1} = 9, Z_i = 9\}$ $E_{2-of-3(T)}^4 = \{Z_{i-2} = 9, Z_{i-1} = 6, Z_i = 9\}$ $E_{2-of-3(T)}^5 = \{Z_1 = 8, Z_2 = 8\}$ $E_{2-of-3(T)}^6 = \{Z_1 = 9, Z_2 = 9\}$

Table 3.4: The *improved 2-of-2* control charts (Signalling events).

The <i>improved 2-of-2</i> control charts
Upper one-sided <i>improved 2-of-2</i>
$E_{I2-of-2(U)}^1 = \{Z_i = 1\}$ $E_{I2-of-2(U)}^2 = \{Z_{i-1} = 2, Z_i = 2\}$
Lower one-sided <i>improved 2-of-2</i>
$E_{I2-of-2(L)}^1 = \{Z_i = 5\}$ $E_{I2-of-2(L)}^2 = \{Z_{i-1} = 4, Z_i = 4\}$
Two-sided <i>improved 2-of-2</i>
$E_{I2-of-2(T)}^1 = \{Z_i = 1\}$ $E_{I2-of-2(T)}^2 = \{Z_{i-1} = 2, Z_i = 2\}$ $E_{I2-of-2(T)}^3 = \{Z_i = 5\}$ $E_{I2-of-2(T)}^4 = \{Z_{i-1} = 4, Z_i = 4\}$

Table 3.5: The *improved 2-of-3* control charts (Signalling events).

The <i>improved 2-of-3</i> control charts
Upper one-sided <i>improved 2-of-3</i>
$E_{12-of-3(U)}^1 = \{Z_i = 1\}$ $E_{12-of-3(U)}^2 = \{Z_{i-2} = 7, Z_{i-1} = 2, Z_i = 2\}$ $E_{12-of-3(U)}^3 = \{Z_{i-2} = 2, Z_{i-1} = 7, Z_i = 2\}$ $E_{12-of-3(U)}^4 = \{Z_1 = 2, Z_2 = 2\}$
Lower one-sided <i>improved 2-of-3</i>
$E_{12-of-3(L)}^1 = \{Z_i = 5\}$ $E_{12-of-3(L)}^2 = \{Z_{i-2} = 6, Z_{i-1} = 4, Z_i = 4\}$ $E_{12-of-3(L)}^3 = \{Z_{i-2} = 4, Z_{i-1} = 6, Z_i = 4\}$ $E_{12-of-3(L)}^4 = \{Z_1 = 4, Z_2 = 4\}$
Two-sided <i>improved 2-of-3</i>
$E_{12-of-3(T)}^1 = \{Z_i = 1\}$ $E_{12-of-3(T)}^2 = \{Z_{i-2} = 3, Z_{i-1} = 2, Z_i = 2\}$ $E_{12-of-3(T)}^3 = \{Z_{i-2} = 2, Z_{i-1} = 3, Z_i = 2\}$ $E_{12-of-3(T)}^4 = \{Z_i = 5\}$ $E_{12-of-3(T)}^5 = \{Z_{i-2} = 3, Z_{i-1} = 4, Z_i = 4\}$ $E_{12-of-3(T)}^6 = \{Z_{i-2} = 4, Z_{i-1} = 3, Z_i = 4\}$ $E_{12-of-3(T)}^7 = \{Z_1 = 2, Z_2 = 2\}$ $E_{12-of-3(T)}^8 = \{Z_1 = 4, Z_2 = 4\}$

Remark 3.19:

By comparing all five different charts (the *1-of-1* charts, the *2-of-2* charts, the *2-of-3* charts, the *improved 2-of-2* charts and the *improved 2-of-3* charts) there are a number of points worth mentioning.

Firstly the *1-of-1*, the *2-of-2* and the *2-of-3* charts all look the same, this can be seen in panels (a), (c) and (e) of Figure 3.2 for the upper, lower and two-sided charts respectively. The only difference between the three charts is the placement of their control limits and their signalling rules. The *2-of-2* and *2-of-3* charts have narrower limits compared to the *1-of-1* charts. Secondly the *improved 2-of-2* and the *improved 2-of-3* charts look the same this can be seen in panels (b), (d) and (f) of Figure 3.2. The only difference between these two charts is the placement of their control limits and their signalling rules.

3.3 Transition probability matrices

When using the Markov chain approach to calculate the run-length distribution and the characteristics of the run-length distribution, the transition probability matrix \mathbf{M} needs to be constructed first. The essential transition probability matrix \mathbf{Q} , i.e. a submatrix of \mathbf{M} is of special interest, since only \mathbf{Q} is required in order to calculate the run-length distribution and the characteristics of the run-length distribution (see equations (2.5), (2.6), (2.7), (2.8), (2.9) and (2.10)).

Before the transition probability matrix can be constructed, the state space of the Markov chain needs to be defined, which includes all possible events on the control chart. A state is associated with a specific location of the plotting statistic on the control chart, or a sequence of plotting statistics on the control chart. The state space and transition probability matrices for each of the different control charts considered in this dissertation are set up in the following section.

Remark 3.20:

A point that needs to be stressed is the inclusion of the dummy state “ ϕ ” to the state space Ω . The process always starts in the dummy state “ ϕ ” with probability one. A question that needs to be asked is, what this means in a SPC context, or what the state “ ϕ ” represents on the control chart? Since the dummy state “ ϕ ” is introduced so that the process starts IC with certainty, the dummy state “ ϕ ” is associated with the first plotting statistic, T_0 , plotting IC. For an upper one-sided, lower one-sided and

two-sided charts, this is equivalent to T_0 plotting below the UCL (zone 7), above the LCL (zone 6) and between the UCL and the LCL (zone 3) respectively. And for the upper one-sided *improved*, the lower one-sided *improved* and the two-sided *improved* charts this is equivalent to T_0 plotting below the UCL_A (zone 7), above the LCL_A (zone 6) and between the UCL_A and the LCL_A (zone 3) respectively.

“The number of rational subgroups to be collected or the number of charting statistics to be plotted on a control chart before the first OOC signal is observed is the run-length of a chart.”, see Human and Graham (2007). Where the run-length in the Markov chain context is the number of transitions between the states until an absorbing state is entered into, and not the number of states visited until an absorbing state is entered into. Some adjustments are made to accommodate for this difference: Firstly the plotting statistic associated with the dummy state “ ϕ ” is denoted by T_0 (with time subscript 0), the reason for this is demonstrated in Figure 3.28.

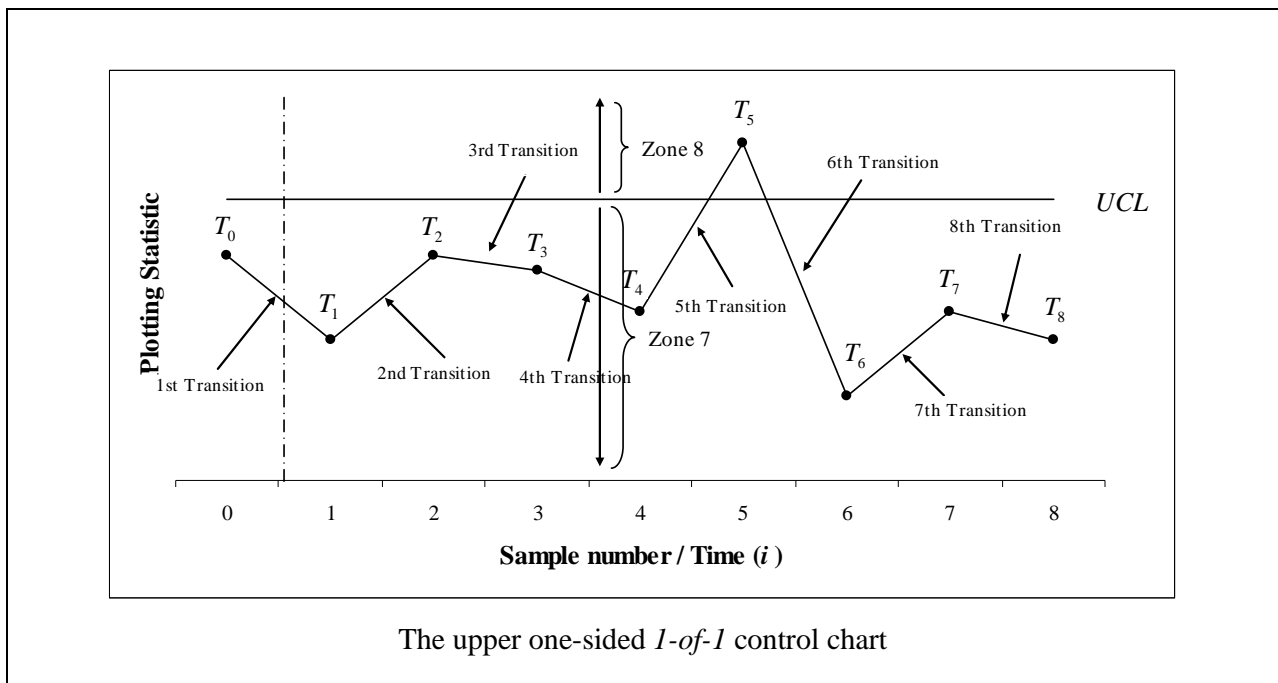


Figure 3.28: Run-length illustration.

An upper one-sided chart is used to demonstrate the adjustments made to accommodate the difference (without loss of generality). Recall that each plotting statistic or sequence of plotting statistics is associated with a state in the state space Ω . T_0 is associated with state ϕ , where T_1, T_2, T_3 and T_4 are associated with state 7, since these plotting statistics plot in zone 7 on the chart and T_5 is

associated with state 8, since the plotting statistic plots in zone 8. In the SPC context the run-length in Figure 3.28 is six, since the chart signals at the sixth plotting statistic (note that the first plotting statistic is T_0 and the sixth plotting statistic is T_5). But in the Markov chain context the run-length is five, since there are only five transitions between the states until the chart signals. To address this problem the plotting statistic T_0 associated with the dummy state “ ϕ ” is not included in the count of the run-length i.e. the count of the number of plotting statistics plotted on the control chart until the chart signals is counted from the first plotting statistic (T_1) onwards. This is a rational approach since the probabilities entered into the transition probability matrix has no influence whether the process visits or revisits state “ ϕ ” and ultimately does not influence T_0 i.e. T_0 always plots IC regardless of the probabilities entered into the transition probability matrix . When using this approach the problem associated with difference between the run-length in the SPC context and Markov chain context is solved. The run-length in Figure 3.28 is therefore five according to this understanding.

Hence the dummy state has a dual purpose, namely that the process starts IC with certainty and that the run-length count starts from the first sample (T_1) up to when the chart signals.

3.3.1 The *1-of-1* control charts

3.3.1.1 The upper one-sided *1-of-1* control chart

The random variable Z_i can assume values 7 and 8 associated with the plotting statistic T_i plotting below the UCL ($T_i < UCL$) (zone 7) and T_i plotting on or above the UCL ($T_i \geq UCL$) (zone 8) respectively. Consequently the state space of the Markov chain $\{Y_t\}$ is $\Omega = \{\phi, 7, \alpha_1\}$, where $\alpha_1 = \{8\}$ is the absorbing state. The run-length of the upper one-sided *1-of-1* control chart is the waiting time for the occurrence of the element in Λ , where $\Lambda = \{\alpha_1\}$.

$$\mathbf{M}_{3 \times 3} = \left[\begin{array}{c|c} \mathbf{Q}_{2 \times 2} & \mathbf{C}_{2 \times 1} \\ \hline \mathbf{0}_{1 \times 2} & \mathbf{I}_{1 \times 1} \end{array} \right] = \left[\begin{array}{c|c|c} p_{\phi, \phi} & p_{\phi, 7} & p_{\phi, 8} \\ \hline p_{7, \phi} & p_{7, 7} & p_{7, 8} \\ \hline p_{8, \phi} & p_{8, 7} & p_{8, 8} \end{array} \right] = \left[\begin{array}{c|c|c} 0 & p_7 & p_8 \\ \hline 0 & p_7 & p_8 \\ \hline 0 & 0 & 1 \end{array} \right]$$

$$\therefore \mathbf{Q}_{2 \times 2} = \begin{bmatrix} 0 & p_7 \\ 0 & p_7 \end{bmatrix}$$

3.3.1.2 The lower one-sided *1-of-1* control chart

The random variable Z_i can only assume values 6 and 9 associated with the plotting statistic T_i plotting above the LCL ($T_i > LCL$) (zone 6), and T_i plotting on or below the LCL ($T_i \leq LCL$) (zone 9) respectively. Consequently the state space of the Markov chain $\{Y_t\}$ is $\Omega = \{\phi, 6, \alpha_1\}$, where $\alpha_1 = \{9\}$ is the absorbing state. The run-length of the lower one-sided *1-of-1* control chart is the waiting time for the occurrence of the element in Λ , where $\Lambda = \{\alpha_1\}$.

$$\mathbf{M}_{3 \times 3} = \left[\begin{array}{c|c} \mathbf{Q}_{2 \times 2} & \mathbf{C}_{2 \times 1} \\ \hline \mathbf{0}_{1 \times 2} & \mathbf{I}_{1 \times 1} \end{array} \right] = \left[\begin{array}{c|c|c} p_{\phi, \phi} & p_{\phi, 6} & p_{\phi, 9} \\ \hline p_{6, \phi} & p_{6, 6} & p_{6, 9} \\ \hline p_{9, \phi} & p_{9, 6} & p_{9, 9} \end{array} \right] = \left[\begin{array}{c|c|c} 0 & p_6 & p_9 \\ \hline 0 & p_6 & p_9 \\ \hline 0 & 0 & 1 \end{array} \right]$$

$$\therefore \mathbf{Q}_{2 \times 2} = \begin{bmatrix} 0 & p_6 \\ 0 & p_6 \end{bmatrix}$$

3.3.1.3 The two-sided *I-of-1* control chart

The random variable Z_i can assume values 3, 8 and 9 associated with the plotting statistic T_i plotting between the control limits ($LCL < T_i < UCL$) (zone 3), on or above the UCL ($T_i \geq UCL$) (zone 8) and T_i plotting on or below the LCL ($T_i \leq LCL$) (zone 9) respectively. Consequently the state space of the Markov chain $\{Y_t\}$ is $\Omega = \{\phi, 3, \alpha_1, \alpha_2\}$, where $\alpha_1 = \{8\}$ and $\alpha_2 = \{9\}$ are the absorbing states. The run-length of the two-sided *I-of-1* control chart is the waiting time for the occurrence of one of the elements in Λ , where $\Lambda = \{\alpha_1, \alpha_2\}$.

$$\mathbf{M}_{4 \times 4} = \begin{bmatrix} \mathbf{Q}_{2 \times 2} & \mathbf{C}_{2 \times 2} \\ \mathbf{0}_{2 \times 2} & \mathbf{I}_{2 \times 2} \end{bmatrix} = \begin{bmatrix} p_{\phi, \phi} & p_{\phi, 3} & p_{\phi, 8} & p_{\phi, 9} \\ p_{3, \phi} & p_{3, 3} & p_{3, 8} & p_{3, 9} \\ p_{8, \phi} & p_{8, 3} & p_{8, 8} & p_{8, 9} \\ p_{9, \phi} & p_{9, 3} & p_{9, 8} & p_{9, 9} \end{bmatrix} = \begin{bmatrix} 0 & p_3 & p_8 & p_9 \\ 0 & p_3 & p_8 & p_9 \\ 0 & 0 & 1 & 0 \\ 0 & 0 & 0 & 1 \end{bmatrix}$$

$$\therefore \mathbf{Q}_{2 \times 2} = \begin{bmatrix} 0 & p_3 \\ 0 & p_3 \end{bmatrix}$$

3.3.2 The 2-of-2 control charts

3.3.2.1 The upper one-sided 2-of-2 control chart

The random variable Z_i can only assume values 7 and 8 associated with the plotting statistic T_i plotting below the UCL ($T_i < UCL$) (zone 7) and T_i plotting on or above the UCL ($T_i \geq UCL$) (zone 8) respectively. Consequently the state space of the Markov chain $\{Y_i\}$ is $\Omega = \{\phi, 7, 8, \alpha_1\}$, where $\alpha_1 = \{88\}$ is the absorbing state associated with two consecutive plotting statistics plotting on or above the UCL . The run-length of the upper one-sided 2-of-2 control chart is the waiting time for the occurrence of the element in Λ , where $\Lambda = \{\alpha_1\}$.

$$\mathbf{M}_{4 \times 4} = \left[\begin{array}{c|c} \mathbf{Q}_{3 \times 3} & \mathbf{C}_{3 \times 1} \\ \hline \mathbf{0}_{1 \times 3} & \mathbf{I}_{1 \times 1} \end{array} \right] = \left[\begin{array}{cccc|c} P_{\phi,\phi} & P_{\phi,7} & P_{\phi,8} & P_{\phi,88} & \\ P_{7,\phi} & P_{7,7} & P_{7,8} & P_{7,88} & \\ P_{8,\phi} & P_{8,7} & P_{8,8} & P_{8,88} & \\ \hline P_{88,\phi} & P_{88,7} & P_{88,8} & P_{88,88} & \end{array} \right] = \left[\begin{array}{ccc|c} 0 & p_7 & p_8 & 0 \\ 0 & p_7 & p_8 & 0 \\ 0 & p_7 & 0 & p_8 \\ \hline 0 & 0 & 0 & 1 \end{array} \right]$$

$$\therefore \mathbf{Q}_{3 \times 3} = \begin{bmatrix} 0 & p_7 & p_8 \\ 0 & p_7 & p_8 \\ 0 & p_7 & 0 \end{bmatrix}$$

3.3.2.2 The lower one-sided 2-of-2 control chart

The random variable Z_i can only assume values 6 and 9 associated with the plotting statistic T_i plotting above the LCL ($T_i > LCL$) (zone 6) and T_i plotting on or below the LCL ($T_i \leq LCL$) (zone 9) respectively. Consequently the state space of the Markov chain $\{Y_i\}$ is $\Omega = \{\phi, 6, 9, \alpha_1\}$, where $\alpha_1 = \{99\}$ is the absorbing state associated with two consecutive plotting statistics plotting on or below the LCL . The run-length of the lower one-sided 2-of-2 control chart is the waiting time for the occurrence of the element in Λ , where $\Lambda = \{\alpha_1\}$.

$$\mathbf{M}_{4 \times 4} = \left[\begin{array}{c|c} \mathbf{Q}_{3 \times 3} & \mathbf{C}_{3 \times 1} \\ \hline \mathbf{0}_{1 \times 3} & \mathbf{I}_{1 \times 1} \end{array} \right] = \left[\begin{array}{cccc|c} P_{\phi,\phi} & P_{\phi,6} & P_{\phi,9} & P_{\phi,99} & \\ P_{6,\phi} & P_{6,6} & P_{6,9} & P_{6,99} & \\ P_{9,\phi} & P_{9,6} & P_{9,9} & P_{99,99} & \\ \hline P_{99,\phi} & P_{99,6} & P_{99,9} & P_{99,99} & \end{array} \right] = \left[\begin{array}{ccc|c} 0 & p_6 & p_9 & 0 \\ 0 & p_6 & p_9 & 0 \\ 0 & p_6 & 0 & p_9 \\ \hline 0 & 0 & 0 & 1 \end{array} \right]$$

$$\therefore \mathbf{Q}_{3 \times 3} = \begin{bmatrix} 0 & p_6 & p_9 \\ 0 & p_6 & p_9 \\ 0 & p_6 & 0 \end{bmatrix}$$

3.3.2.3 The two-sided 2-of-2 control chart

The random variable Z_i can assume values 3, 8 and 9 associated with the plotting statistic T_i plotting between the control limits ($LCL < T_i < UCL$) (zone 3), on or above the UCL ($T_i \geq UCL$) (zone 8) and T_i plotting on or below LCL the ($T_i \leq LCL$) (zone 9) respectively. Consequently the state space of the Markov chain $\{Y_t\}$ is $\Omega = \{\phi, 3, 8, 9, \alpha_1, \alpha_2\}$, where $\alpha_1 = \{88\}$ and $\alpha_2 = \{99\}$ are the absorbing states associated with two consecutive plotting statistics plotting on or above (below) the UCL (LCL). The run-length of the two-sided 2-of-2 control chart is the waiting time for the occurrence of one of the elements in Λ , where $\Lambda = \{\alpha_1, \alpha_2\}$.

$$\begin{aligned} \mathbf{M}_{6 \times 6} &= \left[\begin{array}{c|c} \mathbf{Q}_{4 \times 4} & \mathbf{C}_{4 \times 2} \\ \hline \mathbf{0}_{2 \times 4} & \mathbf{I}_{2 \times 2} \end{array} \right] = \begin{bmatrix} P_{\phi,\phi} & P_{\phi,3} & P_{\phi,8} & P_{\phi,9} & P_{\phi,88} & P_{\phi,99} \\ P_{3,\phi} & P_{3,3} & P_{3,8} & P_{3,9} & P_{3,88} & P_{3,99} \\ P_{8,\phi} & P_{8,3} & P_{8,8} & P_{8,9} & P_{8,88} & P_{8,99} \\ P_{9,\phi} & P_{9,3} & P_{9,8} & P_{9,9} & P_{9,88} & P_{9,99} \\ \hline P_{88,\phi} & P_{88,3} & P_{88,8} & P_{88,9} & P_{88,88} & P_{88,99} \\ P_{99,\phi} & P_{99,3} & P_{99,8} & P_{99,9} & P_{99,88} & P_{99,99} \end{bmatrix} \\ &= \begin{bmatrix} 0 & p_3 & p_8 & p_9 & 0 & 0 \\ 0 & p_3 & p_8 & p_9 & 0 & 0 \\ 0 & p_3 & 0 & p_9 & p_8 & 0 \\ 0 & p_3 & p_8 & 0 & 0 & p_9 \\ \hline 0 & 0 & 0 & 0 & 1 & 0 \\ 0 & 0 & 0 & 0 & 0 & 1 \end{bmatrix} \\ &\therefore \mathbf{Q}_{4 \times 4} = \begin{bmatrix} 0 & p_3 & p_8 & p_9 \\ 0 & p_3 & p_8 & p_9 \\ 0 & p_3 & 0 & p_9 \\ 0 & p_3 & p_8 & 0 \end{bmatrix} \end{aligned}$$

3.3.3 The 2-of-3 control charts

3.3.3.1 The upper one-sided 2-of-3 control chart

The random variable Z_i can assume values 7 and 8 associated with the plotting statistic T_i plotting below the UCL ($T_i < UCL$) (zone 7), and T_i plotting on or above the UCL ($T_i \geq UCL$) (zone 8) respectively. Consequently the state space of the Markov chain $\{Y_i\}$ is $\Omega = \{\phi, 7, 8, 78, 87, \alpha_1, \alpha_2, \alpha_3\}$, where $\alpha_1 = \{88\}$, $\alpha_2 = \{788\}$ and $\alpha_3 = \{878\}$ are the absorbing states. The run-length of the upper one-sided 2-of-3 control chart is the waiting time for the occurrence of one of the elements in Λ , where $\Lambda = \{\alpha_1, \alpha_2, \alpha_3\}$.

$$\mathbf{M}_{8 \times 8} = \left[\begin{array}{c|c} \mathbf{Q}_{5 \times 5} & \mathbf{C}_{5 \times 3} \\ \hline \mathbf{0}_{3 \times 5} & \mathbf{I}_{3 \times 3} \end{array} \right] = \left[\begin{array}{ccccc|ccc} P_{\phi,\phi} & P_{\phi,7} & P_{\phi,8} & P_{\phi,78} & P_{\phi,87} & P_{\phi,88} & P_{\phi,788} & P_{\phi,878} \\ P_{7,\phi} & P_{7,7} & P_{7,8} & P_{7,78} & P_{7,87} & P_{7,88} & P_{7,788} & P_{7,878} \\ P_{8,\phi} & P_{8,7} & P_{8,8} & P_{8,78} & P_{8,87} & P_{8,88} & P_{8,788} & P_{8,878} \\ P_{78,\phi} & P_{78,7} & P_{78,8} & P_{78,78} & P_{78,87} & P_{78,88} & P_{78,788} & P_{78,878} \\ P_{87,\phi} & P_{87,7} & P_{87,8} & P_{87,78} & P_{87,87} & P_{87,88} & P_{87,788} & P_{87,878} \\ \hline P_{88,\phi} & P_{88,7} & P_{88,8} & P_{88,78} & P_{88,87} & P_{88,88} & P_{88,788} & P_{88,878} \\ P_{788,\phi} & P_{788,7} & P_{788,8} & P_{788,78} & P_{788,87} & P_{788,88} & P_{788,788} & P_{788,878} \\ P_{878,\phi} & P_{878,7} & P_{878,8} & P_{878,78} & P_{878,87} & P_{878,88} & P_{878,788} & P_{878,878} \end{array} \right] \\
 = \left[\begin{array}{ccccc|ccc} 0 & p_7 & p_8 & 0 & 0 & 0 & 0 & 0 \\ 0 & p_7 & 0 & p_8 & 0 & 0 & 0 & 0 \\ 0 & 0 & 0 & 0 & p_7 & p_8 & 0 & 0 \\ 0 & 0 & 0 & 0 & p_7 & 0 & p_8 & 0 \\ 0 & p_7 & 0 & 0 & 0 & 0 & 0 & p_8 \\ \hline 0 & 0 & 0 & 0 & 0 & 1 & 0 & 0 \\ 0 & 0 & 0 & 0 & 0 & 0 & 1 & 0 \\ 0 & 0 & 0 & 0 & 0 & 0 & 0 & 1 \end{array} \right] \\
 \therefore \mathbf{Q}_{5 \times 5} = \left[\begin{array}{ccccc} 0 & p_7 & p_8 & 0 & 0 \\ 0 & p_7 & 0 & p_8 & 0 \\ 0 & 0 & 0 & 0 & p_7 \\ 0 & 0 & 0 & 0 & p_7 \\ 0 & p_7 & 0 & 0 & 0 \end{array} \right]$$

3.3.3.2 The lower one-sided 2-of-3 control chart

The random variable Z_i can only assume values 6 and 9, associated with the plotting statistic T_i plotting above the LCL ($T_i > LCL$) (zone 6), and T_i plotting on or below the LCL ($T_i \leq LCL$) (zone 9) respectively. Consequently the state space of the Markov chain $\{Y_t\}$ is $\Omega = \{\phi, 6, 9, 69, 96, \alpha_1, \alpha_2, \alpha_3\}$, where $\alpha_1 = \{99\}$, $\alpha_2 = \{699\}$ and $\alpha_3 = \{969\}$ are the absorbing states. The run-length of the lower one-sided 2-of-3 control chart is the waiting time for the occurrence of one of the elements in Λ , where $\Lambda = \{\alpha_1, \alpha_2, \alpha_3\}$.

$$\begin{aligned}
 \mathbf{M}_{8 \times 8} &= \begin{bmatrix} \mathbf{Q}_{5 \times 5} & \mathbf{C}_{5 \times 3} \\ \mathbf{0}_{3 \times 5} & \mathbf{I}_{3 \times 3} \end{bmatrix} = \begin{bmatrix} P_{\phi,\phi} & P_{\phi,6} & P_{\phi,9} & P_{\phi,69} & P_{\phi,96} & P_{\phi,99} & P_{\phi,699} & P_{\phi,969} \\ P_{6,\phi} & P_{6,6} & P_{6,9} & P_{6,69} & P_{6,96} & P_{6,99} & P_{6,699} & P_{6,969} \\ P_{9,\phi} & P_{9,6} & P_{9,9} & P_{9,69} & P_{9,96} & P_{9,99} & P_{9,699} & P_{9,969} \\ P_{69,\phi} & P_{69,6} & P_{69,9} & P_{69,69} & P_{69,96} & P_{69,99} & P_{69,699} & P_{69,969} \\ P_{96,\phi} & P_{96,6} & P_{96,9} & P_{96,69} & P_{96,96} & P_{96,99} & P_{96,699} & P_{96,969} \\ P_{99,\phi} & P_{99,6} & P_{99,9} & P_{99,69} & P_{99,96} & P_{99,99} & P_{99,699} & P_{99,969} \\ P_{699,\phi} & P_{699,6} & P_{699,9} & P_{699,69} & P_{699,96} & P_{699,99} & P_{699,699} & P_{699,969} \\ P_{969,\phi} & P_{969,6} & P_{969,9} & P_{969,69} & P_{969,96} & P_{969,99} & P_{969,699} & P_{969,969} \end{bmatrix} \\
 &= \begin{bmatrix} 0 & p_6 & p_9 & 0 & 0 & 0 & 0 & 0 \\ 0 & p_6 & 0 & p_9 & 0 & 0 & 0 & 0 \\ 0 & 0 & 0 & 0 & p_6 & p_9 & 0 & 0 \\ 0 & 0 & 0 & 0 & p_6 & 0 & p_9 & 0 \\ 0 & p_6 & 0 & 0 & 0 & 0 & 0 & p_9 \\ \hline 0 & 0 & 0 & 0 & 0 & 1 & 0 & 0 \\ 0 & 0 & 0 & 0 & 0 & 0 & 1 & 0 \\ 0 & 0 & 0 & 0 & 0 & 0 & 0 & 1 \end{bmatrix} \\
 \therefore \mathbf{Q}_{5 \times 5} &= \begin{bmatrix} 0 & p_6 & p_9 & 0 & 0 \\ 0 & p_6 & 0 & p_9 & 0 \\ 0 & 0 & 0 & 0 & p_6 \\ 0 & 0 & 0 & 0 & p_6 \\ 0 & p_6 & 0 & 0 & 0 \end{bmatrix}
 \end{aligned}$$

3.3.3.3 The two-sided 2-of-3 control chart

The random variable Z_i can assume values 3, 8 and 9 associated with the plotting statistic T_i plotting between the control limits ($LCL < T_i < UCL$) (zone 3), on or above the UCL ($T_i \geq UCL$) (zone 8) and T_i plotting on or below the LCL ($T_i \leq LCL$) (zone 9) respectively. Consequently the state space of the Markov chain $\{Y_i\}$ is $\Omega = \{\phi, 3, 8, 9, 38, 39, 83, 93, \alpha_1, \alpha_2, \alpha_3, \alpha_4, \alpha_5, \alpha_6\}$, where $\alpha_1 = \{88\}$, $\alpha_2 = \{99\}$, $\alpha_3 = \{388\}$, $\alpha_4 = \{399\}$, $\alpha_5 = \{838\}$ and $\alpha_6 = \{939\}$ are the absorbing states. The run-length of the two-sided 2-of-3 control chart is the waiting time for the occurrence of one of the elements in Λ , where $\Lambda = \{\alpha_1, \alpha_2, \alpha_3, \alpha_4, \alpha_5, \alpha_6\}$.

$$\mathbf{M}_{14 \times 14} = \begin{bmatrix} \mathbf{Q}_{8 \times 8} & \mathbf{C}_{8 \times 6} \\ \mathbf{0}_{6 \times 8} & \mathbf{I}_{6 \times 6} \end{bmatrix}$$

$$= \begin{bmatrix} P_{\phi, \phi} & P_{\phi, 3} & P_{\phi, 8} & P_{\phi, 9} & P_{\phi, 38} & P_{\phi, 39} & P_{\phi, 83} & P_{\phi, 93} & P_{\phi, 88} & P_{\phi, 99} & P_{\phi, 388} & P_{\phi, 399} & P_{\phi, 838} & P_{\phi, 939} \\ P_{3, \phi} & P_{3, 3} & P_{3, 8} & P_{3, 9} & P_{3, 38} & P_{3, 39} & P_{3, 83} & P_{3, 93} & P_{3, 88} & P_{3, 99} & P_{3, 388} & P_{3, 399} & P_{3, 838} & P_{3, 939} \\ P_{8, \phi} & P_{8, 3} & P_{8, 8} & P_{8, 9} & P_{8, 38} & P_{8, 39} & P_{8, 83} & P_{8, 93} & P_{8, 88} & P_{8, 99} & P_{8, 388} & P_{8, 399} & P_{8, 838} & P_{8, 939} \\ P_{9, \phi} & P_{9, 3} & P_{9, 8} & P_{9, 9} & P_{9, 38} & P_{9, 39} & P_{9, 83} & P_{9, 93} & P_{9, 88} & P_{9, 99} & P_{9, 388} & P_{9, 399} & P_{9, 838} & P_{9, 939} \\ P_{38, \phi} & P_{38, 3} & P_{38, 8} & P_{38, 9} & P_{38, 38} & P_{38, 39} & P_{38, 83} & P_{38, 93} & P_{38, 88} & P_{38, 99} & P_{38, 388} & P_{38, 399} & P_{38, 838} & P_{38, 939} \\ P_{39, \phi} & P_{39, 3} & P_{39, 8} & P_{39, 9} & P_{39, 38} & P_{39, 39} & P_{39, 83} & P_{39, 93} & P_{39, 88} & P_{39, 99} & P_{39, 388} & P_{39, 399} & P_{39, 838} & P_{39, 939} \\ P_{83, \phi} & P_{83, 3} & P_{83, 8} & P_{83, 9} & P_{83, 38} & P_{83, 39} & P_{83, 83} & P_{83, 93} & P_{83, 88} & P_{83, 99} & P_{83, 388} & P_{83, 399} & P_{83, 838} & P_{83, 939} \\ P_{93, \phi} & P_{93, 3} & P_{93, 8} & P_{93, 9} & P_{93, 38} & P_{93, 39} & P_{93, 83} & P_{93, 93} & P_{93, 88} & P_{93, 99} & P_{93, 388} & P_{93, 399} & P_{93, 838} & P_{93, 939} \\ \hline P_{88, \phi} & P_{88, 3} & P_{88, 8} & P_{88, 9} & P_{88, 38} & P_{88, 39} & P_{88, 83} & P_{88, 93} & P_{88, 88} & P_{88, 99} & P_{88, 388} & P_{88, 399} & P_{88, 838} & P_{88, 939} \\ P_{99, \phi} & P_{99, 3} & P_{99, 8} & P_{99, 9} & P_{99, 38} & P_{99, 39} & P_{99, 83} & P_{99, 93} & P_{99, 88} & P_{99, 99} & P_{99, 388} & P_{99, 399} & P_{99, 838} & P_{99, 939} \\ P_{388, \phi} & P_{388, 3} & P_{388, 8} & P_{388, 9} & P_{388, 38} & P_{388, 39} & P_{388, 83} & P_{388, 93} & P_{388, 88} & P_{388, 99} & P_{388, 388} & P_{388, 399} & P_{388, 838} & P_{388, 939} \\ P_{399, \phi} & P_{399, 3} & P_{399, 8} & P_{399, 9} & P_{399, 38} & P_{399, 39} & P_{399, 83} & P_{399, 93} & P_{399, 88} & P_{399, 99} & P_{399, 388} & P_{399, 399} & P_{399, 838} & P_{399, 939} \\ P_{838, \phi} & P_{838, 3} & P_{838, 8} & P_{838, 9} & P_{838, 38} & P_{838, 39} & P_{838, 83} & P_{838, 93} & P_{838, 88} & P_{838, 99} & P_{838, 388} & P_{838, 399} & P_{838, 838} & P_{838, 939} \\ P_{939, \phi} & P_{939, 3} & P_{939, 8} & P_{939, 9} & P_{939, 38} & P_{939, 39} & P_{939, 83} & P_{939, 93} & P_{939, 88} & P_{939, 99} & P_{939, 388} & P_{939, 399} & P_{939, 838} & P_{939, 939} \end{bmatrix}$$

$$= \begin{bmatrix} 0 & p_3 & p_8 & p_9 & 0 & 0 & 0 & 0 & 0 & 0 & 0 & 0 & 0 & 0 \\ 0 & p_3 & 0 & 0 & p_8 & p_9 & 0 & 0 & 0 & 0 & 0 & 0 & 0 & 0 \\ 0 & 0 & 0 & p_9 & 0 & 0 & p_3 & 0 & p_8 & 0 & 0 & 0 & 0 & 0 \\ 0 & 0 & p_8 & 0 & 0 & 0 & 0 & p_3 & 0 & p_9 & 0 & 0 & 0 & 0 \\ 0 & 0 & 0 & p_9 & 0 & 0 & p_3 & 0 & 0 & 0 & p_8 & 0 & 0 & 0 \\ 0 & 0 & p_8 & 0 & 0 & 0 & 0 & p_3 & 0 & 0 & 0 & p_9 & 0 & 0 \\ 0 & p_3 & 0 & 0 & 0 & p_9 & 0 & 0 & 0 & 0 & 0 & 0 & p_8 & 0 \\ 0 & p_3 & 0 & 0 & p_8 & 0 & 0 & 0 & 0 & 0 & 0 & 0 & 0 & p_9 \\ \hline 0 & 0 & 0 & 0 & 0 & 0 & 0 & 0 & 1 & 0 & 0 & 0 & 0 & 0 \\ 0 & 0 & 0 & 0 & 0 & 0 & 0 & 0 & 0 & 1 & 0 & 0 & 0 & 0 \\ 0 & 0 & 0 & 0 & 0 & 0 & 0 & 0 & 0 & 0 & 1 & 0 & 0 & 0 \\ 0 & 0 & 0 & 0 & 0 & 0 & 0 & 0 & 0 & 0 & 0 & 1 & 0 & 0 \\ 0 & 0 & 0 & 0 & 0 & 0 & 0 & 0 & 0 & 0 & 0 & 0 & 1 & 0 \\ 0 & 0 & 0 & 0 & 0 & 0 & 0 & 0 & 0 & 0 & 0 & 0 & 0 & 1 \end{bmatrix}$$

$$\therefore \mathbf{Q}_{8 \times 8} = \begin{bmatrix} 0 & p_3 & p_8 & p_9 & 0 & 0 & 0 & 0 \\ 0 & p_3 & 0 & 0 & p_8 & p_9 & 0 & 0 \\ 0 & 0 & 0 & p_9 & 0 & 0 & p_3 & 0 \\ 0 & 0 & p_8 & 0 & 0 & 0 & 0 & p_3 \\ 0 & 0 & 0 & p_9 & 0 & 0 & p_3 & 0 \\ 0 & 0 & p_8 & 0 & 0 & 0 & 0 & p_3 \\ 0 & p_3 & 0 & 0 & 0 & p_9 & 0 & 0 \\ 0 & p_3 & 0 & 0 & p_8 & 0 & 0 & 0 \end{bmatrix}$$

Remark 3.21:

The transition probability matrix \mathbf{M} , is constructed in such a manner that when the Markov chain is in state $\{9\}$ or $\{39\}$ at sample $i-1$, and the plotting statistic T_i plots on or above the UCL (zone 8), the Markov chain moves to state $\{8\}$ and if the following plotting statistic also plots on or above the UCL (zone 8) the chart signals since the process moves to the absorbing state $\{88\}$, illustrated in panel (a) of Figure 3.29. If the Markov chain is in state $\{8\}$ or $\{38\}$ at sample $i-1$, and the plotting statistic T_i plots on or below the LCL (zone 9), the Markov chain moves to state $\{9\}$ and if the following plotting statistic plots on or below the LCL (zone 9) the process moves to the absorbing state $\{99\}$, illustrated in Figure 3.29 panel (b). These sequences of plotting statistics illustrated in Figure 3.29 are interpreted as upward or downward shifts in the process since in each panel in Figure 3.29 there is at least two consecutive plotting statistics plotted above (below) the UCL (LCL).

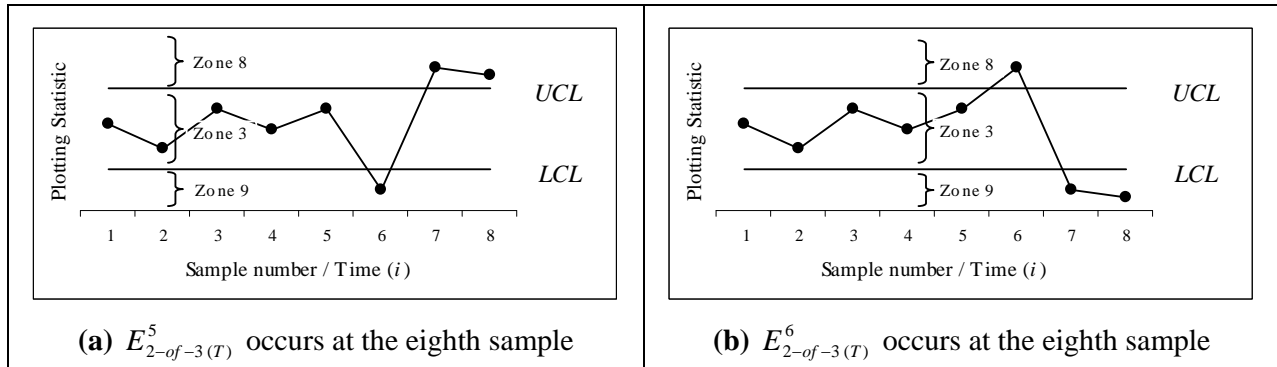


Figure 3.29: Illustrations to help explain some of the signalling events and transitions in the transition probability matrix of the two-sided 2-of-3 control chart.

Remark 3.22:

Note that Human et al. (2009)'s 2-of-3 control charts excluded the signalling events $E_{2-of-3}^3(U) = \{Z_1 = 8, Z_2 = 8\}$, $E_{2-of-3}^3(L) = \{Z_1 = 9, Z_2 = 9\}$, $E_{2-of-3}^5(T) = \{Z_1 = 8, Z_2 = 8\}$ and $E_{2-of-3}^6(T) = \{Z_1 = 9, Z_2 = 9\}$, therefore the 2-of-3 control charts given here differ slightly to Human et al. (2009)'s 2-of-3 control charts. Consequently the 2-of-3 control chart transition probability matrices also differ slightly. The motivation for the alterations is that the *improved* runs-rules control charts has a clear advantage over and above the runs-rules control charts when there is a large shift in the process. The transition probability matrices are needed to study the OOC performance of the control charts, which are necessary to show the advantage of *improved* runs-rules. Performance comparisons between runs-rules and *improved* runs-rules control charts are very limited using Human et al. (2009)'s transition probability matrices, since given large shifts in the process and using Human et al. (2009)'s transition probability matrix, the run-length tends to infinity, which is undesirable.

3.3.4 The *improved 2-of-2* control charts

3.3.4.1 The upper one-sided *improved 2-of-2* control chart

The random variable Z_i can assume values 1, 2 and 7, associated with the plotting statistic T_i plotting on or above UCL_B ($T_i \geq UCL_B$) (zone 1), plotting between UCL_A and UCL_B ($UCL_A \leq T_i < UCL_B$) (zone 2) and plotting below UCL_A ($T_i < UCL_A$) (zone 7) respectively. Consequently the state space of the Markov chain $\{Y_t\}$ is, $\Omega = \{\phi, 7, 2, \alpha_1, \alpha_2\}$, where $\alpha_1 = \{1\}$ and $\alpha_2 = \{22\}$ are the absorbing states. The run-length of the upper one-sided *improved 2-of-2* control chart is the waiting time for the occurrence of one of the elements in Λ , where $\Lambda = \{\alpha_1, \alpha_2\}$.

$$\mathbf{M}_{5 \times 5} = \left[\begin{array}{c|c} \mathbf{Q}_{3 \times 3} & \mathbf{C}_{3 \times 2} \\ \hline \mathbf{0}_{2 \times 3} & \mathbf{I}_{2 \times 2} \end{array} \right] = \left[\begin{array}{ccc|cc} P_{\phi,\phi} & P_{\phi,7} & P_{\phi,2} & P_{\phi,1} & P_{\phi,22} \\ P_{7,\phi} & P_{7,7} & P_{7,2} & P_{7,1} & P_{7,22} \\ P_{2,\phi} & P_{2,7} & P_{2,2} & P_{2,1} & P_{2,22} \\ \hline P_{1,\phi} & P_{1,7} & P_{1,2} & P_{1,1} & P_{1,22} \\ P_{22,\phi} & P_{22,7} & P_{22,2} & P_{22,1} & P_{22,22} \end{array} \right] = \left[\begin{array}{ccc|cc} 0 & p_7 & p_2 & p_1 & 0 \\ 0 & p_7 & p_2 & p_1 & 0 \\ 0 & p_7 & 0 & p_1 & p_2 \\ \hline 0 & 0 & 0 & 1 & 0 \\ 0 & 0 & 0 & 0 & 1 \end{array} \right]$$

$$\therefore \mathbf{Q}_{3 \times 3} = \begin{bmatrix} 0 & p_7 & p_2 \\ 0 & p_7 & p_2 \\ 0 & p_7 & 0 \end{bmatrix}$$

3.3.4.2 The lower one-sided *improved 2-of-2* control chart

The random variable Z_i can assume values 5, 4 and 6, associated with the plotting statistic T_i plotting on or below LCL_B ($T_i \leq LCL_B$) (zone 5), plotting between LCL_A and LCL_B ($LCL_B < T_i \leq LCL_A$) (zone 4) and plotting above LCL_A ($T_i > LCL_A$) (zone 6) respectively. Consequently the state space of the Markov chain $\{Y_t\}$ is, $\Omega = \{\phi, 6, 4, \alpha_1, \alpha_2\}$, where $\alpha_1 = \{5\}$ and $\alpha_2 = \{44\}$ are the absorbing states. The run-length of the lower one-sided *improved 2-of-2* control chart is the waiting time for the occurrence of one of the elements in Λ , where $\Lambda = \{\alpha_1, \alpha_2\}$.

$$\mathbf{M}_{5 \times 5} = \left[\begin{array}{c|c} \mathbf{Q}_{3 \times 3} & \mathbf{C}_{3 \times 2} \\ \hline \mathbf{0}_{2 \times 3} & \mathbf{I}_{2 \times 2} \end{array} \right] = \left[\begin{array}{ccc|cc} P_{\phi,\phi} & P_{\phi,6} & P_{\phi,4} & P_{\phi,5} & P_{\phi,44} \\ P_{6,\phi} & P_{6,6} & P_{6,4} & P_{6,5} & P_{6,44} \\ P_{4,\phi} & P_{4,6} & P_{4,4} & P_{4,5} & P_{4,44} \\ \hline P_{5,\phi} & P_{5,6} & P_{5,4} & P_{5,5} & P_{5,44} \\ P_{44,\phi} & P_{44,6} & P_{44,4} & P_{44,5} & P_{44,44} \end{array} \right] = \left[\begin{array}{ccc|cc} 0 & p_6 & p_4 & p_5 & 0 \\ 0 & p_6 & p_4 & p_5 & 0 \\ 0 & p_6 & 0 & p_5 & p_4 \\ \hline 0 & 0 & 0 & 1 & 0 \\ 0 & 0 & 0 & 0 & 1 \end{array} \right]$$

$$\therefore \mathbf{Q}_{3 \times 3} = \begin{bmatrix} 0 & p_6 & p_4 \\ 0 & p_6 & p_4 \\ 0 & p_6 & 0 \end{bmatrix}$$

3.3.4.3 The two-sided *improved 2-of-2* control chart

The random variable Z_i can assume values 1, 2, 3, 4 and 5, associated with the plotting statistic T_i plotting on or above UCL_B ($T_i \geq UCL_B$) (zone 1), between UCL_A and UCL_B ($UCL_A \leq T_i < UCL_B$) (zone 2), between LCL_A and UCL_A ($LCL_A < T_i < UCL_A$) (zone 3), between LCL_A and LCL_B ($LCL_B < T_i \leq LCL_A$) (zone 4), and T_i plotting on or below LCL_B ($T_i \leq LCL_B$) (zone 5) respectively. Consequently the state space of the Markov chain $\{Y_i\}$ is, $\Omega = \{\phi, 3, 2, 4, \alpha_1, \alpha_2, \alpha_3, \alpha_4\}$, where $\alpha_1 = \{1\}$, $\alpha_2 = \{5\}$, $\alpha_3 = \{22\}$ and $\alpha_4 = \{44\}$ are the absorbing states. The run-length of the two-sided *improved 2-of-2* control chart is the waiting time for the occurrence of one of the elements in Λ , where $\Lambda = \{\alpha_1, \alpha_2, \alpha_3, \alpha_4\}$.

$$\mathbf{M}_{8 \times 8} = \begin{bmatrix} \mathbf{Q}_{4 \times 4} & \mathbf{C}_{4 \times 4} \\ \mathbf{0}_{4 \times 4} & \mathbf{I}_{4 \times 4} \end{bmatrix} = \begin{bmatrix} p_{\phi,\phi} & p_{\phi,3} & p_{\phi,2} & p_{\phi,4} & p_{\phi,1} & p_{\phi,5} & p_{\phi,22} & p_{\phi,44} \\ p_{3,\phi} & p_{3,3} & p_{3,2} & p_{3,4} & p_{3,1} & p_{3,5} & p_{3,22} & p_{3,44} \\ p_{2,\phi} & p_{2,3} & p_{2,2} & p_{2,4} & p_{2,1} & p_{2,5} & p_{2,22} & p_{2,44} \\ p_{4,\phi} & p_{4,3} & p_{4,2} & p_{4,4} & p_{4,1} & p_{4,5} & p_{4,22} & p_{4,44} \\ p_{1,\phi} & p_{1,3} & p_{1,2} & p_{1,4} & p_{1,1} & p_{1,5} & p_{1,22} & p_{1,44} \\ p_{5,\phi} & p_{5,3} & p_{5,2} & p_{5,4} & p_{5,1} & p_{5,5} & p_{5,22} & p_{5,44} \\ p_{22,\phi} & p_{22,3} & p_{22,2} & p_{22,4} & p_{22,1} & p_{22,5} & p_{22,22} & p_{22,44} \\ p_{44,\phi} & p_{44,3} & p_{44,2} & p_{44,4} & p_{44,1} & p_{44,5} & p_{44,22} & p_{44,44} \end{bmatrix}$$

$$= \begin{bmatrix} 0 & p_3 & p_2 & p_4 & p_1 & p_5 & 0 & 0 \\ 0 & p_3 & p_2 & p_4 & p_1 & p_5 & 0 & 0 \\ 0 & p_3 & 0 & p_4 & p_1 & p_5 & p_2 & 0 \\ 0 & p_3 & p_2 & 0 & p_1 & p_5 & 0 & p_4 \\ 0 & 0 & 0 & 0 & 1 & 0 & 0 & 0 \\ 0 & 0 & 0 & 0 & 0 & 1 & 0 & 0 \\ 0 & 0 & 0 & 0 & 0 & 0 & 1 & 0 \\ 0 & 0 & 0 & 0 & 0 & 0 & 0 & 1 \end{bmatrix}$$

$$\therefore \mathbf{Q}_{4 \times 4} = \begin{bmatrix} 0 & p_3 & p_2 & p_4 \\ 0 & p_3 & p_2 & p_4 \\ 0 & p_3 & 0 & p_4 \\ 0 & p_3 & p_2 & 0 \end{bmatrix}$$

3.3.5 The improved 2-of-3 control charts

3.3.5.1 The upper one-sided improved 2-of-3 control chart

The random variable Z_i can assume values 1, 2 and 7, associated with the plotting statistic T_i plotting on or above UCL_B ($T_i \geq UCL_B$) (zone 1), plotting between UCL_A and UCL_B ($UCL_A \leq T_i < UCL_B$) (zone 2) and plotting below UCL_A ($T_i < UCL_A$) (zone 7) respectively. Consequently the state space of the Markov chain $\{Y_i\}$ is, $\Omega = \{\phi, 7, 2, 72, 27, \alpha_1, \alpha_2, \alpha_3, \alpha_4\}$, where $\alpha_1 = \{1\}$, $\alpha_2 = \{22\}$, $\alpha_3 = \{722\}$ and $\alpha_4 = \{272\}$ are the absorbing states. The run-length of the upper one-sided improved 2-of-3 control chart is the waiting time for the occurrence of one of the elements in Λ , where $\Lambda = \{\alpha_1, \alpha_2, \alpha_3, \alpha_4\}$.

$$\mathbf{M}_{9 \times 9} = \left[\begin{array}{c|c} \mathbf{Q}_{5 \times 5} & \mathbf{C}_{5 \times 4} \\ \hline \mathbf{0}_{4 \times 5} & \mathbf{I}_{4 \times 4} \end{array} \right] = \begin{bmatrix} P_{\phi,\phi} & P_{\phi,7} & P_{\phi,2} & P_{\phi,72} & P_{\phi,27} & P_{\phi,1} & P_{\phi,22} & P_{\phi,722} & P_{\phi,272} \\ P_{7,\phi} & P_{7,7} & P_{7,2} & P_{7,72} & P_{7,27} & P_{7,1} & P_{7,22} & P_{7,722} & P_{7,272} \\ P_{2,\phi} & P_{2,7} & P_{2,2} & P_{2,72} & P_{2,27} & P_{2,1} & P_{2,22} & P_{2,722} & P_{2,272} \\ P_{72,\phi} & P_{72,7} & P_{72,2} & P_{72,72} & P_{72,27} & P_{72,1} & P_{72,22} & P_{72,722} & P_{72,272} \\ P_{27,\phi} & P_{27,7} & P_{27,2} & P_{27,72} & P_{27,27} & P_{27,1} & P_{27,22} & P_{27,722} & P_{27,272} \\ \hline P_{1,\phi} & P_{1,7} & P_{1,2} & P_{1,72} & P_{1,27} & P_{1,1} & P_{1,22} & P_{1,722} & P_{1,272} \\ P_{22,\phi} & P_{22,7} & P_{22,2} & P_{22,72} & P_{22,27} & P_{22,1} & P_{22,22} & P_{22,722} & P_{22,272} \\ P_{722,\phi} & P_{722,7} & P_{722,2} & P_{722,72} & P_{722,27} & P_{722,1} & P_{722,22} & P_{722,722} & P_{722,272} \\ P_{272,\phi} & P_{272,7} & P_{272,2} & P_{272,72} & P_{272,27} & P_{272,1} & P_{272,22} & P_{272,722} & P_{272,272} \end{bmatrix} \\
 = \begin{bmatrix} 0 & p_7 & p_2 & 0 & 0 & p_1 & 0 & 0 & 0 \\ 0 & p_7 & 0 & p_2 & 0 & p_1 & 0 & 0 & 0 \\ 0 & 0 & 0 & 0 & p_7 & p_1 & p_2 & 0 & 0 \\ 0 & 0 & 0 & 0 & p_7 & p_1 & 0 & p_2 & 0 \\ 0 & p_7 & 0 & 0 & 0 & p_1 & 0 & 0 & p_2 \\ \hline 0 & 0 & 0 & 0 & 0 & 1 & 0 & 0 & 0 \\ 0 & 0 & 0 & 0 & 0 & 0 & 1 & 0 & 0 \\ 0 & 0 & 0 & 0 & 0 & 0 & 0 & 1 & 0 \\ 0 & 0 & 0 & 0 & 0 & 0 & 0 & 0 & 1 \end{bmatrix} \\
 \therefore \mathbf{Q}_{5 \times 5} = \begin{bmatrix} 0 & p_7 & p_2 & 0 & 0 \\ 0 & p_7 & 0 & p_2 & 0 \\ 0 & 0 & 0 & 0 & p_7 \\ 0 & 0 & 0 & 0 & p_7 \\ 0 & p_7 & 0 & 0 & 0 \end{bmatrix}$$

3.3.5.2 The lower one-sided *improved 2-of-3* control chart

The random variable Z_i can assume values 5, 4 and 6, associated with the plotting statistic T_i plotting on or below LCL_B ($T_i \leq LCL_B$) (zone 5), plotting between LCL_A and LCL_B ($LCL_B < T_i \leq LCL_A$) (zone 4) and plotting above LCL_A ($T_i > LCL_A$) (zone 6) respectively. Consequently the state space of the Markov chain $\{Y_i\}$ is $\Omega = \{\phi, 6, 4, 64, 46, \alpha_1, \alpha_2, \alpha_3, \alpha_4\}$, where $\alpha_1 = \{5\}$, $\alpha_2 = \{44\}$, $\alpha_3 = \{644\}$ and $\alpha_4 = \{464\}$ are the absorbing states. The run-length of the lower one-sided *improved 2-of-3* control chart is the waiting time for the occurrence of one of the elements in Λ , where $\Lambda = \{\alpha_1, \alpha_2, \alpha_3, \alpha_4\}$.

$$\mathbf{M}_{9 \times 9} = \left[\begin{array}{c|c} \mathbf{Q}_{5 \times 5} & \mathbf{C}_{5 \times 4} \\ \hline \mathbf{0}_{4 \times 5} & \mathbf{I}_{4 \times 4} \end{array} \right] = \begin{bmatrix} P_{\phi,\phi} & P_{\phi,6} & P_{\phi,4} & P_{\phi,64} & P_{\phi,46} & P_{\phi,5} & P_{\phi,44} & P_{\phi,644} & P_{\phi,464} \\ P_{6,\phi} & P_{6,6} & P_{6,4} & P_{6,64} & P_{6,46} & P_{6,5} & P_{6,44} & P_{6,644} & P_{6,464} \\ P_{4,\phi} & P_{4,6} & P_{4,4} & P_{4,64} & P_{4,46} & P_{4,5} & P_{4,44} & P_{4,644} & P_{4,464} \\ P_{64,\phi} & P_{64,6} & P_{64,4} & P_{64,64} & P_{64,46} & P_{64,5} & P_{64,44} & P_{64,644} & P_{64,464} \\ P_{46,\phi} & P_{46,6} & P_{46,4} & P_{46,64} & P_{46,46} & P_{46,5} & P_{46,44} & P_{46,644} & P_{46,464} \\ \hline P_{5,\phi} & P_{5,6} & P_{5,4} & P_{5,64} & P_{5,46} & P_{5,5} & P_{5,44} & P_{5,644} & P_{5,464} \\ P_{44,\phi} & P_{44,6} & P_{44,4} & P_{44,64} & P_{44,46} & P_{44,5} & P_{44,44} & P_{44,644} & P_{44,464} \\ P_{644,\phi} & P_{644,6} & P_{644,4} & P_{644,64} & P_{644,46} & P_{644,5} & P_{644,44} & P_{644,644} & P_{644,464} \\ P_{464,\phi} & P_{464,6} & P_{464,4} & P_{464,64} & P_{464,46} & P_{464,5} & P_{464,44} & P_{464,644} & P_{464,464} \end{bmatrix} \\
 = \begin{bmatrix} 0 & p_6 & p_4 & 0 & 0 & p_5 & 0 & 0 & 0 \\ 0 & p_6 & 0 & p_4 & 0 & p_5 & 0 & 0 & 0 \\ 0 & 0 & 0 & 0 & p_6 & p_5 & p_4 & 0 & 0 \\ 0 & 0 & 0 & 0 & p_6 & p_5 & 0 & p_4 & 0 \\ 0 & p_6 & 0 & 0 & 0 & p_5 & 0 & 0 & p_4 \\ \hline 0 & 0 & 0 & 0 & 0 & 1 & 0 & 0 & 0 \\ 0 & 0 & 0 & 0 & 0 & 0 & 1 & 0 & 0 \\ 0 & 0 & 0 & 0 & 0 & 0 & 0 & 1 & 0 \\ 0 & 0 & 0 & 0 & 0 & 0 & 0 & 0 & 1 \end{bmatrix} \\
 \therefore \mathbf{Q}_{5 \times 5} = \begin{bmatrix} 0 & p_6 & p_4 & 0 & 0 \\ 0 & p_6 & 0 & p_4 & 0 \\ 0 & 0 & 0 & 0 & p_6 \\ 0 & 0 & 0 & 0 & p_6 \\ 0 & p_6 & 0 & 0 & 0 \end{bmatrix}$$

3.3.5.3 The two-sided *improved 2-of-3* control chart

The random variable Z_i can assume values 1, 2, 3, 4 and 5, associated with the plotting statistic T_i plotting on or above UCL_B ($T_i \geq UCL_B$) (zone 1), between UCL_A and UCL_B ($UCL_A \leq T_i < UCL_B$) (zone 2), between LCL_A and UCL_A ($LCL_A < T_i < UCL_A$) (zone 3), between LCL_A and LCL_B ($LCL_B < T_i \leq LCL_A$) (zone 4), and T_i plotting on or below LCL_B ($T_i \leq LCL_B$) (zone 5) respectively. Consequently the state space of the Markov chain $\{Y_t\}$ is, $\Omega = \{\phi, 3, 2, 32, 23, 4, 34, 43, \alpha_1, \alpha_2, \alpha_3, \alpha_4, \alpha_5, \alpha_6, \alpha_7, \alpha_8\}$, where $\alpha_1 = \{1\}$, $\alpha_2 = \{5\}$, $\alpha_3 = \{22\}$, $\alpha_4 = \{44\}$, $\alpha_5 = \{322\}$, $\alpha_6 = \{232\}$, $\alpha_7 = \{344\}$ and $\alpha_8 = \{434\}$ are the absorbing states. The run-length of the two-sided *improved 2-of-3* control chart is the waiting time for the occurrence of one of the elements in Λ , where $\Lambda = \{\alpha_1, \alpha_2, \alpha_3, \alpha_4, \alpha_5, \alpha_6, \alpha_7, \alpha_8\}$.

$$\mathbf{M}_{16 \times 16} = \left[\begin{array}{c|c} \mathbf{Q}_{8 \times 8} & \mathbf{C}_{8 \times 8} \\ \hline \mathbf{0}_{8 \times 8} & \mathbf{I}_{8 \times 8} \end{array} \right] =$$

$P_{\phi, \phi}$	$P_{\phi, 3}$	$P_{\phi, 2}$	$P_{\phi, 32}$	$P_{\phi, 23}$	$P_{\phi, 4}$	$P_{\phi, 34}$	$P_{\phi, 43}$	$P_{\phi, 1}$	$P_{\phi, 5}$	$P_{\phi, 22}$	$P_{\phi, 44}$	$P_{\phi, 322}$	$P_{\phi, 232}$	$P_{\phi, 344}$	$P_{\phi, 434}$
$P_{3, \phi}$	$P_{3, 3}$	$P_{3, 2}$	$P_{3, 32}$	$P_{3, 23}$	$P_{3, 4}$	$P_{3, 34}$	$P_{3, 43}$	$P_{3, 1}$	$P_{3, 5}$	$P_{3, 22}$	$P_{3, 44}$	$P_{3, 322}$	$P_{3, 232}$	$P_{3, 344}$	$P_{3, 434}$
$P_{2, \phi}$	$P_{2, 3}$	$P_{2, 2}$	$P_{2, 32}$	$P_{2, 23}$	$P_{2, 4}$	$P_{2, 34}$	$P_{2, 43}$	$P_{2, 1}$	$P_{2, 5}$	$P_{2, 22}$	$P_{2, 44}$	$P_{2, 322}$	$P_{2, 232}$	$P_{2, 344}$	$P_{2, 434}$
$P_{32, \phi}$	$P_{32, 3}$	$P_{32, 2}$	$P_{32, 32}$	$P_{32, 23}$	$P_{32, 4}$	$P_{32, 34}$	$P_{32, 43}$	$P_{32, 1}$	$P_{32, 5}$	$P_{32, 22}$	$P_{32, 44}$	$P_{32, 322}$	$P_{32, 232}$	$P_{32, 344}$	$P_{32, 434}$
$P_{23, \phi}$	$P_{23, 3}$	$P_{23, 2}$	$P_{23, 32}$	$P_{23, 23}$	$P_{23, 4}$	$P_{23, 34}$	$P_{23, 43}$	$P_{23, 1}$	$P_{23, 5}$	$P_{23, 22}$	$P_{23, 44}$	$P_{23, 322}$	$P_{23, 232}$	$P_{23, 344}$	$P_{23, 434}$
$P_{4, \phi}$	$P_{4, 3}$	$P_{4, 2}$	$P_{4, 32}$	$P_{4, 23}$	$P_{4, 4}$	$P_{4, 34}$	$P_{4, 43}$	$P_{4, 1}$	$P_{4, 5}$	$P_{4, 22}$	$P_{4, 44}$	$P_{4, 322}$	$P_{4, 232}$	$P_{4, 344}$	$P_{4, 434}$
$P_{34, \phi}$	$P_{34, 3}$	$P_{34, 2}$	$P_{34, 32}$	$P_{34, 23}$	$P_{34, 4}$	$P_{34, 34}$	$P_{34, 43}$	$P_{34, 1}$	$P_{34, 5}$	$P_{34, 22}$	$P_{34, 44}$	$P_{34, 322}$	$P_{34, 232}$	$P_{34, 344}$	$P_{34, 434}$
$P_{43, \phi}$	$P_{43, 3}$	$P_{43, 2}$	$P_{43, 32}$	$P_{43, 23}$	$P_{43, 4}$	$P_{43, 34}$	$P_{43, 43}$	$P_{43, 1}$	$P_{43, 5}$	$P_{43, 22}$	$P_{43, 44}$	$P_{43, 322}$	$P_{43, 232}$	$P_{43, 344}$	$P_{43, 434}$
$P_{1, \phi}$	$P_{1, 3}$	$P_{1, 2}$	$P_{1, 32}$	$P_{1, 23}$	$P_{1, 4}$	$P_{1, 34}$	$P_{1, 43}$	$P_{1, 1}$	$P_{1, 5}$	$P_{1, 22}$	$P_{1, 44}$	$P_{1, 322}$	$P_{1, 232}$	$P_{1, 344}$	$P_{1, 434}$
$P_{5, \phi}$	$P_{5, 3}$	$P_{5, 2}$	$P_{5, 32}$	$P_{5, 23}$	$P_{5, 4}$	$P_{5, 34}$	$P_{5, 43}$	$P_{5, 1}$	$P_{5, 5}$	$P_{5, 22}$	$P_{5, 44}$	$P_{5, 322}$	$P_{5, 232}$	$P_{5, 344}$	$P_{5, 434}$
$P_{22, \phi}$	$P_{22, 3}$	$P_{22, 2}$	$P_{22, 32}$	$P_{22, 23}$	$P_{22, 4}$	$P_{22, 34}$	$P_{22, 43}$	$P_{22, 1}$	$P_{22, 5}$	$P_{22, 22}$	$P_{22, 44}$	$P_{22, 322}$	$P_{22, 232}$	$P_{22, 344}$	$P_{22, 434}$
$P_{44, \phi}$	$P_{44, 3}$	$P_{44, 2}$	$P_{44, 32}$	$P_{44, 23}$	$P_{44, 4}$	$P_{44, 34}$	$P_{44, 43}$	$P_{44, 1}$	$P_{44, 5}$	$P_{44, 22}$	$P_{44, 44}$	$P_{44, 322}$	$P_{44, 232}$	$P_{44, 344}$	$P_{44, 434}$
$P_{322, \phi}$	$P_{322, 3}$	$P_{322, 2}$	$P_{322, 32}$	$P_{322, 23}$	$P_{322, 4}$	$P_{322, 34}$	$P_{322, 43}$	$P_{322, 1}$	$P_{322, 5}$	$P_{322, 22}$	$P_{322, 44}$	$P_{322, 322}$	$P_{322, 232}$	$P_{322, 344}$	$P_{322, 434}$
$P_{232, \phi}$	$P_{232, 3}$	$P_{232, 2}$	$P_{232, 32}$	$P_{232, 23}$	$P_{232, 4}$	$P_{232, 34}$	$P_{232, 43}$	$P_{232, 1}$	$P_{232, 5}$	$P_{232, 22}$	$P_{232, 44}$	$P_{232, 322}$	$P_{232, 232}$	$P_{232, 344}$	$P_{232, 434}$
$P_{344, \phi}$	$P_{344, 3}$	$P_{344, 2}$	$P_{344, 32}$	$P_{344, 23}$	$P_{344, 4}$	$P_{344, 34}$	$P_{344, 43}$	$P_{344, 1}$	$P_{344, 5}$	$P_{344, 22}$	$P_{344, 44}$	$P_{344, 322}$	$P_{344, 232}$	$P_{344, 344}$	$P_{344, 434}$
$P_{434, \phi}$	$P_{434, 3}$	$P_{434, 2}$	$P_{434, 32}$	$P_{434, 23}$	$P_{434, 4}$	$P_{434, 34}$	$P_{434, 43}$	$P_{434, 1}$	$P_{434, 5}$	$P_{434, 22}$	$P_{434, 44}$	$P_{434, 322}$	$P_{434, 232}$	$P_{434, 344}$	$P_{434, 434}$

$$= \begin{bmatrix} 0 & p_3 & p_2 & 0 & 0 & p_4 & 0 & 0 & p_1 & p_5 & 0 & 0 & 0 & 0 & 0 & 0 \\ 0 & p_3 & 0 & p_2 & 0 & 0 & p_4 & 0 & p_1 & p_5 & 0 & 0 & 0 & 0 & 0 & 0 \\ 0 & 0 & 0 & 0 & p_3 & p_4 & 0 & 0 & p_1 & p_5 & p_2 & 0 & 0 & 0 & 0 & 0 \\ 0 & 0 & 0 & 0 & p_3 & p_4 & 0 & 0 & p_1 & p_5 & 0 & 0 & p_2 & 0 & 0 & 0 \\ 0 & p_3 & 0 & 0 & 0 & 0 & p_4 & 0 & p_1 & p_5 & 0 & 0 & 0 & p_2 & 0 & 0 \\ 0 & 0 & p_2 & 0 & 0 & 0 & 0 & p_3 & p_1 & p_5 & 0 & p_4 & 0 & 0 & 0 & 0 \\ 0 & 0 & p_2 & 0 & 0 & 0 & 0 & p_3 & p_1 & p_5 & 0 & 0 & 0 & 0 & p_4 & 0 \\ 0 & p_3 & 0 & p_2 & 0 & 0 & 0 & 0 & p_1 & p_5 & 0 & 0 & 0 & 0 & 0 & p_4 \\ \hline 0 & 0 & 0 & 0 & 0 & 0 & 0 & 0 & 1 & 0 & 0 & 0 & 0 & 0 & 0 & 0 \\ 0 & 0 & 0 & 0 & 0 & 0 & 0 & 0 & 0 & 1 & 0 & 0 & 0 & 0 & 0 & 0 \\ 0 & 0 & 0 & 0 & 0 & 0 & 0 & 0 & 0 & 0 & 1 & 0 & 0 & 0 & 0 & 0 \\ 0 & 0 & 0 & 0 & 0 & 0 & 0 & 0 & 0 & 0 & 0 & 1 & 0 & 0 & 0 & 0 \\ 0 & 0 & 0 & 0 & 0 & 0 & 0 & 0 & 0 & 0 & 0 & 0 & 1 & 0 & 0 & 0 \\ 0 & 0 & 0 & 0 & 0 & 0 & 0 & 0 & 0 & 0 & 0 & 0 & 0 & 1 & 0 & 0 \\ 0 & 0 & 0 & 0 & 0 & 0 & 0 & 0 & 0 & 0 & 0 & 0 & 0 & 0 & 1 & 0 \\ 0 & 0 & 0 & 0 & 0 & 0 & 0 & 0 & 0 & 0 & 0 & 0 & 0 & 0 & 0 & 1 \end{bmatrix}$$

$$\therefore \mathbf{Q}_{8 \times 8} = \begin{bmatrix} 0 & p_3 & p_2 & 0 & 0 & p_4 & 0 & 0 \\ 0 & p_3 & 0 & p_2 & 0 & 0 & p_4 & 0 \\ 0 & 0 & 0 & 0 & p_3 & p_4 & 0 & 0 \\ 0 & 0 & 0 & 0 & p_3 & p_4 & 0 & 0 \\ 0 & p_3 & 0 & 0 & 0 & 0 & p_4 & 0 \\ 0 & 0 & p_2 & 0 & 0 & 0 & 0 & p_3 \\ 0 & 0 & p_2 & 0 & 0 & 0 & 0 & p_3 \\ 0 & p_3 & 0 & p_2 & 0 & 0 & 0 & 0 \end{bmatrix}$$

Remark 3.23:

The transition probability matrix \mathbf{M} , is constructed in such a manner that when the Markov chain is in state $\{4\}$ or $\{34\}$ at time $i-2$, and the plotting statistic T_{i-1} plots between the UCL_A and the UCL_B ($UCL_A \leq T_{i-1} < UCL_B$) (zone 2), the Markov chain moves to state $\{2\}$ at time $i-1$, if the following plotting statistic T_i plots between the UCL_A and the UCL_B ($UCL_A \leq T_i < UCL_B$) (zone 2) the chart signals at time i since the process moves to the absorbing state $\{22\}$. Similarly if the Markov chain is in state $\{2\}$ or $\{32\}$ at time $i-2$, and the plotting statistic T_{i-1} plots between the LCL_A and LCL_B ($LCL_B < T_i \leq LCL_A$) (zone 4) the Markov chain moves to state $\{4\}$ at time $i-1$ and if the

following plotting statistic T_i plots between the LCL_A and LCL_B ($LCL_B < T_i \leq LCL_A$) (zone 4) the process moves to the absorbing state $\{44\}$. Refer to the two-sided 2-of-3 control chart and Figure 3.29 for a similar discussion on these transitions and their interpretation.

3.4 Control limits

Considering the control charts with *improved* runs-rules, an additional control limit is added to the ordinary control chart in the case of the one-sided control chart, and two additional control limits in the case of the two-sided control chart. A natural question that follows is what are the effects on the control charts when the *inner* and *outer* control limits lie on top of each other, or when the *inner* and *outer* control limits are swapped?

Recall that the *inner* control limits (*A* control limits) are associated with the runs-rules, namely the 2-of-2- and 2-of-3 runs-rules and the *outer* control limits (*B* control limits) are associated with the 1-of-1 rule i.e. when a plotting statistic plots on or above (below) the UCL_B (LCL_B) the chart signals. The *B* control limit(s) were introduced, so that the chart signals immediately following a large process shift.

3.4.1 Upper one-sided control charts

Figure 3.30 graphically illustrates all the possible combinations of the *A* and *B* control limits on the upper one-sided *improved* runs-rules control chart.

In panel (a) of Figure 3.30, is the usual combination of control limits namely where UCL_B lies above UCL_A .

Panel (b) of Figure 3.30 illustrates the case where the *A* and *B* control limits are the same (the *inner* and *outer* control limits lie on top of each other). In this case the runs-rules associated with the *A* control limit is negated, since when a plotting statistic plots on or above the UCL_A / UCL_B ($UCL_A = UCL_B$) the control chart signals immediately. Therefore when the UCL_B and UCL_A lies on top of each other, the *improved* runs-rules chart reduces to an ordinary 1-of-1 upper one-sided chart with upper control limit equal to UCL_A / UCL_B .

Panel (c) of Figure 3.30 illustrates the case where the A control limit lies above the B control limit. In this case the runs-rules associated with the A control limit is also negated, since when a plotting statistic plots on or above the UCL_B the control chart signals immediately. Therefore when the UCL_A lies above the UCL_B the one-sided *improved* runs-rules chart reduce to an ordinary *1-of-1* upper one-sided chart, with upper control limit equal to UCL_B .

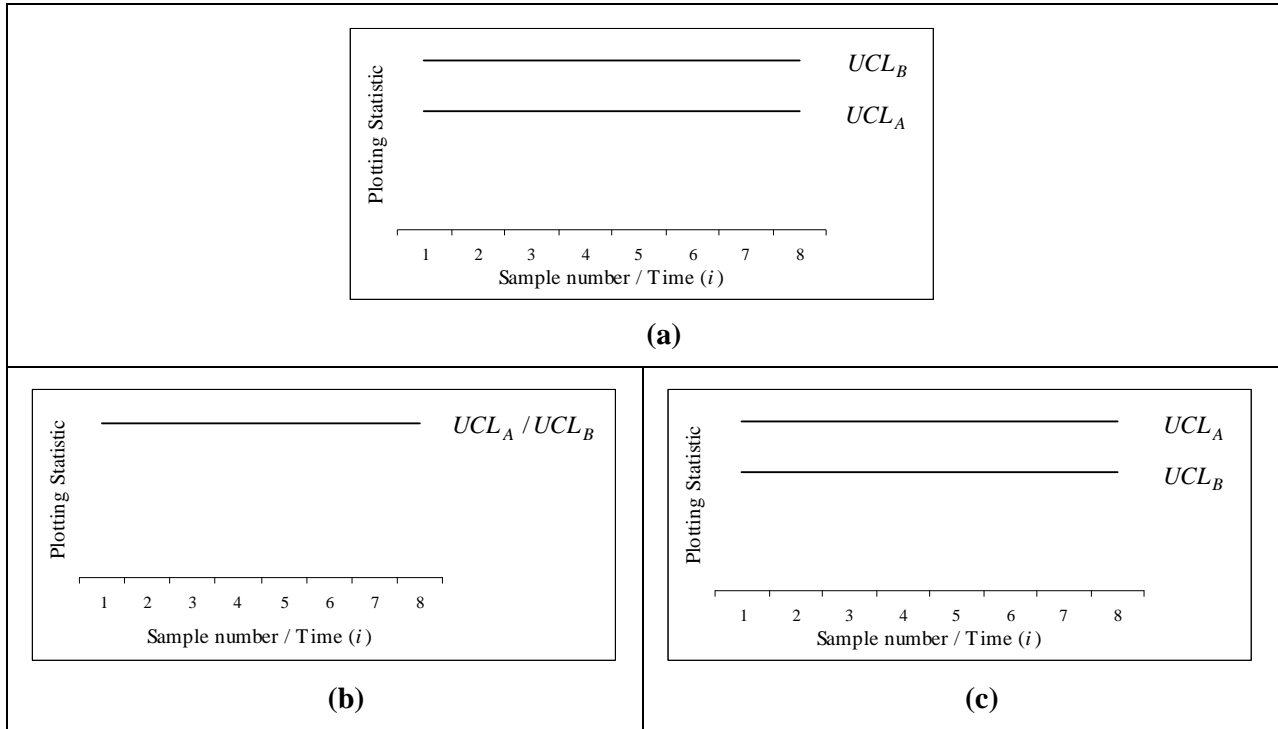


Figure 3.30: Illustrations of combinations of the upper one-sided *improved* runs-rules control limits.

3.4.2 Lower one-sided control charts

A similar argument as with the upper one-sided control charts can be given, in order to show that both lower one-sided *improved* runs-rules control charts illustrated in panels (b) and (c) of Figure 3.31, reduces to a lower one-sided *I-of-1* control chart, with lower control limits equal to LCL_A / LCL_B and LCL_B respectively.

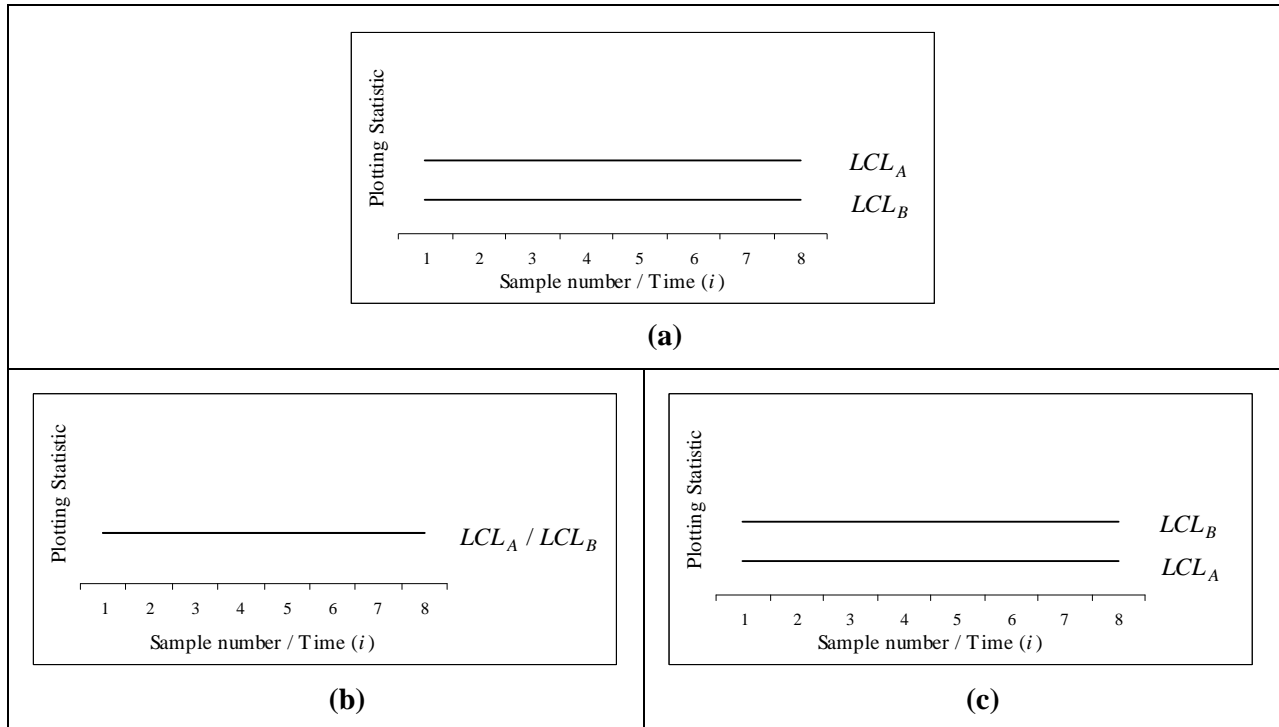


Figure 3.31: Illustrations of combinations of the lower one-sided *improved* runs-rules control limits.

3.4.3 Two-sided control charts

Panel (a) of Figure 3.32 graphically illustrates the two-sided *improved* runs-rules control chart where the *A* control limits associated with the runs-rules lies inside the *B* control limits associated with the *I-of-1* signalling rule. This arrangement of the *A* and *B* control limits is the usual arrangement.

Panels (b) and (c) of Figure 3.32 illustrates the case where the chart has normal lower *improved* runs-rules control limits i.e. LCL_B lies below LCL_A , but has a *I-of-1* signalling rule for an upward

shift in the process. The control limits for the upper *1-of-1* signalling rule for the control charts in panels (b) and (c) are UCL_A / UCL_B and UCL_B respectively.

Panels (d) and (e) of Figure 3.32 illustrates the case where the chart has normal upper *improved* runs-rules control limits i.e. UCL_A lies below UCL_B , but has a *1-of-1* signalling rule for a downward shift in the process. The control limits for the lower *1-of-1* signalling rule, for the control charts illustrated in panels (d) and (e) are LCL_A / LCL_B and LCL_B respectively.

Panels (f) and (g) illustrates the cases where the *A* and *B* control limits lie on top of each other and the case where the *B* control limits lie inside the *A* control limits respectively. In both cases these control charts reduce to ordinary two-sided *1-of-1* control charts.

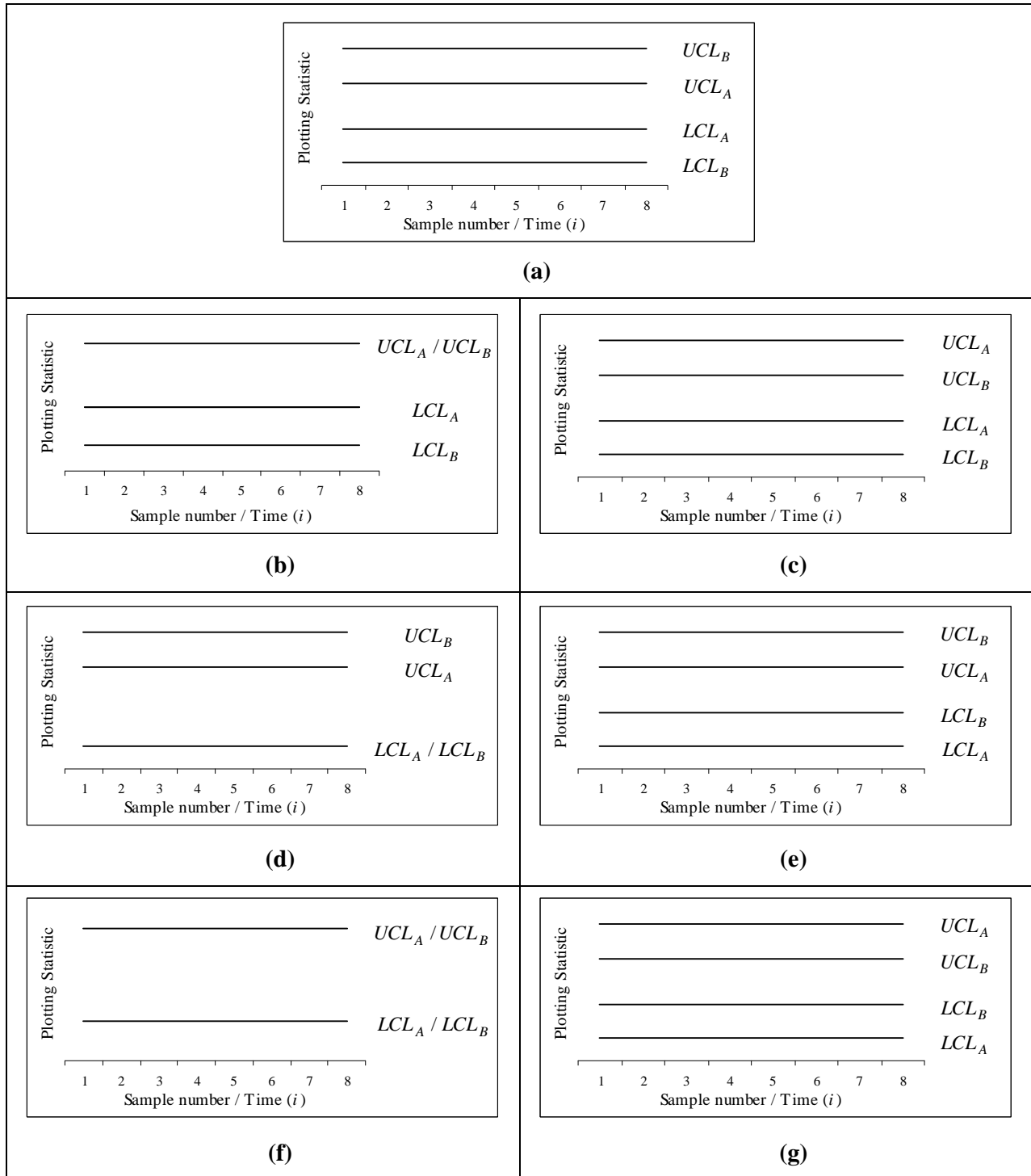


Figure 3.32: Illustrations of combinations of the two-sided *improved runs-rules control limits*.

3.5 Summary of Chapter 3

The reader should now be familiar with the signalling rules and the essential transition probability matrices of the *1-of-1*, the *2-of-2*, the *2-of-3*, the *improved 2-of-2* and the *improved 2-of-3* control charts.

3.6 Following two chapters

The foundation that is laid down in Chapters 2 and 3 are applied in the following two chapters. In Chapter 4 the run-length distribution of the sign chart is calculated, where in Chapter 5 the run-length distribution of the precedence chart is calculated. In both Chapters 4 and 5 the run-length distribution is calculated using a Markov chain approach.

Chapter 4

Sign control charts (Case K)

4.0 Chapter 4 overview and objective

In Chapter 3 the operations of the runs-rules and the *improved* runs-rules have been outlined. Chapter 2 introduced the Markov chain approach to calculate the run-length distribution and some characteristics of the run-length distribution. However, a plotting statistic and control limits are yet to be defined and used in conjunction with the runs-rules and the *improved* runs-rules charts. In this chapter the well-known sign statistic is used as a plotting statistic together with the *improved* runs-rules; this leads to the so-called *improved* runs-rules sign control charts. An overview of the basic and the runs-rules enhanced sign charts by Amin et al. (1995) and Human et al. (2009), respectively are also presented.

The objectives in Chapter 4 are to introduce the *improved* runs-rules sign chart and to derive the run-length distribution of the *improved* runs-rules sign chart using a Markov chain approach. Performance analysis is carried out to illustrate that the *improved* runs-rules sign charts are superior in performance to runs-rules sign charts for large shifts, while maintaining the same sensitivity in the detection of small shifts.

After reading this chapter the reader should be familiar with:

- The history of the sign chart,
- The well-known sign statistic (i.e. the plotting statistic of the sign chart),
- The application of the sign charts,
- The design of the sign charts,
- How the performance of the *improved* runs-rules sign charts compare to the runs-rules enhanced sign charts, and
- The strengths and limitations of the *improved* runs-rules sign charts, compared to the runs-rules enhanced sign charts.

4.1 Introduction

The sign chart is a Shewhart-type chart which uses the sign statistic as plotting statistic and can be used to monitor any specified $100\pi^{\text{th}}$ ($0 < \pi < 1$) process percentile of interest. Note that since it is assumed that the percentile of interest is known, this scenario is referred to as the “Standards Known” case and is abbreviated as Case K.

Amin et al. (1995) developed a nonparametric Shewhart-type chart based on the sign statistic which can be used to monitor the location of a process. This chart is known as the basic sign chart and is based on the simplest signalling rule, namely the *1-of-1* signalling rule i.e. the chart signals when the first plotting statistic plots on or outside the control limits. The *1-of-1* sign chart uses only the most recent plotting statistic in determining the state of the process and is thus insensitive to small process shifts. Human et al. (2009) addressed the *1-of-1* sign chart’s insensitivity to small process shifts by introducing the *2-of-2* and the *2-of-3* runs-rules and showed that the sign chart with runs-rules, have very good properties compared to the *1-of-1* sign chart.

However, runs-rules charts have a limitation, in that they are unable to quickly detect large shifts in the process, as discussed in Chapter 3. The *2-of-2* (*2-of-3*) chart requires at least the last two (three) plotting statistics before the chart can signal, regardless of the size of the shift. To address this limitation, the *improved 2-of-2* and the *improved 2-of-3* runs-rules are introduced to the sign chart.

Amin et al. (1995), p.1607-1608 introduced warning limits to the sign chart that were also studied by Page (1962), Weindling et al. (1970) and Champ et al. (1987) for the \bar{X} control chart. Amin et al. (1995)’s motivation for introducing warning limits to the sign chart, was to improve the efficiency in detecting small shifts. Coincidentally one of the sign charts of Amin et al. (1995) with warning limits is exactly the same as the *improved 2-of-2* sign chart as proposed and considered in this dissertation. The motivation in this dissertation for introducing *improved* runs-rules is to improve the efficiency of the runs-rules charts in detecting large shifts which is different from Amin et al. (1995)’s motivation, (for introducing warning limits) namely to improve the efficiency in detecting small shifts.

Note that the values (*ARL*’s) in Table 2 on p.1606 of Amin et al. (1995) could be reproduced using the formulas provided in this dissertation.

Note that, whereas Amin et al. (1995) only gave a formula to calculate the *ARL* for their sign chart with warning limits, in this dissertation (with regard to the *improved 2-of-2* sign chart over and above

the sign chart of Amin et al. (1995) with warning limits) the run-length distribution, cumulative run-length distribution, *ARL* and *VRL* are derived using a Markov chain approach and formulae for the *FAR* is provided. The *improved 2-of-3* sign chart's run-length distribution is derived, which is unavailable in the literature. Furthermore, the *improved* runs-rules charts are shown to be superior for large process shifts, while they maintain the same sensitivity as the runs-rules charts for small shifts.

It is worth noting that Khoo and Ariffin (2006) implemented *improved* runs-rules to the \bar{X} chart to address the limitation that the runs-rules charts are unable to detect large shifts quickly. The application of the *improved 2-of-3* runs-rules sign charts that are considered in this dissertation are slightly different at start up to Khoo and Ariffin (2006)'s *improved* runs-rules for reasons discussed in Chapter 3 Section 3.2.3; namely to address the problem that the chart does not signal following the event that all the plotting statistics plot on or outside the control limits from start up for the *2-of-3* charts.

4.2 Assumptions

Let $X_{i1}, X_{i2}, \dots, X_{in}$ denote a random sample of size $n \geq 1$ (see Graham et al. (2011)) at time $i = 1, 2, 3, \dots$. Assume that the samples are independent and that each observation follows a continuous distribution with cumulative distribution function denoted by $F_X(x)$. The unique $100\pi^{\text{th}}$ ($0 < \pi < 1$) percentile is denoted by $\theta = F_X^{-1}(\pi)$, $0 < \pi < 1$ (Human et al. (2009)).

4.3 Applications and general information on the sign chart

The sign chart is generally used to monitor the location i.e. the $100\pi^{\text{th}}$ ($0 < \pi < 1$) percentile, of a process or distribution. Two special situations arise and these are: (i) when $\pi = 0.5$ and the underlying process distribution is symmetric, then the sign chart monitors the mean of the process, and (ii) if $\pi = 0.5$ and the underlying process distribution is not symmetric, then the sign chart monitors for a change in the median of the process, where $\theta_0 = F_X^{-1}(0.5)$ denotes the median. It is assumed that θ_0 is specified.

The sign chart is a nonparametric chart, i.e. its IC run-length distribution does not depend on the underlying process distribution. An advantage of the sign chart is that it does not require the underlying continuous process distribution to be symmetric (see e.g. Gibbons and Chakraborti,

(2003)). Furthermore the sign chart does not require the actual measurements, but only the number or count of observations within each sample that are larger or smaller than the known or specified value of the percentile of interest. Consequently, the sign chart can be applied with only binary data, i.e. when the only information available is whether a measurement is larger or smaller than the known or specified percentile of interest. Another advantage of the sign chart is that the variance need not be established in order to set up the sign chart to monitor the location.

4.4 Plotting statistic

The point that is plotted on the chart is typically referred to as a plotting statistic or charting statistic, refer to Chapter 1 Section 1.5.2 for a discussion on plotting statistics.

Amin et al. (1995) considered the statistic

$$SN_i = \sum_{j=1}^n \text{sign}(X_{ij} - \theta_0), i = 1, 2, 3, \dots \quad (4.1)$$

$$\text{where } \text{sign}(g) = \begin{cases} 1 & \text{if } g > 0 \\ 0 & \text{if } g = 0 \\ -1 & \text{if } g < 0 \end{cases}$$

as plotting statistic for their sign chart.

Amin et al. (1995) pointed out that SN_i is just the difference between the number of observations greater than θ_0 and the number smaller than θ_0 in the i^{th} sample of size n , where θ_0 denotes the specified value or the percentile of interest. Amin et al. (1995) favoured SN_i as the plotting statistic given in equation (4.1) since $E(SN_i) = 0$, i.e. the control limits could be placed symmetrically around zero.

However, Human et al. (2009) considered the classical sign statistic

$$T_i = \sum_{j=1}^n I(X_{ij} > \theta_0) \quad i = 1, 2, 3, \dots \quad (4.2)$$

$$\text{where } I(X_{ij} > \theta_0) = \begin{cases} 1 & \text{if } X_{ij} > \theta_0 \\ 0 & \text{if } X_{ij} < \theta_0 \end{cases}$$

The plotting statistic T_i denotes the number of observations greater than θ_0 in the i^{th} sample of size n , where θ_0 denotes the known (or the specified or the target) value of the percentile of interest. Note that T_i follows a Binomial distribution with parameters n and p , where $p = P(X_{ij} > \theta_0)$. If the percentile of interest is equal to its specified value i.e. $\theta = \theta_0$ the process is said to be IC and p equals $p_0 = P(X_{ij} > \theta_0 | IC)$. Note that, the probability $P(X_{ij} = \theta_0)$ is theoretically zero since the process distribution is assumed to be continuous. Amin et al. (1995) used SN_i as plotting statistic since the control limits are then symmetric about zero. This had the result that the control limits could be conveniently placed symmetric about zero. However, T_i is used as the plotting statistic in this dissertation since T_i follows a $BIN(n, p)$ distribution and the properties of a Binomial distribution are well known.

Remark 4.1

Note that the two statistics T_i and SN_i are equivalent since they are linearly related:

$$T_i = (SN_i + n) / 2 \quad i = 1, 2, 3, \dots \quad (4.3)$$

Consequently, monitoring a process using T_i as plotting statistic will be the same as monitoring the process using SN_i as plotting statistic, where equivalent control limits are used.

4.5 Control limits

The upper and lower control limits for the *1-of-1* and runs-rules control charts are:

$$UCL_A / UCL = c \text{ and } LCL_A / LCL = b. \quad (4.4)$$

The upper and lower control limits of the *improved* runs-rules control charts are:

$$UCL_B = d, UCL_A / UCL = c, LCL_A / LCL = b \text{ and } LCL_B = a. \quad (4.5)$$

Refer to Chapter 3 Section 3.1 for an explanation on the four control limits. Refer to Chapter 3 Remark 3.1 for clarity on the notation used in equations (4.4) and (4.5).

The values of the control limits i.e. a, b, c and d (where $a < b < c < d$) are all integers between (and including) zero and n .

The choice of control limits is later discussed in Section 4.8.

4.6 Run-length distribution of the sign charts

A Markov chain approach is used to calculate the run-length distribution. The essential transition probability matrices of all the control charts are given and the formulas that are used to calculate the elements (i.e. the transition probabilities) of the essential transition probability matrices are provided. A performance comparison is carried out between the *improved* runs-rules sign charts and the runs-rules sign charts. Recall that, the essential transition probability matrices were all constructed in Section 3.3 of Chapter 3.

4.6.1 Transition probabilities

Recall from Section 4.4 that the sign statistic T_i follows a Binomial distribution with parameters n and p where $p = P(X_{ij} > \theta_0)$. Furthermore, each element of the essential transition probability matrix is in fact a probability whose value depends on the “zone” in which T_i plots on the chart; these zones were graphically illustrated in Chapter 3 Figure 3.1. So, it follows that:

$$p_1 = P(T_i \geq UCL_B) = 1 - \sum_{x=0}^{UCL_B-1} \binom{n}{x} p^x (1-p)^{n-x} \quad (4.6)$$

$$p_2 = P(UCL_A \leq T_i < UCL_B) = \sum_{x=0}^{UCL_B-1} \binom{n}{x} p^x (1-p)^{n-x} - \sum_{x=0}^{UCL_A-1} \binom{n}{x} p^x (1-p)^{n-x} \quad (4.7)$$

$$p_3 = P(LCL_A / LCL < T_i < UCL_A / UCL) = \sum_{x=0}^{UCL_A-1} \binom{n}{x} p^x (1-p)^{n-x} - \sum_{x=0}^{LCL_A} \binom{n}{x} p^x (1-p)^{n-x} \quad (4.8)$$

$$p_4 = P(LCL_B < T_i \leq LCL_A) = \sum_{x=0}^{LCL_A} \binom{n}{x} p^x (1-p)^{n-x} - \sum_{x=0}^{LCL_B} \binom{n}{x} p^x (1-p)^{n-x} \quad (4.9)$$

$$p_5 = P(T_i \leq LCL_B) = \sum_{x=0}^{LCL_B} \binom{n}{x} p^x (1-p)^{n-x} \quad (4.10)$$

$$p_6 = P(T_i > LCL_A / LCL) = 1 - \sum_{x=0}^{LCL_A} \binom{n}{x} p^x (1-p)^{n-x} \quad (4.11)$$

$$p_7 = P(T_i < UCL_A / UCL) = \sum_{x=0}^{UCL_A-1} \binom{n}{x} p^x (1-p)^{n-x} \quad (4.12)$$

$$p_8 = P(T_i \geq UCL) = 1 - \sum_{x=0}^{UCL-1} \binom{n}{x} p^x (1-p)^{n-x} \quad (4.13)$$

$$p_9 = P(T_i \leq LCL) = \sum_{x=0}^{LCL} \binom{n}{x} p^x (1-p)^{n-x} \quad (4.14)$$

To understand the formulae for p_1, p_2, \dots, p_9 . Note that the formulae for the probabilities are sums of Binomial probabilities (the control limits are integers between zero and n). T_i follows a Binomial distribution with parameters n and p where $p = P(X_{ij} > \theta_0)$.

4.6.2 Essential transition probability matrices

The essential transition probability matrices for all the charts were constructed in Section 3.3 of Chapter 3 and are again given here for completeness.

4.6.2.1 The *I-of-I* sign charts

The essential transition probability matrices of the upper one-sided *I-of-I*, lower one-sided *I-of-I* and two-sided *I-of-I* charts are given by:

Upper one-sided *I-of-I* sign chart essential transition probability matrix:

$$\mathbf{Q}_{1-of-1(U)} = \begin{bmatrix} 0 & p_7 \\ 0 & p_7 \end{bmatrix} \quad (4.15)$$

Lower one-sided *I-of-I* sign chart essential transition probability matrix:

$$\mathbf{Q}_{1-of-1(L)} = \begin{bmatrix} 0 & p_9 \\ 0 & p_9 \end{bmatrix} \quad (4.16)$$

Two-sided *I-of-I* sign chart essential transition probability matrix:

$$\mathbf{Q}_{1-of-1(T)} = \begin{bmatrix} 0 & p_3 \\ 0 & p_3 \end{bmatrix} \quad (4.17)$$

4.6.2.2 The 2-of-2 sign charts

The essential transition probability matrices of the upper one-sided 2-of-2, lower one-sided 2-of-2 and two-sided 2-of-2 charts are given by:

Upper one-sided 2-of-2 sign chart essential transition probability matrix:

$$\mathbf{Q}_{2\text{-of-2}(U)} = \begin{bmatrix} 0 & p_7 & p_8 \\ 0 & p_7 & p_8 \\ 0 & p_7 & 0 \end{bmatrix} \quad (4.18)$$

Lower one-sided 2-of-2 sign chart essential transition probability matrix:

$$\mathbf{Q}_{2\text{-of-2}(L)} = \begin{bmatrix} 0 & p_6 & p_9 \\ 0 & p_6 & p_9 \\ 0 & p_6 & 0 \end{bmatrix} \quad (4.19)$$

Two-sided 2-of-2 sign chart essential transition probability matrix:

$$\mathbf{Q}_{2\text{-of-2}(T)} = \begin{bmatrix} 0 & p_3 & p_8 & p_9 \\ 0 & p_3 & p_8 & p_9 \\ 0 & p_3 & 0 & p_9 \\ 0 & p_3 & p_8 & 0 \end{bmatrix} \quad (4.20)$$

4.6.2.3 The 2-of-3 sign charts

The essential transition probability matrices of the upper one-sided 2-of-3, lower one-sided 2-of-3 and two-sided 2-of-3 charts are given by:

Upper one-sided 2-of-3 sign chart essential transition probability matrix:

$$\mathbf{Q}_{2\text{-of-3}(U)} = \begin{bmatrix} 0 & p_7 & p_8 & 0 & 0 \\ 0 & p_7 & 0 & p_8 & 0 \\ 0 & 0 & 0 & 0 & p_7 \\ 0 & 0 & 0 & 0 & p_7 \\ 0 & p_7 & 0 & 0 & 0 \end{bmatrix} \quad (4.21)$$

Lower one-sided 2-of-3 sign chart essential transition probability matrix:

$$\mathbf{Q}_{2\text{-of-3}(L)} = \begin{bmatrix} 0 & p_6 & p_9 & 0 & 0 \\ 0 & p_6 & 0 & p_9 & 0 \\ 0 & 0 & 0 & 0 & p_6 \\ 0 & 0 & 0 & 0 & p_6 \\ 0 & p_6 & 0 & 0 & 0 \end{bmatrix} \quad (4.22)$$

Two-sided 2-of-3 sign chart essential transition probability matrix:

$$\mathbf{Q}_{2\text{-of-3}(T)} = \begin{bmatrix} 0 & p_3 & p_8 & p_9 & 0 & 0 & 0 & 0 \\ 0 & p_3 & 0 & 0 & p_8 & p_9 & 0 & 0 \\ 0 & 0 & 0 & p_9 & 0 & 0 & p_3 & 0 \\ 0 & 0 & p_8 & 0 & 0 & 0 & 0 & p_3 \\ 0 & 0 & 0 & p_9 & 0 & 0 & p_3 & 0 \\ 0 & 0 & p_8 & 0 & 0 & 0 & 0 & p_3 \\ 0 & p_3 & 0 & 0 & 0 & p_9 & 0 & 0 \\ 0 & p_3 & 0 & 0 & p_8 & 0 & 0 & 0 \end{bmatrix} \quad (4.23)$$

Note that the essential transition probability matrices of the 2-of-3 charts are marginally different from the essential transition probability matrices in Human et al. (2009). A discussion on this point is given in Remark 3.22 of Chapter 3.

4.6.2.4 The *improved 2-of-2* sign charts

The essential transition probability matrices of the upper one-sided *improved 2-of-2*, lower one-sided *improved 2-of-2* and two-sided *improved 2-of-2* charts are given by:

Upper one-sided *improved 2-of-2* sign chart essential transition probability matrix:

$$\mathbf{Q}_{12\text{-of-2}(U)} = \begin{bmatrix} 0 & p_7 & p_2 \\ 0 & p_7 & p_2 \\ 0 & p_7 & 0 \end{bmatrix} \quad (4.24)$$

Lower one-sided *improved 2-of-2* sign chart essential transition probability matrix:

$$\mathbf{Q}_{12\text{-of-2}(L)} = \begin{bmatrix} 0 & p_6 & p_4 \\ 0 & p_6 & p_4 \\ 0 & p_6 & 0 \end{bmatrix} \quad (4.25)$$

Two-sided *improved 2-of-2* sign chart essential transition probability matrix:

$$\mathbf{Q}_{12\text{-of-}2(T)} = \begin{bmatrix} 0 & p_3 & p_2 & p_4 \\ 0 & p_3 & p_2 & p_4 \\ 0 & p_3 & 0 & p_4 \\ 0 & p_3 & p_2 & 0 \end{bmatrix} \quad (4.26)$$

4.6.2.5 The *improved 2-of-3* sign charts

The essential transition probability matrices of the upper one-sided *improved 2-of-3*, lower one-sided *improved 2-of-3* and two-sided *improved 2-of-3* charts are given by:

Upper one-sided *improved 2-of-3* sign chart essential transition probability matrix:

$$\mathbf{Q}_{12\text{-of-}3(U)} = \begin{bmatrix} 0 & p_7 & p_2 & 0 & 0 \\ 0 & p_7 & 0 & p_2 & 0 \\ 0 & 0 & 0 & 0 & p_7 \\ 0 & 0 & 0 & 0 & p_7 \\ 0 & p_7 & 0 & 0 & 0 \end{bmatrix} \quad (4.27)$$

Lower one-sided *improved 2-of-3* sign chart essential transition probability matrix:

$$\mathbf{Q}_{12\text{-of-}3(L)} = \begin{bmatrix} 0 & p_6 & p_4 & 0 & 0 \\ 0 & p_6 & 0 & p_4 & 0 \\ 0 & 0 & 0 & 0 & p_6 \\ 0 & 0 & 0 & 0 & p_6 \\ 0 & p_6 & 0 & 0 & 0 \end{bmatrix} \quad (4.28)$$

Two-sided *improved 2-of-3* sign chart essential transition probability matrix:

$$\mathbf{Q}_{12\text{-of-}3(T)} = \begin{bmatrix} 0 & p_3 & p_2 & 0 & 0 & p_4 & 0 & 0 \\ 0 & p_3 & 0 & p_2 & 0 & 0 & p_4 & 0 \\ 0 & 0 & 0 & 0 & p_3 & p_4 & 0 & 0 \\ 0 & 0 & 0 & 0 & p_3 & p_4 & 0 & 0 \\ 0 & p_3 & 0 & 0 & 0 & 0 & p_4 & 0 \\ 0 & 0 & p_2 & 0 & 0 & 0 & 0 & p_3 \\ 0 & 0 & p_2 & 0 & 0 & 0 & 0 & p_3 \\ 0 & p_3 & 0 & p_2 & 0 & 0 & 0 & 0 \end{bmatrix} \quad (4.29)$$

4.6.3 Run-length distribution and associated characteristics of the charts

From Theorems 2.1 and 2.3 the following run-length distribution formulae follow:

$$P(N = j) = \xi \mathbf{Q}^{j-1} (\mathbf{I} - \mathbf{Q}) \mathbf{1}, \text{ for } j = 1, 2, 3, \dots \text{ with } \mathbf{Q}^0 = \mathbf{I} \quad (\text{pdf of the run-length distribution}) \quad (4.30)$$

$$P(N \leq j) = 1 - \xi \mathbf{Q}^j \mathbf{1}, \text{ for } j = 1, 2, 3, \dots \quad (\text{cdf of the run-length distribution}) \quad (4.31)$$

$$E(N) = \xi (\mathbf{I} - \mathbf{Q})^{-1} \mathbf{1} \quad (\text{expected value of the run-length distribution}) \quad (4.32)$$

$$\text{Var}(N) = \xi (\mathbf{I} + \mathbf{Q}) (\mathbf{I} - \mathbf{Q})^{-2} \mathbf{1} - \left(\xi (\mathbf{I} - \mathbf{Q})^{-1} \mathbf{1} \right)^2 \quad (\text{variance of the run-length distribution}) \quad (4.33)$$

where: $\mathbf{Q} = \mathbf{Q}_{h \times h}$ is the essential transition probability matrix,

$$\xi = \xi_{1 \times h} = (1, 0, 0, \dots, 0),$$

$$\mathbf{1} = \mathbf{1}_{h \times 1} = (1, 1, 1, \dots, 1)^T,$$

$\mathbf{I} = \mathbf{I}_{h \times h}$ is the identity matrix,

N is the run-length random variable,

j is the integer value that N can assume, and

h is an integer value representing the number of transient states.

To calculate the run-length distribution and some associated characteristics of a chart under consideration, the appropriate essential transition probability matrix needs to substitute into equations (4.30), (4.31), (4.32) and (4.33). SAS[®]9.2 and Mathcad[®]14.0 are software packages that are capable of evaluating these expressions.

Refer to Section 1.6.3 and Table 1.1 of Chapter 1 for elaboration on equations (4.30) – (4.33).

4.7 False alarm rates

A single compact *FAR* formula for the different sign charts is not available. Consequently a formula for each chart is given below.

Note that all the probabilities given below are IC probabilities, in other words it is the probability of T_i plotting in a zone on the chart given the process is IC.

$$FAR_{1-af-1(U)} = p_8 \quad \text{for time} = 1,2,3,\dots \quad (4.34)$$

$$FAR_{1-af-1(L)} = p_9 \quad \text{for time} = 1,2,3,\dots \quad (4.35)$$

$$FAR_{1-af-1(T)} = p_8 + p_9 \quad \text{for time} = 1,2,3,\dots \quad (4.36)$$

$$FAR_{2-af-2(U)} = \begin{cases} 0 & \text{for time} = 1 \\ p_8^2 & \text{for time} = 2,3,4,\dots \end{cases} \quad (4.37)$$

$$FAR_{2-af-2(L)} = \begin{cases} 0 & \text{for time} = 1 \\ p_9^2 & \text{for time} = 2,3,4,\dots \end{cases} \quad (4.38)$$

$$FAR_{2-af-2(T)} = \begin{cases} 0 & \text{for time} = 1 \\ p_8^2 + p_9^2 & \text{for time} = 2,3,4,\dots \end{cases} \quad (4.39)$$

$$FAR_{2-af-3(U)} = \begin{cases} 0 & \text{for time} = 1 \\ p_8^2 & \text{for time} = 2 \\ 2p_7p_8^2 & \text{for time} = 3,4,5,\dots \end{cases} \quad (4.40)$$

$$FAR_{2-af-3(L)} = \begin{cases} 0 & \text{for time} = 1 \\ p_9^2 & \text{for time} = 2 \\ 2p_6p_9^2 & \text{for time} = 3,4,5,\dots \end{cases} \quad (4.41)$$

$$FAR_{2-af-3(T)} = \begin{cases} 0 & \text{for time} = 1 \\ p_8^2 + p_9^2 & \text{for time} = 2 \\ 2p_3p_8^2 + 2p_3p_9^2 + p_8p_9^2 + p_9p_8^2 & \text{for time} = 3,4,5,\dots \end{cases} \quad (4.42)$$

$$FAR_{I2-af-2(U)} = \begin{cases} p_1 & \text{for time} = 1 \\ p_1 + p_2^2 & \text{for time} = 2,3,4,\dots \end{cases} \quad (4.43)$$

$$FAR_{I_{2-of-2}(L)} = \begin{cases} p_5 & \text{for time} = 1 \\ p_5 + p_4^2 & \text{for time} = 2,3,4,\dots \end{cases} \quad (4.44)$$

$$FAR_{I_{2-of-2}(T)} = \begin{cases} p_1 + p_5 & \text{for time} = 1 \\ p_1 + p_5 + p_2^2 + p_4^2 & \text{for time} = 2,3,4,\dots \end{cases} \quad (4.45)$$

$$FAR_{I_{2-of-3}(U)} = \begin{cases} p_1 & \text{for time} = 1 \\ p_1 + p_2^2 & \text{for time} = 2 \\ p_1 + 2p_7p_2^2 & \text{for time} = 3,4,5,\dots \end{cases} \quad (4.46)$$

$$FAR_{I_{2-of-3}(L)} = \begin{cases} p_5 & \text{for time} = 1 \\ p_5 + p_4^2 & \text{for time} = 2 \\ p_5 + 2p_6p_4^2 & \text{for time} = 3,4,5,\dots \end{cases} \quad (4.47)$$

$$FAR_{I_{2-of-3}(T)} = \begin{cases} p_1 + p_5 & \text{for time} = 1 \\ p_1 + p_5 + p_2^2 + p_4^2 & \text{for time} = 2 \\ p_1 + p_5 + 2p_3p_2^2 + 2p_3p_4^2 + p_4p_2^2 + p_2p_4^2 & \text{for time} = 3,4,5,\dots \end{cases} \quad (4.48)$$

Where the p_i 's are defined in (4.6)-(4.14) with $p = p_0$, i.e. IC probabilities.

Remark 4.2

An advantage of using the Markov chain approach is that it can be used to calculate the IC and OOC run-length distribution and some IC and OOC characteristics of the run-length distribution. In order to calculate a chart's IC run-length distribution and characteristics, IC probabilities p_1, p_2, \dots, p_9 needs to be substituted into the essential transition probability matrix, i.e. $\theta = \theta_0$. Conversely, to calculate a control chart's OOC run-length distribution and characteristics, OOC probabilities p_1, p_2, \dots, p_9 need to be substituted into the essential transition probability matrix, i.e. $\theta \neq \theta_0$.

Remark 4.3

If $\theta = \theta_0$, the process is IC and the probability that the chart signals depends only on:

- (i) The sample size n ,
- (ii) Some or all of the control limits UCL_B , UCL_A/UCL , LCL_A/LCL and LCL_B , and
- (iii) The specified value of the $100\pi^{\text{th}}$ ($0 < \pi < 1$) percentile denoted by θ_0 .

Therefore any signalling events based on the T_i 's are distribution-free since the IC probability of a signal does not depend on the underlying process distribution as long as the process distribution is continuous and identical at every point in time. Consequently the IC run-length distribution, and hence the sign chart is distribution-free.

Remark 4.4

Note that when the process is OOC i.e. $\theta \neq \theta_0$ the run-length distribution depends on the underlying process distribution. The underlying process distribution influences the parameter p of the Binomial distribution. Therefore p is no longer be equal to p_0 (i.e. $p \neq p_0$).

Consequently the transition probabilities in equations (4.6) to (4.14) will be influenced. These transition probabilities are used to populate the essential transition probability matrix which are used to calculate the run-length distribution as can be seen in equations (4.30) to (4.33). Therefore p depends on the underlying process distribution and ultimately so does the run-length distribution.

Remark 4.5

The run-length distribution and the characteristics of the sign charts can now be calculated since the following is established; the plotting statistic, essential transition probability matrices, the ability to calculate the probabilities inside the essential transition probability matrices (transition probabilities) and formulae to calculate the run-length distribution and the characteristics of the *1-of-1*, *2-of-2*, *2-of-3*, *improved 2-of-2* and *improved 2-of-3* sign charts.

Charting constants/control limits for the sign charts are required for practical implementation by the quality practitioner. Performance comparisons are required to illustrate that *improved* runs-rules sign charts are an improvement over the runs-rules sign charts. This is done through the examination of the characteristics of charts such as the average run-length (*ARL*), the false alarm rate (*FAR*), the standard deviation of the run-length (*SDRL*) and percentiles of the run-length distribution (see e.g. Human et al. (2009)). Refer to Section 1.12.2 of Chapter 1 for an elaboration on the performance analysis of a chart using the characteristic of the run-length distribution.

4.8 Design of the *improved* runs-rules sign charts

In practice one is interested in a chart that has good properties, for instance a large IC *ARL* and small *FAR* (for more detail refer to Chapter 1). The IC properties of a nonparametric (sign) chart depend on the design parameters which include:

- (i) the sample size n
- (ii) the charting constants a, b, c and d , and
- (iii) the target value θ_0 .

The design of the sign charts is given where the median is chosen to be monitored. The median is a popular percentile that is used to monitor the location, hence $\pi = 0.5$ and $p = p_0 = P(X_{ij} > \theta_0 | IC) = 0.5$. Note that in general the sign chart can be used to monitor any desired percentile.

The charting constants can assume any integer values between and including zero and n . However, the charting constants are chosen such that the IC *ARL* assumes values that are informative/usable to the quality practitioner. Note that the charting constants are chosen symmetrically for the median i.e. $LCL_B = a$, $LCL_A / LCL = b$, $UCL_A / UCL = c = n - b$ and $UCL_B = d = n - a$.

These IC characteristics (*ARL* and *FAR*) of the *improved* runs-rules sign charts are calculated by evaluating exact expressions using Proc IML in SAS[®]9.2.

Remark 4.6

Note that since the median is monitored the IC distribution of the sign (plotting) statistic is symmetric, $(T_i \sim \text{Bin}(n, 0.5))$. Since the plotting statistic is symmetric it follows naturally to select the control limits (charting constants) so that they are symmetric. Based on symmetric control limits the IC run-length distribution of the upper and the lower one-sided *improved 2-of-2* and *improved 2-of-3* charts are equal and that the IC performance of the lower and the upper one-sided *improved* sign charts, for monitoring the median, are identical.

It will be shown that the run-length distributions of the upper and the lower *improved 2-of-2* charts are equal and that the performance of the lower and the upper *improved* one-sided sign charts, for monitoring the median, are identical. Recall that equations (4.30) to (4.33) are used to calculate the run-length distribution and the characteristics of the run-length distribution. Equations (4.30) to (4.33) depend only on:

$\mathbf{Q} = \mathbf{Q}_{h \times h}$ the essential transition probability matrix,

$$\boldsymbol{\xi} = \boldsymbol{\xi}_{1 \times h} = (1, 0, 0, \dots, 0),$$

$$\mathbf{1} = \mathbf{1}_{h \times 1} = (1, 1, 1, \dots, 1)^T,$$

$\mathbf{I} = \mathbf{I}_{h \times h}$ is the identity matrix,

where h is the number of transient states. The upper and the lower *improved 2-of-2* charts have the same number of transient states. The only difference between the upper and the lower *improved 2-of-2* charts is the essential transition probability matrix. From investigating matrices (4.24) and (4.25) it is clear that the essential transition probability matrices will be the same if:

$$p_2 = p_4, \text{ and}$$

$$p_6 = p_7.$$

Where:

$$p_2 = P(UCL_A \leq T_i < UCL_B) = \sum_{x=0}^{UCL_B-1} \binom{n}{x} p^x (1-p)^{n-x} - \sum_{x=0}^{UCL_A-1} \binom{n}{x} p^x (1-p)^{n-x} \quad (\text{see equation (4.7)}),$$

or alternatively:

$$p_2 = P(n-b \leq T_i < n-a) = \sum_{x=0}^{n-a-1} \binom{n}{x} p^x (1-p)^{n-x} - \sum_{x=0}^{n-b-1} \binom{n}{x} p^x (1-p)^{n-x}, \text{ and}$$

$$p_4 = P(LCL_B < T_i \leq LCL_A) = \sum_{x=0}^{LCL_A} \binom{n}{x} p^x (1-p)^{n-x} - \sum_{x=0}^{LCL_B} \binom{n}{x} p^x (1-p)^{n-x} \quad (\text{see equation (4.9)}),$$

or alternatively:

$$p_4 = P(a < T_i \leq b) = \sum_{x=0}^b \binom{n}{x} p^x (1-p)^{n-x} - \sum_{x=0}^a \binom{n}{x} p^x (1-p)^{n-x}.$$

p_2 will equal p_4 if:

$P(n-b \leq T_i < n-a) = P(a < T_i \leq b)$ which is the case since the control limits are symmetrically selected, and plotting statistic is symmetric, ($T_i \sim \text{Bin}(n, 0.5)$), i.e.

$$\text{i.e. } \sum_{x=0}^{n-a-1} \binom{n}{x} p^x (1-p)^{n-x} - \sum_{x=0}^{n-b-1} \binom{n}{x} p^x (1-p)^{n-x} = \sum_{x=0}^b \binom{n}{x} p^x (1-p)^{n-x} - \sum_{x=0}^a \binom{n}{x} p^x (1-p)^{n-x}$$

Similarly p_6 will equal p_7 .

Consequently the essential transition probability matrices of the upper and the lower one-sided *improved 2-of-2* charts are equal since their corresponding transition probabilities are equal. This in turn results in an equal run-length distribution of the upper and the lower one-sided *improved 2-of-2* charts. Consequently, when monitoring the process median, the performances of the upper and the lower one-sided *improved 2-of-2* sign charts are equal.

A similar argument can be provided to prove that based on symmetric control limits that the run-length distribution of the upper and the lower *improved 2-of-3* charts are equal and that the performance of the lower and the upper one-sided *improved* sign charts, for monitoring the median, are identical i.e. they are equal in distribution. This is omitted here.

4.8.1 Tables presenting the IC characteristics of the *improved* runs-rules sign charts

Tables 4.2, 4.3, 4.4 and 4.5 provide the IC characteristics (*ARL* and *FAR*) of the *improved* runs-rules sign charts. These Tables will aid in selecting appropriate control limits in the application of the *improved* runs-rules sign charts. Following the presentation and explanation of Tables 4.2, 4.3, 4.4 and 4.5 an example is given to illustrate the use of the Tables 4.2, 4.3, 4.4 and 4.5, and also the application of the *improved* runs-rules sign charts.

Table 4.1 is provided to clarify the notation used in the Tables 4.2, 4.3, 4.4 and 4.5.

Table 4.1: Description of the notation used in Tables 4.1, 4.2, 4.3 and 4.4.

Notation	Description
n	Sample size.
a	Integer representing the value of the outer lower control limit (LCL_B).
b	Integer representing the value of the inner lower control limit (LCL_A).
c	Integer representing the value of the inner upper control limit (UCL_A).
d	Integer representing the value of the outer upper control limit (UCL_B).
ARL_0	In control ARL .
$FAR1$	False alarm rate for time = 1.
$FAR234$	False alarm rate for time = 2, 3, 4,....
$FAR2$	False alarm rate for time = 2.
$FAR345$	False alarm rate for time = 3, 4, 5,....
$I2\text{-of-2}$ (U & L)	Upper and lower one-sided <i>improved 2-of-2</i> charts.
$I2\text{-of-2}$ (Two-Sided)	Two-sided <i>improved 2-of-2</i> chart.
$I2\text{-of-3}$ (U & L)	Upper and lower one-sided <i>improved 2-of-3</i> charts.
$I2\text{-of-3}$ (Two-Sided)	Two-sided <i>improved 2-of-3</i> chart.

4.8.2 The use of Tables 4.2, 4.3, 4.4 and 4.5

An illustration is discussed to explain the use of Tables 4.2, 4.3, 4.4 and 4.5. Consider a two-sided *improved 2-of-2* sign chart, with a sample size of 20, used to monitor a process median. Suitable charting constants/control limits need to be selected to obtain desirable properties for the chart.

In Table 4.2 the first column provides the choice of sample sizes. The last 16 rows of Table 4.2 provides information on the upper and the lower one-sided *improved 2-of-2* sign chart and the two-sided *improved 2-of-2* sign chart with a sample size of 20. However, since the two-sided *improved 2-of-2* sign chart is considered, only the last three columns are of interest.

Columns two, three, four and five provide the combinations of control limits. Now focus is placed on the last 16 rows and columns two, three, four, five, nine, ten and eleven since all the information on the two-sided *improved 2-of-2* sign chart is provided in these cells.

Suppose that control limits need to be selected so that the IC *ARL* of the *improved* two-sided chart is approximately 370. Column nine contains the IC *ARL* values. The seventh row from the bottom of Table 4.2 contains an IC *ARL* value of 381.78. Note that since the sign statistic is a discrete statistic, an IC *ARL* of 370 is not possible for the two-sided *improved 2-of-2* sign chart with a sample size of 20. The control limits that provides an IC *ARL* of 381.78 can be obtained from the Table, $LCL_B = 3$, $LCL_A = 4$, $UCL_A = 16$ and $UCL_B = 17$, where $FAR_1=0.00258$ and $FAR_{234}=0.00262$.

4.8.3 Discussion on Tables 4.2, 4.3, 4.4 and 4.5

A general observation can be made regarding Tables 4.2, 4.3, 4.4 and 4.5 that as the sample size increases that the possible combinations of *ARL* and *FAR* increases. It can be seen that the one-sided charts has a greater combination of practical *ARL* and *FAR* combinations.

For the upper one-sided *improved 2-of-2* (two-sided *improved 2-of-2*) sign chart a sample size of at least nine (ten) is required to obtain a practical IC *ARL* of 443.11 (466.85). Where for the upper one-sided *improved 2-of-3* (two-sided *improved 2-of-3*) sign chart a sample size of at least nine (ten) is required to obtain a practical IC *ARL* of 393.01 (430.41).

From the discussions in this section and in the discussion in the previous section where the application of Tables 4.2, 4.3, 4.4 and 4.5 is discussed it can be seen that the Tables provide a great deal of information. However, the use of Tables 4.2, 4.3, 4.4 and 4.5 is simple and should be useful to the quality practitioner.

Table 4.2: The in-control characteristics (*ARL* and *FAR*) of the upper one-sided, lower one-sided and two-sided *improved 2-of-2* sign charts for the median ($n=5-20$).

Sample Size	LCL_B	LCL_A	UCL_A	UCL_B	<i>I2-of-2</i> (U & L)			<i>I2-of-2</i> (Two-Sided)		
n	$a=n-d$	$b=n-c$	$c=n-b$	$d=n-a$	ARL_0	FAR_1	FAR_{234}	ARL_0	FAR_1	FAR_{234}
5	0	1	4	5	19.10	0.03125	0.05566	9.55	0.06250	0.11133
	0	2	3	5	5.53	0.03125	0.25098			
	1	2	3	4	3.82	0.18750	0.28516			
6	0	1	5	6	42.26	0.01563	0.02441	21.13	0.03125	0.04883
	0	2	4	6	10.34	0.01563	0.12329			
	1	2	4	5	6.50	0.10938	0.16431			
7	0	1	6	7	93.91	0.00781	0.01080	46.96	0.01563	0.02161
	0	2	5	7	21.24	0.00781	0.05566			
	1	2	5	6	11.68	0.06250	0.08942			
8	0	1	7	8	206.05	0.00391	0.00488	103.02	0.00781	0.00977
	0	2	6	8	47.07	0.00391	0.02368	23.54	0.00781	0.04736
	1	2	6	7	21.77	0.03516	0.04712			
9	0	1	8	9	443.11	0.00195	0.00226	221.55	0.00391	0.00452
	0	2	7	9	110.45	0.00195	0.00968	55.23	0.00391	0.01936
	1	2	7	8	41.41	0.01953	0.02448			
10	0	1	9	10	933.70	0.00098	0.00107	466.85	0.00195	0.00214
	0	2	8	10	269.22	0.00098	0.00386	134.61	0.00195	0.00772
	0	3	7	10	38.58	0.00098	0.03018			
	1	2	8	9	79.41	0.01074	0.01267	39.71	0.02148	0.02535
15	0	3	12	15	3001.87	0.00003	0.00034	1500.93	0.00006	0.00068
	0	4	11	15	299.43	0.00003	0.00354	149.71	0.00006	0.00707
	0	5	10	15	50.50	0.00003	0.02279	25.25	0.00006	0.04557
	1	3	12	14	1289.60	0.00049	0.00078	644.80	0.00098	0.00156
	1	4	11	14	266.81	0.00049	0.00394	133.41	0.00098	0.00788
	1	5	10	14	49.63	0.00049	0.02311	24.82	0.00098	0.04621
	2	3	12	13	257.55	0.00369	0.00389	128.77	0.00739	0.00777
	2	4	11	13	151.17	0.00369	0.00678	75.58	0.00739	0.01356
	2	5	10	13	44.29	0.00369	0.02536	22.15	0.00739	0.05071
	3	4	11	12	51.96	0.01758	0.01931	25.98	0.03516	0.03863
	4	5	10	11	14.94	0.05923	0.06763			
20	0	5	15	20	2378.10	0.00000	0.00043	1189.05	0.00000	0.00086
	0	6	14	20	318.05	0.00000	0.00333	159.02	0.00000	0.00665
	0	7	13	20	65.35	0.00000	0.01732	32.67	0.00000	0.03463
	1	5	15	19	2278.88	0.00002	0.00045	1139.44	0.00004	0.00089
	1	6	14	19	316.33	0.00002	0.00334	158.17	0.00004	0.00668
	1	7	13	19	65.28	0.00002	0.01733	32.64	0.00004	0.03466
	2	5	15	18	1631.92	0.00020	0.00062	815.96	0.00040	0.00124
	2	6	14	18	300.91	0.00020	0.00350	150.45	0.00040	0.00701
	2	7	13	18	64.69	0.00020	0.01746	32.34	0.00040	0.03493
	3	4	16	17	763.55	0.00129	0.00131	381.78	0.00258	0.00262
	3	6	14	17	232.75	0.00129	0.00447	116.37	0.00258	0.00893
	3	7	13	17	61.32	0.00129	0.01827	30.66	0.00258	0.03653
	4	5	15	16	163.28	0.00591	0.00613	81.64	0.01182	0.01226
	4	6	14	16	118.27	0.00591	0.00859	59.13	0.01182	0.01717
	4	7	13	16	50.15	0.00591	0.02170	25.07	0.01182	0.04341
5	6	14	15	45.43	0.02069	0.02206	22.71	0.04139	0.04412	

Table 4.3: The in-control characteristics (*ARL* and *FAR*) of the upper one-sided, lower one-sided and two-sided *improved 2-of-2* sign charts for the median ($n=25$).

Sample Size	LCL_B	LCL_A	UCL_A	UCL_B	<i>I2-of-2</i> (U & L)			<i>I2-of-2</i> (Two-Sided)		
n	$a=n-d$	$b=n-c$	$c=n-b$	$d=n-a$	ARL_0	FAR_1	FAR_{234}	ARL_0	FAR_1	FAR_{234}
25	0	7	18	25	2180.98	0.00000	0.00047	1090.49	0.00000	0.00094
	0	8	17	25	363.07	0.00000	0.00290	181.54	0.00000	0.00581
	0	9	16	25	84.64	0.00000	0.01317	42.32	0.00000	0.02634
	0	10	15	25	26.93	0.00000	0.04502			
	1	7	18	24	2177.59	0.00000	0.00047	1088.80	0.00000	0.00094
	1	8	17	24	362.98	0.00000	0.00290	181.49	0.00000	0.00581
	1	9	16	24	84.64	0.00000	0.01317	42.32	0.00000	0.02634
	1	10	15	24	26.93	0.00000	0.04502			
	2	7	18	23	2137.72	0.00001	0.00048	1068.86	0.00002	0.00096
	2	8	17	23	361.93	0.00001	0.00291	180.96	0.00002	0.00582
	2	9	16	23	84.59	0.00001	0.01318	42.29	0.00002	0.02636
	2	10	15	23	26.92	0.00001	0.04503			
	3	6	19	22				3837.93	0.00016	0.00026
	3	7	18	22	1874.53	0.00008	0.00054	937.27	0.00016	0.00109
	3	8	17	22	354.02	0.00008	0.00297	177.01	0.00016	0.00594
	3	9	16	22	84.19	0.00008	0.01323	42.10	0.00016	0.02646
	3	10	15	22	26.89	0.00008	0.04506			
	4	5	20	21				1092.27	0.00091	0.00092
	4	6	19	21				995.98	0.00091	0.00100
	4	7	18	21	1117.50	0.00046	0.00090	558.75	0.00091	0.00181
	4	8	17	21	316.02	0.00046	0.00331	158.01	0.00091	0.00662
	4	9	16	21	82.10	0.00046	0.01352	41.05	0.00091	0.02704
	4	10	15	21	26.70	0.00046	0.04528			
	5	6	19	20	483.94	0.00204	0.00207	241.97	0.00408	0.00413
	5	7	18	20	413.98	0.00204	0.00242	206.99	0.00408	0.00485
	5	8	17	20	217.71	0.00204	0.00473	108.85	0.00408	0.00945
	5	9	16	20	74.31	0.00204	0.01475	37.15	0.00408	0.02949
	5	10	15	20	25.95	0.00204	0.04620			
6	7	18	19	133.00	0.00732	0.00752	66.50	0.01463	0.01504	
6	8	17	19	106.52	0.00732	0.00948	53.26	0.01463	0.01897	
6	9	16	19	56.37	0.00732	0.01886	28.18	0.01463	0.03772	
7	8	17	18	44.15	0.02164	0.02268	22.08	0.04329	0.04536	

Table 4.4: The in-control characteristics (*ARL* and *FAR*) of the upper one-sided, lower one-sided and two-sided *improved 2-of-3* sign charts for the median ($n=5-20$).

Sample Size	LCL_B	LCL_A	UCL_A	UCL_B	<i>I2-of-3</i> (U & L)				<i>I2-of-3</i> (Two-Sided)			
n	$a=n-d$	$b=n-c$	$c=n-b$	$d=n-a$	ARL_0	FAR_1	FAR_2	FAR_{345}	ARL_0	FAR_1	FAR_2	FAR_{345}
5	0	1	4	5	15.21	0.03125	0.05566	0.07092	7.95	0.06250	0.11133	0.13116
6	0	1	5	6	33.62	0.01563	0.02441	0.03128	17.22	0.03125	0.04883	0.06036
7	0	1	6	7	76.62	0.00781	0.01080	0.01342	38.76	0.01563	0.02161	0.02642
	0	2	5	7	14.50	0.00781	0.05566	0.08183				
8	0	1	7	8	175.01	0.00391	0.00488	0.00579	87.97	0.00781	0.00977	0.01151
	0	2	6	8	30.30	0.00391	0.02368	0.03774	16.04	0.00781	0.04736	0.06961
9	0	1	8	9	393.01	0.00195	0.00226	0.00256	196.94	0.00391	0.00452	0.00510
	0	2	7	9	68.55	0.00195	0.00968	0.01601	35.52	0.00391	0.01936	0.03061
	1	2	7	8	35.90	0.01953	0.02448	0.02853	18.18	0.03906	0.04895	0.05598
10	0	1	9	10	860.10	0.00098	0.00107	0.00117	430.41	0.00195	0.00214	0.00233
	0	2	8	10	165.08	0.00098	0.00386	0.00643	84.35	0.00195	0.00772	0.01254
	0	3	7	10	24.00	0.00098	0.03018	0.04935	12.93	0.00195	0.06037	0.08860
	1	2	8	9	70.41	0.01074	0.01267	0.01439	35.43	0.02148	0.02535	0.02853
	1	3	7	9	21.09	0.01074	0.03671	0.05374				
15	0	3	12	15	1611.81	0.00003	0.00034	0.00064	812.53	0.00006	0.00068	0.00126
	0	4	11	15	163.08	0.00003	0.00354	0.00663	83.83	0.00006	0.00707	0.01284
	0	5	10	15	30.37	0.00003	0.02279	0.03867	16.24	0.00006	0.04557	0.07048
	1	2	13	14					983.07	0.00098	0.00100	0.00102
	1	3	12	14	953.93	0.00049	0.00078	0.00106	479.16	0.00098	0.00156	0.00211
	1	4	11	14	153.83	0.00049	0.00394	0.00698	78.92	0.00098	0.00788	0.01355
	1	5	10	14	30.11	0.00049	0.02311	0.03890	16.09	0.00098	0.04621	0.07095
	2	3	12	13	246.03	0.00369	0.00389	0.00407	123.11	0.00739	0.00777	0.00813
	2	4	11	13	109.92	0.00369	0.00678	0.00950	55.88	0.00739	0.01356	0.01861
	2	5	10	13	28.42	0.00369	0.02536	0.04048	15.09	0.00739	0.05071	0.07427
	3	4	11	12	48.32	0.01758	0.01931	0.02084	24.27	0.03516	0.03863	0.04142
	4	5	10	11	13.79	0.05923	0.06763	0.07350				
20	0	4	16	20					7189.62	0.00000	0.00007	0.00014
	0	5	15	20	1226.68	0.00000	0.00043	0.00084	619.56	0.00000	0.00086	0.00166
	0	6	14	20	172.18	0.00000	0.00333	0.00627	88.46	0.00000	0.00665	0.01215
	0	7	13	20	38.51	0.00000	0.01732	0.03007	20.42	0.00000	0.03463	0.05559
	1	4	16	19					5670.31	0.00004	0.00011	0.00018
	1	5	15	19	1200.76	0.00002	0.00045	0.00086	606.32	0.00004	0.00089	0.00170
	1	6	14	19	171.72	0.00002	0.00334	0.00628	88.22	0.00004	0.00668	0.01218
	1	7	13	19	38.49	0.00002	0.01733	0.03008	20.41	0.00004	0.03466	0.05561
	2	5	15	18	999.90	0.00020	0.00062	0.00102	504.00	0.00040	0.00124	0.00203
	2	6	14	18	167.51	0.00020	0.00350	0.00642	85.98	0.00040	0.00701	0.01246
	2	7	13	18	38.32	0.00020	0.01746	0.03018	20.31	0.00040	0.03493	0.05582
	3	4	16	17	751.54	0.00129	0.00131	0.00133	375.81	0.00258	0.00262	0.00266
	3	5	15	17	498.44	0.00129	0.00167	0.00203	250.12	0.00258	0.00333	0.00404
	3	6	14	17	145.96	0.00129	0.00447	0.00728	74.60	0.00258	0.00893	0.01418
	3	7	13	17	37.31	0.00129	0.01827	0.03078	19.74	0.00258	0.03653	0.05704
	4	5	15	16	157.99	0.00591	0.00613	0.00634	79.05	0.01182	0.01226	0.01266
	4	6	14	16	94.02	0.00591	0.00859	0.01096	47.58	0.01182	0.01717	0.02157
	4	7	13	16	33.55	0.00591	0.02170	0.03334				
5	6	14	15	43.16	0.02069	0.02206	0.02327	21.64	0.04139	0.04412	0.04633	

Table 4.5: The in-control characteristics (*ARL* and *FAR*) of the upper one-sided, lower one-sided and two-sided *improved 2-of-3* sign charts for the median ($n=25$).

Sample Size	LCL_B	LCL_A	UCL_A	UCL_B	<i>I2-of-3</i> (U & L)				<i>I2-of-3</i> (Two-Sided)			
n	$a=n-d$	$b=n-c$	$c=n-b$	$d=n-a$	ARL_0	$FAR1$	$FAR2$	$FAR345$	ARL_0	$FAR1$	$FAR2$	$FAR345$
25	0	6	19	25					4771.42	0.00000	0.00011	0.00021
	0	7	18	25	1125.30	0.00000	0.00047	0.00092	568.62	0.00000	0.00094	0.00181
	0	8	17	25	195.59	0.00000	0.00290	0.00549	100.31	0.00000	0.00581	0.01067
	0	9	16	25	48.99	0.00000	0.01317	0.02332	25.80	0.00000	0.02634	0.04361
	1	6	19	24					4738.69	0.00000	0.00011	0.00021
	1	7	18	24	1124.44	0.00000	0.00047	0.00092	568.18	0.00000	0.00094	0.00181
	1	8	17	24	195.56	0.00000	0.00290	0.00549	100.30	0.00000	0.00581	0.01067
	1	9	16	24	48.99	0.00000	0.01317	0.02332	25.80	0.00000	0.02634	0.04361
	2	6	19	23					4378.24	0.00002	0.00013	0.00023
	2	7	18	23	1114.14	0.00001	0.00048	0.00093	562.91	0.00002	0.00096	0.00183
	2	8	17	23	195.28	0.00001	0.00291	0.00550	100.15	0.00002	0.00582	0.01069
	2	9	16	23	48.97	0.00001	0.01318	0.02332	25.79	0.00002	0.02636	0.04362
	3	6	19	22					2765.35	0.00016	0.00026	0.00036
	3	7	18	22	1041.02	0.00008	0.00054	0.00099	525.58	0.00016	0.00109	0.00196
	3	8	17	22	193.16	0.00008	0.00297	0.00555	99.03	0.00016	0.00594	0.01080
	3	9	16	22	48.86	0.00008	0.01323	0.02336	25.73	0.00016	0.02646	0.04371
	4	5	20	21					1086.37	0.00091	0.00092	0.00092
	4	6	19	21	1825.46	0.00046	0.00050	0.00055	913.29	0.00091	0.00100	0.00110
	4	7	18	21	764.74	0.00046	0.00090	0.00133	385.01	0.00091	0.00181	0.00265
	4	8	17	21	182.28	0.00046	0.00331	0.00586	93.29	0.00091	0.00662	0.01140
	4	9	16	21	48.26	0.00046	0.01352	0.02359	25.39	0.00091	0.02704	0.04417
	5	6	19	20	477.65	0.00204	0.00207	0.00209	238.85	0.00408	0.00413	0.00419
	5	7	18	20	360.93	0.00204	0.00242	0.00279	180.97	0.00408	0.00485	0.00556
	5	8	17	20	147.30	0.00204	0.00473	0.00712	74.97	0.00408	0.00945	0.01395
	5	9	16	20	45.88	0.00204	0.01475	0.02454	24.05	0.00408	0.02949	0.04610
	6	7	18	19	129.68	0.00732	0.00752	0.00772	64.87	0.01463	0.01504	0.01542
	6	8	17	19	89.41	0.00732	0.00948	0.01142	45.10	0.01463	0.01897	0.02257
	6	9	16	19	39.35	0.00732	0.01886	0.02776				
7	8	17	18	42.47	0.02164	0.02268	0.02361	21.28	0.04329	0.04536	0.04706	

Remark 4.7

The sign statistic is a discrete statistic i.e. the sign statistic can only assume a finite number of possible values. Consequently the sign chart can only assume a finite number of possible *ARL* and *FAR* combinations for a choice of n . The possible *ARL* and *FAR* combinations increases as n increase.

Example 4.1

An example where the median is monitored is presented to illustrate the application of the sign chart. A two-sided *improved 2-of-2* sign chart and a two-sided *improved 2-of-3* sign chart is presented in this example.

In this example the median of the inside diameter measurements of forged automobile engine piston rings are monitored. The observations that were used for this example is given on p.223 in Table 5.3 of Montgomery (2005), the observations was supplemented with additional observations given on p.250 in Exercise 5.10 of Montgomery (2005). Note that the data is modified by grouping two consecutive samples of size five together to obtain 19 samples (i.e. a total of 190 observations) of size ten each. This grouping of two samples of size five each was done purely for illustration purposes in this Example, so that samples of size ten each could be obtained which would yield combinations of control limits that provide a “practical” IC ARL.

In order to apply the sign charts the charting constants are required. Tables 4.6 and 4.7 are provided to aid in choosing appropriate charting constants.

Table 4.6: The in-control characteristics (ARL and FAR) of the two-sided *improved 2-of-2* sign chart for the median ($n=10$).

<i>I2-of-2 (Two-Sided)</i>						
LCL_B	LCL_A	UCL_A	UCL_B	ARL_0	$FAR1$	$FAR234$
$a=n-d$	$b=n-c$	$c=n-b$	$d=n-a$			
0	1	9	10	466.85	0.00195	0.00214
0	2	8	10	134.61	0.00195	0.00772
1	2	8	9	39.71	0.02148	0.02535

Table 4.7: The in-control characteristics (ARL and FAR) of the two-sided *improved 2-of-3* sign chart for the median ($n=10$).

<i>I2-of-3 (Two-Sided)</i>							
LCL_B	LCL_A	UCL_A	UCL_B	ARL_0	$FAR1$	$FAR2$	$FAR345$
$a=n-d$	$b=n-c$	$c=n-b$	$d=n-a$				
0	1	9	10	430.41	0.00195	0.00214	0.00233
0	2	8	10	84.35	0.00195	0.00772	0.01254
0	3	7	10	12.93	0.00195	0.06037	0.0886

When choosing $LCL_B=0$, $LCL_A=1$, $UCL_A=9$ and $UCL_B=10$ the ARL_0 is 467 and 430 for the two-sided *improved 2-of-2* and the two-sided *improved 2-of-3* sign charts respectively as can be seen in Tables 4.6 and 4.7. With this the choice of control limits, the two-sided *improved 2-of-2* and the two-sided *improved 2-of-3* sign charts appears visually identical, since the plotting statistic is calculated in the same manner and the control limits are the same as can be seen in and Figure 4.1. The only difference is the signalling rules and ultimately the characteristics of the charts.

A plot of the sign statistics is presented in Figure 4.1. Note that for this set of observations both the two-sided *improved 2-of-2* and the two-sided *improved 2-of-3* sign charts signal at the 19th sample. Note that if the two-sided *2-of-2* and the two-sided *2-of-3* sign charts were considered, neither one would have signalled at the 19th sample since the 19th sample would have been the first plotting statistic plotting on or above the UCL_A/UCL . The two-sided *1-of-1* sign chart would not be appropriate to compare in this case since the control limits would be wider than UCL_A/UCL (to obtain a similar IC ARL), so the chart may signal or not depending if the plotting statistic plots on or above UCL_A/UCL .

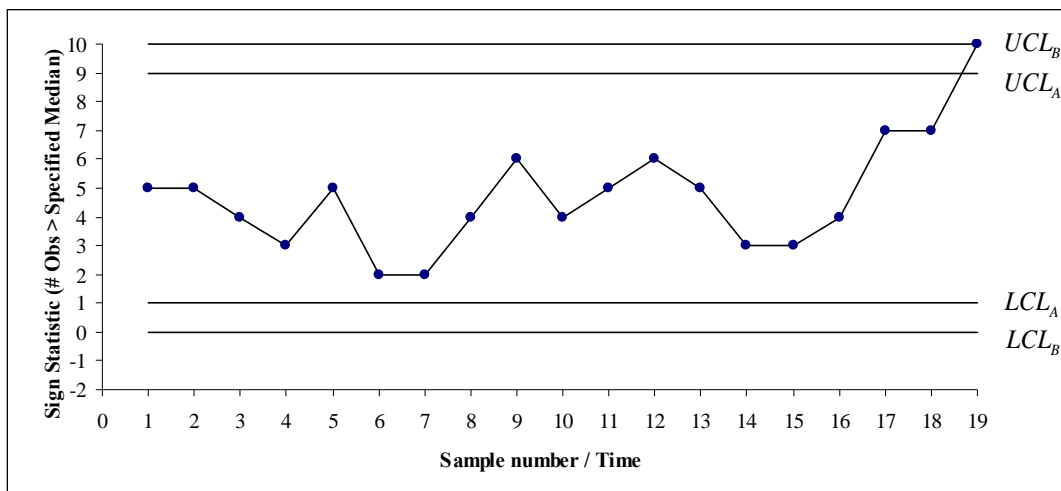


Figure 4.1: The two-sided *improved 2-of-2* and two-sided *improved 2-of-3* sign charts for monitoring the median for Montgomery (2005) piston-ring data.

4.9 Performance of the *improved* runs-rules sign charts

Performance analysis between two competing charts is performed when their IC ARL (ARL_0) values are equal or, at least approximately so. The chart that detects a shift in the least amount of observations (smallest OOC ARL) is declared to be the superior chart. Refer to Section 1.12 of Chapter 1 for a discussion on the performance of a chart.

The *improved* runs-rules charts are compared to the runs-rules charts to illustrate the advantages of the *improved* runs-rules charts over the runs-rules charts. These performance comparisons were done by evaluating exact expressions using Proc IML in SAS[®]9.2.

Recall the claims that *improved* runs-rules sign charts are superior in performance for large shifts in the process, while maintaining the same sensitivity in the detection of small shifts compared to runs-rules sign charts. Performance analysis is done to confirm these claims.

The performance comparisons between the *improved* runs-rules sign charts and runs-rules sign charts are done by considering the Normal (symmetric distribution), Students- t (symmetric with heavy tails) and Exponentially (skew) distributions as the underlying process distributions as illustrated in Figure 4.2. Performance analysis is done using different underlying process distributions to investigate the performance of the *improved* runs-rules sign charts under different conditions. It will be shown in the performance analysis that the *improved* runs-rules sign charts do not perform equally well when altering the underlying process distribution.

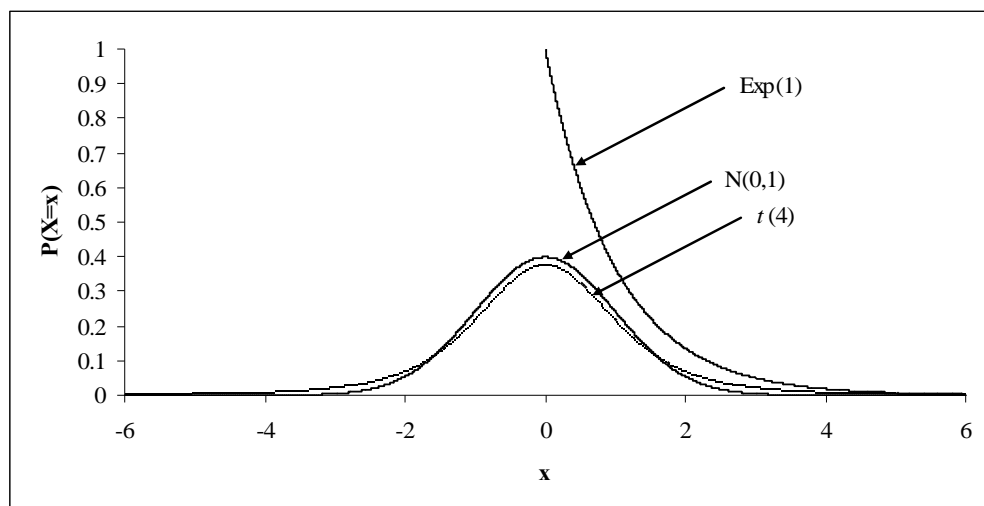


Figure 4.2: Different underlying process distributions that are used to perform performance comparisons.

4.9.1 Discussion on the performance analysis Tables

Refer to Table 4.8 to clarify the notation used in Tables 4.9 to 4.22.

Table 4.8: Description of notation used in Tables 4.9 – 4.22.

Notation	Description
$N(0,1)$	Standard Normal underlying process distribution.
$T(4)$	Students $t(4)$ underlying process distribution.
$Exp(1)$	Exponential ($\theta = 1$) underlying process distribution.
<i>Shift</i> (σ Units)	Shift in the underlying process distribution in standard deviation units.
<i>2-of-2</i> (U&L)	Upper and lower one-sided <i>2-of-2</i> runs-rules sign charts.
<i>I2-of-2</i> (U&L)	Upper and lower one-sided <i>improved 2-of-2</i> runs-rules sign charts.
<i>2-of-2</i> (U)	Upper one-sided <i>2-of-2</i> runs-rules sign chart.
<i>I2-of-2</i> (U)	Upper one-sided <i>improved 2-of-2</i> runs-rules sign chart.
<i>2-of-2</i> (L)	Lower one-sided <i>2-of-2</i> runs-rules sign chart.
<i>I2-of-2</i> (L)	Lower one-sided <i>improved 2-of-2</i> runs-rules sign chart.
<i>2-of-2</i> (T)	Two-sided <i>2-of-2</i> runs-rules sign chart.
<i>I2-of-2</i> (T)	Two-sided <i>improved 2-of-2</i> runs-rules sign chart.
<i>2-of-3</i> (U&L)	Upper and lower one-sided <i>2-of-3</i> runs-rules sign charts.
<i>I2-of-3</i> (U&L)	Upper and lower one-sided <i>improved 2-of-3</i> runs-rules sign charts.
<i>2-of-3</i> (U)	Upper one-sided <i>2-of-3</i> runs-rules sign chart.
<i>I2-of-3</i> (U)	Upper one-sided <i>improved 2-of-3</i> runs-rules sign chart.
<i>2-of-3</i> (L)	Lower one-sided <i>2-of-3</i> runs-rules sign chart.
<i>I2-of-3</i> (L)	Lower one-sided <i>improved 2-of-3</i> runs-rules sign chart.
<i>2-of-3</i> (T)	Two-sided <i>2-of-3</i> runs-rules sign chart.
<i>I2-of-3</i> (T)	Two-sided <i>improved 2-of-3</i> runs-rules sign chart.
<i>ARL</i>	Average run-length.
<i>SDRL</i>	Standard deviation of the run-length.
5^{th}	5^{th} Percentile of the run-length distribution.
Q_1	25^{th} Percentile (first quartile) of the run-length distribution.
<i>MDRL</i>	50^{th} Percentile (median) of the run-length distribution.
Q_3	75^{th} Percentile (third quartile) of the run-length distribution.
95^{th}	95^{th} Percentile of the run-length distribution.

To illustrate the use of Tables 4.9 to 4.22 consider the following situation. A process is monitored using $n=20$ and the underlying process distribution is $N(0,1)$. A comparison needs to be done between the two-sided *2-of-2* runs-rules sign chart and the two-sided *improved 2-of-2* runs-rules sign chart. This can be done by considering Table 4.13.

From Table 4.13, it can be seen that the control limits are $LCL_B=1$, $LCL_A=6$, $UCL_A=14$ and $UCL_B=19$. From the second row it can be seen that the first column contains the shift in the underlying process distribution in standard deviation units. Columns two to eight (nine to fifteen) contain the characteristics (ARL , $SDRL$, the 5^{th} , 25^{th} (Q_1), 50^{th} (MRL), 75^{th} (Q_3) and 95^{th} percentiles) of the two-sided runs-rules sign chart (two-sided *improved* runs-rules sign chart). Refer to Table 4.8 for clarity on the notation.

First, the observation can be made that the IC ARL for the two-sided *2-of-2* runs-rules sign chart and the two-sided *improved 2-of-2* runs-rules sign chart are 159.07 and 158.17, respectively. Since the IC ARL is the same or approximately so, OOC performance analysis is meaningful.

Second, it is seen that since the underlying process distribution is symmetric, upward and downward shifts of the same magnitude render the same performance for both the two-sided runs-rules sign chart and the two-sided *improved* runs-rules sign chart.

Consider an upward shift of a 0.2 standard deviation units (σ unit shift = 0.2), then the OOC ARL is 31.59 and 31.39 for the two-sided runs-rules sign chart and the two-sided *improved* runs-rules sign chart respectively (note that the other characteristics are similar or the same). From this the first claim is supported that the *improved* runs-rules sign charts are as sensitive to small process shifts as the runs-rules sign charts. Now consider an upward shift of 2.2 standard deviation units (σ unit shift = 2.2), then the OOC ARL is 2 and 1.03 for the two-sided runs-rules sign chart and the two-sided *improved* runs-rules sign chart respectively. From this, the second claim is supported that *improved* runs-rules sign charts detect larger shifts in the process more efficiently. The superiority of the *improved* runs-rules sign charts in the presence of large process shifts is also confirmed by the remaining characteristics.

4.9.2 Discussion on the performance analysis results

Considering Tables 4.9 to 4.22 the following observations can be made regarding the performance comparison between the runs-rules and the *improved* runs-rules sign charts:

- From Tables 4.9, 4.10, 4.11 and 4.12 it can be seen that the upper and the lower one-sided *improved 2-of-2* sign charts are as sensitive to small process shifts compared to the upper and the lower one-sided *2-of-2* sign charts while having the ability to detect large process shifts more efficiently. However, for the $t(4)$ distribution and for the $Exp(1)$ distribution (for downward shifts) the *improved 2-of-2* charts the OOC ARL seem to converge slower to one i.e. less efficient in the detection of large process shifts.
- From Tables 4.13, 4.14 and 4.15 it can be seen that the two-sided *improved 2-of-2* sign chart is as sensitive to small process shifts compared to the two-sided *2-of-2* sign chart while having the ability to detect large process shifts more efficiently. Note that for certain underlying distributions the two-sided *improved 2-of-2* sign chart is able to detect large process shifts more efficiently than for other distributions. However, the chart is less efficient in detecting large process shifts in the case of a downward shift when the underlying process distribution is $Exp(1)$ as can be seen in Table 4.15.
- Close inspection of Tables 4.16, 4.17, 4.18, 4.19, 4.20, 4.21 and 4.22 lead to the same conclusions regarding the *improved 2-of-3* runs-rules sign charts.
- From investigating the performance analysis it can be concluded that, in general the *improved* runs-rules sign charts are as sensitive to small shifts as the runs-rules sign charts, while at least have the ability to detect large process shifts more efficient than runs-rules sign charts.

Remark 4.8

Note that Tables 4.9 to 4.22 are rich in information regarding the OOC performance of the runs-rules and the *improved* runs-rules sign charts and can be a discussion topic on its own. However, in this dissertation the main concern is to confirm the two claims that the *improved* runs-rules sign charts are superior in performance to the runs-rules sign charts for large shifts in the process, while maintaining the same sensitivity in the detection of small shifts. These two claims are confirmed in the previous discussion.

Remark 4.9

The OOC characteristics for the upper and the lower one-sided charts are presented in the same tables for the $N(0,1)$ and the $t(4)$ distributions since these distributions are symmetric. The shifts for the lower one-sided charts are presented in brackets in the column titled “Shift”.

Table 4.9: The OOC characteristics of the upper and the lower one-sided 2-of-2 sign charts and the improved 2-of-2 sign charts for the median ($n=20$) where $LCL_B=1$, $LCL_A=6$, $UCL_A=14$ and $UCL_B=19$.

$N(0,1)$ Distribution														
σ Units	2-of-2 (U&L)							I2-of-2 (U&L)						
Shift	ARL	SDRL	5th	Q_1	MDRL	Q_3	95th	ARL	SDRL	5th	Q_1	MDRL	Q_3	95th
-0.2 (0.2)	8474.71	8473.22	436	2439	5875	11748	25385	8414.54	8413.06	433	2422	5833	11664	25205
-0.1 (0.1)	1449.97	1448.49	76	418	1005	2010	4341	1441.17	1439.70	75	416	999	1997	4314
0	318.13	316.68	18	93	221	440	950	316.33	314.89	18	92	220	438	945
0.1 (-0.1)	89.23	87.81	6	27	62	123	264	88.71	87.31	6	27	62	122	263
0.2 (-0.2)	31.71	30.34	3	10	22	43	92	31.51	30.15	3	10	22	43	92
0.3 (-0.3)	14.03	12.70	2	5	10	19	39	13.93	12.61	2	5	10	19	39
0.4 (-0.4)	7.53	6.22	2	3	6	10	20	7.46	6.17	2	3	6	10	20
0.5 (-0.5)	4.76	3.45	2	2	4	6	12	4.71	3.41	2	2	4	6	12
0.6 (-0.6)	3.44	2.09	2	2	3	4	8	3.38	2.06	2	2	2	4	8
0.7 (-0.7)	2.76	1.34	2	2	2	3	6	2.69	1.33	2	2	2	3	5
0.8 (-0.8)	2.39	0.89	2	2	2	2	4	2.30	0.90	1	2	2	2	4
0.9 (-0.9)	2.19	0.60	2	2	2	2	4	2.07	0.65	1	2	2	2	4
1 (-1)	2.09	0.40	2	2	2	2	3	1.92	0.52	1	2	2	2	2
1.1 (-1.1)	2.04	0.26	2	2	2	2	2	1.80	0.48	1	2	2	2	2
1.2 (-1.2)	2.02	0.16	2	2	2	2	2	1.70	0.49	1	1	2	2	2
1.3 (-1.3)	2.01	0.10	2	2	2	2	2	1.59	0.50	1	1	2	2	2
1.4 (-1.4)	2.00	0.06	2	2	2	2	2	1.49	0.50	1	1	1	2	2
1.5 (-1.5)	2.00	0.03	2	2	2	2	2	1.39	0.49	1	1	1	2	2
1.6 (-1.6)	2.00	0.02	2	2	2	2	2	1.30	0.46	1	1	1	2	2
1.7 (-1.7)	2.00	0.01	2	2	2	2	2	1.22	0.42	1	1	1	1	2
1.8 (-1.8)	2.00	0.00	2	2	2	2	2	1.16	0.37	1	1	1	1	2
1.9 (-1.9)	2.00	0.00	2	2	2	2	2	1.11	0.31	1	1	1	1	2
2 (-2)	2.00	0.00	2	2	2	2	2	1.08	0.26	1	1	1	1	2
2.1 (-2.1)	2.00	0.00	2	2	2	2	2	1.05	0.22	1	1	1	1	1
2.2 (-2.2)	2.00	0.00	2	2	2	2	2	1.03	0.17	1	1	1	1	1
2.3 (-2.3)	2.00	0.00	2	2	2	2	2	1.02	0.14	1	1	1	1	1
2.4 (-2.4)	2.00	0.00	2	2	2	2	2	1.01	0.11	1	1	1	1	1
2.5 (-2.5)	2.00	0.00	2	2	2	2	2	1.01	0.08	1	1	1	1	1
2.6 (-2.6)	2.00	0.00	2	2	2	2	2	1.00	0.06	1	1	1	1	1

Table 4.10: The OOC characteristics of the upper and the lower one-sided 2-of-2 sign charts and the improved 2-of-2 sign charts for the median ($n=20$) where $LCL_B=1$, $LCL_A=6$, $UCL_A=14$ and $UCL_B=19$.

$t(4)$ Distribution														
σ Units	2-of-2 (U&L)							I2-of-2 (U&L)						
Shift	ARL	SDRL	5 th	Q_1	MDRL	Q_3	95 th	ARL	SDRL	5 th	Q_1	MDRL	Q_3	95 th
-0.2 (0.2)	30268.2	30266.7	1554	8709	20981	41960	90673	30017.7	30016.2	1541	8637	20807	41613	89922
-0.1 (0.1)	2516.02	2514.54	130	725	1744	3487	7534	2500.11	2498.64	130	720	1733	3465	7487
0	318.13	316.68	18	93	221	440	950	316.33	314.89	18	92	220	438	945
0.1 (-0.1)	61.97	60.58	4	19	43	85	183	61.61	60.22	4	19	43	85	182
0.2 (-0.2)	18.29	16.95	2	6	13	25	52	18.16	16.83	2	6	13	25	52
0.3 (-0.3)	7.76	6.45	2	3	6	10	21	7.69	6.39	2	3	6	10	20
0.4 (-0.4)	4.39	3.07	2	2	3	6	11	4.34	3.03	2	2	3	5	10
0.5 (-0.5)	3.07	1.70	2	2	2	4	6	3.01	1.67	2	2	2	4	6
0.6 (-0.6)	2.49	1.02	2	2	2	3	4	2.41	1.02	2	2	2	2	4
0.7 (-0.7)	2.22	0.65	2	2	2	2	4	2.11	0.69	1	2	2	2	4
0.8 (-0.8)	2.10	0.41	2	2	2	2	3	1.93	0.53	1	2	2	2	3
0.9 (-0.9)	2.04	0.26	2	2	2	2	2	1.81	0.48	1	2	2	2	2
1 (-1)	2.02	0.16	2	2	2	2	2	1.70	0.49	1	1	2	2	2
1.1 (-1.1)	2.01	0.10	2	2	2	2	2	1.60	0.50	1	1	2	2	2
1.2 (-1.2)	2.00	0.06	2	2	2	2	2	1.50	0.50	1	1	1	2	2
1.3 (-1.3)	2.00	0.04	2	2	2	2	2	1.41	0.49	1	1	1	2	2
1.4 (-1.4)	2.00	0.02	2	2	2	2	2	1.34	0.47	1	1	1	2	2
1.5 (-1.5)	2.00	0.01	2	2	2	2	2	1.27	0.44	1	1	1	2	2
1.6 (-1.6)	2.00	0.01	2	2	2	2	2	1.21	0.41	1	1	1	1	2
1.7 (-1.7)	2.00	0.00	2	2	2	2	2	1.17	0.37	1	1	1	1	2
1.8 (-1.8)	2.00	0.00	2	2	2	2	2	1.13	0.34	1	1	1	1	2
1.9 (-1.9)	2.00	0.00	2	2	2	2	2	1.10	0.30	1	1	1	1	2
2 (-2)	2.00	0.00	2	2	2	2	2	1.08	0.27	1	1	1	1	2
2.1 (-2.1)	2.00	0.00	2	2	2	2	2	1.06	0.24	1	1	1	1	2
2.2 (-2.2)	2.00	0.00	2	2	2	2	2	1.05	0.22	1	1	1	1	1
2.3 (-2.3)	2.00	0.00	2	2	2	2	2	1.04	0.19	1	1	1	1	1
2.4 (-2.4)	2.00	0.00	2	2	2	2	2	1.03	0.17	1	1	1	1	1
2.5 (-2.5)	2.00	0.00	2	2	2	2	2	1.02	0.15	1	1	1	1	1
2.6 (-2.6)	2.00	0.00	2	2	2	2	2	1.02	0.14	1	1	1	1	1
2.7 (-2.7)	2.00	0.00	2	2	2	2	2	1.02	0.12	1	1	1	1	1
2.8 (-2.8)	2.00	0.00	2	2	2	2	2	1.01	0.11	1	1	1	1	1
2.9 (-2.9)	2.00	0.00	2	2	2	2	2	1.01	0.10	1	1	1	1	1
3 (-3)	2.00	0.00	2	2	2	2	2	1.01	0.09	1	1	1	1	1

Table 4.11: The OOC characteristics of the upper one-sided 2-of-2 sign charts and the improved 2-of-2 sign charts for the median ($n=20$) where $LCL_B=1$, $LCL_A=6$, $UCL_A=14$ and $UCL_B=19$.

Exp(1) Distribution														
σ Units	2-of-2 (U)							I2-of-2 (U)						
Shift	ARL	SDRL	5 th	Q_1	MDRL	Q_3	95 th	ARL	SDRL	5 th	Q_1	MDRL	Q_3	95 th
-0.2	14869.17	14867.68	764	4279	10307	20612	44541	14756.61	14755.12	758	4246	10229	20456	44204
-0.1	2008.01	2006.53	104	579	1392	2783	6013	1995.54	1994.07	104	575	1384	2766	5975
0	318.13	316.68	18	93	221	440	950	316.33	314.89	18	92	220	438	945
0.1	62.36	60.96	5	19	44	86	184	61.99	60.60	4	19	43	85	183
0.2	16.10	14.77	2	6	12	22	46	15.99	14.67	2	6	11	22	45
0.3	5.78	4.47	2	2	4	7	15	5.73	4.43	2	2	4	7	15
0.4	2.97	1.58	2	2	2	4	6	2.91	1.56	2	2	2	4	6
0.5	2.15	0.53	2	2	2	2	3	2.02	0.60	1	2	2	2	3
0.6	2.00	0.08	2	2	2	2	2	1.54	0.50	1	1	2	2	2
0.7	2.00	0.00	2	2	2	2	2	1.00	0.00	1	1	1	1	1
0.8	2.00	0.00	2	2	2	2	2	1.00	0.00	1	1	1	1	1
0.9	2.00	0.00	2	2	2	2	2	1.00	0.00	1	1	1	1	1
1	2.00	0.00	2	2	2	2	2	1.00	0.00	1	1	1	1	1
1.1	2.00	0.00	2	2	2	2	2	1.00	0.00	1	1	1	1	1
1.2	2.00	0.00	2	2	2	2	2	1.00	0.00	1	1	1	1	1
1.3	2.00	0.00	2	2	2	2	2	1.00	0.00	1	1	1	1	1
1.4	2.00	0.00	2	2	2	2	2	1.00	0.00	1	1	1	1	1
1.5	2.00	0.00	2	2	2	2	2	1.00	0.00	1	1	1	1	1
1.6	2.00	0.00	2	2	2	2	2	1.00	0.00	1	1	1	1	1
1.7	2.00	0.00	2	2	2	2	2	1.00	0.00	1	1	1	1	1
1.8	2.00	0.00	2	2	2	2	2	1.00	0.00	1	1	1	1	1
1.9	2.00	0.00	2	2	2	2	2	1.00	0.00	1	1	1	1	1
2	2.00	0.00	2	2	2	2	2	1.00	0.00	1	1	1	1	1
2.1	2.00	0.00	2	2	2	2	2	1.00	0.00	1	1	1	1	1
2.2	2.00	0.00	2	2	2	2	2	1.00	0.00	1	1	1	1	1
2.3	2.00	0.00	2	2	2	2	2	1.00	0.00	1	1	1	1	1
2.4	2.00	0.00	2	2	2	2	2	1.00	0.00	1	1	1	1	1
2.5	2.00	0.00	2	2	2	2	2	1.00	0.00	1	1	1	1	1
2.6	2.00	0.00	2	2	2	2	2	1.00	0.00	1	1	1	1	1
2.7	2.00	0.00	2	2	2	2	2	1.00	0.00	1	1	1	1	1
2.8	2.00	0.00	2	2	2	2	2	1.00	0.00	1	1	1	1	1
2.9	2.00	0.00	2	2	2	2	2	1.00	0.00	1	1	1	1	1
3	2.00	0.00	2	2	2	2	2	1.00	0.00	1	1	1	1	1

Table 4.12: The OOC characteristics of the lower one-sided 2-of-2 sign charts and the improved 2-of-2 sign charts for the median ($n=20$) where $LCL_B=1$, $LCL_A=6$, $UCL_A=14$ and $UCL_B=19$.

σ Units	Exp(1) Distribution													
	2-of-2 (L)							I2-of-2 (L)						
	Shift	ARL	SDRL	5 th	Q_1	MDRL	Q_3	95 th	ARL	SDRL	5 th	Q_1	MDRL	Q_3
0.2	42668.0	42666.5	2190	12276	29576	59150	127819	42298.1	42296.6	2171	12169	29319	58637	126711
0.1	2491.19	2489.71	129	718	1727	3453	7460	2475.46	2473.98	128	713	1716	3431	7413
0	318.13	316.68	18	93	221	440	950	316.33	314.89	18	92	220	438	945
-0.1	71.57	70.17	5	22	50	99	212	71.16	69.76	5	21	50	98	210
-0.2	24.46	23.10	2	8	17	33	71	24.30	22.95	2	8	17	33	70
-0.3	11.36	10.04	2	4	8	15	31	11.28	9.97	2	4	8	15	31
-0.4	6.60	5.29	2	3	5	9	17	6.54	5.24	2	3	5	9	17
-0.5	4.50	3.18	2	2	4	6	11	4.44	3.14	2	2	3	6	11
-0.6	3.44	2.09	2	2	3	4	8	3.39	2.06	2	2	2	4	8
-0.7	2.86	1.46	2	2	2	3	6	2.80	1.44	2	2	2	3	6
-0.8	2.52	1.06	2	2	2	3	5	2.45	1.06	2	2	2	3	4
-0.9	2.32	0.79	2	2	2	2	4	2.22	0.81	1	2	2	2	4
-1	2.19	0.60	2	2	2	2	4	2.07	0.65	1	2	2	2	4
-1.1	2.12	0.45	2	2	2	2	3	1.96	0.55	1	2	2	2	3
-1.2	2.07	0.35	2	2	2	2	2	1.88	0.50	1	2	2	2	2
-1.3	2.04	0.26	2	2	2	2	2	1.81	0.48	1	2	2	2	2
-1.4	2.02	0.20	2	2	2	2	2	1.74	0.48	1	1	2	2	2
-1.5	2.01	0.15	2	2	2	2	2	1.68	0.49	1	1	2	2	2
-1.6	2.01	0.11	2	2	2	2	2	1.62	0.50	1	1	2	2	2
-1.7	2.00	0.08	2	2	2	2	2	1.56	0.50	1	1	2	2	2
-1.8	2.00	0.06	2	2	2	2	2	1.50	0.50	1	1	2	2	2
-1.9	2.00	0.05	2	2	2	2	2	1.45	0.50	1	1	1	2	2
-2	2.00	0.03	2	2	2	2	2	1.40	0.49	1	1	1	2	2
-2.1	2.00	0.02	2	2	2	2	2	1.35	0.48	1	1	1	2	2
-2.2	2.00	0.02	2	2	2	2	2	1.31	0.46	1	1	1	2	2
-2.3	2.00	0.01	2	2	2	2	2	1.27	0.44	1	1	1	2	2
-2.4	2.00	0.01	2	2	2	2	2	1.23	0.42	1	1	1	1	2
-2.5	2.00	0.01	2	2	2	2	2	1.20	0.40	1	1	1	1	2
-2.6	2.00	0.00	2	2	2	2	2	1.17	0.37	1	1	1	1	2
-2.7	2.00	0.00	2	2	2	2	2	1.14	0.35	1	1	1	1	2
-2.8	2.00	0.00	2	2	2	2	2	1.12	0.33	1	1	1	1	2
-2.9	2.00	0.00	2	2	2	2	2	1.10	0.30	1	1	1	1	2
-3	2.00	0.00	2	2	2	2	2	1.09	0.28	1	1	1	1	2

Table 4.13: The OOC characteristics of the two-sided 2-of-2 sign charts and the improved 2-of-2 sign charts for the median ($n=20$) where $LCL_B=1$, $LCL_A=6$, $UCL_A=14$ and $UCL_B=19$.

$N(0,1)$ Distribution														
σ Units	2-of-2 (T)							I2-of-2 (T)						
Shift	ARL	SDRL	5 th	Q_1	MDRL	Q_3	95 th	ARL	SDRL	5 th	Q_1	MDRL	Q_3	95 th
2.2	2.00	0.00	2	2	2	2	2	1.03	0.17	1	1	1	1	1
2.1	2.00	0.00	2	2	2	2	2	1.05	0.22	1	1	1	1	1
2	2.00	0.00	2	2	2	2	2	1.08	0.26	1	1	1	1	2
1.9	2.00	0.00	2	2	2	2	2	1.11	0.31	1	1	1	1	2
1.8	2.00	0.00	2	2	2	2	2	1.16	0.37	1	1	1	1	2
1.7	2.00	0.01	2	2	2	2	2	1.22	0.42	1	1	1	1	2
1.6	2.00	0.02	2	2	2	2	2	1.30	0.46	1	1	1	2	2
1.5	2.00	0.03	2	2	2	2	2	1.39	0.49	1	1	1	2	2
1.4	2.00	0.06	2	2	2	2	2	1.49	0.50	1	1	1	2	2
1.3	2.01	0.10	2	2	2	2	2	1.59	0.50	1	1	2	2	2
1.2	2.02	0.16	2	2	2	2	2	1.70	0.49	1	1	2	2	2
1.1	2.04	0.26	2	2	2	2	2	1.80	0.48	1	2	2	2	2
1	2.09	0.40	2	2	2	2	3	1.92	0.52	1	2	2	2	2
0.9	2.19	0.60	2	2	2	2	4	2.07	0.65	1	2	2	2	4
0.8	2.39	0.89	2	2	2	2	4	2.30	0.90	1	2	2	2	4
0.7	2.76	1.34	2	2	2	3	6	2.69	1.33	2	2	2	3	5
0.6	3.44	2.09	2	2	3	4	8	3.38	2.06	2	2	2	4	8
0.5	4.76	3.45	2	2	4	6	12	4.71	3.41	2	2	4	6	12
0.4	7.53	6.22	2	3	6	10	20	7.46	6.17	2	3	6	10	20
0.3	14.02	12.69	2	5	10	19	39	13.92	12.60	2	5	10	19	39
0.2	31.59	30.22	3	10	22	43	92	31.39	30.03	3	10	22	43	91
0.1	84.05	82.64	6	25	59	116	249	83.57	82.16	6	25	58	115	248
0	159.07	157.61	10	47	111	220	474	158.17	156.72	9	47	110	219	471
-0.1	84.05	82.64	6	25	59	116	249	83.57	82.16	6	25	58	115	248
-0.2	31.59	30.22	3	10	22	43	92	31.39	30.03	3	10	22	43	91
-0.3	14.02	12.69	2	5	10	19	39	13.92	12.60	2	5	10	19	39
-0.4	7.53	6.22	2	3	6	10	20	7.46	6.17	2	3	6	10	20
-0.5	4.76	3.45	2	2	4	6	12	4.71	3.41	2	2	4	6	12
-0.6	3.44	2.09	2	2	3	4	8	3.38	2.06	2	2	2	4	8
-0.7	2.76	1.34	2	2	2	3	6	2.69	1.33	2	2	2	3	5
-0.8	2.39	0.89	2	2	2	2	4	2.30	0.90	1	2	2	2	4
-0.9	2.19	0.60	2	2	2	2	4	2.07	0.65	1	2	2	2	4
-1	2.09	0.40	2	2	2	2	3	1.92	0.52	1	2	2	2	2
-1.1	2.04	0.26	2	2	2	2	2	1.80	0.48	1	2	2	2	2
-1.2	2.02	0.16	2	2	2	2	2	1.70	0.49	1	1	2	2	2
-1.3	2.01	0.10	2	2	2	2	2	1.59	0.50	1	1	2	2	2
-1.4	2.00	0.06	2	2	2	2	2	1.49	0.50	1	1	1	2	2
-1.5	2.00	0.03	2	2	2	2	2	1.39	0.49	1	1	1	2	2
-1.6	2.00	0.02	2	2	2	2	2	1.30	0.46	1	1	1	2	2
-1.7	2.00	0.01	2	2	2	2	2	1.22	0.42	1	1	1	1	2
-1.8	2.00	0.00	2	2	2	2	2	1.16	0.37	1	1	1	1	2
-1.9	2.00	0.00	2	2	2	2	2	1.11	0.31	1	1	1	1	2
-2	2.00	0.00	2	2	2	2	2	1.08	0.26	1	1	1	1	2
-2.1	2.00	0.00	2	2	2	2	2	1.05	0.22	1	1	1	1	1
-2.2	2.00	0.00	2	2	2	2	2	1.03	0.17	1	1	1	1	1

Table 4.14: The OOC characteristics of the two-sided 2-of-2 sign charts and the improved 2-of-2 sign charts for the median ($n=20$) where $LCL_B=1$, $LCL_A=6$, $UCL_A=14$ and $UCL_B=19$.

$t(4)$ Distribution														
σ Units	2-of-2 (T)							I2-of-2 (T)						
Shift	ARL	SDRL	5 th	Q_1	MDRL	Q_3	95 th	ARL	SDRL	5 th	Q_1	MDRL	Q_3	95 th
2.2	2.00	0.00	2	2	2	2	2	1.05	0.22	1	1	1	1	1
2.1	2.00	0.00	2	2	2	2	2	1.06	0.24	1	1	1	1	2
2	2.00	0.00	2	2	2	2	2	1.08	0.27	1	1	1	1	2
1.9	2.00	0.00	2	2	2	2	2	1.10	0.30	1	1	1	1	2
1.8	2.00	0.00	2	2	2	2	2	1.13	0.34	1	1	1	1	2
1.7	2.00	0.00	2	2	2	2	2	1.17	0.37	1	1	1	1	2
1.6	2.00	0.01	2	2	2	2	2	1.21	0.41	1	1	1	1	2
1.5	2.00	0.01	2	2	2	2	2	1.27	0.44	1	1	1	2	2
1.4	2.00	0.02	2	2	2	2	2	1.34	0.47	1	1	1	2	2
1.3	2.00	0.04	2	2	2	2	2	1.41	0.49	1	1	1	2	2
1.2	2.00	0.06	2	2	2	2	2	1.50	0.50	1	1	1	2	2
1.1	2.01	0.10	2	2	2	2	2	1.60	0.50	1	1	2	2	2
1	2.02	0.16	2	2	2	2	2	1.70	0.49	1	1	2	2	2
0.9	2.04	0.26	2	2	2	2	2	1.81	0.48	1	2	2	2	2
0.8	2.10	0.41	2	2	2	2	3	1.93	0.53	1	2	2	2	3
0.7	2.22	0.65	2	2	2	2	4	2.11	0.69	1	2	2	2	4
0.6	2.49	1.02	2	2	2	3	4	2.41	1.02	2	2	2	2	4
0.5	3.07	1.70	2	2	2	4	6	3.01	1.67	2	2	2	4	6
0.4	4.39	3.07	2	2	3	6	11	4.34	3.03	2	2	3	5	10
0.3	7.76	6.45	2	3	6	10	21	7.69	6.39	2	3	6	10	20
0.2	18.28	16.94	2	6	13	25	52	18.15	16.82	2	6	13	25	52
0.1	60.48	59.08	4	18	42	83	178	60.13	58.74	4	18	42	83	177
0	159.07	157.61	10	47	111	220	474	158.17	156.72	9	47	110	219	471
-0.1	60.48	59.08	4	18	42	83	178	60.13	58.74	4	18	42	83	177
-0.2	18.28	16.94	2	6	13	25	52	18.15	16.82	2	6	13	25	52
-0.3	7.76	6.45	2	3	6	10	21	7.69	6.39	2	3	6	10	20
-0.4	4.39	3.07	2	2	3	6	11	4.34	3.03	2	2	3	5	10
-0.5	3.07	1.70	2	2	2	4	6	3.01	1.67	2	2	2	4	6
-0.6	2.49	1.02	2	2	2	3	4	2.41	1.02	2	2	2	2	4
-0.7	2.22	0.65	2	2	2	2	4	2.11	0.69	1	2	2	2	4
-0.8	2.10	0.41	2	2	2	2	3	1.93	0.53	1	2	2	2	3
-0.9	2.04	0.26	2	2	2	2	2	1.81	0.48	1	2	2	2	2
-1	2.02	0.16	2	2	2	2	2	1.70	0.49	1	1	2	2	2
-1.1	2.01	0.10	2	2	2	2	2	1.60	0.50	1	1	2	2	2
-1.2	2.00	0.06	2	2	2	2	2	1.50	0.50	1	1	1	2	2
-1.3	2.00	0.04	2	2	2	2	2	1.41	0.49	1	1	1	2	2
-1.4	2.00	0.02	2	2	2	2	2	1.34	0.47	1	1	1	2	2
-1.5	2.00	0.01	2	2	2	2	2	1.27	0.44	1	1	1	2	2
-1.6	2.00	0.01	2	2	2	2	2	1.21	0.41	1	1	1	1	2
-1.7	2.00	0.00	2	2	2	2	2	1.17	0.37	1	1	1	1	2
-1.8	2.00	0.00	2	2	2	2	2	1.13	0.34	1	1	1	1	2
-1.9	2.00	0.00	2	2	2	2	2	1.10	0.30	1	1	1	1	2
-2	2.00	0.00	2	2	2	2	2	1.08	0.27	1	1	1	1	2
-2.1	2.00	0.00	2	2	2	2	2	1.06	0.24	1	1	1	1	2
-2.2	2.00	0.00	2	2	2	2	2	1.05	0.22	1	1	1	1	1

Table 4.15: The OOC characteristics of the two-sided 2-of-2 sign charts and the improved 2-of-2 sign charts for the median ($n=20$) where $LCL_B=1$, $LCL_A=6$, $UCL_A=14$ and $UCL_B=19$.

Exp(1) Distribution														
σ Units	2-of-2 (T)							I2-of-2 (T)						
Shift	ARL	SDRL	5 th	Q_1	MDRL	Q_3	95 th	ARL	SDRL	5 th	Q_1	MDRL	Q_3	95 th
2.2	2.00	0.00	2	2	2	2	2	1.00	0.00	1	1	1	1	1
2.1	2.00	0.00	2	2	2	2	2	1.00	0.00	1	1	1	1	1
2	2.00	0.00	2	2	2	2	2	1.00	0.00	1	1	1	1	1
1.9	2.00	0.00	2	2	2	2	2	1.00	0.00	1	1	1	1	1
1.8	2.00	0.00	2	2	2	2	2	1.00	0.00	1	1	1	1	1
1.7	2.00	0.00	2	2	2	2	2	1.00	0.00	1	1	1	1	1
1.6	2.00	0.00	2	2	2	2	2	1.00	0.00	1	1	1	1	1
1.5	2.00	0.00	2	2	2	2	2	1.00	0.00	1	1	1	1	1
1.4	2.00	0.00	2	2	2	2	2	1.00	0.00	1	1	1	1	1
1.3	2.00	0.00	2	2	2	2	2	1.00	0.00	1	1	1	1	1
1.2	2.00	0.00	2	2	2	2	2	1.00	0.00	1	1	1	1	1
1.1	2.00	0.00	2	2	2	2	2	1.00	0.00	1	1	1	1	1
1	2.00	0.00	2	2	2	2	2	1.00	0.00	1	1	1	1	1
0.9	2.00	0.00	2	2	2	2	2	1.00	0.00	1	1	1	1	1
0.8	2.00	0.00	2	2	2	2	2	1.00	0.00	1	1	1	1	1
0.7	2.00	0.00	2	2	2	2	2	1.00	0.00	1	1	1	1	1
0.6	2.00	0.08	2	2	2	2	2	1.54	0.50	1	1	2	2	2
0.5	2.15	0.53	2	2	2	2	3	2.02	0.60	1	2	2	2	3
0.4	2.97	1.58	2	2	2	4	6	2.91	1.56	2	2	2	4	6
0.3	5.78	4.47	2	2	4	7	15	5.72	4.43	2	2	4	7	15
0.2	16.10	14.76	2	6	12	22	46	15.99	14.66	2	6	11	22	45
0.1	60.83	59.43	4	18	43	84	179	60.48	59.08	4	18	42	83	178
0	159.07	157.61	10	47	111	220	474	158.17	156.72	9	47	110	219	471
-0.1	69.11	67.70	5	21	48	95	204	68.71	67.31	5	21	48	95	203
-0.2	24.42	23.06	2	8	17	33	70	24.26	22.91	2	8	17	33	70
-0.3	11.36	10.04	2	4	8	15	31	11.28	9.96	2	4	8	15	31
-0.4	6.60	5.29	2	3	5	9	17	6.54	5.24	2	3	5	9	17
-0.5	4.50	3.18	2	2	4	6	11	4.44	3.14	2	2	3	6	11
-0.6	3.44	2.09	2	2	3	4	8	3.39	2.06	2	2	2	4	8
-0.7	2.86	1.46	2	2	2	3	6	2.80	1.44	2	2	2	3	6
-0.8	2.52	1.06	2	2	2	3	5	2.45	1.06	2	2	2	3	4
-0.9	2.32	0.79	2	2	2	2	4	2.22	0.81	1	2	2	2	4
-1	2.19	0.60	2	2	2	2	4	2.07	0.65	1	2	2	2	4
-1.1	2.12	0.45	2	2	2	2	3	1.96	0.55	1	2	2	2	3
-1.2	2.07	0.35	2	2	2	2	2	1.88	0.50	1	2	2	2	2
-1.3	2.04	0.26	2	2	2	2	2	1.81	0.48	1	2	2	2	2
-1.4	2.02	0.20	2	2	2	2	2	1.74	0.48	1	1	2	2	2
-1.5	2.01	0.15	2	2	2	2	2	1.68	0.49	1	1	2	2	2
-1.6	2.01	0.11	2	2	2	2	2	1.62	0.50	1	1	2	2	2
-1.7	2.00	0.08	2	2	2	2	2	1.56	0.50	1	1	2	2	2
-1.8	2.00	0.06	2	2	2	2	2	1.50	0.50	1	1	2	2	2
-1.9	2.00	0.05	2	2	2	2	2	1.45	0.50	1	1	1	2	2
-2	2.00	0.03	2	2	2	2	2	1.40	0.49	1	1	1	2	2
-2.1	2.00	0.02	2	2	2	2	2	1.35	0.48	1	1	1	2	2
-2.2	2.00	0.02	2	2	2	2	2	1.31	0.46	1	1	1	2	2

Table 4.16: The OOC characteristics of the upper and the lower one-sided 2-of-3 sign charts and the improved 2-of-3 sign charts for the median ($n=20$) where $LCL_B=1$, $LCL_A=6$, $UCL_A=14$ and $UCL_B=19$.

$N(0,1)$ Distribution														
σ Units	2-of-3 (U&L)							I2-of-3 (U&L)						
Shift	ARL	SDRL	5 th	Q_1	MDRL	Q_3	95 th	ARL	SDRL	5 th	Q_1	MDRL	Q_3	95 th
-0.2 (0.2)	4306.15	4304.19	223	1240	2985	5969	12896	4290.89	4288.93	222	1236	2975	5948	12850
-0.1 (0.1)	753.30	751.37	40	218	523	1044	2253	751.03	749.11	40	217	521	1040	2246
0	172.20	170.36	11	51	120	238	512	171.72	169.88	11	51	120	237	511
0.1 (-0.1)	51.46	49.72	4	16	36	71	151	51.32	49.58	4	16	36	70	150
0.2 (-0.2)	19.86	18.22	3	7	14	27	56	19.80	18.16	3	7	14	27	56
0.3 (-0.3)	9.62	8.06	2	4	7	13	26	9.58	8.04	2	4	7	13	26
0.4 (-0.4)	5.64	4.13	2	3	4	7	14	5.62	4.12	2	3	4	7	14
0.5 (-0.5)	3.86	2.35	2	2	3	5	9	3.83	2.34	2	2	3	5	9
0.6 (-0.6)	2.98	1.44	2	2	3	3	6	2.94	1.44	2	2	2	3	6
0.7 (-0.7)	2.51	0.92	2	2	2	3	4	2.47	0.93	2	2	2	3	4
0.8 (-0.8)	2.26	0.60	2	2	2	2	3	2.19	0.64	1	2	2	2	3
0.9 (-0.9)	2.13	0.39	2	2	2	2	3	2.02	0.50	1	2	2	2	3
1 (-1)	2.06	0.26	2	2	2	2	3	1.90	0.45	1	2	2	2	2
1.1 (-1.1)	2.03	0.17	2	2	2	2	2	1.80	0.45	1	2	2	2	2
1.2 (-1.2)	2.01	0.10	2	2	2	2	2	1.70	0.48	1	1	2	2	2
1.3 (-1.3)	2.00	0.06	2	2	2	2	2	1.59	0.50	1	1	2	2	2
1.4 (-1.4)	2.00	0.04	2	2	2	2	2	1.49	0.50	1	1	1	2	2
1.5 (-1.5)	2.00	0.02	2	2	2	2	2	1.39	0.49	1	1	1	2	2
1.6 (-1.6)	2.00	0.01	2	2	2	2	2	1.30	0.46	1	1	1	2	2
1.7 (-1.7)	2.00	0.01	2	2	2	2	2	1.22	0.42	1	1	1	1	2
1.8 (-1.8)	2.00	0.00	2	2	2	2	2	1.16	0.37	1	1	1	1	2
1.9 (-1.9)	2.00	0.00	2	2	2	2	2	1.11	0.31	1	1	1	1	2
2 (-2)	2.00	0.00	2	2	2	2	2	1.08	0.26	1	1	1	1	2
2.1 (-2.1)	2.00	0.00	2	2	2	2	2	1.05	0.22	1	1	1	1	1
2.2 (-2.2)	2.00	0.00	2	2	2	2	2	1.03	0.17	1	1	1	1	1
2.3 (-2.3)	2.00	0.00	2	2	2	2	2	1.02	0.14	1	1	1	1	1
2.4 (-2.4)	2.00	0.00	2	2	2	2	2	1.01	0.11	1	1	1	1	1
2.5 (-2.5)	2.00	0.00	2	2	2	2	2	1.01	0.08	1	1	1	1	1
2.6 (-2.6)	2.00	0.00	2	2	2	2	2	1.00	0.06	1	1	1	1	1
2.7 (-2.7)	2.00	0.00	2	2	2	2	2	1.00	0.05	1	1	1	1	1
2.8 (-2.8)	2.00	0.00	2	2	2	2	2	1.00	0.03	1	1	1	1	1
2.9 (-2.9)	2.00	0.00	2	2	2	2	2	1.00	0.03	1	1	1	1	1
3 (-3)	2.00	0.00	2	2	2	2	2	1.00	0.02	1	1	1	1	1

Table 4.17: The OOC characteristics of the upper and the lower one-sided 2-of-3 sign charts and the improved 2-of-3 sign charts for the median ($n=20$) where $LCL_B=1$, $LCL_A=6$, $UCL_A=14$ and $UCL_B=19$.

$t(4)$ Distribution														
σ Units	2-of-3 (U&L)							I2-of-3 (U&L)						
Shift	ARL	SDRL	5 th	Q_1	MDRL	Q_3	95 th	ARL	SDRL	5 th	Q_1	MDRL	Q_3	95 th
-0.2 (0.2)	15264.3	15262.3	785	4393	10581	21160	45724	15201.1	15199.1	782	4374	10537	21072	45535
-0.1 (0.1)	1295.38	1293.44	68	374	898	1795	3877	1291.31	1289.38	68	373	896	1789	3865
0	172.20	170.36	11	51	120	238	512	171.72	169.88	11	51	120	237	511
0.1 (-0.1)	36.66	34.95	3	12	26	50	106	36.56	34.85	3	12	26	50	106
0.2 (-0.2)	12.14	10.56	2	5	9	16	33	12.10	10.53	2	5	9	16	33
0.3 (-0.3)	5.79	4.27	2	3	4	7	14	5.76	4.26	2	3	4	7	14
0.4 (-0.4)	3.62	2.10	2	2	3	4	8	3.59	2.10	2	2	3	4	8
0.5 (-0.5)	2.73	1.17	2	2	2	3	5	2.69	1.17	2	2	2	3	5
0.6 (-0.6)	2.33	0.69	2	2	2	3	3	2.27	0.72	2	2	2	2	3
0.7 (-0.7)	2.15	0.42	2	2	2	2	3	2.05	0.52	1	2	2	2	3
0.8 (-0.8)	2.06	0.27	2	2	2	2	3	1.91	0.45	1	2	2	2	3
0.9 (-0.9)	2.03	0.17	2	2	2	2	2	1.80	0.45	1	2	2	2	2
1 (-1)	2.01	0.10	2	2	2	2	2	1.70	0.48	1	1	2	2	2
1.1 (-1.1)	2.00	0.06	2	2	2	2	2	1.60	0.50	1	1	2	2	2
1.2 (-1.2)	2.00	0.04	2	2	2	2	2	1.50	0.50	1	1	1	2	2
1.3 (-1.3)	2.00	0.02	2	2	2	2	2	1.41	0.49	1	1	1	2	2
1.4 (-1.4)	2.00	0.01	2	2	2	2	2	1.34	0.47	1	1	1	2	2
1.5 (-1.5)	2.00	0.01	2	2	2	2	2	1.27	0.44	1	1	1	2	2
1.6 (-1.6)	2.00	0.01	2	2	2	2	2	1.21	0.41	1	1	1	1	2
1.7 (-1.7)	2.00	0.00	2	2	2	2	2	1.17	0.37	1	1	1	1	2
1.8 (-1.8)	2.00	0.00	2	2	2	2	2	1.13	0.34	1	1	1	1	2
1.9 (-1.9)	2.00	0.00	2	2	2	2	2	1.10	0.30	1	1	1	1	2
2 (-2)	2.00	0.00	2	2	2	2	2	1.08	0.27	1	1	1	1	2
2.1 (-2.1)	2.00	0.00	2	2	2	2	2	1.06	0.24	1	1	1	1	2
2.2 (-2.2)	2.00	0.00	2	2	2	2	2	1.05	0.22	1	1	1	1	1
2.3 (-2.3)	2.00	0.00	2	2	2	2	2	1.04	0.19	1	1	1	1	1
2.4 (-2.4)	2.00	0.00	2	2	2	2	2	1.03	0.17	1	1	1	1	1
2.5 (-2.5)	2.00	0.00	2	2	2	2	2	1.02	0.15	1	1	1	1	1
2.6 (-2.6)	2.00	0.00	2	2	2	2	2	1.02	0.14	1	1	1	1	1
2.7 (-2.7)	2.00	0.00	2	2	2	2	2	1.02	0.12	1	1	1	1	1
2.8 (-2.8)	2.00	0.00	2	2	2	2	2	1.01	0.11	1	1	1	1	1
2.9 (-2.9)	2.00	0.00	2	2	2	2	2	1.01	0.10	1	1	1	1	1
3 (-3)	2.00	0.00	2	2	2	2	2	1.01	0.09	1	1	1	1	1

Table 4.18: The OOC characteristics of the upper and the lower one-sided 2-of-3 sign charts and the improved 2-of-3 sign charts for the median ($n=20$) where $LCL_B=1$, $LCL_A=6$, $UCL_A=14$ and $UCL_B=19$.

<i>Exp(1) Distribution</i>														
σ Units	2-of-3 (U)							I2-of-3 (U)						
Shift	ARL	SDRL	5 th	Q_1	MDRL	Q_3	95 th	ARL	SDRL	5 th	Q_1	MDRL	Q_3	95 th
-0.2	7525.79	7523.82	388	2166	5217	10432	22541	7497.31	7495.34	386	2158	5197	10393	22456
-0.1	1037.37	1035.44	55	300	720	1437	3104	1034.17	1032.24	55	299	717	1433	3094
0	172.20	170.36	11	51	120	238	512	171.72	169.88	11	51	120	237	511
0.1	36.87	35.16	4	12	26	50	107	36.77	35.06	4	12	26	50	107
0.2	10.86	9.29	2	4	8	14	29	10.82	9.26	2	4	8	14	29
0.3	4.53	3.02	2	2	3	6	11	4.50	3.01	2	2	3	6	11
0.4	2.66	1.08	2	2	2	3	5	2.62	1.09	2	2	2	3	5
0.5	2.10	0.34	2	2	2	2	3	1.98	0.47	1	2	2	2	3
0.6	2.00	0.05	2	2	2	2	2	1.54	0.50	1	1	2	2	2
0.7	2.00	0.00	2	2	2	2	2	1.00	0.00	1	1	1	1	1
0.8	2.00	0.00	2	2	2	2	2	1.00	0.00	1	1	1	1	1
0.9	2.00	0.00	2	2	2	2	2	1.00	0.00	1	1	1	1	1
1	2.00	0.00	2	2	2	2	2	1.00	0.00	1	1	1	1	1
1.1	2.00	0.00	2	2	2	2	2	1.00	0.00	1	1	1	1	1
1.2	2.00	0.00	2	2	2	2	2	1.00	0.00	1	1	1	1	1
1.3	2.00	0.00	2	2	2	2	2	1.00	0.00	1	1	1	1	1
1.4	2.00	0.00	2	2	2	2	2	1.00	0.00	1	1	1	1	1
1.5	2.00	0.00	2	2	2	2	2	1.00	0.00	1	1	1	1	1
1.6	2.00	0.00	2	2	2	2	2	1.00	0.00	1	1	1	1	1
1.7	2.00	0.00	2	2	2	2	2	1.00	0.00	1	1	1	1	1
1.8	2.00	0.00	2	2	2	2	2	1.00	0.00	1	1	1	1	1
1.9	2.00	0.00	2	2	2	2	2	1.00	0.00	1	1	1	1	1
2	2.00	0.00	2	2	2	2	2	1.00	0.00	1	1	1	1	1
2.1	2.00	0.00	2	2	2	2	2	1.00	0.00	1	1	1	1	1
2.2	2.00	0.00	2	2	2	2	2	1.00	0.00	1	1	1	1	1
2.3	2.00	0.00	2	2	2	2	2	1.00	0.00	1	1	1	1	1
2.4	2.00	0.00	2	2	2	2	2	1.00	0.00	1	1	1	1	1
2.5	2.00	0.00	2	2	2	2	2	1.00	0.00	1	1	1	1	1
2.6	2.00	0.00	2	2	2	2	2	1.00	0.00	1	1	1	1	1
2.7	2.00	0.00	2	2	2	2	2	1.00	0.00	1	1	1	1	1
2.8	2.00	0.00	2	2	2	2	2	1.00	0.00	1	1	1	1	1
2.9	2.00	0.00	2	2	2	2	2	1.00	0.00	1	1	1	1	1
3	2.00	0.00	2	2	2	2	2	1.00	0.00	1	1	1	1	1

Table 4.19: The OOC characteristics of the lower one-sided 2-of-3 sign charts and the improved 2-of-3 sign charts for the median ($n=20$) where $LCL_B=1$, $LCL_A=6$, $UCL_A=14$ and $UCL_B=19$.

Exp(1) Distribution														
σ Units	2-of-3 (L)							I2-of-3 (L)						
Shift	ARL	SDRL	5 th	Q_1	MDRL	Q_3	95 th	ARL	SDRL	5 th	Q_1	MDRL	Q_3	95 th
0.2	21488.7	21486.7	1104	6183	14895	29789	64370	21395.3	21393.4	1099	6156	14831	29660	64091
0.1	1282.78	1280.84	68	370	890	1778	3839	1278.76	1276.82	67	369	887	1772	3827
0	172.20	170.36	11	51	120	238	512	171.72	169.88	11	51	120	237	511
-0.1	41.90	40.18	4	13	30	57	122	41.78	40.06	4	13	29	57	122
-0.2	15.72	14.11	2	6	11	21	44	15.67	14.07	2	6	11	21	44
-0.3	8.01	6.48	2	3	6	10	21	7.98	6.45	2	3	6	10	21
-0.4	5.05	3.54	2	3	4	6	12	5.02	3.53	2	3	4	6	12
-0.5	3.69	2.18	2	2	3	4	8	3.66	2.17	2	2	3	4	8
-0.6	2.98	1.44	2	2	3	3	6	2.95	1.44	2	2	2	3	6
-0.7	2.59	1.00	2	2	2	3	5	2.54	1.01	2	2	2	3	5
-0.8	2.35	0.72	2	2	2	3	4	2.30	0.75	2	2	2	3	4
-0.9	2.21	0.53	2	2	2	2	3	2.13	0.59	1	2	2	2	3
-1	2.13	0.39	2	2	2	2	3	2.02	0.50	1	2	2	2	3
-1.1	2.08	0.29	2	2	2	2	3	1.94	0.45	1	2	2	2	3
-1.2	2.05	0.22	2	2	2	2	2	1.86	0.44	1	2	2	2	2
-1.3	2.03	0.17	2	2	2	2	2	1.80	0.45	1	2	2	2	2
-1.4	2.02	0.13	2	2	2	2	2	1.74	0.47	1	1	2	2	2
-1.5	2.01	0.10	2	2	2	2	2	1.68	0.48	1	1	2	2	2
-1.6	2.01	0.07	2	2	2	2	2	1.62	0.49	1	1	2	2	2
-1.7	2.00	0.05	2	2	2	2	2	1.56	0.50	1	1	2	2	2
-1.8	2.00	0.04	2	2	2	2	2	1.50	0.50	1	1	2	2	2
-1.9	2.00	0.03	2	2	2	2	2	1.45	0.50	1	1	1	2	2
-2	2.00	0.02	2	2	2	2	2	1.40	0.49	1	1	1	2	2
-2.1	2.00	0.02	2	2	2	2	2	1.35	0.48	1	1	1	2	2
-2.2	2.00	0.01	2	2	2	2	2	1.31	0.46	1	1	1	2	2
-2.3	2.00	0.01	2	2	2	2	2	1.27	0.44	1	1	1	2	2
-2.4	2.00	0.01	2	2	2	2	2	1.23	0.42	1	1	1	1	2
-2.5	2.00	0.00	2	2	2	2	2	1.20	0.40	1	1	1	1	2
-2.6	2.00	0.00	2	2	2	2	2	1.17	0.37	1	1	1	1	2
-2.7	2.00	0.00	2	2	2	2	2	1.14	0.35	1	1	1	1	2
-2.8	2.00	0.00	2	2	2	2	2	1.12	0.33	1	1	1	1	2
-2.9	2.00	0.00	2	2	2	2	2	1.10	0.30	1	1	1	1	2
-3	2.00	0.00	2	2	2	2	2	1.09	0.28	1	1	1	1	2

Table 4.20: The OOC characteristics of the two-sided 2-of-3 sign charts and the improved 2-of-3 sign charts for the median ($n=25$) where $LCL_B=1$, $LCL_A=7$, $UCL_A=18$ and $UCL_B=24$.

$N(0,1)$ Distribution														
σ Units	2-of-3 (T)							I2-of-3 (T)						
Shift	ARL	SDRL	5th	Q_1	MDRL	Q_3	95th	ARL	SDRL	5th	Q_1	MDRL	Q_3	95th
2.2	2.00	0.00	2	2	2	2	2	1.05	0.21	1	1	1	1	1
2.1	2.00	0.00	2	2	2	2	2	1.07	0.26	1	1	1	1	2
2	2.00	0.00	2	2	2	2	2	1.11	0.31	1	1	1	1	2
1.9	2.00	0.00	2	2	2	2	2	1.16	0.37	1	1	1	1	2
1.8	2.00	0.00	2	2	2	2	2	1.23	0.42	1	1	1	1	2
1.7	2.00	0.00	2	2	2	2	2	1.31	0.46	1	1	1	2	2
1.6	2.00	0.01	2	2	2	2	2	1.40	0.49	1	1	1	2	2
1.5	2.00	0.02	2	2	2	2	2	1.50	0.50	1	1	2	2	2
1.4	2.00	0.03	2	2	2	2	2	1.61	0.49	1	1	2	2	2
1.3	2.00	0.06	2	2	2	2	2	1.71	0.46	1	1	2	2	2
1.2	2.01	0.11	2	2	2	2	2	1.81	0.42	1	2	2	2	2
1.1	2.03	0.18	2	2	2	2	2	1.90	0.38	1	2	2	2	2
1	2.07	0.28	2	2	2	2	3	1.99	0.39	1	2	2	2	3
0.9	2.17	0.45	2	2	2	2	3	2.12	0.50	2	2	2	2	3
0.8	2.35	0.71	2	2	2	3	4	2.32	0.73	2	2	2	3	4
0.7	2.72	1.16	2	2	2	3	5	2.70	1.16	2	2	2	3	5
0.6	3.46	1.94	2	2	3	4	7	3.45	1.94	2	2	3	4	7
0.5	5.02	3.51	2	3	4	6	12	5.01	3.51	2	3	4	6	12
0.4	8.68	7.13	2	4	6	11	23	8.66	7.12	2	3	6	11	23
0.3	18.78	17.15	3	7	14	25	53	18.76	17.13	3	7	13	25	53
0.2	53.49	51.74	4	17	38	73	157	53.45	51.70	4	17	38	73	157
0.1	203.96	202.10	12	60	142	282	607	203.80	201.94	12	60	142	282	607
0	568.64	566.71	31	165	395	788	1700	568.18	566.25	31	165	394	787	1698
-0.1	203.96	202.10	12	60	142	282	607	203.80	201.94	12	60	142	282	607
-0.2	53.49	51.74	4	17	38	73	157	53.45	51.70	4	17	38	73	157
-0.3	18.78	17.15	3	7	14	25	53	18.76	17.13	3	7	13	25	53
-0.4	8.68	7.13	2	4	6	11	23	8.66	7.12	2	3	6	11	23
-0.5	5.02	3.51	2	3	4	6	12	5.01	3.51	2	3	4	6	12
-0.6	3.46	1.94	2	2	3	4	7	3.45	1.94	2	2	3	4	7
-0.7	2.72	1.16	2	2	2	3	5	2.70	1.16	2	2	2	3	5
-0.8	2.35	0.71	2	2	2	3	4	2.32	0.73	2	2	2	3	4
-0.9	2.17	0.45	2	2	2	2	3	2.12	0.50	2	2	2	2	3
-1	2.07	0.28	2	2	2	2	3	1.99	0.39	1	2	2	2	3
-1.1	2.03	0.18	2	2	2	2	2	1.90	0.38	1	2	2	2	2
-1.2	2.01	0.11	2	2	2	2	2	1.81	0.42	1	2	2	2	2
-1.3	2.00	0.06	2	2	2	2	2	1.71	0.46	1	1	2	2	2
-1.4	2.00	0.03	2	2	2	2	2	1.61	0.49	1	1	2	2	2
-1.5	2.00	0.02	2	2	2	2	2	1.50	0.50	1	1	2	2	2
-1.6	2.00	0.01	2	2	2	2	2	1.40	0.49	1	1	1	2	2
-1.7	2.00	0.00	2	2	2	2	2	1.31	0.46	1	1	1	2	2
-1.8	2.00	0.00	2	2	2	2	2	1.23	0.42	1	1	1	1	2
-1.9	2.00	0.00	2	2	2	2	2	1.16	0.37	1	1	1	1	2
-2	2.00	0.00	2	2	2	2	2	1.11	0.31	1	1	1	1	2
-2.1	2.00	0.00	2	2	2	2	2	1.07	0.26	1	1	1	1	2
-2.2	2.00	0.00	2	2	2	2	2	1.05	0.21	1	1	1	1	1

Table 4.21: The OOC characteristics of the two-sided 2-of-3 sign charts and the improved 2-of-3 sign charts for the median ($n=25$) where $LCL_B=1$, $LCL_A=7$, $UCL_A=18$ and $UCL_B=24$.

$t(4)$ Distribution														
σ Units	2-of-3 (T)							I2-of-3 (T)						
Shift	ARL	SDRL	5 th	Q_1	MDRL	Q_3	95 th	ARL	SDRL	5 th	Q_1	MDRL	Q_3	95 th
2.2	2.00	0.00	2	2	2	2	2	1.07	0.26	1	1	1	1	2
2.1	2.00	0.00	2	2	2	2	2	1.09	0.29	1	1	1	1	2
2	2.00	0.00	2	2	2	2	2	1.12	0.32	1	1	1	1	2
1.9	2.00	0.00	2	2	2	2	2	1.15	0.36	1	1	1	1	2
1.8	2.00	0.00	2	2	2	2	2	1.19	0.39	1	1	1	1	2
1.7	2.00	0.00	2	2	2	2	2	1.24	0.42	1	1	1	1	2
1.6	2.00	0.00	2	2	2	2	2	1.29	0.46	1	1	1	2	2
1.5	2.00	0.01	2	2	2	2	2	1.36	0.48	1	1	1	2	2
1.4	2.00	0.01	2	2	2	2	2	1.44	0.50	1	1	1	2	2
1.3	2.00	0.02	2	2	2	2	2	1.53	0.50	1	1	2	2	2
1.2	2.00	0.04	2	2	2	2	2	1.62	0.49	1	1	2	2	2
1.1	2.00	0.06	2	2	2	2	2	1.72	0.46	1	1	2	2	2
1	2.01	0.11	2	2	2	2	2	1.81	0.42	1	2	2	2	2
0.9	2.03	0.18	2	2	2	2	2	1.90	0.38	1	2	2	2	2
0.8	2.08	0.29	2	2	2	2	3	2.00	0.40	1	2	2	2	3
0.7	2.19	0.49	2	2	2	2	3	2.15	0.53	2	2	2	2	3
0.6	2.45	0.84	2	2	2	3	4	2.43	0.85	2	2	2	3	4
0.5	3.06	1.52	2	2	3	3	6	3.04	1.52	2	2	3	3	6
0.4	4.57	3.06	2	2	3	6	11	4.56	3.06	2	2	3	6	11
0.3	8.99	7.45	2	4	7	12	24	8.98	7.44	2	4	7	12	24
0.2	26.30	24.63	3	9	19	36	75	26.28	24.61	3	9	19	36	75
0.1	128.02	126.20	8	38	89	177	380	127.92	126.10	8	38	89	177	380
0	568.64	566.71	31	165	395	788	1700	568.18	566.25	31	165	394	787	1698
-0.1	128.02	126.20	8	38	89	177	380	127.92	126.10	8	38	89	177	380
-0.2	26.30	24.63	3	9	19	36	75	26.28	24.61	3	9	19	36	75
-0.3	8.99	7.45	2	4	7	12	24	8.98	7.44	2	4	7	12	24
-0.4	4.57	3.06	2	2	3	6	11	4.56	3.06	2	2	3	6	11
-0.5	3.06	1.52	2	2	3	3	6	3.04	1.52	2	2	3	3	6
-0.6	2.45	0.84	2	2	2	3	4	2.43	0.85	2	2	2	3	4
-0.7	2.19	0.49	2	2	2	2	3	2.15	0.53	2	2	2	2	3
-0.8	2.08	0.29	2	2	2	2	3	2.00	0.40	1	2	2	2	3
-0.9	2.03	0.18	2	2	2	2	2	1.90	0.38	1	2	2	2	2
-1	2.01	0.11	2	2	2	2	2	1.81	0.42	1	2	2	2	2
-1.1	2.00	0.06	2	2	2	2	2	1.72	0.46	1	1	2	2	2
-1.2	2.00	0.04	2	2	2	2	2	1.62	0.49	1	1	2	2	2
-1.3	2.00	0.02	2	2	2	2	2	1.53	0.50	1	1	2	2	2
-1.4	2.00	0.01	2	2	2	2	2	1.44	0.50	1	1	1	2	2
-1.5	2.00	0.01	2	2	2	2	2	1.36	0.48	1	1	1	2	2
-1.6	2.00	0.00	2	2	2	2	2	1.29	0.46	1	1	1	2	2
-1.7	2.00	0.00	2	2	2	2	2	1.24	0.42	1	1	1	1	2
-1.8	2.00	0.00	2	2	2	2	2	1.19	0.39	1	1	1	1	2
-1.9	2.00	0.00	2	2	2	2	2	1.15	0.36	1	1	1	1	2
-2	2.00	0.00	2	2	2	2	2	1.12	0.32	1	1	1	1	2
-2.1	2.00	0.00	2	2	2	2	2	1.09	0.29	1	1	1	1	2
-2.2	2.00	0.00	2	2	2	2	2	1.07	0.26	1	1	1	1	2

Table 4.22: The OOC characteristics of the two-sided 2-of-3 sign charts and the improved 2-of-3 sign charts for the median ($n=25$) where $LCL_B=1$, $LCL_A=7$, $UCL_A=18$ and $UCL_B=24$.

<i>Exp(1) Distribution</i>														
σ Units	2-of-3 (T)							I2-of-3 (T)						
Shift	ARL	SDRL	5 th	Q ₁	MDRL	Q ₃	95 th	ARL	SDRL	5 th	Q ₁	MDRL	Q ₃	95 th
2.2	2.00	0.00	2	2	2	2	2	1.00	0.00	1	1	1	1	1
2.1	2.00	0.00	2	2	2	2	2	1.00	0.00	1	1	1	1	1
2	2.00	0.00	2	2	2	2	2	1.00	0.00	1	1	1	1	1
1.9	2.00	0.00	2	2	2	2	2	1.00	0.00	1	1	1	1	1
1.8	2.00	0.00	2	2	2	2	2	1.00	0.00	1	1	1	1	1
1.7	2.00	0.00	2	2	2	2	2	1.00	0.00	1	1	1	1	1
1.6	2.00	0.00	2	2	2	2	2	1.00	0.00	1	1	1	1	1
1.5	2.00	0.00	2	2	2	2	2	1.00	0.00	1	1	1	1	1
1.4	2.00	0.00	2	2	2	2	2	1.00	0.00	1	1	1	1	1
1.3	2.00	0.00	2	2	2	2	2	1.00	0.00	1	1	1	1	1
1.2	2.00	0.00	2	2	2	2	2	1.00	0.00	1	1	1	1	1
1.1	2.00	0.00	2	2	2	2	2	1.00	0.00	1	1	1	1	1
1	2.00	0.00	2	2	2	2	2	1.00	0.00	1	1	1	1	1
0.9	2.00	0.00	2	2	2	2	2	1.00	0.00	1	1	1	1	1
0.8	2.00	0.00	2	2	2	2	2	1.00	0.00	1	1	1	1	1
0.7	2.00	0.00	2	2	2	2	2	1.00	0.00	1	1	1	1	1
0.6	2.00	0.05	2	2	2	2	2	1.67	0.47	1	1	2	2	2
0.5	2.13	0.39	2	2	2	2	3	2.07	0.45	1	2	2	2	3
0.4	2.95	1.40	2	2	2	3	6	2.93	1.40	2	2	2	3	6
0.3	6.31	4.80	2	3	5	8	16	6.30	4.79	2	3	5	8	16
0.2	22.37	20.72	3	8	16	30	64	22.35	20.70	3	8	16	30	64
0.1	129.05	127.23	8	38	90	178	383	128.95	127.13	8	38	90	178	383
0	568.64	566.71	31	165	395	788	1700	568.18	566.25	31	165	394	787	1698
-0.1	154.17	152.33	10	46	107	213	458	154.05	152.21	10	46	107	213	458
-0.2	38.21	36.50	4	12	27	52	111	38.18	36.47	4	12	27	52	111
-0.3	14.41	12.81	2	5	10	19	40	14.40	12.80	2	5	10	19	40
-0.4	7.39	5.86	2	3	6	10	19	7.38	5.86	2	3	6	10	19
-0.5	4.70	3.19	2	3	4	6	11	4.69	3.19	2	3	4	6	11
-0.6	3.47	1.95	2	2	3	4	7	3.45	1.95	2	2	3	4	7
-0.7	2.83	1.28	2	2	2	3	6	2.82	1.28	2	2	2	3	5
-0.8	2.48	0.88	2	2	2	3	4	2.46	0.89	2	2	2	3	4
-0.9	2.28	0.62	2	2	2	2	3	2.25	0.64	2	2	2	2	3
-1	2.16	0.45	2	2	2	2	3	2.12	0.50	2	2	2	2	3
-1.1	2.10	0.33	2	2	2	2	3	2.03	0.41	1	2	2	2	3
-1.2	2.05	0.24	2	2	2	2	3	1.96	0.38	1	2	2	2	2
-1.3	2.03	0.18	2	2	2	2	2	1.90	0.38	1	2	2	2	2
-1.4	2.02	0.13	2	2	2	2	2	1.85	0.40	1	2	2	2	2
-1.5	2.01	0.10	2	2	2	2	2	1.79	0.42	1	2	2	2	2
-1.6	2.00	0.07	2	2	2	2	2	1.74	0.45	1	1	2	2	2
-1.7	2.00	0.05	2	2	2	2	2	1.68	0.47	1	1	2	2	2
-1.8	2.00	0.04	2	2	2	2	2	1.62	0.49	1	1	2	2	2
-1.9	2.00	0.03	2	2	2	2	2	1.57	0.50	1	1	2	2	2
-2	2.00	0.02	2	2	2	2	2	1.51	0.50	1	1	2	2	2
-2.1	2.00	0.01	2	2	2	2	2	1.46	0.50	1	1	1	2	2
-2.2	2.00	0.01	2	2	2	2	2	1.41	0.49	1	1	1	2	2

Remark 4.10

Note that to do performance analysis; a sufficiently large sample size is required so that there exists an outer set of control limits that has an absolute minimal influence on the IC *ARL* of the *improved* runs-rules charts. This is done so that the IC *ARL* for both runs-rules and *improved* runs-rules charts are almost exactly the same by choosing the inner set of control limits of the *improved* runs-rules charts and the control limits of the runs-rules charts the same. Consequently, the sample size is chosen to be 20 in the performance analysis for the 2-*of*-2 charts and the one-sided 2-*of*-3 charts. The sample size is chosen to be 25 in the performance analysis for the two-sided 2-*of*-3 charts.

4.10 Final comments regarding the *improved* runs-rules sign charts

From investigating the performance analysis it can be concluded that the *improved* runs-rules sign charts are superior in performance to the runs-rules sign charts for large shifts, while maintaining the same sensitivity in the detection of small shifts. Consequently the *improved* runs-rules sign charts are superior in performance compared to the runs-rules sign charts.

However, the *improved* runs-rules sign charts do have limitations. First, the *improved* runs-rules sign charts require the sample size to be larger than what is required for the runs-rules charts. The sample size needs to be at least 9 for the one-sided *improved* 2-*of*-2 and the 2-*of*-3 sign charts and needs to be at least 10 for the two-sided *improved* 2-*of*-2 and the 2-*of*-3 sign charts so that sufficient and practically usable *ARL* and *FAR* combinations are obtained. Second, the *improved* runs-rules sign charts are more complex than the runs-rules charts. Note that for the sacrifice in simplicity there are rewards in the performance of the chart.

Summary of the strengths and the limitations of the *improved* runs-rules sign charts:

Strengths:

- Does not require a specified underlying process distribution (nonparametric),
- Does not require the variance of the process to be established,
- Can monitor any desirable percentile of the underlying process distribution,
- Does not require the actual measurements, but only the number or count of observations within each sample that are larger or smaller than the known or specified value of the percentile of interest to be able to calculate the plotting statistic,

- As sensitive to small process shifts as the runs-rules sign charts, and
- Superior in the detection of large process shifts.

Limitations:

- Requires sample sizes to be larger than the runs-rules sign charts to obtain practical ARL_0 and FAR control limit combinations, and
- The *improved* runs-rules sign charts are more complex charts.

4.11 Summary of Chapter 4

The *improved* runs-rules are introduced to the sign chart in Chapter 4. The run-length distribution of the *improved* runs-rules sign charts are derived using a Markov chain approach. Performance analysis is carried out to illustrate that the *improved* runs-rules sign charts are superior in performance to the runs-rules sign charts for large shifts in the process, while maintaining the same sensitivity in the detection of small shifts.

4.12 Following chapter

The sign chart requires the value of the percentile that needs to be monitored to be specified (i.e. Case K). When the value of the percentile that needs to be monitored is unspecified (i.e. Case U) then the sign chart is no longer appropriate. The precedence chart is then the appropriate chart. In Chapter 5 the *improved* runs-rules precedence chart is introduced.

Chapter 5

Precedence control charts (Case U)

5.0 Chapter 5 overview and objective

In Chapter 4 *improved* runs-rules are introduced to the sign chart. However, in order to apply the sign chart the percentile of the underlying process distribution that is monitored needs to be known or specified (i.e. Case K). In this chapter the situation is considered where the percentile of the underlying process distribution that is monitored is unknown or unspecified (i.e. Case U). An appropriate chart for Case U is the precedence chart. The precedence chart is a nonparametric chart that can be used to monitor any unknown $100\pi^{\text{th}}$ ($0 < \pi < 1$) percentile of a continuous process distribution, i.e. monitoring the location of a process where the $100\pi^{\text{th}}$ ($0 < \pi < 1$) percentile is unknown or unspecified. Chakraborti et al. (2004) introduced the precedence statistic as plotting statistic to the *1-of-1* precedence charts. Human et al. (2009) introduced runs-rules to the precedence charts to address the *1-of-1* precedence charts lack of sensitivity to small shifts. In this chapter *improved* runs-rules are introduced to the precedence charts as an improvement over the runs-rules enhanced precedence charts. A Markov chain and a conditioning by expectation approach are used to calculate the unconditional run-length distribution and the unconditional characteristics of the *improved* runs-rules precedence charts. Performance analysis is carried out to illustrate that the *improved* runs-rules precedence charts are superior in performance to the runs-rules precedence charts for large shifts, while maintaining the same sensitivity in the detection of small shifts.

After reading this chapter the reader should be familiar with:

- The history of the precedence chart,
- The precedence statistic and the plotting statistic of the precedence chart,
- The application of the precedence chart,
- The design of the precedence charts,
- How the performance of the *improved* runs-rules precedence charts compare to the runs-rules enhanced precedence charts, and

- The strengths and the limitations of the *improved* runs-rules precedence charts compared to the runs-rules enhanced precedence charts.

5.1 Introduction

The precedence charts are based on the median test, which is essentially a modified sign test for two independent samples and is a member of a more general class of nonparametric two-sample tests. The nonparametric two-sample tests are referred to as precedence tests of precedence statistics (see e.g. Gibbons and Chakraborti (2003)). The precedence charts can be used to monitor any unknown $100\pi^{\text{th}}$ ($0 < \pi < 1$) process percentile of interest. Similar to the sign chart the precedence chart is a nonparametric chart, consequently the properties of the chart remain unchanged while the process remains IC and the underlying process is continuous.

Chakraborti et al. (2004) introduced a class of Phase II Shewhart-type nonparametric charts, which are referred to as the (basic) *1-of-1* precedence charts or simply the precedence charts. Chakraborti et al. (2004) showed that the *1-of-1* precedence charts are preferred from a robustness point of view, since these charts have attractive *ARL* properties and would be particularly useful in situations where one uses a classical Shewhart \bar{X} -chart to monitor a process (Human et al. (2009)).

The *1-of-1* precedence charts consider only the last plotting statistic in determining whether the process is IC or OOC. Consequently the precedence chart is insensitive to small shifts. Human et al. (2009) addressed this limitation, namely lack of sensitivity to small process shifts by introducing runs-rules to the Phase II nonparametric precedence charts of Chakraborti et al. (2004).

Unfortunately the runs-rules that Human et al. (2009) introduced to the precedence charts are unable to detect large process shifts quickly; since at least two or three of the last plotting statistics are required before the chart can signal in the case of the *2-of-2* and the *2-of-3* charts respectively. As with the sign charts, the implementation of the *improved* runs-rules are proposed to the precedence charts, which is similar to what Khoo and Ariffin (2006) introduced to the \bar{X} chart.

The precedence charts require an IC Phase I reference sample from which the control limits are estimated. The process is then monitored in Phase II using these estimated control limits from Phase I. Since the monitoring of the process in Phase II depends on the estimated control limits from Phase I, the performance of the precedence charts depends on the estimated control limits from Phase I.

Chakraborti et al. (2004) noted that the *I-of-I* precedence charts have a Geometric distribution given a set of estimated control limits from Phase I. A conditioning argument (see Chakraborti (2000)) is then used to find an expression for the precedence chart's unconditional run-length distribution, which yields the exact IC run-length distribution and the exact IC run-length characteristics. Human et al. (2009) used a Markov chain approach to calculate the conditional run-length distribution; a conditioning argument was then used to find an expression for the unconditional run-length distribution, which yields the exact IC run-length distribution of the runs-rules enhanced precedence charts.

For the proposed precedence charts with *improved* runs-rules incorporated, a Markov chain approach is used to calculate the conditional run-length distribution, conditioned on the estimated control limits from Phase I. A similar conditioning argument as used by Chakraborti et al. (2004) and Human et al. (2009) is then used to find an expression for the exact run-length distribution, i.e. the unconditional run-length distribution.

Throughout Chapter 5 the focus is on the median chart since the median is by far the most popular percentile and the median is a robust estimator of the location. Charts based on other percentiles can be developed with a similar approach (Chakraborti et al. (2004)).

5.2 Assumptions

Suppose that an IC reference sample of size m from Phase I denoted by (X_1, X_2, \dots, X_m) is available from an unknown continuous process distribution with an unknown continuous cdf $F_X(x) = F(x - \theta)$ where θ is the location parameter and F is some continuous cdf with a median of zero. The Phase I reference sample (X_1, X_2, \dots, X_m) is used to estimate the control limits for Phase II monitoring.

In Phase II a test sample denoted by $(Y_{i,1}, Y_{i,2}, \dots, Y_{i,n})$ is sequentially taken at sampling stage (time) $i = 1, 2, 3, \dots$. Each Phase II test sample $(Y_{i,1}, Y_{i,2}, \dots, Y_{i,n})$ is a random sample (rational subgroup) of size $n > 1$ from an unknown continuous distribution with cdf $G_Y(y) = F(y - \theta_i)$ where θ_i is the location parameter of the i^{th} test sample.

It is assumed that the Phase II test samples $(Y_{i,1}, Y_{i,2}, \dots, Y_{i,n})$, $i = 1, 2, 3, \dots$ are drawn sequentially and independently of one another and from the Phase I reference sample (X_1, X_2, \dots, X_m) .

5.3 Plotting statistic and control limits

The plotting statistic of the precedence chart can be represented in many ways. The plotting statistic that is used in this dissertation is an order statistics from the Phase II test samples. Background is given on the plotting statistic of the precedence chart.

Let W_j denote the number of Phase I reference sample observations that precede (not greater than) the j^{th} order statistic from a Phase II test sample. In the literature the statistic W_j has been referred to as a precedence statistic and any test based on W_j has been referred to as a precedence test.

When the process is IC, the exact probability distribution of the precedence statistic can be obtained either by mathematical statistical techniques or by combinatorial arguments. This is given by:

$$P(W_j = w) = \frac{\binom{j+w-1}{w} \binom{m+n-j-w}{m-w}}{\binom{m+n}{m}}, \quad w = 0, 1, \dots, m \quad (5.1)$$

Note that the IC distribution of the precedence statistic W_j depends only on selected values of m , n and j and not on the underlying process distributions (F and G). Hence any chart based on the precedence statistic is nonparametric as per the definition of a nonparametric chart, provided that the process distributions in Phase I and Phase II are continuous and identical (Chakraborti et al. (2004)).

The probability that the precedence chart does not signal (W_j plotting between two integers/control limits) can be expressed in terms of the j^{th} order statistic from Phase II ($Y_{(j:n)}$) plotting between two order statistics from Phase I i.e.:

$$P(\text{Chart does not signal}) = P(X_{(a:m)} < Y_{(j:n)} < X_{(b:m)}) = P(a \leq W_j \leq b-1) \quad (5.2)$$

(Chakraborti et al. (2004))

Consequently the plotting statistic chosen to be used in the precedence chart is the j^{th} order statistic from a Phase II test sample.

The monitoring of a process is carried out as follows: In Phase I an IC reference sample of size m is obtained from which the control limits are estimated. Note that the estimated control limits are order statistic(s) from the Phase I reference sample. In Phase II new incoming samples are taken sequentially from the process. For each new incoming sample a plotting statistic (an order statistic) is calculated/observed at time $i = 1, 2, 3, \dots$, each plotting statistic is then compared to the control limits. If a sequence of plotting statistics of interest occur on the control chart, the chart signals and a search is initiated to determine if an assignable cause is present. This will be explained further.

The plotting statistic is denoted by T_i , where T_i at time $i = 1, 2, 3, \dots$ is the j^{th} order statistic from the i^{th} Phase II test sample $(Y_{i1}, Y_{i2}, \dots, Y_{in})$, $i = 1, 2, 3, \dots$ denoted by $Y_{(jn)}^i$ for $1 < j \leq n$.

To find the control limits for Phase II monitoring the Phase I reference sample of size m is arranged in ascending order given by:

$$X_{(1:m)} < X_{(2:m)} < X_{(3:m)} < \dots < X_{(m:m)},$$

where $X_{(k:m)}$ denotes the k^{th} order statistic of the reference sample of size m . The control limits for the basic (*I-of-I*), the runs-rules and the *improved* runs-rules precedence charts are order statistics from the Phase I reference sample. The order statistics $X_{(a:m)}$, $X_{(b:m)}$, $X_{(c:m)}$ and $X_{(d:m)}$ (for $1 \leq a < b < c < d \leq m$ i.e. $X_{(a:m)} < X_{(b:m)} < X_{(c:m)} < X_{(d:m)}$) denote the control limits of the precedence charts and are given by:

$$\begin{aligned} \hat{UCL}_B &= X_{(d:m)} \\ \hat{UCL}_A / \hat{UCL} &= X_{(c:m)} \\ \hat{LCL}_A / \hat{LCL} &= X_{(b:m)} \\ \hat{LCL}_B &= X_{(a:m)} \end{aligned}$$

Figure 5.1 illustrate the order statistics from the Phase I reference sample that is used as control limits in Phase II monitoring.

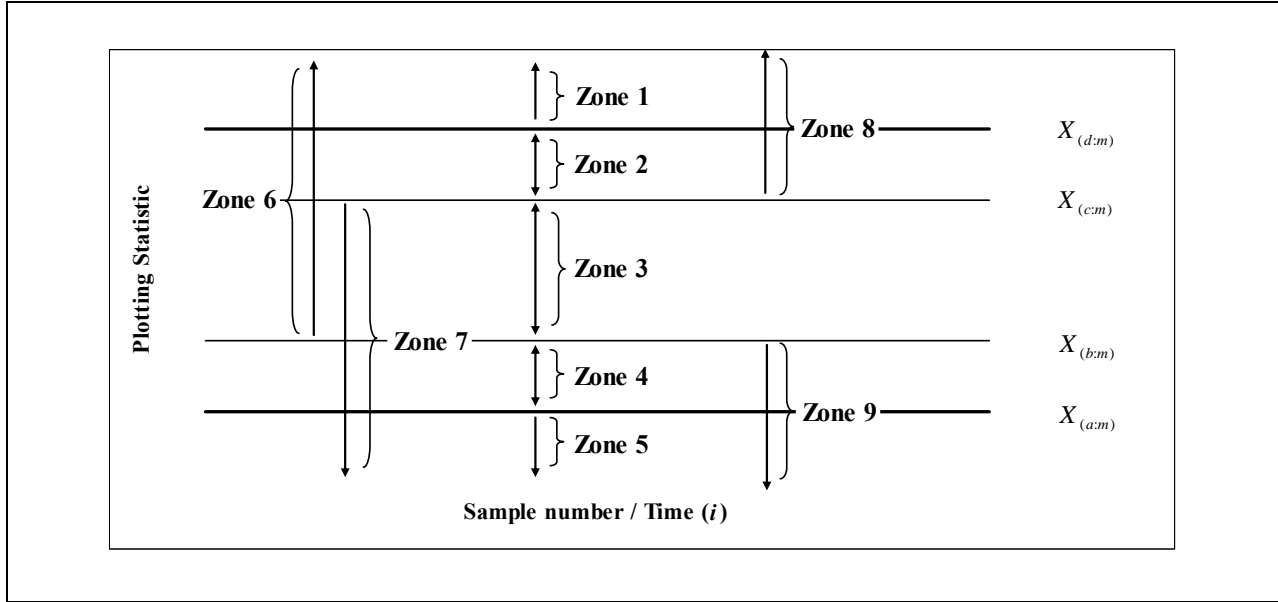


Figure 5.1: Illustration of the control limits and the zones on the precedence charts.

Note that when monitoring the process in Phase II, the plotting statistic $T_i = Y_{(j:n)}^i$ that is calculated from each test sample is not compared to known control limits LCL_B , LCL_A / LCL , UCL_A / UCL and UCL_B as was the case with the sign chart, but are compared to estimated control limits \hat{LCL}_B , \hat{LCL}_A / \hat{LCL} , \hat{UCL}_A / \hat{UCL} and \hat{UCL}_B from the Phase I reference sample. Also note that it is possible to apply the precedence chart as soon as the necessary order statistic is available, which is an advantage in applications where the observations are observed in ascending or descending order.

Remark 5.1

Precedence charts can be used to monitor any unknown $100\pi^{th}$ ($0 < \pi < 1$) process percentile of interest. However, the emphasis in this chapter is on the median chart, since the median is the most popular percentile. Charts based on other percentiles can be developed in a similar manner (Chakraborti et al. (2004)). To simplify matters further it is assumed, without loss of generality, that the Phase II sample size n ($n = 2s + 1$) is odd, therefore the median of the test sample $Y_{(j:n)}^i$ is uniquely defined with $j = s + 1$ (Human et al. (2009)).

5.4 The run-length distribution and some characteristics of the precedence charts

In order calculate the run-length distribution of each precedence chart, a Markov Chain approach is used to calculate the conditional run-length distribution conditioned on the estimated control limits from a Phase I analysis. A conditioning argument (see Chakraborti (2000)) is then used to find an expression for the exact unconditional run-length distribution.

All the necessary results, probabilities and essential transition probability matrices are given in Appendix 5. These results, probabilities and essential transition probability matrices are then used to derive the run-length distribution of all of the considered precedence charts. The expressions are given below but for full details refer to Appendix 5.

5.4.1 The $1-of-1$ precedence charts

5.4.1.1 The upper one-sided $1-of-1$ precedence chart

The unconditional run-length distribution and some characteristics of the unconditional run-length distribution of the upper one-sided $1-of-1$ precedence chart are given by:

$$P(N_{1-of-1(U)} = j) = \int_0^1 P_C(N_{1-of-1(U)} = j) f_c(\kappa) d\kappa = \int_0^1 \xi(\mathbf{Q})^{j-1} (\mathbf{I} - \mathbf{Q}) \mathbf{1} f_c(\kappa) d\kappa \quad (5.3)$$

$$ARL_{1-of-1(U)} = \int_0^1 CARL_{1-of-1(U)} f_c(\kappa) d\kappa = \int_0^1 \xi(\mathbf{I} - \mathbf{Q})^{-1} \mathbf{1} f_c(\kappa) d\kappa \quad (5.4)$$

$$\begin{aligned}
 VRL_{1-of-1(U)} &= \int_0^1 CVRL_{1-of-1(U)} f_c(\kappa) d\kappa + \int_0^1 (CARL_{1-of-1(U)})^2 f_c(\kappa) d\kappa - \left(\int_0^1 CARL_{1-of-1(U)} f_c(\kappa) d\kappa \right)^2 \\
 &= \int_0^1 \xi(\mathbf{I} + \mathbf{Q})(\mathbf{I} - \mathbf{Q})^{-2} \mathbf{1} - (\xi(\mathbf{I} - \mathbf{Q})^{-1} \mathbf{1})^2 f_c(\kappa) d\kappa \\
 &\quad + \int_0^1 (\xi(\mathbf{I} - \mathbf{Q})^{-1} \mathbf{1})^2 f_c(\kappa) d\kappa - \left(\int_0^1 \xi(\mathbf{I} - \mathbf{Q})^{-1} \mathbf{1} f_c(\kappa) d\kappa \right)^2
 \end{aligned} \tag{5.5}$$

$$FAR_{1-of-1(U)} = \int_0^1 CFAR_{1-of-1(U)} f_c(\kappa) d\kappa = \int_0^1 (p_{8C} | G = F) f_c(\kappa) d\kappa \tag{5.6}$$

For more information regarding the equations (5.3), (5.4), (5.5) and (5.6) refer to Appendix 5 equations (A5.77), (A5.78), (A5.79) and (A5.80).

Refer to Section 3.2.1.1 of Chapter 3 for an explanation of the subscripts used in the equations of the unconditional run-length distribution and the characteristics of the unconditional run-length distribution. Also note that the C in $CARL$, $CVRL$ and $CFAR$ indicate that the ARL , VRL and FAR is conditional.

5.4.1.2 The lower one-sided $1-of-1$ precedence chart

The unconditional run-length distribution and some characteristics of the unconditional run-length distribution of the lower one-sided $1-of-1$ precedence chart are given by:

$$P(N_{1-of-1(L)} = j) = \int_0^1 P_C(N_{1-of-1(L)} = j) f_b(t) dt = \int_0^1 \xi(\mathbf{Q})^{j-1} (\mathbf{I} - \mathbf{Q}) \mathbf{1} f_b(t) dt \tag{5.7}$$

$$ARL_{1-of-1(L)} = \int_0^1 CARL_{1-of-1(L)} f_b(t) dt = \int_0^1 \xi(\mathbf{I} - \mathbf{Q})^{-1} \mathbf{1} f_b(t) dt \tag{5.8}$$

$$\begin{aligned}
 VRL_{1-of-1(L)} &= \int_0^1 CVRL_{1-of-1(L)} f_b(t) dt + \int_0^1 (CARL_{1-of-1(L)})^2 f_b(t) dt - \left(\int_0^1 CARL_{1-of-1(L)} f_b(t) dt \right)^2 \\
 &= \int_0^1 (\xi(\mathbf{I} + \mathbf{Q})(\mathbf{I} - \mathbf{Q})^{-2} \mathbf{1} - (\xi(\mathbf{I} - \mathbf{Q})^{-1} \mathbf{1})^2) f_b(t) dt \\
 &\quad + \int_0^1 (\xi(\mathbf{I} - \mathbf{Q})^{-1} \mathbf{1})^2 f_b(t) dt - \left(\int_0^1 \xi(\mathbf{I} - \mathbf{Q})^{-1} \mathbf{1} f_b(t) dt \right)^2
 \end{aligned} \tag{5.9}$$

$$FAR_{1-of-1(L)} = \int_0^1 CFAR_{1-of-1(L)} f_b(t) dt = \int_0^1 (p_{9C} | G = F) f_b(t) dt \tag{5.10}$$

For more information regarding the equations (5.7), (5.8), (5.9) and (5.10) refer to equations (A5.81), (A5.82), (A5.83) and (A5.84) of Appendix 5.

5.4.1.3 The two-sided *l-of-l* precedence chart

The unconditional run-length distribution and some characteristics of the unconditional run-length distribution of the two-sided *l-of-l* precedence chart are given by:

$$P(N_{1-of-1(T)} = j) = \int_0^1 \int_0^\kappa P_C(N_{1-of-1(T)} = j) f_{bc}(t, \kappa) dtd\kappa = \int_0^1 \int_0^\kappa \xi(\mathbf{Q})^{j-1} (\mathbf{I} - \mathbf{Q}) \mathbf{1} f_{bc}(t, \kappa) dtd\kappa \quad (5.10)$$

$$ARL_{1-of-1(T)} = \int_0^1 \int_0^\kappa CARL_{1-of-1(T)} f_{bc}(t, \kappa) dtd\kappa = \int_0^1 \int_0^\kappa \xi(\mathbf{I} - \mathbf{Q})^{-1} \mathbf{1} f_{bc}(t, \kappa) dtd\kappa \quad (5.11)$$

$$\begin{aligned} VRL_{1-of-1(T)} &= \int_0^1 \int_0^\kappa CVRL_{1-of-1(T)} f_{bc}(t, \kappa) dtd\kappa + \int_0^1 \int_0^\kappa (CARL_{1-of-1(T)})^2 f_{bc}(t, \kappa) dtd\kappa \\ &\quad - \left(\int_0^1 \int_0^\kappa CARL_{1-of-1(T)} f_{bc}(t, \kappa) dtd\kappa \right)^2 \\ &= \int_0^1 \int_0^\kappa \left(\xi(\mathbf{I} + \mathbf{Q})(\mathbf{I} - \mathbf{Q})^{-2} \mathbf{1} - (\xi(\mathbf{I} - \mathbf{Q})^{-1} \mathbf{1})^2 \right) f_{bc}(t, \kappa) dtd\kappa \\ &\quad + \int_0^1 \int_0^\kappa (\xi(\mathbf{I} - \mathbf{Q})^{-1} \mathbf{1})^2 f_{bc}(t, \kappa) dtd\kappa - \left(\int_0^1 \int_0^\kappa \xi(\mathbf{I} - \mathbf{Q})^{-1} \mathbf{1} f_{bc}(t, \kappa) dtd\kappa \right)^2 \end{aligned} \quad (5.12)$$

$$FAR_{1-of-1(T)} = \int_0^1 \int_0^\kappa UFAR_{1-of-1(T)} f_{bc}(t, \kappa) dtd\kappa = \int_0^1 \int_0^\kappa (p_{8C} + p_{9C} | G = F) f_{bc}(t, \kappa) dtd\kappa \quad (5.13)$$

For more information regarding the equations (5.10), (5.11), (5.12) and (5.13) refer to equations (A5.85), (A5.86), (A5.87) and (A5.88) of Appendix 5.

5.4.2 The 2-of-2 precedence charts

5.4.2.1 The upper one-sided 2-of-2 precedence chart

The unconditional run-length distribution and some characteristics of the unconditional run-length distribution of the upper one-sided 2-of-2 precedence chart are given by:

$$P(N_{2\text{-of-}2(U)} = j) = \int_0^1 P_C(N_{2\text{-of-}2(U)} = j) f_c(\kappa) d\kappa = \int_0^1 \xi(\mathbf{Q})^{j-1} (\mathbf{I} - \mathbf{Q}) \mathbf{1} f_c(\kappa) d\kappa \quad (5.14)$$

$$ARL_{2\text{-of-}2(U)} = \int_0^1 CARL_{2\text{-of-}2(U)} f_c(\kappa) d\kappa = \int_0^1 \xi(\mathbf{I} - \mathbf{Q})^{-1} \mathbf{1} f_c(\kappa) d\kappa \quad (5.15)$$

$$\begin{aligned} VRL_{2\text{-of-}2(U)} &= \int_0^1 CVRL_{2\text{-of-}2(U)} f_c(\kappa) d\kappa + \int_0^1 (CARL_{2\text{-of-}2(U)})^2 f_c(\kappa) d\kappa - \left(\int_0^1 CARL_{2\text{-of-}2(U)} f_c(\kappa) d\kappa \right)^2 \\ &= \int_0^1 \left(\xi(\mathbf{I} + \mathbf{Q})(\mathbf{I} - \mathbf{Q})^{-2} \mathbf{1} - (\xi(\mathbf{I} - \mathbf{Q})^{-1} \mathbf{1})^2 \right) f_c(\kappa) d\kappa \\ &\quad + \int_0^1 (\xi(\mathbf{I} - \mathbf{Q})^{-1} \mathbf{1})^2 f_c(\kappa) d\kappa - \left(\int_0^1 \xi(\mathbf{I} - \mathbf{Q})^{-1} \mathbf{1} f_c(\kappa) d\kappa \right)^2 \end{aligned} \quad (5.16)$$

$$FAR_{2\text{-of-}2(U)} = \int_0^1 CFAR_{2\text{-of-}2(U)} f_c(\kappa) d\kappa = \int_0^1 \left((p_{8C})^2 | G = F \right) f_c(\kappa) d\kappa \quad (5.17)$$

For more information regarding the equations (5.14), (5.15), (5.16) and (5.17) refer to equations (A5.89), (A5.90), (A5.91) and (A5.92) of Appendix 5. See also Human et al. (2009).

5.4.2.2 The lower one-sided 2-of-2 precedence chart

The unconditional run-length distribution and some characteristics of the unconditional run-length distribution of the lower one-sided 2-of-2 precedence chart are given by:

$$P(N_{2\text{-of-}2(L)} = j) = \int_0^1 P_C(N_{2\text{-of-}2(L)} = j) f_b(t) dt = \int_0^1 \xi(\mathbf{Q})^{j-1} (\mathbf{I} - \mathbf{Q}) \mathbf{1} f_b(t) dt \quad (5.18)$$

$$ARL_{2\text{-of-}2(L)} = \int_0^1 CARL_{2\text{-of-}2(L)} f_b(t) dt = \int_0^1 \xi(\mathbf{I} - \mathbf{Q})^{-1} \mathbf{1} f_b(t) dt \quad (5.19)$$

$$\begin{aligned}
 VRL_{2-of-2(L)} &= \int_0^1 CVRL_{2-of-2(L)} f_b(t) dt + \int_0^1 (CARL_{2-of-2(L)})^2 f_b(t) dt - \left(\int_0^1 CARL_{2-of-2(L)} f_b(t) dt \right)^2 \\
 &= \int_0^1 \left(\xi(\mathbf{I} + \mathbf{Q})(\mathbf{I} - \mathbf{Q})^{-2} \mathbf{1} - (\xi(\mathbf{I} - \mathbf{Q})^{-1} \mathbf{1})^2 \right) f_b(t) dt \\
 &\quad + \int_0^1 \left(\xi(\mathbf{I} - \mathbf{Q})^{-1} \mathbf{1} \right)^2 f_b(t) dt - \left(\int_0^1 \xi(\mathbf{I} - \mathbf{Q})^{-1} \mathbf{1} f_b(t) dt \right)^2
 \end{aligned} \tag{5.20}$$

$$FAR_{2-of-2(L)} = \int_0^1 CFAR_{2-of-2(L)} f_b(t) dt = \int_0^1 \left((p_{9C})^2 \mid G = F \right) f_b(t) dt \tag{5.21}$$

For more information regarding the equations (5.18), (5.19), (5.20) and (5.21) refer to equations (A5.93), (A5.94), (A5.95) and (A5.96) of Appendix 5.

5.4.2.3 The two-sided 2-of-2 precedence chart

The unconditional run-length distribution and some characteristics of the unconditional run-length distribution of the two-sided 2-of-2 precedence chart are given by:

$$P(N_{2-of-2(T)} = j) = \int_0^1 \int_0^\kappa P_C(N_{2-of-2(T)} = j) f_{bc}(t, \kappa) dtd\kappa = \int_0^1 \int_0^\kappa \xi(\mathbf{Q})^{j-1} (\mathbf{I} - \mathbf{Q}) \mathbf{1} f_{bc}(t, \kappa) dtd\kappa \tag{5.22}$$

$$ARL_{2-of-2(T)} = \int_0^1 \int_0^\kappa CARL_{2-of-2(T)} f_{bc}(t, \kappa) dtd\kappa = \int_0^1 \int_0^\kappa \xi(\mathbf{I} - \mathbf{Q})^{-1} \mathbf{1} f_{bc}(t, \kappa) dtd\kappa \tag{5.23}$$

$$\begin{aligned}
 VRL_{2-of-2(T)} &= \int_0^1 \int_0^\kappa CVRL_{2-of-2(T)} f_{bc}(t, \kappa) dtd\kappa + \int_0^1 \int_0^\kappa (CARL_{2-of-2(T)})^2 f_{bc}(t, \kappa) dtd\kappa \\
 &\quad - \left(\int_0^1 \int_0^\kappa CARL_{2-of-2(T)} f_{bc}(t, \kappa) dtd\kappa \right)^2 \\
 &= \int_0^1 \int_0^\kappa \left(\xi(\mathbf{I} + \mathbf{Q})(\mathbf{I} - \mathbf{Q})^{-2} \mathbf{1} - (\xi(\mathbf{I} - \mathbf{Q})^{-1} \mathbf{1})^2 \right) f_{bc}(t, \kappa) dtd\kappa \\
 &\quad + \int_0^1 \int_0^\kappa \left(\xi(\mathbf{I} - \mathbf{Q})^{-1} \mathbf{1} \right)^2 f_{bc}(t, \kappa) dtd\kappa - \left(\int_0^1 \int_0^\kappa \xi(\mathbf{I} - \mathbf{Q})^{-1} \mathbf{1} f_{bc}(t, \kappa) dtd\kappa \right)^2
 \end{aligned} \tag{5.24}$$

$$FAR_{2-of-2(T)} = \int_0^1 \int_0^\kappa CFAR_{2-of-2(T)} f_{bc}(t, \kappa) dtd\kappa = \int_0^1 \int_0^\kappa \left((p_{8C})^2 + (p_{9C})^2 \mid G = F \right) f_{bc}(t, \kappa) dtd\kappa \tag{5.25}$$

For more information regarding the equations (5.22), (5.23), (5.24) and (5.25) refer to equations (A5.97), (A5.98), (A5.99) and (A5.100) of Appendix 5. See also Human et al. (2009).

5.4.3 The 2-of-3 precedence charts

5.4.3.1 The upper one-sided 2-of-3 precedence chart

The unconditional run-length distribution and some characteristics of the unconditional run-length distribution of the upper one-sided 2-of-3 precedence chart are given by:

$$P(N_{2-of-3(U)} = j) = \int_0^1 P_C(N_{2-of-3(U)} = j) f_c(\kappa) d\kappa = \int_0^1 \xi(\mathbf{Q})^{j-1} (\mathbf{I} - \mathbf{Q}) \mathbf{1} f_c(\kappa) d\kappa \quad (5.26)$$

$$ARL_{2-of-3(U)} = \int_0^1 CARL_{2-of-3(U)} f_c(\kappa) d\kappa = \int_0^1 \xi(\mathbf{I} - \mathbf{Q})^{-1} \mathbf{1} f_c(\kappa) d\kappa \quad (5.27)$$

$$\begin{aligned} VRL_{2-of-3(U)} &= \int_0^1 CVRL_{2-of-3(U)} f_c(\kappa) d\kappa + \int_0^1 (CARL_{2-of-3(U)})^2 f_c(\kappa) d\kappa - \left(\int_0^1 CARL_{2-of-3(U)} f_c(\kappa) d\kappa \right)^2 \\ &= \int_0^1 \left(\xi(\mathbf{I} + \mathbf{Q})(\mathbf{I} - \mathbf{Q})^{-2} \mathbf{1} - (\xi(\mathbf{I} - \mathbf{Q})^{-1} \mathbf{1})^2 \right) f_c(\kappa) d\kappa \\ &\quad + \int_0^1 (\xi(\mathbf{I} - \mathbf{Q})^{-1} \mathbf{1})^2 f_c(\kappa) d\kappa - \left(\int_0^1 \xi(\mathbf{I} - \mathbf{Q})^{-1} \mathbf{1} f_c(\kappa) d\kappa \right)^2 \end{aligned} \quad (5.28)$$

$$FAR_{2-of-3(U)} = \int_0^1 CFAR_{2-of-3(U)} f_c(\kappa) d\kappa \quad (5.29)$$

For more information regarding the equations (5.26), (5.27), (5.28) and (5.29) refer to equations (A5.101), (A5.102), (A5.103) and (A5.104) of Appendix 5.

5.4.3.2 The lower one-sided 2-of-3 precedence chart

The unconditional run-length distribution and some characteristics of the unconditional run-length distribution of the lower one-sided 2-of-3 precedence chart are given by:

$$P(N_{2-of-3(L)} = j) = \int_0^1 P_C(N_{2-of-3(L)} = j) f_b(t) dt = \int_0^1 \xi(\mathbf{Q})^{j-1} (\mathbf{I} - \mathbf{Q}) \mathbf{1} f_b(t) dt \quad (5.30)$$

$$ARL_{2-of-3(L)} = \int_0^1 CARL_{2-of-3(L)} f_b(t) dt = \int_0^1 \xi(\mathbf{I} - \mathbf{Q})^{-1} \mathbf{1} f_b(t) dt \quad (5.31)$$

$$\begin{aligned}
 VRL_{2-of-3(L)} &= \int_0^1 CVRL_{2-of-3(L)} f_b(t) dt + \int_0^1 (CARL_{2-of-3(L)})^2 f_b(t) dt - \left(\int_0^1 CARL_{2-of-3(L)} f_b(t) dt \right)^2 \\
 &= \int_0^1 \left(\xi(\mathbf{I} + \mathbf{Q})(\mathbf{I} - \mathbf{Q})^{-2} \mathbf{1} - (\xi(\mathbf{I} - \mathbf{Q})^{-1} \mathbf{1})^2 \right) f_b(t) dt \\
 &\quad + \int_0^1 \left(\xi(\mathbf{I} - \mathbf{Q})^{-1} \mathbf{1} \right)^2 f_b(t) dt - \left(\int_0^1 \xi(\mathbf{I} - \mathbf{Q})^{-1} \mathbf{1} f_b(t) dt \right)^2
 \end{aligned} \tag{5.32}$$

$$FAR_{2-of-3(L)} = \int_0^1 CFAR_{2-of-3(L)} f_b(t) dt \tag{5.33}$$

For more information regarding the equations (5.30), (5.31), (5.32) and (5.33) refer to equations (A5.105), (A5.106), (A5.107) and (A5.108) of Appendix 5.

5.4.3.3 The two-sided 2-of-3 precedence chart

The unconditional run-length distribution and some characteristics of the unconditional run-length distribution of the two-sided 2-of-3 precedence chart are given by:

$$P(N_{2-of-3(T)} = j) = \int_0^1 \int_0^\kappa P_C(N_{2-of-3(T)} = j) f_{bc}(t, \kappa) d\iota d\kappa = \int_0^1 \int_0^\kappa \xi(\mathbf{Q})^{j-1} (\mathbf{I} - \mathbf{Q}) \mathbf{1} f_{bc}(t, \kappa) d\iota d\kappa \tag{5.34}$$

$$ARL_{2-of-3(T)} = \int_0^1 \int_0^\kappa CARL_{2-of-3(T)} f_{bc}(t, \kappa) d\iota d\kappa = \int_0^1 \int_0^\kappa \xi(\mathbf{I} - \mathbf{Q})^{-1} \mathbf{1} f_{bc}(t, \kappa) d\iota d\kappa \tag{5.35}$$

$$\begin{aligned}
 VRL_{2-of-3(T)} &= \int_0^1 \int_0^\kappa CVRL_{2-of-3(T)} f_{bc}(t, \kappa) d\iota d\kappa + \int_0^1 \int_0^\kappa (CARL_{2-of-3(T)})^2 f_{bc}(t, \kappa) d\iota d\kappa \\
 &\quad - \left(\int_0^1 \int_0^\kappa CARL_{2-of-3(T)} f_{bc}(t, \kappa) d\iota d\kappa \right)^2 \\
 &= \int_0^1 \int_0^\kappa \left(\xi(\mathbf{I} + \mathbf{Q})(\mathbf{I} - \mathbf{Q})^{-2} \mathbf{1} - (\xi(\mathbf{I} - \mathbf{Q})^{-1} \mathbf{1})^2 \right) f_{bc}(t, \kappa) d\iota d\kappa \\
 &\quad + \int_0^1 \int_0^\kappa \left(\xi(\mathbf{I} - \mathbf{Q})^{-1} \mathbf{1} \right)^2 f_{bc}(t, \kappa) d\iota d\kappa - \left(\int_0^1 \int_0^\kappa \xi(\mathbf{I} - \mathbf{Q})^{-1} \mathbf{1} f_{bc}(t, \kappa) d\iota d\kappa \right)^2
 \end{aligned} \tag{5.36}$$

$$FAR_{2-of-3(T)} = \int_0^1 \int_0^\kappa CFAR_{2-of-3(T)} f_{bc}(t, \kappa) d\iota d\kappa \tag{5.37}$$

For more information regarding the equations (5.34), (5.35), (5.36) and (5.37) refer to equations (A5.109), (A5.110), (A5.111) and (A5.112) of Appendix 5.

5.4.4 The *improved 2-of-2* precedence charts

5.4.4.1 The upper one-sided *improved 2-of-2* precedence chart

The unconditional run-length distribution and some characteristics of the unconditional run-length distribution of the upper one-sided *improved 2-of-2* precedence chart are given by:

$$P(N_{12\text{-of-}2(U)} = j) = \int_0^1 \int_0^\lambda P_C(N_{12\text{-of-}2(U)} = j) f_{cd}(\kappa, \lambda) d\kappa d\lambda = \int_0^1 \int_0^\lambda \xi(\mathbf{Q})^{j-1} (\mathbf{I} - \mathbf{Q}) \mathbf{1} f_{cd}(\kappa, \lambda) d\kappa d\lambda \quad (5.38)$$

$$ARL_{12\text{-of-}2(U)} = \int_0^1 \int_0^\lambda CARL_{12\text{-of-}2(U)} f_{cd}(\kappa, \lambda) d\kappa d\lambda = \int_0^1 \int_0^\lambda \xi(\mathbf{I} - \mathbf{Q})^{-1} \mathbf{1} f_{cd}(\kappa, \lambda) d\kappa d\lambda \quad (5.39)$$

$$\begin{aligned} VRL_{12\text{-of-}2(U)} &= \int_0^1 \int_0^\lambda CVRL_{12\text{-of-}2(U)} f_{cd}(\kappa, \lambda) d\kappa d\lambda + \int_0^1 \int_0^\lambda (CARL_{12\text{-of-}2(U)})^2 f_{cd}(\kappa, \lambda) d\kappa d\lambda \\ &\quad - \left(\int_0^1 \int_0^\lambda CARL_{12\text{-of-}2(U)} f_{cd}(\kappa, \lambda) d\kappa d\lambda \right)^2 \\ &= \int_0^1 \int_0^\lambda \left(\xi(\mathbf{I} + \mathbf{Q})(\mathbf{I} - \mathbf{Q})^{-2} \mathbf{1} - (\xi(\mathbf{I} - \mathbf{Q})^{-1} \mathbf{1})^2 \right) f_{cd}(\kappa, \lambda) d\kappa d\lambda \\ &\quad + \int_0^1 \int_0^\lambda (\xi(\mathbf{I} - \mathbf{Q})^{-1} \mathbf{1})^2 f_{cd}(\kappa, \lambda) d\kappa d\lambda - \left(\int_0^1 \int_0^\lambda \xi(\mathbf{I} - \mathbf{Q})^{-1} \mathbf{1} f_{cd}(\kappa, \lambda) d\kappa d\lambda \right)^2 \end{aligned} \quad (5.40)$$

$$FAR_{12\text{-of-}2(U)} = \int_0^1 \int_0^\lambda CFAR_{12\text{-of-}2(U)} f_{cd}(\kappa, \lambda) d\kappa d\lambda \quad (5.41)$$

For more information regarding the equations (5.38), (5.39), (5.40) and (5.41) refer to equations (A5.113), (A5.114), (A5.115) and (A5.116) of Appendix 5.

5.4.4.2 The lower one-sided *improved 2-of-2* precedence chart

The unconditional run-length distribution and some characteristics of the unconditional run-length distribution of the lower one-sided *improved 2-of-2* precedence chart are given by:

$$P(N_{12\text{-of-}2(L)} = j) = \int_0^1 \int_0^t P_C(N_{12\text{-of-}2(L)} = j) f_{ab}(\theta, t) d\theta dt = \int_0^1 \int_0^t \xi(\mathbf{Q})^{j-1} (\mathbf{I} - \mathbf{Q}) \mathbf{1} f_{ab}(\theta, t) d\theta dt \quad (5.42)$$

$$ARL_{12\text{-of-}2(L)} = \int_0^1 \int_0^t CARL_{12\text{-of-}2(L)} f_{ab}(\theta, t) d\theta dt = \int_0^1 \int_0^t \xi(\mathbf{I} - \mathbf{Q})^{-1} \mathbf{1} f_{ab}(\theta, t) d\theta dt \quad (5.43)$$

$$\begin{aligned}
 VRL_{I2-of-2(L)} &= \int_0^1 \int_0^t CVRL_{I2-of-2(L)} f_{ab}(\theta, \iota) d\theta d\iota + \int_0^1 \int_0^t (CARL_{I2-of-2(L)})^2 f_{ab}(\theta, \iota) d\theta d\iota \\
 &\quad - \left(\int_0^1 \int_0^y CARL_{I2-of-2(L)} f_{ab}(\theta, \iota) d\theta d\iota \right)^2 \\
 &= \int_0^1 \int_0^t \left(\xi(\mathbf{I} + \mathbf{Q})(\mathbf{I} - \mathbf{Q})^{-2} \mathbf{1} - (\xi(\mathbf{I} - \mathbf{Q})^{-1} \mathbf{1})^2 \right) f_{ab}(\theta, \iota) d\theta d\iota \\
 &\quad + \int_0^1 \int_0^t (\xi(\mathbf{I} - \mathbf{Q})^{-1} \mathbf{1})^2 f_{ab}(\theta, \iota) d\theta d\iota - \left(\int_0^1 \int_0^t \xi(\mathbf{I} - \mathbf{Q})^{-1} \mathbf{1} f_{ab}(\theta, \iota) d\theta d\iota \right)^2
 \end{aligned} \tag{5.44}$$

$$FAR_{I2-of-2(L)} = \int_0^1 \int_0^t CFAR_{I2-of-2(L)} f_{ab}(\theta, \iota) d\theta d\iota \tag{5.45}$$

For more information regarding the equations (5.42), (5.43), (5.44) and (5.45) refer to equations (A5.117), (A5.118), (A5.119) and (A5.120) of Appendix 5.

5.4.4.3 The two-sided *improved 2-of-2* precedence chart

The unconditional run-length distribution and some characteristics of the unconditional run-length distribution of the two-sided *improved 2-of-2* precedence chart are given by:

$$\begin{aligned}
 P(N_{I2-of-2(T)} = j) &= \int_0^1 \int_0^\lambda \int_0^\kappa \int_0^t P_C(N_{I2-of-2(T)} = j) f_{abcd}(\theta, \iota, \kappa, \lambda) d\theta d\iota d\kappa d\lambda \\
 &= \int_0^1 \int_0^\lambda \int_0^\kappa \int_0^t \xi(\mathbf{Q})^{j-1} (\mathbf{I} - \mathbf{Q}) \mathbf{1} f_{abcd}(\theta, \iota, \kappa, \lambda) d\theta d\iota d\kappa d\lambda
 \end{aligned} \tag{5.46}$$

$$\begin{aligned}
 ARL_{I2-of-2(T)} &= \int_0^1 \int_0^\lambda \int_0^\kappa \int_0^t CARL_{I2-of-2(T)} f_{abcd}(\theta, \iota, \kappa, \lambda) d\theta d\iota d\kappa d\lambda \\
 &= \int_0^1 \int_0^\lambda \int_0^\kappa \int_0^t \xi(\mathbf{I} - \mathbf{Q})^{-1} \mathbf{1} f_{abcd}(\theta, \iota, \kappa, \lambda) d\theta d\iota d\kappa d\lambda
 \end{aligned} \tag{5.47}$$

$$\begin{aligned}
 VRL_{12\text{-of-}2(T)} &= \int_0^1 \int_0^\lambda \int_0^\kappa \int_0^t CVRL_{12\text{-of-}2(T)} f_{abcd}(\theta, \iota, \kappa, \lambda) d\theta d\iota \kappa d\lambda \\
 &+ \int_0^1 \int_0^\lambda \int_0^\kappa \int_0^t (CARL_{12\text{-of-}2(T)})^2 f_{abcd}(\theta, \iota, \kappa, \lambda) d\theta d\iota \kappa d\lambda \\
 &- \left(\int_0^1 \int_0^\lambda \int_0^\kappa \int_0^t CARL_{12\text{-of-}2(T)} f_{abcd}(\theta, \iota, \kappa, \lambda) d\theta d\iota \kappa d\lambda \right)^2 \\
 &= \int_0^1 \int_0^\lambda \int_0^\kappa \int_0^t \left(\xi(\mathbf{I} + \mathbf{Q})(\mathbf{I} - \mathbf{Q})^{-2} \mathbf{1} - (\xi(\mathbf{I} - \mathbf{Q})^{-1} \mathbf{1})^2 \right) f_{abcd}(\theta, \iota, \kappa, \lambda) d\theta d\iota \kappa d\lambda \\
 &+ \int_0^1 \int_0^\lambda \int_0^\kappa \int_0^t (\xi(\mathbf{I} - \mathbf{Q})^{-1} \mathbf{1})^2 f_{abcd}(\theta, \iota, \kappa, \lambda) d\theta d\iota \kappa d\lambda \\
 &- \left(\int_0^1 \int_0^\lambda \int_0^\kappa \int_0^t \xi(\mathbf{I} - \mathbf{Q})^{-1} \mathbf{1} f_{abcd}(\theta, \iota, \kappa, \lambda) d\theta d\iota \kappa d\lambda \right)^2
 \end{aligned} \tag{5.48}$$

$$FAR_{12\text{-of-}2(T)} = \int_0^1 \int_0^\lambda \int_0^\kappa \int_0^t CFAR_{12\text{-of-}2(T)} f_{abcd}(\theta, \iota, \kappa, \lambda) d\theta d\iota \kappa d\lambda \tag{5.49}$$

For more information regarding the equations (5.46), (5.47), (5.48) and (5.49) refer to equations (A5.121), (A5.122), (A5.123) and (A5.124) of Appendix 5.

5.4.5 The *improved 2-of-3* precedence charts

5.4.5.1 The upper one-sided *improved 2-of-3* precedence chart

The unconditional run-length distribution and some characteristics of the unconditional run-length distribution of the upper one-sided *improved 2-of-3* precedence chart are given by:

$$P(N_{12\text{-of-}3(U)} = j) = \int_0^1 \int_0^\lambda P_C(N_{12\text{-of-}3(U)} = j) f_{cd}(\kappa, \lambda) d\kappa d\lambda = \int_0^1 \int_0^\lambda \xi(\mathbf{Q})^{j-1} (\mathbf{I} - \mathbf{Q}) \mathbf{1} f_{cd}(\kappa, \lambda) d\kappa d\lambda \tag{5.50}$$

$$ARL_{12\text{-of-}3(U)} = \int_0^1 \int_0^\lambda CARL_{12\text{-of-}3(U)} f_{cd}(\kappa, \lambda) d\kappa d\lambda = \int_0^1 \int_0^\lambda \xi(\mathbf{I} - \mathbf{Q})^{-1} \mathbf{1} f_{cd}(\kappa, \lambda) d\kappa d\lambda \tag{5.51}$$

$$\begin{aligned}
 VRL_{12\text{-of-}3(U)} &= \int_0^1 \int_0^\lambda CVRL_{12\text{-of-}3(U)} f_{cd}(\kappa, \lambda) d\kappa d\lambda + \int_0^1 \int_0^\lambda (CARL_{12\text{-of-}3(U)})^2 f_{cd}(\kappa, \lambda) d\kappa d\lambda \\
 &- \left(\int_0^1 \int_0^\lambda CARL_{12\text{-of-}3(U)} f_{cd}(\kappa, \lambda) d\kappa d\lambda \right)^2
 \end{aligned}$$

$$\begin{aligned}
 &= \int_0^1 \int_0^\lambda \left(\xi(\mathbf{I} + \mathbf{Q})(\mathbf{I} - \mathbf{Q})^{-2} \mathbf{1} - \left(\xi(\mathbf{I} - \mathbf{Q})^{-1} \mathbf{1} \right)^2 \right) f_{cd}(\kappa, \lambda) d\kappa d\lambda \\
 &\quad + \int_0^1 \int_0^\lambda \left(\xi(\mathbf{I} - \mathbf{Q})^{-1} \mathbf{1} \right)^2 f_{cd}(\kappa, \lambda) d\kappa d\lambda - \left(\int_0^1 \int_0^\lambda \xi(\mathbf{I} - \mathbf{Q})^{-1} \mathbf{1} f_{cd}(\kappa, \lambda) d\kappa d\lambda \right)^2
 \end{aligned} \tag{5.52}$$

$$FAR_{I_{2-of-3}(U)} = \int_0^1 \int_0^\lambda CFAR_{I_{2-of-3}(U)} f_{cd}(\kappa, \lambda) d\kappa d\lambda = \int_0^1 \int_0^\lambda \xi(\mathbf{Q})^{j-1} (\mathbf{I} - \mathbf{Q}) \mathbf{1} f_{cd}(\kappa, \lambda) d\kappa d\lambda \tag{5.53}$$

For more information regarding the equations (5.50), (5.51), (5.52) and (5.53) refer to equations (A5.125), (A5.126), (A5.127) and (A5.128) of Appendix 5.

5.4.5.2 The lower one-sided *improved 2-of-3* precedence chart

The unconditional run-length distribution and some characteristics of the unconditional run-length distribution of the lower one-sided *improved 2-of-3* precedence chart are given by:

$$P(N_{I_{2-of-3}(L)} = j) = \int_0^1 \int_0^t P_C(N_{I_{2-of-3}(L)} = j) f_{ab}(\theta, t) d\theta dt = \int_0^1 \int_0^t \xi(\mathbf{Q})^{j-1} (\mathbf{I} - \mathbf{Q}) \mathbf{1} f_{ab}(\theta, t) d\theta dt \tag{5.54}$$

$$ARL_{I_{2-of-3}(L)} = \int_0^1 \int_0^t CARL_{I_{2-of-3}(L)} f_{ab}(\theta, t) d\theta dt = \int_0^1 \int_0^t \xi(\mathbf{I} - \mathbf{Q})^{-1} \mathbf{1} f_{ab}(\theta, t) d\theta dt \tag{5.55}$$

$$\begin{aligned}
 VRL_{I_{2-of-3}(L)} &= \int_0^1 \int_0^t CVRL_{I_{2-of-3}(L)} f_{ab}(\theta, t) d\theta dt + \int_0^1 \int_0^t \left(CARL_{I_{2-of-3}(L)} \right)^2 f_{ab}(\theta, t) d\theta dt \\
 &\quad - \left(\int_0^1 \int_0^t CARL_{I_{2-of-3}(L)} f_{ab}(\theta, t) d\theta dt \right)^2 \\
 &= \int_0^1 \int_0^t \left(\xi(\mathbf{I} + \mathbf{Q})(\mathbf{I} - \mathbf{Q})^{-2} \mathbf{1} - \left(\xi(\mathbf{I} - \mathbf{Q})^{-1} \mathbf{1} \right)^2 \right) f_{ab}(\theta, t) d\theta dt \\
 &\quad + \int_0^1 \int_0^t \left(\xi(\mathbf{I} - \mathbf{Q})^{-1} \mathbf{1} \right)^2 f_{ab}(\theta, t) d\theta dt - \left(\int_0^1 \int_0^t \xi(\mathbf{I} - \mathbf{Q})^{-1} \mathbf{1} f_{ab}(\theta, t) d\theta dt \right)^2
 \end{aligned} \tag{5.56}$$

$$FAR_{I_{2-of-3}(L)} = \int_0^1 \int_0^t CFAR_{I_{2-of-3}(L)} f_{ab}(\theta, t) d\theta dt \tag{5.57}$$

For more information regarding the equations (5.54), (5.55), (5.56) and (5.57) refer to equations (A5.129), (A5.130), (A5.131) and (A5.132) of Appendix 5.

5.4.5.3 The two-sided *improved 2-of-3* precedence chart

The unconditional run-length distribution and some characteristics of the unconditional run-length distribution of the two-sided *improved 2-of-3* precedence chart are given by:

$$\begin{aligned}
 P(N_{I2-of-3(T)} = j) &= \int_0^1 \int_0^\lambda \int_0^\kappa \int_0^t P_C(N_{I2-of-3(T)} = j) f_{abcd}(\theta, \iota, \kappa, \lambda) d\theta d\iota d\kappa d\lambda \\
 &= \int_0^1 \int_0^\lambda \int_0^\kappa \int_0^t \xi(\mathbf{Q})^{j-1} (\mathbf{I} - \mathbf{Q}) \mathbf{1} f_{abcd}(\theta, \iota, \kappa, \lambda) d\theta d\iota d\kappa d\lambda
 \end{aligned} \tag{5.58}$$

$$\begin{aligned}
 ARL_{I2-of-3(T)} &= \int_0^1 \int_0^\lambda \int_0^\kappa \int_0^t CARL_{I2-of-3(T)} f_{abcd}(\theta, \iota, \kappa, \lambda) d\theta d\iota d\kappa d\lambda \\
 &= \int_0^1 \int_0^\lambda \int_0^\kappa \int_0^t \xi(\mathbf{I} - \mathbf{Q})^{-1} \mathbf{1} f_{abcd}(\theta, \iota, \kappa, \lambda) d\theta d\iota d\kappa d\lambda
 \end{aligned} \tag{5.59}$$

$$\begin{aligned}
 VRL_{I2-of-3(T)} &= \int_0^1 \int_0^\lambda \int_0^\kappa \int_0^t CVRL_{I2-of-3(T)} f_{abcd}(\theta, \iota, \kappa, \lambda) d\theta d\iota d\kappa d\lambda \\
 &\quad + \int_0^1 \int_0^\lambda \int_0^\kappa \int_0^t (CARL_{I2-of-3(T)})^2 f_{abcd}(\theta, \iota, \kappa, \lambda) d\theta d\iota d\kappa d\lambda \\
 &\quad - \left(\int_0^1 \int_0^\lambda \int_0^\kappa \int_0^t CARL_{I2-of-3(T)} f_{abcd}(\theta, \iota, \kappa, \lambda) d\theta d\iota d\kappa d\lambda \right)^2 \\
 &= \int_0^1 \int_0^\lambda \int_0^\kappa \int_0^t \left(\xi(\mathbf{I} + \mathbf{Q})(\mathbf{I} - \mathbf{Q})^{-2} \mathbf{1} - (\xi(\mathbf{I} - \mathbf{Q})^{-1} \mathbf{1})^2 \right) f_{abcd}(\theta, \iota, \kappa, \lambda) d\theta d\iota d\kappa d\lambda \\
 &\quad + \int_0^1 \int_0^\lambda \int_0^\kappa \int_0^t (\xi(\mathbf{I} - \mathbf{Q})^{-1} \mathbf{1})^2 f_{abcd}(\theta, \iota, \kappa, \lambda) d\theta d\iota d\kappa d\lambda \\
 &\quad - \left(\int_0^1 \int_0^\lambda \int_0^\kappa \int_0^t \xi(\mathbf{I} - \mathbf{Q})^{-1} \mathbf{1} f_{abcd}(\theta, \iota, \kappa, \lambda) d\theta d\iota d\kappa d\lambda \right)^2
 \end{aligned} \tag{5.60}$$

$$FAR_{I2-of-3(T)} = \int_0^1 \int_0^\lambda \int_0^\kappa \int_0^t CFAR_{I2-of-3(T)} f_{abcd}(\theta, \iota, \kappa, \lambda) d\theta d\iota d\kappa d\lambda \tag{5.61}$$

For more information regarding the equations (5.58), (5.59), (5.60) and (5.61) refer to equations (A5.133), (A5.134), (A5.135) and (A5.136) of Appendix 5.

5.5 Design of the *improved* runs-rules precedence charts

The background and the explicit formulas for the precedence charts have been established. But what are still lacking are the charting constants for the *improved* runs-rules precedence charts. Therefore the order statistics from the IC reference sample need to be established that are used as the control limits in Phase II monitoring. This would ensure a chart which has desirable properties.

Note that the equations that are used to calculate the run-length distribution and the characteristics of the two-sided *improved* precedence charts are complicated (see equations (5.46)-(5.49) and equations (5.58)-(5.61)). Solving these equations is resource intensive. Simulations can be utilized for an approximation, but solving the equations is preferred. Consequently the focus will be on the upper one-sided *improved* runs-rules precedence charts. The software package Mathcad[®]14.0 is used to solve the equations that are used to calculate the characteristics of the upper one-sided *improved* runs-rules precedence charts.

Tables 5.2 and 5.3 were constructed by allowing the outer control limit UCL_B to be as large as possible (i.e. making UCL_B as un-influential as possible) while at the same time choosing the inner control limit UCL_A such that the $UARL$ is as close as possible to 370. The effect is then observed when the outer control limit is gradually brought closer to the UCL_A . From Tables 5.2 and 5.3 it can be seen that as the UCL_B is decreased, the unconditional average run-length ($UARL$) is at first unaffected, then the $UARL$ starts to decrease as expected. Based on the IC performance analysis, when reference sample size is 100 and 200 the $UARL$ is immediately affected as the UCL_B decreases.

There are two motivations for the manner in which Tables 5.2 and 5.3 were populated i.e. by starting to let the outer control limit UCL_B be as large as possible while at the same time choosing the inner control limit UCL_A such that the $UARL$ is as close as possible to 370 and then gradually bringing the UCL_B closer to the UCL_A . The first motivation is to limit the combinations of charting constants that need to be investigated since there are many possibilities. The second motivation is that the performance comparisons are simplified since a combination of charting constants can quite easily be found that provide a similar (same) IC ARL to the runs-rules enhanced precedence charts.

To illustrate the use of Tables 5.2 and 5.3 consider rows one to seven and the far right cells of Table 5.3. These cells contain the characteristics of the upper one-sided *improved 2-of-3* precedence chart when the reference sample is of size 500, the test sample is of size 7 and the 393rd (UCL_A) and

500th (UCL_B) order statistics from the reference sample are used as control limits to monitor the median. From this cell the following information can be obtained $ARL_{12-of-3(U)} = 361.49$, $FAR1_{12-of-3(U)} = 0.00000001$, $FAR2_{12-of-3(U)} = 0.00211750$ and $FAR345_{12-of-3(U)} = 0.00401624$. See Table 5.1 for clarity on the notation.

Tables 5.2 and 5.3 provide a great deal of information. These Tables should be of great usefulness to the quality practitioner in selecting appropriate control limits.

Following the presentation of Tables 5.2 and 5.3 an example is presented to illustrate the use of Tables 5.2 and 5.3 and also the application of the *improved* runs-rules precedence charts.

Table 5.1: Description of the notation used in Tables 5.2 and 5.3.

Notation	Description
n	Test sample size.
m	Reference sample size.
c	Integer representing the order statistic number from Phase I that is used as UCL_A .
d	Integer representing the order statistic number from Phase I that is used as UCL_B .
j	Integer representing the order statistic number from Phase II that is used as the plotting statistic.
IC ARL	Unconditional IC ARL.
$FAR1$	Unconditional false alarm rate for time = 1.
$FAR234$	Unconditional false alarm rate for time = 2, 3, 4,....
$FAR2$	Unconditional false alarm rate for time = 2.
$FAR345$	Unconditional false alarm rate for time = 3, 4, 5,....

Table 5.2: Unconditional IC *ARL*, unconditional *FAR* at time 1 and 2,3,4... respectively and the charting constants (*c,d*) for the upper one-sided improved 2-of-2 precedence chart for $m = 100, 200, 500$ and $(n,j)=(5,3),(7,4)$.

	$n=5, j=3$			$n=7, j=4$		
	$m=100$	$m=200$	$m=500$	$m=100$	$m=200$	$m=500$
IC <i>ARL</i>	390.45	349.63	365.00	303.91	383.78	352.22
<i>FAR</i>	0.00005334	0.00000706	0.00000048	0.00000678	0.00000047	0.00000001
<i>FAR</i>₂₃₄	0.00740930	0.00512795	0.00361770	0.01133275	0.00542242	0.00396963
(<i>c,d</i>)	(79,100)	(159,200)	(401,500)	(74,100)	(152,200)	(382,500)
IC <i>ARL</i>	349.94	317.89	362.08	297.97	377.38	352.05
<i>FAR</i>	0.00051782	0.00038136	0.00002714	0.00009703	0.00005590	0.00000166
<i>FAR</i>₂₃₄	0.00778414	0.00544478	0.00363992	0.01140042	0.00546881	0.00397098
(<i>c,d</i>)	(79,98)	(159,195)	(401,495)	(74,98)	(152,195)	(382,495)
IC <i>ARL</i>	281.28	239.06	350.80	279.99	343.08	350.92
<i>FAR</i>	0.00175854	0.00187392	0.00012313	0.00043158	0.00041777	0.00001206
<i>FAR</i>₂₃₄	0.00879061	0.00671368	0.00373121	0.01165212	0.00577221	0.00398024
(<i>c,d</i>)	(79,96)	(159,190)	(401,490)	(74,96)	(152,190)	(382,490)
IC <i>ARL</i>	207.78	155.81	328.27	247.96	273.57	347.39
<i>FAR</i>	0.00409341	0.00514267	0.00038085	0.00123317	0.00152033	0.00004721
<i>FAR</i>₂₃₄	0.01069985	0.00951387	0.00393757	0.01225836	0.00669983	0.00400990
(<i>c,d</i>)	(79,94)	(159,185)	(401,485)	(74,94)	(152,185)	(382,485)
IC <i>ARL</i>	145.84	96.04	295.51	206.18	191.94	339.70
<i>FAR</i>	0.00779507	0.01072807	0.00078110	0.00276654	0.00391215	0.00012126
<i>FAR</i>₂₃₄	0.01376099	0.01435966	0.00430221	0.01342680	0.00872557	0.00407739
(<i>c,d</i>)	(79,92)	(159,180)	(401,480)	(74,92)	(152,180)	(382,480)
IC <i>ARL</i>	100.22	59.64	256.55	162.04	123.96	326.30
<i>FAR</i>	0.01309294	0.01906042	0.00142281	0.00532072	0.00819766	0.00028059
<i>FAR</i>₂₃₄	0.01820764	0.02172273	0.00486596	0.01539354	0.01239459	0.00420459
(<i>c,d</i>)	(79,90)	(159,175)	(401,475)	(74,90)	(152,175)	(382,475)
IC <i>ARL</i>	68.99	38.42	216.28	121.91	77.72	306.46
<i>FAR</i>	0.02017518	0.03046625	0.00233323	0.00919351	0.01498703	0.00049152
<i>FAR</i>₂₃₄	0.02426358	0.03205126	0.00566744	0.01841729	0.01830187	0.00441737
(<i>c,d</i>)	(79,88)	(159,170)	(401,470)	(74,88)	(152,170)	(382,470)
IC <i>ARL</i>	48.25	25.86	178.61	89.14	49.18	280.67
<i>FAR</i>	0.02919065	0.04517478	0.00355142	0.01467797	0.02485491	0.00089128
<i>FAR</i>₂₃₄	0.03214747	0.04578421	0.00674304	0.02277628	0.02708197	0.00474463
(<i>c,d</i>)	(79,86)	(159,165)	(401,465)	(74,86)	(152,165)	(382,465)

Table 5.3: Unconditional IC *ARL*, unconditional *FAR* at time 1, 2 and 3,4,5... respectively and the charting constants (*c,d*) for the upper one-sided improved 2-of-3 nonparametric chart for $m = 100, 200, 500$ and $(n,j)=(5,3),(7,4)$.

	$n=5, j=3$			$n=7, j=4$		
	$m=100$	$m=200$	$m=500$	$m=100$	$m=200$	$m=500$
IC <i>ARL</i>	375.52	381.94	363.52	411.00	376.14	361.49
<i>FAR1</i>	0.00005334	0.00000706	0.00000050	0.00000678	0.00000047	0.00000001
<i>FAR2</i>	0.00475813	0.00273040	0.00197355	0.00581425	0.00321304	0.00211750
<i>FAR345</i>	0.00857053	0.00510493	0.00375400	0.01033252	0.00596127	0.00401624
(<i>c,d</i>)	(81,100)	(164,200)	(412,500)	(77,100)	(156,200)	(393,500)
IC <i>ARL</i>	338.19	345.57	360.74	400.34	370.17	361.32
<i>FAR1</i>	0.00051782	0.00038136	0.00002713	0.00009703	0.00005590	0.00000167
<i>FAR2</i>	0.00514999	0.00306232	0.00199661	0.00588790	0.00326143	0.00211895
<i>FAR345</i>	0.00890389	0.00540012	0.00377491	0.01039343	0.00600366	0.00401753
(<i>c,d</i>)	(81,98)	(164,195)	(412,495)	(77,98)	(156,195)	(393,495)
IC <i>ARL</i>	274.41	257.02	349.96	369.79	337.95	360.18
<i>FAR1</i>	0.00175854	0.00187392	0.00012308	0.00043158	0.00041777	0.00001174
<i>FAR2</i>	0.00620188	0.00439138	0.00147987	0.00616174	0.00357775	0.00212855
<i>FAR345</i>	0.00980350	0.00658673	0.00386081	0.01062060	0.00628133	0.00402623
(<i>c,d</i>)	(81,96)	(164,190)	(412,490)	(77,96)	(156,190)	(393,490)
IC <i>ARL</i>	205.20	165.48	328.34	318.77	271.88	356.60
<i>FAR1</i>	0.00409341	0.00514267	0.00038084	0.00123317	0.00152033	0.00004703
<i>FAR2</i>	0.00819648	0.00732316	0.00230506	0.00682091	0.00454512	0.00215932
<i>FAR345</i>	0.01152340	0.00922503	0.00405527	0.01117011	0.00713328	0.00405405
(<i>c,d</i>)	(81,94)	(164,185)	(412,485)	(77,94)	(156,185)	(393,485)
IC <i>ARL</i>	145.82	100.87	296.68	256.43	192.94	348.81
<i>FAR1</i>	0.00779507	0.01072807	0.00078122	0.00276654	0.00391215	0.00012130
<i>FAR2</i>	0.01139276	0.01239353	0.00268312	0.00809038	0.00665666	0.00222954
<i>FAR345</i>	0.01431125	0.01384659	0.00439933	0.01223604	0.00900565	0.00411752
(<i>c,d</i>)	(81,92)	(164,180)	(412,480)	(77,92)	(156,180)	(393,480)
IC <i>ARL</i>	101.26	61.98	258.70	194.59	125.88	335.21
<i>FAR1</i>	0.01309294	0.01906042	0.00142281	0.00532072	0.00819766	0.00028072
<i>FAR2</i>	0.01603250	0.02009117	0.00326737	0.01022504	0.01047909	0.00236197
<i>FAR345</i>	0.01841853	0.02099078	0.00493190	0.01404651	0.01243255	0.00423734
(<i>c,d</i>)	(81,90)	(164,175)	(412,475)	(77,90)	(156,175)	(393,475)
IC <i>ARL</i>	70.18	39.46	219.08	141.53	79.38	315.05
<i>FAR1</i>	0.02017518	0.03046624	0.00233302	0.00919351	0.01498703	0.00049145
<i>FAR2</i>	0.02234616	0.03087704	0.00409792	0.01350283	0.01662884	0.00258325
<i>FAR345</i>	0.02410957	0.03123572	0.00569006	0.01686358	0.01803541	0.00443770
(<i>c,d</i>)	(81,88)	(164,170)	(412,470)	(77,88)	(156,170)	(393,470)
IC <i>ARL</i>	49.21	26.19	181.68	100.38	50.25	288.78
<i>FAR1</i>	0.02919065	0.04517478	0.00355148	0.01467796	0.02485491	0.00089118
<i>FAR2</i>	0.03055755	0.04519885	0.00521257	0.01822056	0.02576048	0.00292356
<i>FAR345</i>	0.03166874	0.04521988	0.00671165	0.02098636	0.02653684	0.00474606
(<i>c,d</i>)	(81,86)	(164,165)	(412,465)	(77,86)	(156,165)	(393,465)

Remark 5.2

The precedence statistic is a discrete statistic as the sign statistic i.e. the precedence statistic can only assume a finite number of possible values. Consequently the precedence chart can only assume a finite number of possible $UARL$ and unconditional false alarm rate ($UFAR$) combinations for a choice of m and n . The possible $UARL$ and $UFAR$ combinations increases as m and n increases.

Example 5.1

An example is presented to illustrate the application of the precedence charts. An upper one-sided *improved 2-of-2* precedence chart and an upper one-sided *improved 2-of-3* precedence chart are presented in this example.

In this example the inside diameter measurements of forged automobile engine piston rings are monitored. The IC Phase I reference sample consisting of twenty-five samples of size five each (i.e. a total of 125 observations) given on p.223 in Table 5.3 of Montgomery (2005).

In order to apply the precedence charts the charting constants are required, Table 5.4 is given to aid in choosing appropriate charting constants.

Table 5.4: Unconditional characteristics of the upper one-sided *improved 2-of-2* precedence chart and upper one-sided *improved 2-of-3* precedence chart when $m=125$, $n=5$ and $j=3$.

<i>I2-of-2(U)</i>					<i>I2-of-3(U)</i>					
c	d	ARL_0	$FAR1$	$FAR234$	c	d	ARL_0	$FAR1$	$FAR2$	$FAR345$
99	125	373.382	0.000028	0.006433	102	125	402.5662	0.000028	0.003667	0.006721
99	124	365.0477	0.000110	0.006500	102	124	393.1183	0.000110	0.003738	0.006783
99	123	350.6366	0.000273	0.006637	102	123	376.9063	0.000273	0.003879	0.006905
99	122	330.4585	0.000539	0.006854	102	122	354.3849	0.000539	0.004109	0.007105
99	121	305.6776	0.000933	0.007178	102	121	326.9381	0.000933	0.004450	0.007403

When constructing a control chart one typically require the chart to have a large unconditional IC ARL . From Table 5.4 it can be seen that to obtain an ARL_0 (unconditional) of 350.64 for the upper one-sided *improved 2-of-2* chart, charting constants $c=99$ and $d=123$ need to be selected. Therefore in order to obtain an ARL_0 (unconditional) of 350.64 one need choose the inner and the outer upper control limits to be the 99th and the 123rd order statistics from the Phase I reference sample of size 125 respectively. Similarly for the upper one-sided *improved 2-of-3* chart, the 102nd and the 122nd order

statistics from the phase I reference sample of size 125 need to be selected as the inner and the outer upper control limits respectively, to obtain an ARL_0 (unconditional) of 354.38.

The control limits for the upper one-sided *improved 2-of-2* precedence chart are given by:

$$\hat{UCL}_A = X_{99:125} = 74.009 \text{ and } \hat{UCL}_B = X_{123:125} = 74.021$$

The control limits for the upper one-sided *improved 2-of-3* precedence chart are given by:

$$\hat{UCL}_A = X_{102:125} = 74.010 \text{ and } \hat{UCL}_B = X_{122:125} = 74.020$$

The upper one-sided *improved 2-of-2* and the upper one-sided *improved 2-of-3* precedence charts are presented in Figures 5.2 and 5.3 respectively. The 15 samples from Phase II of size five each is given on p.250 under exercise 5.10 of Montgomery (2005).

A plot of the medians is presented in Figures 5.2 and 5.3. The first 25 medians are from the IC phase I reference sample. The last 15 medians are from Phase II monitoring. Considering Figure 5.2 the upper one-sided *improved 2-of-2* precedence chart detects the first signal at sample number 35 since two consecutive plotting statistics plotted on or above the UCL_A . Considering Figure 5.3 the upper one-sided *improved 2-of-3* chart detects the first signal at sample number 35 since two of the last three plotting statistics plotted on or above the UCL_A .

Note that for the upper one-sided *2-of-2* precedence chart the chart will signal at sample number 35 since two consecutive plotting statistics plotted on or above the UCL_A / UCL . Note that for the upper one-sided *2-of-3* precedence chart the chart will signal at sample number 35 since two of the last three plotting statistics plotted on or above the UCL_A / UCL . For illustration purposes assume that the one-sided *1-of-1* precedence chart control limit is equal to UCL_A / UCL in Figure 5.2 (Figure 5.3), then the chart would signal at the 20th (26th) sample since a single plotting statistics plotted on or above the UCL_A / UCL .

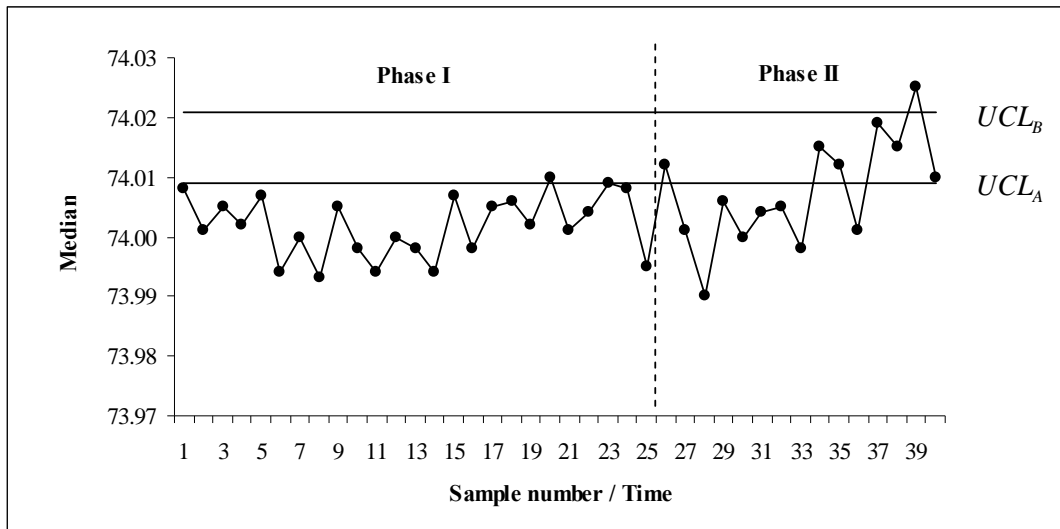


Figure 5.2: The upper one-sided *improved 2-of-2* precedence chart for the Montgomery (2005) piston-ring data.

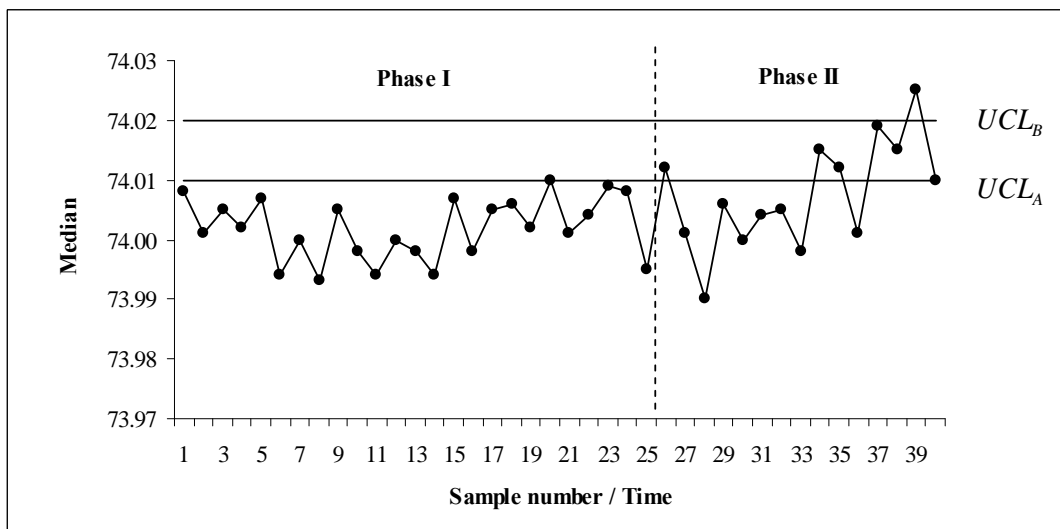


Figure 5.3: The upper one-sided *improved 2-of-3* precedence chart for the Montgomery (2005) piston-ring data.

The example illustrates that the application of the *improved runs-rules* precedence charts are quite simple. The challenge is to determine appropriate charting constants so that the chart has desirable properties.

5.6 Performance of the *improved* runs-rules precedence charts

Improved runs-rules are introduced to address a shortcoming of the runs-rules charts, namely the inability to detect large shifts quickly. Performance comparisons between the upper one-sided *2-of-2* precedence chart and the upper one-sided *improved 2-of-2* precedence chart is done. Performance comparisons are also made between the upper one-sided *2-of-3* precedence chart and the upper one-sided *improved 2-of-3* precedence chart.

The performance comparisons between the *improved* runs-rules precedence charts and the runs-rules precedence charts are done by considering the Normal (symmetric distribution), Students-*t* (symmetric with heavy tails) and Exponential (skew) distribution as the underlying process distribution as illustrated in Figure 5.4. It will be shown in the performance analysis that the *improved* runs-rules precedence charts do not perform equally well for all underlying process distributions.

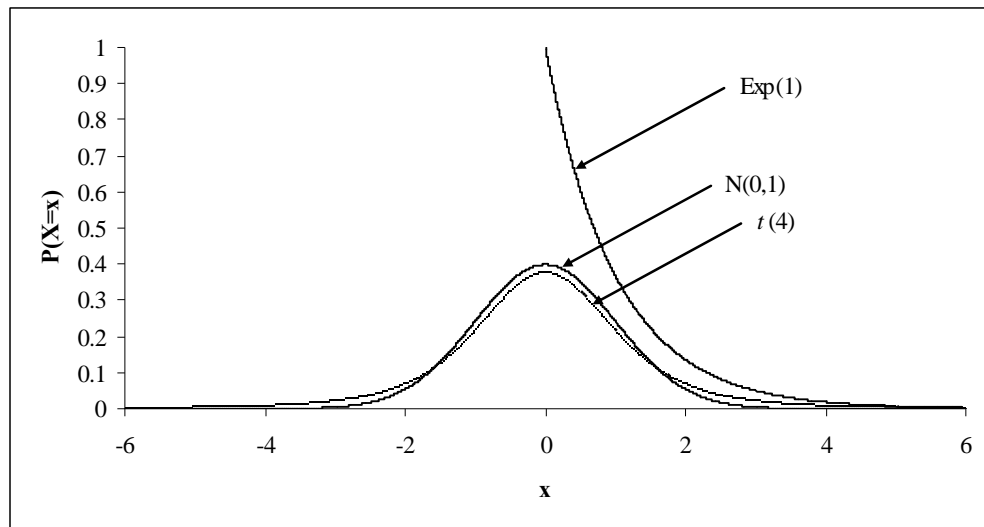


Figure 5.4: Different underlying process distributions that are used to perform performance comparisons.

5.6.1 Discussion on the performance analysis Tables

Refer to Table 5.5 to clarify the notation used in Tables 5.6 to 5.11.

Table 5.5: Description of notation used in Tables 5.6 to 5.11.

Notation	Description
$N(0,1)$	Standard Normal underlying process distribution.
$t(4)$	Students $t(4)$ underlying process distribution.
$Exp(1)$	Exponential ($\theta = 1$) underlying process distribution.
<i>Shift</i> (σ Units)	Shift in the underlying process distribution in standard deviation units.
2-of-2 (U)	Upper one-sided 2-of-2 runs-rules precedence chart.
I2-of-2 (U)	Upper one-sided <i>improved</i> 2-of-2 runs-rules precedence chart.
2-of-3 (U)	Upper one-sided 2-of-3 runs-rules precedence chart.
I2-of-3 (U)	Upper one-sided <i>improved</i> 2-of-3 runs-rules precedence chart.
ARL	Unconditional average run-length.
IQR	Unconditional inter quartile range of the run-length.
5 th	Unconditional 5 th percentile of the run-length distribution.
Q_1	Unconditional 25 th percentile (first quartile) of the run-length distribution.
MDRL	Unconditional 50 th percentile (median) of the run-length distribution.
Q_3	Unconditional 75 th percentile (third quartile) of the run-length distribution.
95 th	Unconditional 95 th percentile of the run-length distribution.

To illustrate the use of Tables 5.6 to 5.11 consider the following situation. A process is monitored using an upper one-sided 2-of-2 runs-rules precedence chart and the underlying process distribution is $t(4)$ distributed. A comparison needs to be done between the upper one-sided 2-of-2 runs-rules precedence chart and the upper one-sided *improved* 2-of-2 runs-rules precedence chart. This can be done by considering Table 5.8.

From the first row of Table 5.8 it can be seen that the reference sample size is 500 ($m = 500$), the test sample size is 7 ($n = 7$), the control limits are $UCL_A = 382$ and $UCL_B = 490$. From the caption it can be seen that the underlying process distribution is $t(4)$. From the third row it can be seen that the first column contains the shift in the underlying process distribution (in standard deviation units). Still considering the third row it can be seen that columns two to eight (nine to fifteen) contains the

characteristics of the upper one-sided runs-rules precedence chart (upper one-sided *improved* runs-rules precedence chart). Refer to Table 5.5 for clarity on the notation.

The observation can be made that when the process is IC, that the IC *ARL* for the upper one-sided runs-rules precedence chart and the upper one-sided *improved* runs-rules precedence chart is 350.83 and 351.52 respectively. Since the IC *ARL* is the same or approximately so, OOC performance analysis is meaningful.

Consider an upward shift in the process of a 0.25 standard deviation units (σ unit shift = 0.25), then the OOC *ARL* is 36.84 and 36.72 for the upper one-sided runs-rules precedence chart and the upper one-sided *improved* runs-rules precedence chart respectively (note that the other characteristics are also similar or the same). From this the first claim is supported that the *improved* runs-rules precedence charts are as sensitive to small process shifts as the runs-rules precedence charts. Now consider an upward shift in the process of 4 standard deviation units (σ unit shift = 4), then the OOC *ARL* is 2 and 1.00 for the upper one-sided 2-of-2 runs-rules precedence chart and the upper one-sided *improved* 2-of-2 runs-rules precedence charts respectively. From this the second claim is supported that the *improved* runs-rules precedence charts detect larger shifts in the process more efficiently. The superiority of the *improved* runs-rules precedence charts in the presence of larger process shifts is also confirmed by the remaining characteristics.

From the performance analysis illustration between the upper one-sided 2-of-2 runs-rules precedence chart and the upper one-sided *improved* 2-of-2 runs-rules precedence chart in Table 5.8, the use of the performance analysis Tables (Tables 5.6 to 5.11) is established.

5.6.2 Discussion on the performance analysis results

Considering Tables 5.6 to 5.11 the following observations can be made regarding the performance comparison between the runs-rules and the *improved* runs-rules precedence charts:

- From Tables 5.6, 5.7 and 5.8 it can be seen that the upper one-sided *improved* 2-of-2 precedence chart is as sensitive to small process shifts compared to the upper one-sided 2-of-2 precedence chart, while having the ability to detect large process shifts more efficiently. However, for the *Exp*(1) distribution (for upward shifts) the upper one-sided *improved* 2-of-2 chart, that the OOC *ARL* seem to converge slower to one i.e. less efficient in the detection of large process shifts compared to the $t(4)$ and the $N(0,1)$ distributions.

- From Tables 5.9, 5.10 and 5.11 it can be seen that the upper one-sided *improved 2-of-3* precedence chart is as sensitive to small process shifts compared to the upper one-sided *2-of-3* precedence chart, while having the ability to detect large process shifts more efficiently. Note that for certain underlying distributions the upper one-sided *improved 2-of-3* precedence chart is able to detect large process shifts more efficient than for other distributions. The chart is less efficient in detecting large process shifts in the case of an upward shift when the underlying process distribution is $Exp(1)$. This can be seen in Table 5.9 in the *ARL* column (ninth column) when the shift increases the *ARL* does not converge as quickly to one as for the other distributions.

Remark 5.3

Note that Tables 5.6 to 5.11 are rich in information regarding the OOC performance for the runs-rules and the *improved* runs-rules precedence charts and can be a discussion topic on its own. However, in this dissertation the main concern is to confirm the two claims that the *improved* runs-rules precedence charts are superior in performance to the runs-rules precedence charts for large shifts in the process, while maintaining the same sensitivity in the detection of small shifts. These two claims are confirmed in the previous discussion.

The performance comparisons are presented in Tables 5.6-5.11. These results are obtained by means of computer simulation (250 000 repetitions) using proc IML in SAS[®]9.2.

Considering Tables 5.6-5.11 it can be seen that the *improved* runs-rules precedence charts are as sensitive to small process shifts compared to the runs-rules precedence charts while having the ability to detect large process shifts quickly.

Table 5.6: Unconditional characteristics of the upper one-sided 2-of-2 and the upper one-sided improved 2-of-2 precedence charts when the underlying process distribution is $Exp(1)$.

<i>Exp(1) Distribution (n=7, j=4, m=500, c=382, d=490)</i>														
σ Units	2-of-2 (U)							I2-of-2 (U)						
Shift	ARL	IQR	5 th	Q ₁	MDRL	Q ₃	95 th	ARL	IQR	5 th	Q ₁	MDRL	Q ₃	95 th
-0.05	491.41	511	20	112	284	623	1647	488.34	509	20	111	283	620	1636
0	351.28	363	15	82	205	445	1174	350.52	363	15	81	203	444	1170
0.25	73.98	76	4	19	45	95	240	74.17	77	4	19	45	96	241
0.5	18.95	18	2	6	12	24	58	18.94	18	2	6	12	24	58
0.75	6.33	6	2	2	4	8	17	6.33	6	2	2	4	8	17
1	2.97	2	2	2	2	4	6	2.98	2	2	2	2	4	6
1.25	2.10	0	2	2	2	2	3	2.10	0	2	2	2	2	3
1.5	2.00	0	2	2	2	2	2	2.00	0	2	2	2	2	2
1.75	2.00	0	2	2	2	2	2	1.99	0	2	2	2	2	2
2	2.00	0	2	2	2	2	2	1.98	0	2	2	2	2	2
2.25	2.00	0	2	2	2	2	2	1.95	0	1	2	2	2	2
2.5	2.00	0	2	2	2	2	2	1.89	0	1	2	2	2	2
2.75	2.00	0	2	2	2	2	2	1.78	0	1	2	2	2	2
3	2.00	0	2	2	2	2	2	1.62	1	1	1	2	2	2
3.25	2.00	0	2	2	2	2	2	1.40	1	1	1	1	2	2
3.5	2.00	0	2	2	2	2	2	1.21	0	1	1	1	1	2
3.75	2.00	0	2	2	2	2	2	1.08	0	1	1	1	1	2
4	2.00	0	2	2	2	2	2	1.02	0	1	1	1	1	1

Table 5.7: Unconditional characteristics of the upper one-sided 2-of-2 and the upper one-sided improved 2-of-2 precedence charts when the underlying process distribution is $N(0,1)$.

<i>N(0,1) Distribution (n=7, j=4, m=500, c=382, d=490)</i>														
σ Units	2-of-2 (U)							I2-of-2 (U)						
Shift	ARL	IQR	5 th	Q ₁	MDRL	Q ₃	95 th	ARL	IQR	5 th	Q ₁	MDRL	Q ₃	95 th
-0.05	550.30	570	22	124	315	694	1847	547.73	570	22	123	313	693	1852
0	352.38	365	15	81	205	446	1177	353.17	368	15	81	205	449	1177
0.25	53.10	56	4	14	34	70	167	52.75	55	4	14	33	69	167
0.5	13.62	13	2	5	9	18	40	13.53	13	2	5	9	18	39
0.75	5.58	5	2	2	4	7	14	5.53	5	2	2	4	7	14
1	3.27	2	2	2	2	4	7	3.21	2	2	2	2	4	7
1.25	2.44	0	2	2	2	2	4	2.37	0	2	2	2	2	4
1.5	2.14	0	2	2	2	2	3	1.99	0	1	2	2	2	3
1.75	2.04	0	2	2	2	2	2	1.75	1	1	1	2	2	2
2	2.01	0	2	2	2	2	2	1.53	1	1	1	2	2	2
2.25	2.00	0	2	2	2	2	2	1.32	1	1	1	1	2	2
2.5	2.00	0	2	2	2	2	2	1.16	0	1	1	1	1	2
2.75	2.00	0	2	2	2	2	2	1.06	0	1	1	1	1	2
3	2.00	0	2	2	2	2	2	1.02	0	1	1	1	1	1
3.25	2.00	0	2	2	2	2	2	1.01	0	1	1	1	1	1
3.5	2.00	0	2	2	2	2	2	1.00	0	1	1	1	1	1
3.75	2.00	0	2	2	2	2	2	1.00	0	1	1	1	1	1
4	2.00	0	2	2	2	2	2	1.00	0	1	1	1	1	1

Table 5.8: Unconditional characteristics of the upper one-sided 2-of-2 and the upper one-sided improved 2-of-2 precedence charts when the underlying process distribution is $t(4)$.

$t(4)$ Distribution ($n=7, j=4, m=500, c=382, d=490$)														
σ Units	2-of-2 (U)							I2-of-2 (U)						
Shift	ARL	IQR	5 th	Q ₁	MDRL	Q ₃	95 th	ARL	IQR	5 th	Q ₁	MDRL	Q ₃	95 th
-0.05	595.46	616	24	135	342	751	1997	590.72	617	24	133	340	750	1977
0	350.83	364	15	81	205	445	1168	351.52	367	15	81	206	448	1167
0.25	36.84	38	3	10	23	48	115	36.72	38	3	10	23	48	115
0.5	7.98	7	2	3	6	10	22	7.97	7	2	3	6	10	22
0.75	3.45	2	2	2	2	4	8	3.44	2	2	2	2	4	8
1	2.38	0	2	2	2	2	4	2.37	0	2	2	2	2	4
1.25	2.09	0	2	2	2	2	3	2.07	0	2	2	2	2	3
1.5	2.02	0	2	2	2	2	2	1.94	0	1	2	2	2	2
1.75	2.00	0	2	2	2	2	2	1.80	0	1	2	2	2	2
2	2.00	0	2	2	2	2	2	1.58	1	1	1	2	2	2
2.25	2.00	0	2	2	2	2	2	1.35	1	1	1	1	2	2
2.5	2.00	0	2	2	2	2	2	1.16	0	1	1	1	1	2
2.75	2.00	0	2	2	2	2	2	1.06	0	1	1	1	1	2
3	2.00	0	2	2	2	2	2	1.02	0	1	1	1	1	1
3.25	2.00	0	2	2	2	2	2	1.00	0	1	1	1	1	1
3.5	2.00	0	2	2	2	2	2	1.00	0	1	1	1	1	1
3.75	2.00	0	2	2	2	2	2	1.00	0	1	1	1	1	1
4	2.00	0	2	2	2	2	2	1.00	0	1	1	1	1	1

Table 5.9: Unconditional characteristics of the upper one-sided 2-of-3 and the upper one-sided improved 2-of-3 precedence charts when the underlying process distribution is $Exp(1)$.

$Exp(1)$ Distribution ($n=7, j=4, m=500, c=393, d=490$)														
σ Units	2-of-3 (U)							I2-of-3 (U)						
Shift	ARL	IQR	5 th	Q ₁	MDRL	Q ₃	95 th	ARL	IQR	5 th	Q ₁	MDRL	Q ₃	95 th
-0.05	502.92	516	21	112	284	628	1706	501.41	517	21	112	284	629	1704
0	361.74	370	16	82	206	452	1219	360.47	372	15	81	205	453	1207
0.25	76.05	77	5	19	45	96	250	76.22	78	5	19	45	97	250
0.5	19.86	19	3	6	13	25	61	19.82	19	3	6	13	25	61
0.75	6.80	5	2	3	5	8	18	6.80	5	2	3	5	8	19
1	3.24	2	2	2	3	4	7	3.24	2	2	2	3	4	7
1.25	2.21	0	2	2	2	2	3	2.20	0	2	2	2	2	3
1.5	2.01	0	2	2	2	2	2	2.00	0	2	2	2	2	2
1.75	2.00	0	2	2	2	2	2	1.99	0	2	2	2	2	2
2	2.00	0	2	2	2	2	2	1.98	0	2	2	2	2	2
2.25	2.00	0	2	2	2	2	2	1.95	0	1	2	2	2	2
2.5	2.00	0	2	2	2	2	2	1.89	0	1	2	2	2	2
2.75	2.00	0	2	2	2	2	2	1.78	0	1	2	2	2	2
3	2.00	0	2	2	2	2	2	1.61	1	1	1	2	2	2
3.25	2.00	0	2	2	2	2	2	1.40	1	1	1	1	2	2
3.5	2.00	0	2	2	2	2	2	1.21	0	1	1	1	1	2
3.75	2.00	0	2	2	2	2	2	1.08	0	1	1	1	1	2
4	2.00	0	2	2	2	2	2	1.02	0	1	1	1	1	1

Table 5.10: Unconditional characteristics of the upper one-sided 2-of-3 and the upper one-sided improved 2-of-3 precedence charts when the underlying process distribution is $N(0,1)$.

$N(0,1)$ Distribution ($n=7, j=4, m=500, c=393, d=490$)														
σ Units	2-of-3 (U)							I2-of-3 (U)						
Shift	ARL	IQR	5 th	Q_1	MDRL	Q_3	95 th	ARL	IQR	5 th	Q_1	MDRL	Q_3	95 th
-0.05	576.04	590	23	125	322	715	1968	573.88	584	23	125	318	709	1956
0	360.60	371	15	81	205	452	1222	359.92	369	15	81	204	450	1216
0.25	50.64	52	4	14	32	66	160	50.27	51	4	14	32	65	159
0.5	12.70	13	2	4	9	17	36	12.63	12	2	4	9	16	36
0.75	5.27	4	2	3	4	7	13	5.24	4	2	3	4	7	13
1	3.15	1	2	2	3	3	7	3.11	1	2	2	3	3	6
1.25	2.41	1	2	2	2	3	4	2.34	1	1	2	2	3	4
1.5	2.14	0	2	2	2	2	3	1.99	0	1	2	2	2	3
1.75	2.04	0	2	2	2	2	2	1.75	1	1	1	2	2	2
2	2.01	0	2	2	2	2	2	1.53	1	1	1	2	2	2
2.25	2.00	0	2	2	2	2	2	1.32	1	1	1	1	2	2
2.5	2.00	0	2	2	2	2	2	1.16	0	1	1	1	1	2
2.75	2.00	0	2	2	2	2	2	1.07	0	1	1	1	1	2
3	2.00	0	2	2	2	2	2	1.02	0	1	1	1	1	1
3.25	2.00	0	2	2	2	2	2	1.01	0	1	1	1	1	1
3.5	2.00	0	2	2	2	2	2	1.00	0	1	1	1	1	1
3.75	2.00	0	2	2	2	2	2	1.00	0	1	1	1	1	1
4	2.00	0	2	2	2	2	2	1.00	0	1	1	1	1	1

Table 5.11: Unconditional characteristics of the upper one-sided 2-of-3 and the upper one-sided improved 2-of-3 precedence charts when the underlying process distribution is $t(4)$.

$t(4)$ Distribution ($n=7, j=4, m=500, c=393, d=490$)														
σ Units	2-of-3 (U)							I2-of-3 (U)						
Shift	ARL	IQR	5 th	Q_1	MDRL	Q_3	95 th	ARL	IQR	5 th	Q_1	MDRL	Q_3	95 th
-0.05	616.18	633	24	135	346	768	2093	613.74	629	24	134	343	763	2086
0	361.53	374	16	81	206	455	1220	360.87	370	15	82	206	452	1215
0.25	36.19	37	3	10	23	47	114	35.88	36	3	10	23	46	112
0.5	7.71	7	2	3	6	10	21	7.72	7	2	3	6	10	21
0.75	3.37	2	2	2	3	4	7	3.37	2	2	2	3	4	7
1	2.36	1	2	2	2	3	4	2.35	1	2	2	2	3	4
1.25	2.09	0	2	2	2	2	3	2.07	0	2	2	2	2	3
1.5	2.02	0	2	2	2	2	2	1.94	0	1	2	2	2	2
1.75	2.00	0	2	2	2	2	2	1.80	0	1	2	2	2	2
2	2.00	0	2	2	2	2	2	1.58	1	1	1	2	2	2
2.25	2.00	0	2	2	2	2	2	1.35	1	1	1	1	2	2
2.5	2.00	0	2	2	2	2	2	1.16	0	1	1	1	1	2
2.75	2.00	0	2	2	2	2	2	1.06	0	1	1	1	1	2
3	2.00	0	2	2	2	2	2	1.02	0	1	1	1	1	1
3.25	2.00	0	2	2	2	2	2	1.00	0	1	1	1	1	1
3.5	2.00	0	2	2	2	2	2	1.00	0	1	1	1	1	1
3.75	2.00	0	2	2	2	2	2	1.00	0	1	1	1	1	1
4	2.00	0	2	2	2	2	2	1.00	0	1	1	1	1	1

Remark 5.4

Note that in order to perform the performance analysis on the precedence charts; a sufficiently large reference sample size is required, so that there exist an outer set of control limits that has an absolute minimal influence on the IC *UARL* of the *improved* runs-rules precedence charts. This is done so that the IC *UARL* for both the runs-rules and the *improved* runs-rules precedence charts are almost exactly the same by choosing the inner set of control limits of the *improved* runs-rules charts and the control limits of the runs-rules charts the same. Consequently the reference sample size is chosen to be 500 in the performance analysis for the upper one-sided *improved 2-of-2* runs-rules precedence charts and the upper one-sided *improved 2-of-3* runs-rules precedence charts.

Remark 5.5

Note that in Chapter 4 for the *improved* runs-rules sign charts it is required that the sample size should be sufficiently large. The sample size needs to be at least 9 for the one-sided *improved 2-of-2* and the *improved 2-of-3* sign charts and at least 10 for the two-sided *improved 2-of-2* and the *improved 2-of-3* sign charts so that practically usable *ARL* and *FAR* combinations are obtained. However, for the *improved* runs-rules precedence charts the test sample size can be relatively small provided that the reference sample size is large. Note that in the *improved* runs-rules precedence charts performance analysis (Tables 5.6 to 5.11) the test sample was of size seven ($n = 7$).

5.7 Final comments regarding the *improved* runs-rules precedence charts

From the performance analysis it can be concluded that the *improved* runs-rules precedence charts are as sensitive to small shifts as the runs-rules precedence charts, while they have the ability to detect large shifts more efficiently. It is shown that the *improved* runs-rules charts are superior in performance for large shifts, while maintaining the same sensitivity in the detection of small shifts. Consequently, the *improved* runs-rules precedence charts are superior compared to runs-rules precedence charts.

However, the *improved* runs-rules precedence charts do have a practical limitation, they are more complex than the runs-rules precedence charts. Note that for the sacrifice in some simplicity there are rewards in the performance of the chart.

Summary of the strengths and the limitations of the *improved* runs-rules precedence charts:

Strengths:

- Do not require a specified underlying process distribution (nonparametric),
- Can monitor any desirable percentile,
- The percentile of the underlying process distribution that is monitored need not be known or specified,
- Do not require the variance of the process to be established,
- It is possible to apply the precedence chart as soon as the necessary order statistics are available, which is an advantage in applications where the observations are observed in ascending or descending order,
- Are sensitive to small process shifts as the runs-rules precedence charts, and
- Superior in the detection of large process shifts.

Limitations:

- The *improved* runs-rules precedence charts are more complex.

5.8 Summary of Chapter 5

The *improved* runs-rules are introduced to the precedence charts in Chapter 5. The run-length distribution and some characteristics of the run-length distribution of the *improved* runs-rules precedence charts are derived using a Markov chain approach combined with a conditioning by expectation approach. Performance analysis is carried out to illustrate that the *improved* runs-rules precedence charts are superior in performance to the runs-rules precedence charts for large shifts, while maintaining the same sensitivity in the detection of small shifts.

5.9 Following chapter

Chapter 6 provides some concluding remarks.

Chapter 6

Concluding remarks

This mini dissertation introduced the *improved* runs-rules to the sign and the precedence charts. Performance comparisons between the sign charts with runs-rules and the sign charts with *improved* runs-rules in Case K, illustrates that the *improved* runs-rules are superior in performance for large shifts, while maintaining the same sensitivity in the detection of small shifts. Similarly performance comparisons between the precedence charts with runs-rules and the precedence charts with *improved* runs-rules in Case U, illustrates that the *improved* runs-rules are superior in performance for large shifts, while maintaining the same sensitivity in the detection of small shifts.

A part of the research that is not the main focus of this dissertation and not reported here is related to the robustness of the EWMA control chart. A paper titled *Robustness of the EWMA control chart for individual observations* was written, submitted and was first published on the 24th of January 2011 in the *Journal of Applied Statistics*; the authors of the paper are Human, S.W., Kritzinger, P. and Chakraborti, S.

Currently a paper is being written on the *improved 2-of-2* sign chart. The intention is to submit the paper for publication very shortly. In the near future the goal is to write a paper on the *improved 2-of-2* precedence chart.

Note that Khoo and Ariffin introduced *improved* runs-rules to the \bar{X} control chart. *Improved* runs-rules are extended in this dissertation to the sign and precedence charts. In future the *improved* runs-rules can be considered for other nonparametric charts like the Shewhart-type signed-rank chart.

Appendix 1

Introduction

Appendix 1 is the appendix of Chapter 1. Only the variance of the plotting statistic of the EWMA control chart (given in equation (1.3) of Chapter 1) is derived in this appendix.

Proof 1.1 (Equation 1.3)

The exponentially weighted moving average is defined as:

$$T_i = \lambda X_i + (1 - \lambda)T_{i-1} \quad \text{where } 0 < \lambda \leq 1 \text{ and } T_0 = \mu_0 \quad (\text{A1.1})$$

Expanding the equation (A1.1) (exponentially weighted moving average):

$$\begin{aligned} T_i &= \lambda X_i + (1 - \lambda)T_{i-1} \\ &= \lambda X_i + (1 - \lambda)(\lambda X_{i-1} + (1 - \lambda)T_{i-2}) \\ &= \lambda X_i + \lambda(1 - \lambda)X_{i-1} + (1 - \lambda)^2 T_{i-2} \\ &= \lambda X_i + \lambda(1 - \lambda)X_{i-1} + (1 - \lambda)^2 (\lambda X_{i-2} + (1 - \lambda)T_{i-3}) \\ &= \lambda X_i + \lambda(1 - \lambda)X_{i-1} + \lambda(1 - \lambda)^2 X_{i-2} + (1 - \lambda)^3 T_{i-3} \\ &= \lambda X_i + \lambda(1 - \lambda)X_{i-1} + \lambda(1 - \lambda)^2 X_{i-2} + (1 - \lambda)^3 (\lambda X_{i-3} + (1 - \lambda)T_{i-4}) \\ &= \lambda X_i + \lambda(1 - \lambda)X_{i-1} + \lambda(1 - \lambda)^2 X_{i-2} + \lambda(1 - \lambda)^3 X_{i-3} + (1 - \lambda)^4 T_{i-4} \\ &\dots \\ &= \lambda \sum_{j=0}^{i-1} (1 - \lambda)^j X_{i-j} + (1 - \lambda)^i T_0 \end{aligned}$$

$$\text{i.e. } T_i = \lambda \sum_{j=0}^{i-1} (1 - \lambda)^j X_{i-j} + (1 - \lambda)^i T_0 \quad (\text{A1.2})$$

$$\begin{aligned}
 \text{Var}(T_i) &= \text{Var}\left(\lambda \sum_{j=0}^{i-1} (1-\lambda)^j X_{i-j} + (1-\lambda)^i T_0\right) && \text{since } (1-\lambda)^i T_0 \text{ is a constant} \\
 &= \text{Var}\left(\lambda \sum_{j=0}^{i-1} (1-\lambda)^j X_{i-j}\right) \\
 &= \lambda^2 \text{Var}\left(\sum_{j=0}^{i-1} (1-\lambda)^j X_{i-j}\right) \\
 &= \lambda^2 \left(\text{Var}(X_i + (1-\lambda)X_{i-1} + (1-\lambda)^2 X_{i-2} + \dots + (1-\lambda)^{i-2} X_2 + (1-\lambda)^{i-1} X_1)\right) \\
 &= \lambda^2 \left(\sigma^2 + (1-\lambda)^2 \sigma^2 + (1-\lambda)^4 \sigma^2 + \dots + (1-\lambda)^{2i-4} \sigma^2 + (1-\lambda)^{2i-2} \sigma^2\right) \\
 &= \lambda^2 \sigma^2 \left(1 + (1-\lambda)^2 + (1-\lambda)^4 + \dots + (1-\lambda)^{2i-4} + (1-\lambda)^{2i-2}\right) \\
 \text{i.e. } \text{Var}(T_i) &= \lambda^2 \sigma^2 \left(1 + (1-\lambda)^2 + (1-\lambda)^4 + \dots + (1-\lambda)^{2i-4} + (1-\lambda)^{2i-2}\right) && \text{(A1.3)}
 \end{aligned}$$

Recall the following formulae:

$$\text{If } S_n = a + ar + ar^2 + \dots + ar^{n-1}$$

$$\text{Then } S_n = a \frac{(1-r^n)}{1-r}, \quad r \neq 1$$

(A1.4)

Substituting (A1.3) into (A1.4) the following is obtained:

$$\begin{aligned}
 \text{Var}(T_i) &= \lambda^2 \sigma^2 \left(\frac{1 - (1-\lambda)^{2i}}{1 - (1-\lambda)^2}\right) \\
 &= \lambda^2 \sigma^2 \left(\frac{1 - (1-\lambda)^{2i}}{2\lambda - \lambda^2}\right) \\
 &= \lambda \sigma^2 \left(\frac{1 - (1-\lambda)^{2i}}{2 - \lambda}\right) \\
 &= \sigma^2 \left(\frac{\lambda}{2 - \lambda}\right) (1 - (1-\lambda)^{2i})
 \end{aligned}$$

$$\text{i.e. } \text{Var}(T_i) = \sigma^2 \left(\frac{\lambda}{2 - \lambda}\right) (1 - (1-\lambda)^{2i})$$

(A1.5)

□

Appendix 2

Introduction

The proofs of the results and theorems given in Chapter 2 are provided in this appendix. Note that it is not necessary for the reader to read Appendix 2 in order to follow the flow of the dissertation. However, this appendix is a reference to the results.

Proof 2.1 (Result 2.1(i))

For a given j , (i) follows immediately from the multiplication of matrices. (Fu et al., 2002)

□

Proof 2.2 (Result 2.1(ii))

Let:

$$\mathbf{W}_j = \mathbf{I} + \mathbf{Q} + \mathbf{Q}^2 + \mathbf{Q}^3 + \dots + \mathbf{Q}^{j-1} \quad (\text{A2.1})$$

$$\mathbf{QW}_j = \mathbf{Q} + \mathbf{Q}^2 + \mathbf{Q}^3 + \mathbf{Q}^4 + \dots + \mathbf{Q}^j \quad (\text{A2.2})$$

$$\begin{aligned} ((\text{A2.1}) - (\text{A2.2})) : \mathbf{W}_j - \mathbf{QW}_j &= (\mathbf{I} + \mathbf{Q} + \mathbf{Q}^2 + \dots + \mathbf{Q}^{j-1}) - (\mathbf{Q} + \mathbf{Q}^2 + \dots + \mathbf{Q}^j) \\ \mathbf{W}_j(\mathbf{I} - \mathbf{Q}) &= \mathbf{I} - \mathbf{Q}^j \\ \therefore \mathbf{W}_j &= (\mathbf{I} - \mathbf{Q}^j)(\mathbf{I} - \mathbf{Q})^{-1} \quad \text{since } (\mathbf{I} - \mathbf{Q}) \text{ is invertible} \end{aligned}$$

Since all the elements of \mathbf{Q} lie in the interval $[0,1)$, it follows that $\lim_{j \rightarrow \infty} \mathbf{Q}^j = \mathbf{0}$.

$$\begin{aligned} \therefore \lim_{j \rightarrow \infty} \mathbf{W}_j &= \lim_{j \rightarrow \infty} (\mathbf{I} - \mathbf{Q}^j)(\mathbf{I} - \mathbf{Q})^{-1} \\ &= \left(\mathbf{I} - \left(\lim_{j \rightarrow \infty} \mathbf{Q}^j \right) \right) (\mathbf{I} - \mathbf{Q})^{-1} \\ &= (\mathbf{I} - (\mathbf{0}))(\mathbf{I} - \mathbf{Q})^{-1} \\ &= (\mathbf{I})(\mathbf{I} - \mathbf{Q})^{-1} \\ &= (\mathbf{I} - \mathbf{Q})^{-1} \end{aligned}$$

$$\therefore \mathbf{I} + \mathbf{Q} + \mathbf{Q}^2 + \mathbf{Q}^3 + \mathbf{Q}^4 + \dots = (\mathbf{I} - \mathbf{Q})^{-1}$$

$$\therefore \lim_{j \rightarrow \infty} \mathbf{W}_j = (\mathbf{I} - \mathbf{Q})^{-1} \quad (\text{A2.3})$$

□

Proof 2.5 (Theorem 2.1(ii))

It follows from the definition of a moment generating function (Definition 2.5.1 Bain & Engelhardt (1992)) that the random variable N has moment generating function:

$$\begin{aligned}
 M_N(t) &= E(e^{tN}) \\
 &= \sum_{n=1}^{\infty} e^{nt} P(N = n | Y_0 = \phi) \\
 &= \sum_{n=1}^{\infty} e^{nt} (P(N > n-1 | Y_0 = \phi) - P(N > n | Y_0 = \phi)) \\
 &= \left(\sum_{n=1}^{\infty} e^{nt} P(N > n-1 | Y_0 = \phi) \right) - \left(\sum_{n=1}^{\infty} e^{nt} P(N > n | Y_0 = \phi) \right) \\
 &= \left(\sum_{n=1}^{\infty} e^{nt} P(Y_{n-1} < \omega_{h+1} | Y_0 = \phi) \right) - \left(\sum_{n=1}^{\infty} e^{nt} P(Y_n < \omega_{h+1} | Y_0 = \phi) \right) \quad (\text{from A2.5}) \\
 &= \left(\sum_{n=1}^{\infty} e^{nt} \xi \mathbf{Q}^{n-1} \mathbf{1} \right) - \left(\sum_{n=1}^{\infty} e^{nt} \xi \mathbf{Q}^n \mathbf{1} \right) \quad (\text{from A2.4}) \\
 &= \xi \left(\sum_{n=1}^{\infty} e^{nt} \mathbf{Q}^{n-1} - \sum_{n=1}^{\infty} e^{nt} \mathbf{Q}^n \right) \mathbf{1} \\
 &= \xi (e^t \mathbf{I} + e^{2t} \mathbf{Q} + e^{3t} \mathbf{Q}^2 + \dots - e^t \mathbf{Q} - e^{2t} \mathbf{Q}^2 - e^{3t} \mathbf{Q}^3 - \dots) \mathbf{1} \\
 &= \xi (e^t \mathbf{Q} (e^t - 1) + e^{2t} \mathbf{Q}^2 (e^t - 1) + \dots) \mathbf{1} + \xi e^t \mathbf{I} \mathbf{1} \\
 &= (e^t - 1) \xi (e^t \mathbf{Q} + e^{2t} \mathbf{Q}^2 + \dots) \mathbf{1} + \xi e^t \mathbf{I} \mathbf{1} \\
 &= (e^t - 1) \xi (\mathbf{I} - \mathbf{I} + e^t \mathbf{Q} + e^{2t} \mathbf{Q}^2 + \dots) \mathbf{1} + \xi e^t \mathbf{I} \mathbf{1} \\
 &= (e^t - 1) \xi (\mathbf{I} + e^t \mathbf{Q} + e^{2t} \mathbf{Q}^2 + \dots) \mathbf{1} + \xi e^t \mathbf{I} \mathbf{1} - (e^t - 1) \xi \mathbf{I} \mathbf{1} \\
 &= (e^t - 1) \xi \left(\sum_{n=0}^{\infty} e^{nt} \mathbf{Q}^n \right) \mathbf{1} + e^t \xi \mathbf{I} \mathbf{1} - e^t \xi \mathbf{I} \mathbf{1} + \xi \mathbf{I} \mathbf{1} \\
 &= (e^t - 1) \xi \left(\sum_{n=0}^{\infty} e^{nt} \mathbf{Q}^n \right) \mathbf{1} + \xi \mathbf{I} \mathbf{1} \\
 &= (e^t - 1) \xi \left(\sum_{n=0}^{\infty} e^{nt} \mathbf{Q}^n \right) \mathbf{1} + \mathbf{1}
 \end{aligned}$$

From **Result 2.1(ii)** (A2.3) and the equation above it follows that:

$$M_N(t) = (e^t - 1) \xi (\mathbf{I} - e^t \mathbf{Q})^{-1} \mathbf{1} + \mathbf{1} \quad (\text{A2.7})$$

□

(Fu et al. (2002))

Proof 2.6 (Theorem 2.1(iii))

By differentiating the moment generating function (mgf) with respect to t and setting $t = 0$, the moments of the run-length random variable N can be found i.e.:

$$\frac{d}{dt} M_N(t) \Big|_{t=0} = M'_N(0) = E(N)$$

$$\frac{d^2}{dt^2} M_N(t) \Big|_{t=0} = M''_N(0) = E(N^2)$$

$$M_N(t) = (e^t - 1) \xi(\mathbf{I} - e^t \mathbf{Q})^{-1} \mathbf{1} + 1$$

$$\begin{aligned} M'_N(t) &= \frac{d}{dt} M_N(t) \\ &= (1)(e^t - 1) \xi(\mathbf{I} - e^t \mathbf{Q})^{-1} \mathbf{1} + (e^t - 1) \xi(-1)(\mathbf{I} - e^t \mathbf{Q})^{-2} (-e^t \mathbf{Q}) \mathbf{1} \\ &= e^t \xi(\mathbf{I} - e^t \mathbf{Q})^{-1} \mathbf{1} + (e^t - 1) \xi(\mathbf{I} - e^t \mathbf{Q})^{-2} (e^t \mathbf{Q}) \mathbf{1} \\ &= e^t \xi(\mathbf{I} - e^t \mathbf{Q})^{-1} \mathbf{1} + (e^{2t} - e^t) \xi(\mathbf{I} - e^t \mathbf{Q})^{-2} \mathbf{1} \end{aligned}$$

$$\begin{aligned} M''_N(t) &= \frac{d^2}{dt^2} M_N(t) \\ &= \frac{d}{dt} M'_N(t) \\ &= e^t \xi(\mathbf{I} - e^t \mathbf{Q})^{-1} \mathbf{1} + e^t \xi(-1)(\mathbf{I} - e^t \mathbf{Q})^{-2} (-e^t \mathbf{Q}) \mathbf{1} \\ &\quad + (1)(e^{2t} - e^t)' (e^{2t} 2 - e^t) \xi(\mathbf{I} - e^t \mathbf{Q})^{-2} \mathbf{Q} \mathbf{1} \\ &\quad + (e^{2t} - e^t) \xi(-2)(\mathbf{I} - e^t \mathbf{Q})^{-3} (-e^t \mathbf{Q}) \mathbf{Q} \mathbf{1} \\ &= e^t \xi(\mathbf{I} - e^t \mathbf{Q})^{-1} \mathbf{1} + e^{2t} \xi(\mathbf{I} - e^t \mathbf{Q})^{-2} \mathbf{Q} \mathbf{1} \\ &\quad + (2e^{2t} - e^t) \xi(\mathbf{I} - e^t \mathbf{Q})^{-2} \mathbf{Q} \mathbf{1} \\ &\quad + 2(e^{3t} - e^{2t}) \xi(\mathbf{I} - e^t \mathbf{Q})^{-3} \mathbf{Q}^2 \mathbf{1} \end{aligned}$$

$$\begin{aligned} M'_N(0) &= e^0 \xi(\mathbf{I} - e^0 \mathbf{Q})^{-1} \mathbf{1} + (e^{2(0)} - e^0) \xi(\mathbf{I} - e^0 \mathbf{Q})^{-2} \mathbf{Q} \mathbf{1} \\ &= 1 \xi(\mathbf{I} - \mathbf{1Q})^{-1} \mathbf{1} + (1 - 1) \xi(\mathbf{I} - \mathbf{1Q})^{-2} \mathbf{Q} \mathbf{1} \\ &= \xi(\mathbf{I} - \mathbf{Q})^{-1} \mathbf{1} + (0) \xi(\mathbf{I} - \mathbf{Q})^{-2} \mathbf{Q} \mathbf{1} \\ &= \xi(\mathbf{I} - \mathbf{Q})^{-1} \mathbf{1} \end{aligned}$$

$$\begin{aligned}
 M_N''(0) &= e^0 \xi (\mathbf{I} - e^0 \mathbf{Q})^{-1} \mathbf{1} + e^{2(0)} \xi (\mathbf{I} - e^0 \mathbf{Q})^{-2} \mathbf{Q} \mathbf{1} \\
 &\quad + (2e^{2(0)} - e^0) \xi (\mathbf{I} - e^0 \mathbf{Q})^{-2} \mathbf{Q} \mathbf{1} \\
 &\quad + 2(e^{3(0)} - e^{2(0)}) \xi (\mathbf{I} - e^0 \mathbf{Q})^{-3} \mathbf{Q}^2 \mathbf{1} \\
 &= 1 \xi (\mathbf{I} - \mathbf{1} \mathbf{Q})^{-1} \mathbf{1} + 1 \xi (\mathbf{I} - \mathbf{1} \mathbf{Q})^{-2} \mathbf{Q} \mathbf{1} \\
 &\quad + (2(1) - 1) \xi (\mathbf{I} - \mathbf{1} \mathbf{Q})^{-2} \mathbf{Q} \mathbf{1} \\
 &\quad + 2(1 - 1) \xi (\mathbf{I} - \mathbf{1} \mathbf{Q})^{-3} \mathbf{Q} \mathbf{1} \\
 &= \xi (\mathbf{I} - \mathbf{Q})^{-1} \mathbf{1} + \xi (\mathbf{I} - \mathbf{Q})^{-2} \mathbf{Q} \mathbf{1} + \xi (\mathbf{I} - \mathbf{Q})^{-2} \mathbf{Q} \mathbf{1} \\
 &= \xi (\mathbf{I} + (\mathbf{I} - \mathbf{Q})^{-1} \mathbf{Q} + (\mathbf{I} - \mathbf{Q})^{-1} \mathbf{Q}) (\mathbf{I} - \mathbf{Q})^{-1} \mathbf{1} \\
 &= \xi ((\mathbf{I} - \mathbf{Q}) \mathbf{I} + \mathbf{Q} + \mathbf{Q}) (\mathbf{I} - \mathbf{Q})^{-1} (\mathbf{I} - \mathbf{Q})^{-1} \mathbf{1} \\
 &= \xi (\mathbf{I} - \mathbf{Q} + \mathbf{Q} + \mathbf{Q}) (\mathbf{I} - \mathbf{Q})^{-2} \mathbf{1} \\
 &= \xi (\mathbf{I} + \mathbf{Q}) (\mathbf{I} - \mathbf{Q})^{-2} \mathbf{1}
 \end{aligned}$$

$$E(N) = M_N'(0) = \xi (\mathbf{I} - \mathbf{Q})^{-1} \mathbf{1} \quad (\text{A2.8})$$

$$E(N^2) = M_N''(0) = \xi (\mathbf{I} + \mathbf{Q}) (\mathbf{I} - \mathbf{Q})^{-2} \mathbf{1} \quad (\text{A2.9})$$

$$\begin{aligned}
 \text{Var}(N) &= E(N^2) - (E(N))^2 \\
 &= \xi (\mathbf{I} + \mathbf{Q}) (\mathbf{I} - \mathbf{Q})^{-2} \mathbf{1} - (\xi (\mathbf{I} - \mathbf{Q})^{-1} \mathbf{1})^2 \\
 \therefore \text{Var}(N) &= \xi (\mathbf{I} + \mathbf{Q}) (\mathbf{I} - \mathbf{Q})^{-2} \mathbf{1} - (\xi (\mathbf{I} - \mathbf{Q})^{-1} \mathbf{1})^2 \quad (\text{A2.10})
 \end{aligned}$$

$$\text{Stdv}(N) = \sqrt{\text{Var}(N)} = \sqrt{\xi (\mathbf{I} + \mathbf{Q}) (\mathbf{I} - \mathbf{Q})^{-2} \mathbf{1} - (\xi (\mathbf{I} - \mathbf{Q})^{-1} \mathbf{1})^2} \quad (\text{A2.11})$$

□

(Fu et al. (2002))

Proof 2.7 (Theorem 2.2(i))

It follows from the definition of the probability generating function or factorial moment generating function (Definition 2.5.2 Bain & Engelhardt (1992)) that the random variable N has probability generating function:

$$\begin{aligned}
G_N(t) &= E(t^N) \\
&= \sum_{n=1}^{\infty} t^n P(N = n | Y_0 = \phi) \\
&= \sum_{n=1}^{\infty} t^n (P(N > n-1 | Y_0 = \phi) - P(N > n | Y_0 = \phi)) \\
&= \left(\sum_{n=1}^{\infty} t^n P(N > n-1 | Y_0 = \phi) \right) - \left(\sum_{n=1}^{\infty} t^n P(N > n | Y_0 = \phi) \right) \\
&= \left(\sum_{n=1}^{\infty} t^n P(Y_{n-1} < \omega_{h+1} | Y_0 = \phi) \right) - \left(\sum_{n=1}^{\infty} t^n P(Y_n < \omega_{h+1} | Y_0 = \phi) \right) \text{ (from A2.5)} \\
&= \left(\sum_{n=1}^{\infty} t^n \xi \mathbf{Q}^{n-1} \mathbf{1} \right) - \left(\sum_{n=1}^{\infty} t^n \xi \mathbf{Q}^n \mathbf{1} \right) \text{ (from A2.4)} \\
&= \xi \left(\sum_{n=1}^{\infty} t^n \mathbf{Q}^{n-1} - \sum_{n=1}^{\infty} t^n \mathbf{Q}^n \right) \mathbf{1} \\
&= \xi \left((t\mathbf{I} + t^2\mathbf{Q} + t^3\mathbf{Q}^2 + \dots) - (t\mathbf{Q} + t^2\mathbf{Q}^2 + t^3\mathbf{Q}^3 + \dots) \right) \mathbf{1} \\
&= \xi (t\mathbf{Q}(t-1) + t^2\mathbf{Q}^2(t-1) + \dots) \mathbf{1} + \xi t \mathbf{I} \mathbf{1} \\
&= (t-1) \xi (t\mathbf{Q} + t^2\mathbf{Q}^2 + t^3\mathbf{Q}^3 \dots) \mathbf{1} + \xi t \mathbf{I} \mathbf{1} \\
&= (t-1) \xi (\mathbf{I} - \mathbf{I} + t\mathbf{Q} + t^2\mathbf{Q}^2 + \dots) \mathbf{1} + \xi t \mathbf{I} \mathbf{1} \\
&= (t-1) \xi (\mathbf{I} + t\mathbf{Q} + t^2\mathbf{Q}^2 + \dots) \mathbf{1} + \xi t \mathbf{I} \mathbf{1} - (t-1) \xi \mathbf{I} \mathbf{1} \\
&= (t-1) \xi \left(\sum_{n=0}^{\infty} t^n \mathbf{Q}^n \right) \mathbf{1} + t \xi \mathbf{I} \mathbf{1} - t \xi \mathbf{I} \mathbf{1} + \xi \mathbf{I} \mathbf{1} \\
&= (t-1) \xi \left(\sum_{n=0}^{\infty} t^n \mathbf{Q}^n \right) \mathbf{1} + \xi \mathbf{I} \mathbf{1} \\
&= (t-1) \xi \left(\sum_{n=0}^{\infty} t^n \mathbf{Q}^n \right) \mathbf{1} + 1
\end{aligned}$$

From **Result 2.1(ii)** (A2.3) and the equation above it follows that:

$$G_N(t) = (t-1) \xi (\mathbf{I} - t\mathbf{Q})^{-1} \mathbf{1} + 1 \tag{A2.12}$$

□

(Fu and Lou (2003), p.73)

Proof 2.8 (Theorem 2.2(ii))

$$\begin{aligned}
 G'_N(t) &= \frac{d}{dt} \left((t-1)\xi(\mathbf{I}-t\mathbf{Q})^{-1}\mathbf{1} + 1 \right) \\
 &= \xi(\mathbf{I}-t\mathbf{Q})^{-1}\mathbf{1} + (t-1)\xi(-1)(-\mathbf{Q})(\mathbf{I}-t\mathbf{Q})^{-2}\mathbf{1} \\
 &= \xi(\mathbf{I}-t\mathbf{Q})^{-1}\mathbf{1} + (t-1)\xi\mathbf{Q}(\mathbf{I}-t\mathbf{Q})^{-2}\mathbf{1}
 \end{aligned}$$

$$\begin{aligned}
 G''_N(t) &= \frac{d}{dt} G'_N(t) \\
 &= \frac{d}{dt} \left(\xi(\mathbf{I}-t\mathbf{Q})^{-1}\mathbf{1} + (t-1)\xi(-1)(-\mathbf{Q})(\mathbf{I}-t\mathbf{Q})^{-2}\mathbf{1} \right) \\
 &= \xi(-1)(-\mathbf{Q})(\mathbf{I}-t\mathbf{Q})^{-2}\mathbf{1} + \xi(-1)(-\mathbf{Q})(\mathbf{I}-t\mathbf{Q})^{-2}\mathbf{1} \\
 &\quad + (t-1)\xi(-1)(-2)(-\mathbf{Q})(-\mathbf{Q})(\mathbf{I}-t\mathbf{Q})^{-3}\mathbf{1} \\
 &= \xi\mathbf{Q}(\mathbf{I}-t\mathbf{Q})^{-2}\mathbf{1} + \xi\mathbf{Q}(\mathbf{I}-t\mathbf{Q})^{-2}\mathbf{1} + 2(t-1)\xi\mathbf{Q}^2(\mathbf{I}-t\mathbf{Q})^{-3}\mathbf{1}
 \end{aligned}$$

$$\begin{aligned}
 G'_N(1) &= \xi(\mathbf{I}-(1)\mathbf{Q})^{-1}\mathbf{1} + ((1)-1)\xi\mathbf{Q}(\mathbf{I}-(1)\mathbf{Q})^{-2}\mathbf{1} \\
 &= \xi(\mathbf{I}-\mathbf{Q})^{-1}\mathbf{1} + (0)\xi\mathbf{Q}(\mathbf{I}-\mathbf{Q})^{-2}\mathbf{1} \\
 &= \xi(\mathbf{I}-\mathbf{Q})^{-1}\mathbf{1}
 \end{aligned}$$

$$\begin{aligned}
 G''_N(1) &= \xi\mathbf{Q}(\mathbf{I}-(1)\mathbf{Q})^{-2}\mathbf{1} + \xi\mathbf{Q}(\mathbf{I}-(1)\mathbf{Q})^{-2}\mathbf{1} + 2((1)-1)\xi\mathbf{Q}^2(\mathbf{I}-(1)\mathbf{Q})^{-3}\mathbf{1} \\
 &= \xi\mathbf{Q}(\mathbf{I}-\mathbf{Q})^{-2}\mathbf{1} + \xi\mathbf{Q}(\mathbf{I}-\mathbf{Q})^{-2}\mathbf{1} + 2(0)\xi\mathbf{Q}(\mathbf{I}-\mathbf{Q})^{-3}\mathbf{1} \\
 &= 2\xi\mathbf{Q}(\mathbf{I}-\mathbf{Q})^{-2}\mathbf{1}
 \end{aligned}$$

From Theorem 2.5.4 of Bain & Engelhardt (1992) it follows that:

$$\begin{aligned}
 G'_N(1) &= E(N) \\
 G''_N(1) &= E(N(N-1)) = E(N^2 - N) = E(N^2) - E(N)
 \end{aligned}$$

From the above two equations it follows that:

$$\begin{aligned}
 E(N^2) &= (E(N^2) - E(N)) + E(N) \\
 &= G''_N(1) + G'_N(1)
 \end{aligned}$$

From the equations above the variance formulae are as follows:

$$\begin{aligned}
 \text{Var}(N) &= E(N^2) - (E(N))^2 \\
 &= E(N^2) - E(N) + E(N) - (E(N))^2 \\
 &= (E(N^2) - E(N)) + E(N) - (E(N))^2 \\
 &= G_N''(1) + G_N'(1) - (G_N'(1))^2
 \end{aligned}$$

$$\therefore E(N) = G_N'(1) = \xi(\mathbf{I} - \mathbf{Q})^{-1} \mathbf{1} \quad (\text{A2.13})$$

(Fu and Lou (2003), p.73)

$$\begin{aligned}
 E(N^2) &= G_N''(1) + G_N'(1) \\
 &= 2\xi \mathbf{Q}(\mathbf{I} - \mathbf{Q})^{-2} \mathbf{1} + \xi(\mathbf{I} - \mathbf{Q})^{-1} \mathbf{1} \\
 &= \xi(2\mathbf{Q}(\mathbf{I} - \mathbf{Q})^{-1} + \mathbf{I})(\mathbf{I} - \mathbf{Q})^{-1} \mathbf{1} \\
 &= \xi(\mathbf{I} + 2\mathbf{Q}(\mathbf{I} - \mathbf{Q})^{-1})(\mathbf{I} - \mathbf{Q})^{-1} \mathbf{1} \\
 &= \xi(\mathbf{I} + 2\mathbf{Q}(\mathbf{I} + \mathbf{Q} + \mathbf{Q}^2 + \mathbf{Q}^3 + \dots))(\mathbf{I} - \mathbf{Q})^{-1} \mathbf{1} \\
 &= \xi(\mathbf{I} + 2\mathbf{Q} + 2\mathbf{Q}^2 + 2\mathbf{Q}^3 + \dots)(\mathbf{I} - \mathbf{Q})^{-1} \mathbf{1} \\
 &= \xi(\mathbf{I} + \mathbf{Q} + \mathbf{Q}^2 + \mathbf{Q}^3 + \dots + \mathbf{Q} + \mathbf{Q}^2 + \mathbf{Q}^3 + \dots)(\mathbf{I} - \mathbf{Q})^{-1} \mathbf{1} \\
 &= \xi((\mathbf{I} + \mathbf{Q} + \mathbf{Q} + \mathbf{Q} + \dots) + \mathbf{Q}(\mathbf{I} + \mathbf{Q} + \mathbf{Q} + \mathbf{Q} + \dots))(\mathbf{I} - \mathbf{Q})^{-1} \mathbf{1} \\
 &= \xi((\mathbf{I} - \mathbf{Q})^{-1} + \mathbf{Q}(\mathbf{I} - \mathbf{Q})^{-1})(\mathbf{I} - \mathbf{Q})^{-1} \mathbf{1} \\
 &= \xi((\mathbf{I} + \mathbf{Q})(\mathbf{I} - \mathbf{Q})^{-1})(\mathbf{I} - \mathbf{Q})^{-1} \mathbf{1} \\
 &= \xi(\mathbf{I} + \mathbf{Q})(\mathbf{I} - \mathbf{Q})^{-2} \mathbf{1}
 \end{aligned}$$

$$\therefore E(N^2) = \xi(\mathbf{I} + \mathbf{Q})(\mathbf{I} - \mathbf{Q})^{-2} \mathbf{1} \quad (\text{A2.14})$$

$$\begin{aligned}
 \text{Var}(N) &= G_N''(1) + G_N'(1) - (G_N'(1))^2 \\
 &= (G_N''(1) + G_N'(1)) - (G_N'(1))^2 \\
 &= (E(N^2)) - (E(N))^2 \\
 &= \xi(\mathbf{I} + \mathbf{Q})(\mathbf{I} - \mathbf{Q})^{-2} \mathbf{1} - (\xi(\mathbf{I} - \mathbf{Q})^{-1} \mathbf{1})^2
 \end{aligned}$$

$$\therefore \text{Var}(N) = \xi(\mathbf{I} + \mathbf{Q})(\mathbf{I} - \mathbf{Q})^{-2} \mathbf{1} - (\xi(\mathbf{I} - \mathbf{Q})^{-1} \mathbf{1})^2 \quad (\text{A2.15})$$

$$\therefore \text{Stdv}(N) = \sqrt{\xi(\mathbf{I} + \mathbf{Q})(\mathbf{I} - \mathbf{Q})^{-2} \mathbf{1} - (\xi(\mathbf{I} - \mathbf{Q})^{-1} \mathbf{1})^2} \quad (\text{A2.16})$$

□

Proof 2.9 (Theorem 2.3(ii))

Consider equation (A2.4) from **Result 2.2**:

$$\begin{aligned} P(Y_j < \omega_{h+1} | Y_0 = \phi) &= P(N > j | Y_0 = \phi) \\ &= \xi \mathbf{Q}^j \mathbf{1}, \quad \forall j = 1, 2, 3, \dots \end{aligned} \tag{A2.4}$$

$$\therefore P(N > j | Y_0 = \phi) = \xi \mathbf{Q}^j \mathbf{1}, \quad \forall j = 1, 2, 3, \dots \tag{A2.17}$$

It is known that:

$$\begin{aligned} P(N \leq j | Y_0 = \phi) &= 1 - P(N > j | Y_0 = \phi) \\ &= 1 - \xi \mathbf{Q}^j \mathbf{1}, \quad \forall j = 1, 2, 3, \dots \end{aligned}$$

$$\therefore P(N \leq j | Y_0 = \phi) = 1 - \xi \mathbf{Q}^j \mathbf{1}, \quad \forall j = 1, 2, 3, \dots \tag{A2.18}$$

□

Appendix 5

Introduction

The proofs of the results and theorems given and utilized in Chapter 5 are provided in this appendix. Note that it is not necessary for the reader to read Appendix 5 in order to follow the flow of the dissertation. However, this appendix is a reference to the results.

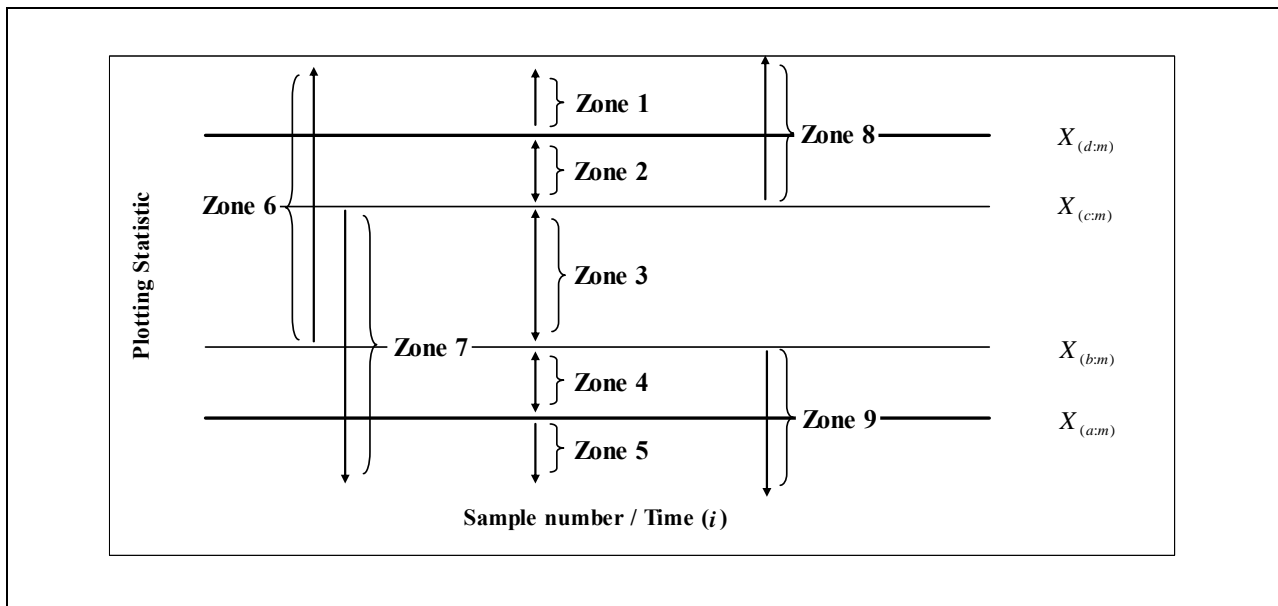


Figure A5.1: Illustration of control limits and zones on the precedence charts.

Recall that:

$$p_1 = P(Z_i = 1) = P(T_i \geq UCL_B) \quad (A5.1)$$

$$p_2 = P(Z_i = 2) = P(UCL_A \leq T_i < UCL_B) \quad (A5.2)$$

$$p_3 = P(Z_i = 3) = P(LCL_A / LCL < T_i < UCL_A / UCL) \quad (A5.3)$$

$$p_4 = P(Z_i = 4) = P(LCL_B < T_i \leq LCL_A) \quad (A5.4)$$

$$p_5 = P(Z_i = 5) = P(T_i \leq LCL_B) \quad (A5.5)$$

$$p_6 = P(Z_i = 6) = P(T_i > LCL_A / LCL) \quad (A5.6)$$

$$p_7 = P(Z_i = 7) = P(T_i < UCL_A / UCL) \quad (A5.7)$$

$$p_8 = P(Z_i = 8) = P(T_i \geq UCL) \quad (\text{A5.8})$$

$$p_9 = P(Z_i = 9) = P(T_i \leq LCL) \quad (\text{A5.9})$$

The estimated control limits from a Phase I reference sample are:

$$\hat{UCL}_B = X_{(d:m)} \quad (\text{A5.10})$$

$$\hat{UCL}_A / \hat{UCL} = X_{(c:m)} \quad (\text{A5.11})$$

$$\hat{LCL}_A / \hat{LCL} = X_{(b:m)} \quad (\text{A5.12})$$

$$\hat{LCL}_B = X_{(a:m)} \quad (\text{A5.13})$$

Let the conditional probabilities, conditioned on the estimated control limits from phase I be denoted by:

$$p_{1C} = P(Z_i = 1) = P(T_i \geq UCL_B / UCL_B = x_{(d:m)}) = P(T_i \geq x_{(d:m)})$$

$$p_{2C} = P(Z_i = 2) = P(UCL_A \leq T_i < UCL_B / UCL_A = x_{(c:m)}, UCL_B = x_{(d:m)}) \\ = P(x_{(c:m)} \leq T_i < x_{(d:m)})$$

$$p_{3C} = P(Z_i = 3) = P(LCL_A / LCL < T_i < UCL_A / UCL \mid LCL_A / LCL = x_{(b:m)}, UCL_A / UCL = x_{(c:m)}) \\ = P(x_{(b:m)} < T_i < x_{(c:m)})$$

$$p_{4C} = P(Z_i = 4) = P(LCL_B < T_i \leq LCL_A / LCL_B = x_{(a:m)}, LCL_A = x_{(b:m)}) \\ = P(x_{(a:m)} < T_i < x_{(b:m)})$$

$$p_{5C} = P(Z_i = 5) = P(T_i \leq LCL_B \mid LCL_B = x_{(a:m)}) = P(T_i \leq x_{(a:m)})$$

$$p_{6C} = P(Z_i = 6) = P(T_i > LCL_A / LCL \mid LCL_A / LCL = x_{(b:m)}) = P(T_i > x_{(b:m)})$$

$$p_{7C} = P(Z_i = 7) = P(T_i < UCL_A / UCL \mid UCL_A / UCL = x_{(c:m)}) = P(T_i < x_{(c:m)})$$

$$p_{8C} = P(Z_i = 8) = P(T_i \geq UCL \mid UCL = x_{(c:m)}) = P(T_i \geq x_{(c:m)})$$

$$p_{9C} = P(Z_i = 9) = P(T_i \leq LCL \mid LCL = x_{(b:m)}) = P(T_i \leq x_{(b:m)})$$

Result AR5.1 (Probability Integral Transformation (PIT))

If X is continuous with cdf $F_X(x)$, then

$$U = F_X(x) \sim UNIF(0,1)$$

Result AR5.2

Let $U_{(1:n)}, U_{(2:n)}, \dots, U_{(n:n)}$ be i.i.d. $UNIF(0,1)$ order statistics where $n > 0$, and let the $U_{(1:m)}, U_{(2:m)}, \dots, U_{(m:m)}$ be i.i.d. $UNIF(0,1)$ order statistics where $m > 0$, independent from the first set.

Then it follows from the Result A5.1 (PIT) that $X_{(i:m)} = F^{-1}(U_{(i:m)}) \forall i$ and $Y_{(j:n)} = G^{-1}(U_{(j:n)}) \forall j$ where $X_{(i:m)}$ and $Y_{(j:n)}$ denote the i^{th} and j^{th} order statistics from samples of size $m \geq 1$ and $n \geq 1$ with cdf's denoted by F and G respectively.

Result AR5.3

If $X \sim UNIF(0,1)$, then

$$f_X(x) = 1 \text{ and}$$

$$F_X(a) = a \text{ if } 0 < a < 1, \text{ and zero otherwise.}$$

Result AR5.4

Suppose that X_1, X_2, \dots, X_m denotes a random sample of size $m > 0$ from a continuous pdf, $f_X(x)$, where $f(x) > 0$ for $c_1 < x < c_2$ and cdf denoted by $F_X(x)$. Then the pdf of the a^{th} order statistic $X_{(a:m)}$ is given by

$$f_{X_{(a:m)}}(\theta) = \frac{m!}{(a-1)!(m-a)!} (F_X(\theta))^{a-1} (1 - F_X(\theta))^{m-a} f_X(\theta),$$

if $c_1 < \theta < c_2$, and zero otherwise.

(see e.g. Gibbons and Chakraborti (2003), p.48)

Result AR5.5

If X_1, X_2, \dots, X_m is a random sample of size $m > 0$ from a population with continuous pdf $f_X(x)$ and cdf $F_X(x)$, then the joint pdf of the order statistics $X_{(b:m)}$ and $X_{(c:m)}$, where $b < c$ is given by:

$$f_{X_{(b:m)}, X_{(c:m)}}(t, \kappa) = \frac{m!}{(b-1)!(c-b-1)!(m-c)!} (F_X(t))^{b-1} f_X(t) \\ \times (F_X(\kappa) - F_X(t))^{c-b-1} (1 - F_X(\kappa))^{m-c} f_X(\kappa)$$

(see e.g. Gibbons and Chakraborti (2003), p.48)

Result AR5.6

If X_1, X_2, \dots, X_m is a random sample of size $m > 0$ from a population with continuous pdf $f(x)$ and cdf $F_X(x)$, then the joint pdf of the order statistics $X_{(a:m)}, X_{(b:m)}, X_{(c:m)}$ and $X_{(d:m)}$ where $a < b < c < d$ is given by:

$$f_{X_{(a:m)}, X_{(b:m)}, X_{(c:m)}, X_{(d:m)}}(\theta, t, \kappa, \lambda) = \frac{m!}{(a-1)!(b-a-1)!(c-b-1)!(d-c-1)!(m-d)!} (F_X(\theta))^{a-1} \\ \times (F_X(t) - F_X(\theta))^{b-a-1} (F_X(\kappa) - F_X(t))^{c-b-1} \\ \times (F_X(\lambda) - F_X(\kappa))^{d-c-1} (1 - F_X(\lambda))^{m-d} \\ \times f_X(\theta) f_X(t) f_X(\kappa) f_X(\lambda)$$

(see e.g. Gibbons and Chakraborti (2003), p.50 for an explanation)

Result AR5.7

If X_1, X_2, \dots, X_m is a random sample of size $m > 0$ from a population with continuous pdf $f_X(x)$ and cdf $F_X(x)$, then the joint pdf of the order statistics $X_{(1:m)}, X_{(2:m)}, \dots, X_{(m:m)}$ is

$$f_{X_{(1:m)}, X_{(2:m)}, \dots, X_{(m:m)}}(c_1, c_2, \dots, c_m) = m! f_X(c_1) f_X(c_2) \dots f_X(c_m)$$

if $c_1 < c_2 < \dots < c_m$, and zero otherwise.

(see e.g. Bain and Engelhardt (1992), p.215)

Result AR5.8

Let U_1, U_2, \dots, U_m be a random sample of size $m > 0$ from a $UNIF(0,1)$ distribution with pdf and c.d.f denoted by $f_U(u) = 1$ and $F_U(u) = u$ respectively, then it follows from Results AR5.3 and AR5.4 that the pdf of the a^{th} order statistics $U_{(a:m)}$ and is given by:

$$\begin{aligned} f_{U_{(a:m)}}(\theta) &= \frac{m!}{(a-1)!(m-a)!} (F_U(\theta))^{a-1} (1-F_U(\theta))^{m-a} f_U(\theta) \\ &= \frac{m!}{(a-1)!(m-a)!} (\theta)^{a-1} (1-\theta)^{m-a} \end{aligned}$$

Result AR5.9

Let U_1, U_2, \dots, U_m be a random sample of size $m > 0$ from a $UNIF(0,1)$ distribution with pdf and c.d.f denoted by $f_U(u) = 1$ and $F_U(u) = u$ respectively, then it follows from Results AR5.3 and AR5.5 that the joint pdf of the b^{th} and c^{th} order statistics $U_{(b:m)} U_{(c:m)}$ where $b < c$ is given by:

$$\begin{aligned} f_{U_{(b:m)}, U_{(c:m)}}(t, \kappa) &= \frac{m!}{(b-1)!(c-b-1)!(m-c)!} (F_U(t))^{b-1} f_U(t) \\ &\quad \times (F_U(\kappa) - F_U(t))^{c-b-1} (1-F_U(\kappa))^{m-c} f_U(\kappa) \\ &= \frac{m!}{(b-1)!(c-b-1)!(m-c)!} (t)^{b-1} \\ &\quad \times (\kappa - t)^{c-b-1} (1-\kappa)^{m-c} \end{aligned}$$

Result AR5.10

Let U_1, U_2, \dots, U_m be a random sample of size $m > 0$ from a $UNIF(0,1)$ distribution with pdf and c.d.f denoted by $f_U(u) = 1$ and $F_U(u) = u$ respectively, then it follows from Results AR5.3 and AR5.6 that the joint pdf of the a^{th} , b^{th} , c^{th} and d^{th} order statistics $U_{(a:m)}$, $U_{(b:m)}$, $U_{(c:m)}$ and $U_{(d:m)}$ where $a < b < c < d$ is given by:

$$\begin{aligned} f_{U_{(a:m)}, U_{(b:m)}, U_{(c:m)}, U_{(d:m)}}(\theta, t, \kappa, \lambda) &= \frac{m!}{(a-1)!(b-a-1)!(c-b-1)!(d-c-1)!(m-d)!} (F_U(\theta))^{a-1} \\ &\quad \times (F_U(t) - F_U(\theta))^{b-a-1} (F_U(\kappa) - F_U(t))^{c-b-1} (F_U(\lambda) - F_U(\kappa))^{d-c-1} \\ &\quad \times (1 - F_U(\lambda))^{m-d} f_U(\theta) f_U(t) f_U(\kappa) f_U(\lambda) \\ &= \frac{m!}{(a-1)!(b-a-1)!(c-b-1)!(d-c-1)!(m-d)!} (\theta)^{a-1} \\ &\quad \times (t - \theta)^{b-a-1} (\kappa - t)^{c-b-1} (\lambda - \kappa)^{d-c-1} (1 - \lambda)^{m-d} \end{aligned}$$

Result AR5.11

The j^{th} order statistic from a sample size of $n > 0$ from an $UNIF(0,1)$ distribution follows a Beta distribution with parameters j and $n-j+1$.

$$I_p(j, n-j+1) = (\beta(j, n-j+1))^{-1} \int_0^p w^{j-1} (1-w)^{n-j} dw \quad \text{where: } j, n-j+1 > 0$$

is the cdf of the $Beta(j, n-j+1)$ distribution, also known as the incomplete beta function.

$$\text{Where } \beta(j, n-j+1) = \frac{(j-1)!(n-j)!}{n!} \quad (\text{Chakraborti et al. (2004)})$$

(see e.g. Gibbons and Chakraborti (2003), p.41)

Result AR5.12

Let $Y_{(j:n)}$ denote the j^{th} order statistic in a sample of size $n > 0$ from a continuous distribution with cdf G , and let $x_{(k:m)}$ be the k^{th} order statistic in a sample of size $m > 0$ from a continuous distribution with cdf F . Also let $U_{(j:n)}$ denote the j^{th} order statistic in a sample of size $n > 0$ from a $UNIF(0,1)$ distribution and $U_{(k:m)}$ denote the k^{th} order statistic in a sample of size $m > 0$ from a $UNIF(0,1)$ distribution.

Then:

$$\begin{aligned}
 P(Y_{(j:n)} \leq X_{(k:m)} \mid X_{(k:m)} = x_{(k:m)}) &= P(Y_{(j:n)} < X_{(k:m)} \mid X_{(k:m)} = x_{(k:m)}) \\
 &= P(G^{-1}(U_{(j:n)}) < F^{-1}(U_{(k:m)}) \mid U_{(k:m)} = u_{(k:m)}) && \text{(Result AR5.2)} \\
 &= P(U_{(j:n)} < GF^{-1}(U_{(k:m)}) \mid U_{(k:m)} = u_{(k:m)}) \\
 &= I_{GF^{-1}(u_{(k:m)})}(j, n - j + 1) && \text{(Result AR5.11)} \\
 &= (\beta(j, n - j + 1))^{-1} \int_0^{GF^{-1}(u_{(k:m)})} w^{j-1} (1-w)^{n-j} dw && \text{(Result AR5.11)}
 \end{aligned}$$

$$\text{i.e. } P(Y_{(j:n)} \leq X_{(k:m)} \mid X_{(k:m)} = x_{(k:m)}) = (\beta(j, n - j + 1))^{-1} \int_0^{GF^{-1}(u_{(k:m)})} w^{j-1} (1-w)^{n-j} dw$$

Result AR5.13

When the process is in-control i.e. the reference sample and test sample distributions denoted by F and G respectively are the same ($F = G$), then it follows from AR5.12 that

$$P(Y_{(j:n)} \leq X_{(k:m)} \mid X_{(k:m)} = x_{(k:m)}) = (\beta(j, n - j + 1))^{-1} \int_0^{u_{(k:m)}} w^{j-1} (1-w)^{n-j} dw$$

Conditional probabilities for the plotting statistic plotting inside the different zones

Let $Y_{(j:n)}^i$ denote the j^{th} order statistic of the i^{th} Phase II test sample of size n .

$$\begin{aligned}
 p_{1C} &= P\left(Y_{(j:n)}^i \geq X_{(d:m)} \mid X_{(d:m)} = x_{(d:m)}\right) \\
 &= 1 - P\left(Y_{(j:n)}^i < X_{(d:m)} \mid X_{(d:m)} = x_{(d:m)}\right) \\
 &= 1 - P\left(U_{(j:n)} < GF^{-1}\left(U_{(d:m)}\right) \mid U_{(d:m)} = u_{(d:m)}\right) \quad (\text{see Result AR5.12}) \\
 &= 1 - \left(\beta(j, n - j + 1)\right)^{-1} \int_0^{GF^{-1}(u_{(d:m)})} w^{j-1} (1 - w)^{n-j} dw \quad (\text{see Result AR5.13}) \quad (\text{A5.14})
 \end{aligned}$$

A similar argument is followed to obtain expressions for p_{2C} , p_{3C} , p_{4C} , p_{5C} , p_{6C} , p_{7C} , p_{8C} and p_{9C} .

$$\begin{aligned}
 p_{2C} &= P\left(X_{(c:m)} \leq Y_{(j:n)} < X_{(d:m)} \mid X_{(c:m)} = x_{(c:m)}, X_{(d:m)} = x_{(d:m)}\right) \\
 &= P\left(Y_{(j:n)} < X_{(d:m)} \mid X_{(d:m)} = x_{(d:m)}\right) - P\left(Y_{(j:n)} < X_{(c:m)} \mid X_{(c:m)} = x_{(c:m)}\right) \\
 &= P\left(U_{(j:n)} < GF^{-1}\left(U_{(d:m)}\right) \mid U_{(d:m)} = u_{(d:m)}\right) - P\left(U_{(j:n)} < GF^{-1}\left(U_{(c:m)}\right) \mid U_{(c:m)} = u_{(c:m)}\right) \quad (\text{see AR5.12}) \\
 &= \left(\beta(j, n - j + 1)\right)^{-1} \left(\int_0^{GF^{-1}(u_{(d:m)})} w^{j-1} (1 - w)^{n-j} dw - \int_0^{GF^{-1}(u_{(c:m)})} w^{j-1} (1 - w)^{n-j} dw \right) \quad (\text{see Result AR5.13}) \quad (\text{A5.15})
 \end{aligned}$$

$$\begin{aligned}
 p_{3C} &= P\left(X_{(b:m)} < Y_{(j:n)} < X_{(c:m)} \mid X_{(b:m)} = x_{(b:m)}, X_{(c:m)} = x_{(c:m)}\right) \\
 &= P\left(Y_{(j:n)} < X_{(c:m)} \mid X_{(c:m)} = x_{(c:m)}\right) - P\left(Y_{(j:n)} < X_{(b:m)} \mid X_{(b:m)} < x_{(b:m)}\right) \\
 &= P\left(U_{(j:n)} < GF^{-1}\left(U_{(c:m)}\right) \mid U_{(c:m)} = u_{(c:m)}\right) - P\left(U_{(j:n)} < GF^{-1}\left(U_{(b:m)}\right) \mid U_{(b:m)} = u_{(b:m)}\right) \quad (\text{see AR5.12}) \\
 &= \left(\beta(j, n - j + 1)\right)^{-1} \left(\int_0^{GF^{-1}(u_{(c:m)})} w^{j-1} (1 - w)^{n-j} dw - \int_0^{GF^{-1}(u_{(b:m)})} w^{j-1} (1 - w)^{n-j} dw \right) \quad (\text{see Result AR5.13}) \quad (\text{A5.16})
 \end{aligned}$$

$$\begin{aligned}
p_{4C} &= P(X_{(a:m)} < Y_{(j:n)} \leq X_{(b:m)} \mid X_{(a:m)} = x_{(a:m)}, X_{(b:m)} = x_{(b:m)}) \\
&= P(Y_{(j:n)} \leq X_{(b:m)} \mid X_{(b:m)} = x_{(b:m)}) - P(Y_{(j:n)} < X_{(a:m)} \mid X_{(a:m)} = x_{(a:m)}) \\
&= P(U_{(j:n)} < GF^{-1}(U_{(b:m)}) \mid U_{(b:m)} = u_{(b:m)}) - P(U_{(j:n)} < GF^{-1}(U_{(a:m)}) \mid U_{(a:m)} = u_{(a:m)}) \quad (\text{see AR5.12}) \\
&= (\beta(j, n - j + 1))^{-1} \left(\int_0^{GF^{-1}(u_{(b:m)})} w^{j-1} (1-w)^{n-j} dw - \int_0^{GF^{-1}(u_{(a:m)})} w^{j-1} (1-w)^{n-j} dw \right) \quad (\text{see Result AR5.13}) \quad (\text{A5.17})
\end{aligned}$$

$$\begin{aligned}
p_{5C} &= P(Y_{(j:n)} \leq X_{(a:m)} \mid X_{(a:m)} = x_{(a:m)}) \\
&= P(U_{(j:n)} < GF^{-1}(U_{(a:m)}) \mid U_{(a:m)} = u_{(a:m)}) \quad (\text{see AR5.12}) \\
&= (\beta(j, n - j + 1))^{-1} \int_0^{GF^{-1}(u_{(a:m)})} w^{j-1} (1-w)^{n-j} dw \quad (\text{see Result AR5.13}) \quad (\text{A5.18})
\end{aligned}$$

$$\begin{aligned}
p_{6C} &= P(Y_{(j:n)} > X_{(b:m)} \mid X_{(b:m)} = x_{(b:m)}) \\
&= 1 - P(Y_{(j:n)} \leq X_{(b:m)} \mid X_{(b:m)} = x_{(b:m)}) \\
&= 1 - P(U_{(j:n)} < GF^{-1}(U_{(b:m)}) \mid U_{(b:m)} = u_{(b:m)}) \quad (\text{see AR5.12}) \\
&= 1 - (\beta(j, n - j + 1))^{-1} \int_0^{GF^{-1}(u_{(b:m)})} w^{j-1} (1-w)^{n-j} dw \quad (\text{see Result AR5.13}) \quad (\text{A5.19})
\end{aligned}$$

$$\begin{aligned}
p_{7C} &= P(Y_{(j:n)} < X_{(c:m)} \mid X_{(c:m)} = x_{(c:m)}) \\
&= P(U_{(j:n)} < GF^{-1}(U_{(c:m)}) \mid U_{(c:m)} = u_{(c:m)}) \quad (\text{see AR5.12}) \\
&= (\beta(j, n - j + 1))^{-1} \int_0^{GF^{-1}(u_{(c:m)})} w^{j-1} (1-w)^{n-j} dw \quad (\text{see Result AR5.13}) \quad (\text{A5.20})
\end{aligned}$$

$$\begin{aligned}
 p_{8C} &= P\left(Y_{(j:n)} \geq X_{(c:m)} \mid X_{(c:m)} = x_{(c:m)}\right) \\
 &= 1 - P\left(Y_{(j:n)} < X_{(c:m)} \mid X_{(c:m)} = x_{(c:m)}\right) \\
 &= 1 - P\left(U_{(j:n)} < GF^{-1}\left(U_{(c:m)}\right) \mid U_{(c:m)} = u_{(c:m)}\right) && \text{(see AR5.12)} \\
 &= 1 - \left(\beta(j, n - j + 1)\right)^{-1} \int_0^{GF^{-1}(u_{(c:m)})} w^{j-1} (1 - w)^{n-j} dw && \text{(see Result AR5.13)} \quad \text{(A5.21)}
 \end{aligned}$$

$$\begin{aligned}
 p_{9C} &= P\left(Y_{(j:n)} \leq X_{(b:m)} \mid X_{(b:m)} = x_{(b:m)}\right) \\
 &= P\left(U_{(j:n)} < GF^{-1}\left(U_{(b:m)}\right) \mid U_{(b:m)} = u_{(b:m)}\right) && \text{(see AR5.12)} \\
 &= \left(\beta(j, n - j + 1)\right)^{-1} \int_0^{GF^{-1}(u_{(b:m)})} w^{j-1} (1 - w)^{n-j} dw && \text{(see Result AR5.13)} \quad \text{(A5.22)}
 \end{aligned}$$

Conditional essential transition probability matrices

The elements of the conditional essential transition probability matrices are all conditional probabilities. For more information regarding these conditional probabilities refer to equations A5.14, A5.15, A5.16, A5.17, A5.18, A5.19, A5.20, A5.21 and A5.22.

The *I-of-I* precedence charts

The essential transition probability matrices of the upper one-sided-, lower one-sided- and two sided *I-of-I* precedence charts are given by:

The upper one-sided *I-of-I* precedence chart essential transition probability matrix:

$$\mathbf{Q}_{1-of-1(U)}^{Con(2 \times 2)} = \begin{bmatrix} 0 & p_{7C} \\ 0 & p_{7C} \end{bmatrix} \quad (A5.23)$$

Before proceeding the notation is first clarified. The subscript of $\mathbf{Q}_{1-of-1(U)}^{Con(2 \times 2)}$ indicate which charts' essential transition probability matrix is considered, in this case it is the upper *I-of-I* chart. The superscript of $\mathbf{Q}_{1-of-1(U)}^{Con(2 \times 2)}$ is *Con* (2×2), the *Con* denotes that the essential transition probability matrix has conditional transition probabilities as elements and the (2×2) indicate the dimensions of the matrix.

The lower one-sided *I-of-I* precedence chart essential transition probability matrix:

$$\mathbf{Q}_{1-of-1(L)}^{Con(2 \times 2)} = \begin{bmatrix} 0 & p_{9C} \\ 0 & p_{9C} \end{bmatrix} \quad (A5.24)$$

The two-sided *I-of-I* precedence chart essential transition probability matrix:

$$\mathbf{Q}_{1-of-1(T)}^{Con(2 \times 2)} = \begin{bmatrix} 0 & p_{3C} \\ 0 & p_{3C} \end{bmatrix} \quad (A5.25)$$

The 2-of-2 precedence charts

The essential transition probability matrices of the upper one-sided-, lower one-sided- and two-sided 2-of-2 precedence charts are given by:

The upper one-sided 2-of-2 precedence chart essential transition probability matrix:

$$\mathbf{Q}_{2\text{-of-}2(U)}^{Con(3 \times 3)} = \begin{bmatrix} 0 & p_{7C} & p_{8C} \\ 0 & p_{7C} & p_{8C} \\ 0 & p_{7C} & 0 \end{bmatrix} \quad (\text{A5.26})$$

The lower one-sided 2-of-2 precedence chart essential transition probability matrix:

$$\mathbf{Q}_{2\text{-of-}2(L)}^{Con(3 \times 3)} = \begin{bmatrix} 0 & p_{6C} & p_{9C} \\ 0 & p_{6C} & p_{9C} \\ 0 & p_{6C} & 0 \end{bmatrix} \quad (\text{A5.27})$$

The two-sided 2-of-2 precedence chart essential transition probability matrix:

$$\mathbf{Q}_{2\text{-of-}2(T)}^{Con(4 \times 4)} = \begin{bmatrix} 0 & p_{3C} & p_{8C} & p_{9C} \\ 0 & p_{3C} & p_{8C} & p_{9C} \\ 0 & p_{3C} & 0 & p_{9C} \\ 0 & p_{3C} & p_{8C} & 0 \end{bmatrix} \quad (\text{A5.28})$$

The 2-of-3 precedence charts

The essential transition probability matrices of the upper one-sided-, lower one-sided- and two-sided 2-of-3 precedence charts are given by:

The upper one-sided 2-of-3 precedence chart essential transition probability matrix:

$$\mathbf{Q}_{2\text{-of-}3(U)}^{Con(5 \times 5)} = \begin{bmatrix} 0 & p_{7C} & p_{8C} & 0 & 0 \\ 0 & p_{7C} & 0 & p_{8C} & 0 \\ 0 & 0 & 0 & 0 & p_{7C} \\ 0 & 0 & 0 & 0 & p_{7C} \\ 0 & p_{7C} & 0 & 0 & 0 \end{bmatrix} \quad (\text{A5.29})$$

The lower one-sided 2-of-3 precedence chart essential transition probability matrix:

$$\mathbf{Q}_{2\text{-of-}3(L)}^{Con(5 \times 5)} = \begin{bmatrix} 0 & p_{6C} & p_{9C} & 0 & 0 \\ 0 & p_{6C} & 0 & p_{9C} & 0 \\ 0 & 0 & 0 & 0 & p_{6C} \\ 0 & 0 & 0 & 0 & p_{6C} \\ 0 & p_{6C} & 0 & 0 & 0 \end{bmatrix} \quad (\text{A5.30})$$

The two-sided 2-of-3 precedence chart essential transition probability matrix:

$$\mathbf{Q}_{2\text{-of-}3(T)}^{Con(8 \times 8)} = \begin{bmatrix} 0 & p_{3C} & p_{8C} & p_{9C} & 0 & 0 & 0 & 0 \\ 0 & p_{3C} & 0 & 0 & p_{8C} & p_{9C} & 0 & 0 \\ 0 & 0 & 0 & p_{9C} & 0 & 0 & p_{3C} & 0 \\ 0 & 0 & p_{8C} & 0 & 0 & 0 & 0 & p_{3C} \\ 0 & 0 & 0 & p_{9C} & 0 & 0 & p_{3C} & 0 \\ 0 & 0 & p_{8C} & 0 & 0 & 0 & 0 & p_{3C} \\ 0 & p_{3C} & 0 & 0 & 0 & p_{9C} & 0 & 0 \\ 0 & p_{3C} & 0 & 0 & p_{8C} & 0 & 0 & 0 \end{bmatrix} \quad (\text{A5.31})$$

Note that the essential transition probability matrices of the 2-of-3 charts are slightly different from the ones in Human et al. (2009). A discussion on this point is given in remark 3.21 of Chapter 3.

The improved 2-of-2 precedence charts

The essential transition probability matrices of the upper one-sided-, lower one-sided- and two sided improved 2-of-2 precedence charts are given by:

The upper one-sided improved 2-of-2 precedence chart essential transition probability matrix:

$$\mathbf{Q}_{12\text{-of-}2(U)}^{Con(3 \times 3)} = \begin{bmatrix} 0 & p_{7C} & p_{2C} \\ 0 & p_{7C} & p_{2C} \\ 0 & p_{7C} & 0 \end{bmatrix} \quad (\text{A5.32})$$

The lower one-sided improved 2-of-2 precedence chart essential transition probability matrix:

$$\mathbf{Q}_{12\text{-of-}2(L)}^{Con(3 \times 3)} = \begin{bmatrix} 0 & p_{6C} & p_{4C} \\ 0 & p_{6C} & p_{4C} \\ 0 & p_{6C} & 0 \end{bmatrix} \quad (\text{A5.33})$$

The two-sided *improved 2-of-2* precedence chart essential transition probability matrix:

$$\mathbf{Q}_{12\text{-of-}2(T)}^{\text{Con } (4 \times 4)} = \begin{bmatrix} 0 & p_{3C} & p_{2C} & p_{4C} \\ 0 & p_{3C} & p_{2C} & p_{4C} \\ 0 & p_{3C} & 0 & p_{4C} \\ 0 & p_{3C} & p_{2C} & 0 \end{bmatrix} \quad (\text{A5.34})$$

The *improved 2-of-3* precedence charts

The essential transition probability matrices of the upper one-sided-, lower one-sided- and two sided *improved 2-of-3* precedence charts are given by:

The upper one-sided *improved 2-of-3* precedence chart essential transition probability matrix:

$$\mathbf{Q}_{12\text{-of-}3(U)}^{\text{Con } (5 \times 5)} = \begin{bmatrix} 0 & p_{7C} & p_{2C} & 0 & 0 \\ 0 & p_{7C} & 0 & p_{2C} & 0 \\ 0 & 0 & 0 & 0 & p_{7C} \\ 0 & 0 & 0 & 0 & p_{7C} \\ 0 & p_{7C} & 0 & 0 & 0 \end{bmatrix} \quad (\text{A5.35})$$

The lower one-sided *improved 2-of-3* precedence chart essential transition probability matrix:

$$\mathbf{Q}_{12\text{-of-}3(L)}^{\text{Con } (5 \times 5)} = \begin{bmatrix} 0 & p_{6C} & p_{4C} & 0 & 0 \\ 0 & p_{6C} & 0 & p_{4C} & 0 \\ 0 & 0 & 0 & 0 & p_{6C} \\ 0 & 0 & 0 & 0 & p_{6C} \\ 0 & p_{6C} & 0 & 0 & 0 \end{bmatrix} \quad (\text{A5.36})$$

The two-sided *improved 2-of-3* precedence chart essential transition probability matrix:

$$\mathbf{Q}_{I2-of-3(T)}^{Con(8 \times 8)} = \begin{bmatrix} 0 & p_{3C} & p_{2C} & 0 & 0 & p_{4C} & 0 & 0 \\ 0 & p_{3C} & 0 & p_{2C} & 0 & 0 & p_{4C} & 0 \\ 0 & 0 & 0 & 0 & p_{3C} & p_{4C} & 0 & 0 \\ 0 & 0 & 0 & 0 & p_{3C} & p_{4C} & 0 & 0 \\ 0 & p_{3C} & 0 & 0 & 0 & 0 & p_{4C} & 0 \\ 0 & 0 & p_{2C} & 0 & 0 & 0 & 0 & p_{3C} \\ 0 & 0 & p_{2C} & 0 & 0 & 0 & 0 & p_{3C} \\ 0 & p_{3C} & 0 & p_{2C} & 0 & 0 & 0 & 0 \end{bmatrix} \quad (\text{A5.37})$$

To find the conditional run-length distribution and the characteristics of the conditional run-length distribution of a chart the associated essential transition probability matrix is substituted into the following formulae:

$$P_c(N = j) = P(N = j | \mathbf{Z} = \mathbf{z}) = \xi (\mathbf{Q}^{Con})^{j-1} (\mathbf{I} - \mathbf{Q}^{Con}) \mathbf{1}, \text{ for } j=1,2,3,\dots, \text{ with } (\mathbf{Q}^{Con})^0 = \mathbf{I} \quad (\text{A5.38})$$

$$P_c(N \leq j) = P(N \leq j | \mathbf{Z} = \mathbf{z}) = 1 - \xi (\mathbf{Q}^{Con})^j \mathbf{1}, \quad j = 1,2,3,\dots \quad (\text{A5.39})$$

$$CARL = E_c(N) = E(N | \mathbf{Z} = \mathbf{z}) = \xi (\mathbf{I} - \mathbf{Q}^{Con})^{-1} \mathbf{1} \quad (\text{A5.40})$$

$$CVRL = VRL_c(N) = VRL(N | \mathbf{Z} = \mathbf{z}) = \xi (\mathbf{I} + \mathbf{Q}^{Con}) (\mathbf{I} - \mathbf{Q}^{Con})^{-2} \mathbf{1} - \left(\xi (\mathbf{I} - \mathbf{Q}^{Con})^{-1} \mathbf{1} \right)^2 \quad (\text{A5.41})$$

Where: $\mathbf{Q}^{Con} = \mathbf{Q}_{h \times h}^{Con}$ is the conditional essential transition probability matrix.

$$\xi = \xi_{1 \times h} = (1, 0, 0, \dots, 0), \quad (\text{A5.42})$$

$$\mathbf{1} = \mathbf{1}_{h \times 1} = (1, 1, 1, \dots, 1)^T, \quad (\text{A5.43})$$

$$\mathbf{I} = \mathbf{I}_{h \times h} \text{ is the identity matrix,} \quad (\text{A5.44})$$

N is the run-length random variable,

j is the integer value that N can assume, and

h is an integer value representing the number of transient states.

(Refer to Theorem 2.1)

Conditional false alarm rate (*CFAR*)

Unfortunately there are no standard formulae to find the *CFAR* like equations A5.38, A5.39, A5.40 and A5.41 are used to find the pdf cdf, average and variance of the conditional run-length distribution. First principles are used to find the *CFAR* for each chart. Note that the when calculating the *CFAR* it is assumed that the process is IC i.e. the reference sample distribution and test sample distribution are the same ($F = G$).

The upper one-sided *I-of-I* precedence chart

For time $i = 1, 2, 3, \dots$

$$\begin{aligned}
 CFAR_{1-of-1(U)} &= (p_{8C} \mid G = F) \\
 &= 1 - (\beta(j, n - j + 1))^{-1} \int_0^{u_{(c;m)}} w^{j-1} (1 - w)^{n-j} dw \quad (\text{see A5.21}) \quad (\text{A5.45})
 \end{aligned}$$

The lower one-sided *I-of-I* precedence chart

For time $i = 1, 2, 3, \dots$

$$\begin{aligned}
 CFAR_{1-of-1(L)} &= (p_{9C} \mid G = F) \\
 &= (\beta(j, n - j + 1))^{-1} \int_0^{u_{(b;m)}} w^{j-1} (1 - w)^{n-j} dw \quad (\text{see A5.22}) \quad (\text{A5.46})
 \end{aligned}$$

The two-sided *I-of-I* precedence chart

For time $i = 1, 2, 3, \dots$

$$\begin{aligned}
 CFAR_{1-of-1(T)} &= (p_{8C} + p_{9C} \mid G = F) \\
 &= (\beta(j, n - j + 1))^{-1} \int_0^{u_{(b;m)}} w^{j-1} (1 - w)^{n-j} dw + \\
 &\quad 1 - (\beta(j, n - j + 1))^{-1} \int_0^{u_{(c;m)}} w^{j-1} (1 - w)^{n-j} dw \quad (\text{see A5.21 and A5.22}) \quad (\text{A5.47})
 \end{aligned}$$

The upper one-sided 2-of-2 precedence chart

For time $i = 1$

$$CFAR_{2\text{-of-}2(U)} = 0$$

For time $i = 2, 3, 4, \dots$

$$\begin{aligned}
 CFAR_{2\text{-of-}2(U)} &= \left((p_{8C})^2 \mid G = F \right) \\
 &= \left(1 - (\beta(j, n - j + 1))^{-1} \int_0^{u_{(c;m)}} w^{j-1} (1 - w)^{n-j} dw \right)^2 \quad (\text{see A5.21}) \quad (\text{A5.48})
 \end{aligned}$$

The lower one-sided 2-of-2 precedence chart

For time $i = 1$

$$CFAR_{2\text{-of-}2(L)} = 0$$

For time $i = 2, 3, 4, \dots$

$$\begin{aligned}
 CFAR_{2\text{-of-}2(L)} &= \left((p_{9C})^2 \mid G = F \right) \\
 &= \left((\beta(j, n - j + 1))^{-1} \int_0^{u_{(b;m)}} w^{j-1} (1 - w)^{n-j} dw \right)^2 \quad (\text{see A5.22}) \quad (\text{A5.49})
 \end{aligned}$$

The two-sided 2-of-2 precedence chart

For time $i = 1$

$$CFAR_{2\text{-of-}2(T)} = 0$$

For time $i = 2, 3, 4, \dots$

$$\begin{aligned} CFAR_{2\text{-of-}2(T)} &= \left((p_{8C})^2 + (p_{9C})^2 \mid G = F \right) \\ &= \left(1 - (\beta(j, n - j + 1))^{-1} \int_0^{u_{(cm)}} w^{j-1} (1 - w)^{n-j} dw \right)^2 \\ &\quad + \left((\beta(j, n - j + 1))^{-1} \int_0^{u_{(bm)}} w^{j-1} (1 - w)^{n-j} dw \right)^2 \end{aligned} \quad \begin{array}{l} \text{(see A5.21 and A5.22)} \\ \text{(A5.50)} \end{array}$$

The upper one-sided 2-of-3 precedence chart

For time $i = 1$

$$CFAR_{2\text{-of-}3(U)} = 0$$

For time $i = 2$

$$\begin{aligned} CFAR_{2\text{-of-}3(U)} &= \left((p_{8C})^2 \mid G = F \right) \\ &= \left(1 - (\beta(j, n - j + 1))^{-1} \int_0^{u_{(cm)}} w^{j-1} (1 - w)^{n-j} dw \right)^2 \end{aligned} \quad \begin{array}{l} \text{(see A5.21)} \\ \text{(A5.51)} \end{array}$$

For time $i = 3, 4, 5, \dots$

$$\begin{aligned} CFAR_{2\text{-of-}3(U)} &= \left(2p_{7C} p_{8C}^2 \mid G = F \right) \\ &= 2 \left((\beta(j, n - j + 1))^{-1} \int_0^{u_{(cm)}} w^{j-1} (1 - w)^{n-j} dw \right) \\ &\quad \times \left(1 - (\beta(j, n - j + 1))^{-1} \int_0^{u_{(cm)}} w^{j-1} (1 - w)^{n-j} dw \right)^2 \end{aligned} \quad \begin{array}{l} \text{(see A5.20 and A5.21)} \\ \text{(A5.52)} \end{array}$$

The lower one-sided 2-of-3 precedence chart

For time $i = 1$

$$CFAR_{2-of-3(L)} = 0$$

For time $i = 2$

$$\begin{aligned} CFAR_{2-of-3(L)} &= (p_{9C}^2 | G = F) \\ &= \left((\beta(j, n - j + 1))^{-1} \int_0^{u_{(b;m)}} w^{j-1} (1 - w)^{n-j} dw \right)^2 \end{aligned} \quad \begin{array}{l} \text{(see A5.22)} \\ \text{(A5.53)} \end{array}$$

For time $i = 3, 4, 5, \dots$

$$\begin{aligned} CFAR_{2-of-3(L)} &= (2p_{6C} p_{9C}^2 | G = F) \\ &= 2 \left(1 - (\beta(j, n - j + 1))^{-1} \int_0^{u_{(b;m)}} w^{j-1} (1 - w)^{n-j} dw \right) \\ &\quad \times \left((\beta(j, n - j + 1))^{-1} \int_0^{u_{(b;m)}} w^{j-1} (1 - w)^{n-j} dw \right)^2 \end{aligned} \quad \begin{array}{l} \text{(see A5.19 and A5.22)} \\ \text{(A5.54)} \end{array}$$

The two-sided 2-of-3 precedence chart

For time $i = 1$

$$CFAR_{2-of-3(T)} = 0$$

For time $i = 2$

$$\begin{aligned} CFAR_{2-of-3(T)} &= (p_{8C}^2 + p_{9C}^2 | G = F) \\ &= \left(1 - (\beta(j, n - j + 1))^{-1} \int_0^{u_{(c;m)}} w^{j-1} (1 - w)^{n-j} dw \right)^2 \\ &\quad + \left((\beta(j, n - j + 1))^{-1} \int_0^{u_{(b;m)}} w^{j-1} (1 - w)^{n-j} dw \right)^2 \end{aligned} \quad \begin{array}{l} \text{(see A5.21 and A5.22)} \\ \text{(A5.55)} \end{array}$$

For time $i = 3, 4, 5, \dots$

$$\begin{aligned}
 CFAR_{2\text{-of-}3(T)} &= \left(2p_{3c}p_{8c}^2 + 2p_{3c}p_{9c}^2 + p_{8c}p_{9c}^2 + p_{9c}p_{8c}^2 \mid G = F \right) \\
 &= \left(2p_{3c}(p_{8c}^2 + p_{9c}^2) + p_{8c}p_{9c}(p_{9c} + p_{8c}) \mid G = F \right) \\
 &= 2 \left((\beta(j, n - j + 1))^{-1} \left(\int_0^{u_{(c;m)}} w^{j-1}(1-w)^{n-j} dw - \int_0^{u_{(b;m)}} w^{j-1}(1-w)^{n-j} dw \right) \right) \\
 &\quad \times \left(\left(1 - (\beta(j, n - j + 1))^{-1} \int_0^{u_{(c;m)}} w^{j-1}(1-w)^{n-j} dw \right)^2 + \left((\beta(j, n - j + 1))^{-1} \int_0^{u_{(b;m)}} w^{j-1}(1-w)^{n-j} dw \right)^2 \right) \\
 &\quad + \left(1 - (\beta(j, n - j + 1))^{-1} \int_0^{u_{(c;m)}} w^{j-1}(1-w)^{n-j} dw \right) \times \left((\beta(j, n - j + 1))^{-1} \int_0^{u_{(b;m)}} w^{j-1}(1-w)^{n-j} dw \right) \\
 &\quad \times \left(\left(1 - (\beta(j, n - j + 1))^{-1} \int_0^{u_{(c;m)}} w^{j-1}(1-w)^{n-j} dw \right) + \left((\beta(j, n - j + 1))^{-1} \int_0^{u_{(b;m)}} w^{j-1}(1-w)^{n-j} dw \right) \right) \\
 &\quad \text{(see A5.16, A5.21 and A5.22)} \tag{A5.56}
 \end{aligned}$$

The upper one-sided *improved 2-of-2* precedence chart

For time $i = 1$

$$\begin{aligned}
 CFAR_{12\text{-of-}2(U)} &= (p_{1c} \mid G = F) \\
 &= 1 - (\beta(j, n - j + 1))^{-1} \int_0^{u_{(d;m)}} w^{j-1}(1-w)^{n-j} dw \quad \text{(see A5.14)} \tag{A5.57}
 \end{aligned}$$

For time $i = 2, 3, 4, \dots$

$$\begin{aligned}
 CFAR_{12\text{-of-}2(U)} &= (p_{1c} + p_{2c}^2 \mid G = F) \\
 &= \left(1 - (\beta(j, n - j + 1))^{-1} \int_0^{u_{(d;m)}} w^{j-1}(1-w)^{n-j} dw \right) \\
 &\quad + \left((\beta(j, n - j + 1))^{-1} \left(\int_0^{u_{(d;m)}} w^{j-1}(1-w)^{n-j} dw - \int_0^{u_{(c;m)}} w^{j-1}(1-w)^{n-j} dw \right) \right)^2 \\
 &\quad \text{(see A5.14 and A5.15)} \tag{A5.58}
 \end{aligned}$$

The lower one-sided *improved 2-of-2* precedence chart

For time $i = 1$

$$\begin{aligned}
 CFAR_{I2-of-2(L)} &= (p_{5C} | G = F) \\
 &= (\beta(j, n - j + 1))^{-1} \int_0^{u(a;m)} w^{j-1} (1 - w)^{n-j} dw \quad (\text{see A5.18}) \quad (\text{A5.59})
 \end{aligned}$$

For time $i = 2, 3, 4, \dots$

$$\begin{aligned}
 CFAR_{I2-of-2(L)} &= (p_{5C} + p_{4C}^2 | G = F) \\
 &= \left((\beta(j, n - j + 1))^{-1} \int_0^{u(a;m)} w^{j-1} (1 - w)^{n-j} dw \right) \\
 &\quad + \left((\beta(j, n - j + 1))^{-1} \left(\int_0^{u(b;m)} w^{j-1} (1 - w)^{n-j} dw - \int_0^{u(a;m)} w^{j-1} (1 - w)^{n-j} dw \right) \right)^2 \\
 &\quad (\text{see A5.17 and A5.18}) \quad (\text{A5.60})
 \end{aligned}$$

The two-sided *improved 2-of-2* precedence chart

For time $i = 1$

$$\begin{aligned}
 CFAR_{I2-of-2(T)} &= (p_{1C} + p_{5C} | G = F) \\
 &= \left(1 - (\beta(j, n - j + 1))^{-1} \int_0^{u(d;m)} w^{j-1} (1 - w)^{n-j} dw \right) + \left((\beta(j, n - j + 1))^{-1} \int_0^{u(a;m)} w^{j-1} (1 - w)^{n-j} dw \right) \\
 &\quad (\text{see A5.14 and A5.18}) \quad (\text{A5.61})
 \end{aligned}$$

For time $i = 2, 3, 4, \dots$

$$\begin{aligned}
 CFAR_{I_{2-of-2}(T)} &= (p_{1C} + p_{5C} + p_{2C}^2 + p_{4C}^2 \mid G = F) \\
 &= \left(1 - (\beta(j, n - j + 1))^{-1} \int_0^{u_{(d;m)}} w^{j-1} (1 - w)^{n-j} dw \right) + \left((\beta(j, n - j + 1))^{-1} \int_0^{u_{(a;m)}} w^{j-1} (1 - w)^{n-j} dw \right) \\
 &\quad + \left((\beta(j, n - j + 1))^{-1} \left(\int_0^{u_{(d;m)}} w^{j-1} (1 - w)^{n-j} dw - \int_0^{u_{(c;m)}} w^{j-1} (1 - w)^{n-j} dw \right) \right)^2 \\
 &\quad + \left((\beta(j, n - j + 1))^{-1} \left(\int_0^{u_{(b;m)}} w^{j-1} (1 - w)^{n-j} dw - \int_0^{u_{(a;m)}} w^{j-1} (1 - w)^{n-j} dw \right) \right)^2 \\
 &\quad \text{(see A5.14, A5.15, A5.17 and A5.18)} \tag{A5.62}
 \end{aligned}$$

The upper one-sided *improved 2-of-3* precedence chart

For time $i = 1$

$$\begin{aligned}
 CFAR_{I_{2-of-3}(U)} &= (p_{1C} \mid G = F) \\
 &= 1 - (\beta(j, n - j + 1))^{-1} \int_0^{u_{(d;m)}} w^{j-1} (1 - w)^{n-j} dw \tag{see A5.14} \tag{A5.63}
 \end{aligned}$$

For time $i = 2$

$$\begin{aligned}
 CFAR_{I_{2-of-3}(U)} &= (p_{1C} + p_{2C}^2 \mid G = F) \\
 &= \left(1 - (\beta(j, n - j + 1))^{-1} \int_0^{u_{(d;m)}} w^{j-1} (1 - w)^{n-j} dw \right) \\
 &\quad + \left((\beta(j, n - j + 1))^{-1} \left(\int_0^{u_{(d;m)}} w^{j-1} (1 - w)^{n-j} dw - \int_0^{u_{(c;m)}} w^{j-1} (1 - w)^{n-j} dw \right) \right)^2 \\
 &\quad \text{(see A5.14 and A5.15)} \tag{A5.64}
 \end{aligned}$$

For time $i = 3, 4, 5, \dots$

$$\begin{aligned}
 CFAR_{I2-of-3(U)} &= (p_{1C} + 2p_{7C}p_{2C}^2 \mid G = F) \\
 &= \left(1 - (\beta(j, n - j + 1))^{-1} \int_0^{u_{(d;m)}} w^{j-1} (1 - w)^{n-j} dw \right) + 2 \left((\beta(j, n - j + 1))^{-1} \int_0^{u_{(c;m)}} w^{j-1} (1 - w)^{n-j} dw \right) \\
 &\quad \times \left((\beta(j, n - j + 1))^{-1} \left(\int_0^{u_{(d;m)}} w^{j-1} (1 - w)^{n-j} dw - \int_0^{u_{(c;m)}} w^{j-1} (1 - w)^{n-j} dw \right) \right)^2 \\
 &\hspace{15em} \text{(see A5.14, A5.15 and A5.20)} \hspace{10em} \text{(A5.65)}
 \end{aligned}$$

The lower one-sided *improved 2-of-3* precedence chart

For time $i = 1$

$$\begin{aligned}
 CFAR_{I2-of-3(L)} &= (p_{5C} \mid G = F) \\
 &= (\beta(j, n - j + 1))^{-1} \int_0^{u_{(a;m)}} w^{j-1} (1 - w)^{n-j} dw \hspace{10em} \text{(see A5.18)} \hspace{10em} \text{(A5.66)}
 \end{aligned}$$

For time $i = 2$

$$\begin{aligned}
 CFAR_{I2-of-3(L)} &= (p_{5C} + p_{4C}^2 \mid G = F) \\
 &= \left((\beta(j, n - j + 1))^{-1} \int_0^{u_{(a;m)}} w^{j-1} (1 - w)^{n-j} dw \right) \\
 &\quad + \left((\beta(j, n - j + 1))^{-1} \left(\int_0^{u_{(b;m)}} w^{j-1} (1 - w)^{n-j} dw - \int_0^{u_{(a;m)}} w^{j-1} (1 - w)^{n-j} dw \right) \right)^2 \\
 &\hspace{15em} \text{(see A5.17 and A5.18)} \hspace{10em} \text{(A5.67)}
 \end{aligned}$$

For time $i = 3, 4, 5, \dots$

$$\begin{aligned}
 CFAR_{I_{2-of-3}(L)} &= (p_{5C} + 2p_{6C}p_{4C}^2 \mid G = F) \\
 &= \left((\beta(j, n-j+1))^{-1} \int_0^{u_{(a,m)}} w^{j-1} (1-w)^{n-j} dw \right) + 2 \left(1 - (\beta(j, n-j+1))^{-1} \int_0^{u_{(b,m)}} w^{j-1} (1-w)^{n-j} dw \right) \\
 &\quad \times \left((\beta(j, n-j+1))^{-1} \left(\int_0^{u_{(b,m)}} w^{j-1} (1-w)^{n-j} dw - \int_0^{u_{(a,m)}} w^{j-1} (1-w)^{n-j} dw \right) \right)^2 \\
 &\hspace{15em} \text{(see A5.17, A5.18 and A5.19)} \hspace{10em} \text{(A5.68)}
 \end{aligned}$$

The two-sided *improved 2-of-3* precedence chart

For time $i = 1$

$$\begin{aligned}
 CFAR_{I_{2-of-3}(T)} &= (p_{1C} + p_{5C} \mid G = F) \\
 &= \left(1 - (\beta(j, n-j+1))^{-1} \int_0^{u_{(d,m)}} w^{j-1} (1-w)^{n-j} dw \right) \\
 &\quad + \left((\beta(j, n-j+1))^{-1} \int_0^{u_{(a,m)}} w^{j-1} (1-w)^{n-j} dw \right) \\
 &\hspace{15em} \text{(see A5.14 and A5.18)} \hspace{10em} \text{(A5.69)}
 \end{aligned}$$

For time $i = 2$

$$\begin{aligned}
 CFAR_{I_{2-of-3}(T)} &= (p_{1C} + p_{5C} + p_{2C}^2 + p_{4C}^2 \mid G = F) \\
 &= \left(1 - (\beta(j, n-j+1))^{-1} \int_0^{u_{(d,m)}} w^{j-1} (1-w)^{n-j} dw \right) + \left((\beta(j, n-j+1))^{-1} \int_0^{u_{(a,m)}} w^{j-1} (1-w)^{n-j} dw \right) \\
 &\quad + \left((\beta(j, n-j+1))^{-1} \left(\int_0^{u_{(d,m)}} w^{j-1} (1-w)^{n-j} dw - \int_0^{u_{(c,m)}} w^{j-1} (1-w)^{n-j} dw \right) \right)^2 \\
 &\quad + \left((\beta(j, n-j+1))^{-1} \left(\int_0^{u_{(b,m)}} w^{j-1} (1-w)^{n-j} dw - \int_0^{u_{(a,m)}} w^{j-1} (1-w)^{n-j} dw \right) \right)^2 \\
 &\hspace{15em} \text{(see A5.14, A5.15, A5.17 and A5.18)} \hspace{10em} \text{(A5.70)}
 \end{aligned}$$

For time $i = 3, 4, 5, \dots$

$$\begin{aligned}
CFAR_{I_{2-of-3}(T)} &= (p_{1C} + p_{5C} + 2p_{2C}^2 p_3 + 2p_{3C} p_{4C}^2 + p_{2C}^2 p_{4C} + p_{2C} p_{4C}^2 \mid G = F) \\
&= (p_{1C} + p_{5C} + 2p_{2C}^2 p_3 + p_{2C}^2 p_{4C} + 2p_{3C} p_{4C}^2 + p_{2C} p_{4C}^2 \mid G = F) \\
&= (p_{1C} + p_{5C} + p_{2C}^2 (2p_3 + p_{4C}) + p_{4C}^2 (2p_{3C} + p_{2C}) \mid G = F) \\
&= \left(1 - (\beta(j, n - j + 1))^{-1} \int_0^{u_{(d;m)}} w^{j-1} (1-w)^{n-j} dw \right) + \left((\beta(j, n - j + 1))^{-1} \int_0^{u_{(a;m)}} w^{j-1} (1-w)^{n-j} dw \right) \\
&\quad + \left((\beta(j, n - j + 1))^{-1} \left(\int_0^{u_{(d;m)}} w^{j-1} (1-w)^{n-j} dw - \int_0^{u_{(c;m)}} w^{j-1} (1-w)^{n-j} dw \right) \right)^2 \\
&\quad \times \left(2 \left((\beta(j, n - j + 1))^{-1} \left(\int_0^{u_{(c;m)}} w^{j-1} (1-w)^{n-j} dw - \int_0^{u_{(b;m)}} w^{j-1} (1-w)^{n-j} dw \right) \right) \right. \\
&\quad \left. + \left((\beta(j, n - j + 1))^{-1} \left(\int_0^{u_{(b;m)}} w^{j-1} (1-w)^{n-j} dw - \int_0^{u_{(a;m)}} w^{j-1} (1-w)^{n-j} dw \right) \right) \right) \\
&\quad + \left((\beta(j, n - j + 1))^{-1} \left(\int_0^{u_{(b;m)}} w^{j-1} (1-w)^{n-j} dw - \int_0^{u_{(a;m)}} w^{j-1} (1-w)^{n-j} dw \right) \right)^2 \\
&\quad \times \left(2 \left((\beta(j, n - j + 1))^{-1} \left(\int_0^{u_{(c;m)}} w^{j-1} (1-w)^{n-j} dw - \int_0^{u_{(b;m)}} w^{j-1} (1-w)^{n-j} dw \right) \right) \right. \\
&\quad \left. + \left((\beta(j, n - j + 1))^{-1} \left(\int_0^{u_{(d;m)}} w^{j-1} (1-w)^{n-j} dw - \int_0^{u_{(c;m)}} w^{j-1} (1-w)^{n-j} dw \right) \right) \right)
\end{aligned}$$

(see A5.14, A5.15, A5.16, A5.17 and A5.18) (A5.71)

Conditional and unconditional run-length distribution and some characteristics of the run-length distribution.

Expressions for the average and the variance of the unconditional run-length distributions can be calculated by making use of the following conditional expectations:

$$E(N) = E_{\mathbf{Z}}(E(N | \mathbf{Z})) \quad (\text{A5.72})$$

$$\begin{aligned} \text{Var}(N) &= E_{\mathbf{Z}}(\text{var}(N | \mathbf{Z})) + \text{var}_{\mathbf{Z}}(E(N | \mathbf{Z})) \\ &= E_{\mathbf{Z}}(\text{var}(N | \mathbf{Z})) + \left(E_{\mathbf{Z}}\left((E(N | \mathbf{Z}))^2 \right) - (E_{\mathbf{Z}}(E(N | \mathbf{Z})))^2 \right) \end{aligned} \quad (\text{A5.73})$$

where \mathbf{Z} denotes a vector of random variables which consists of order statistics yet to be observed. This represents the estimated control limits from the Phase I reference sample. Note that the number of elements in \mathbf{Z} vary from control chart to control chart, e.g. for an upper one-sided *1-of-1* and two-sided *improved 2-of-2* control charts \mathbf{Z} has 1 and 4 elements respectively.

$E(N)$ and $\text{Var}(N)$ denotes the unconditional characteristics whilst $E(N | \mathbf{Z})$ and $\text{Var}(N | \mathbf{Z})$ denote the conditional characteristics for the control chart under consideration.

The *1-of-1* precedence charts

The upper *1-of-1* precedence chart

The conditional run-length distribution, conditional run-length distribution characteristics and *CFAR* are given by:

$$P(N_{1-of-1(U)} = j | \mathbf{Z}) = \xi(\mathbf{Q})^{j-1}(\mathbf{I} - \mathbf{Q})\mathbf{1}, \text{ for } j=1,2,3,\dots \text{ with } (\mathbf{Q})^0 = \mathbf{I} \quad (\text{A5.74})$$

$$\text{CARL}_{1-of-1(U)} = E(N | \mathbf{Z}) = \xi(\mathbf{I} - \mathbf{Q})^{-1}\mathbf{1} \quad (\text{A5.75})$$

$$\text{CVRL}_{1-of-1(U)} = \text{Var}(N | \mathbf{Z}) = \xi(\mathbf{I} + \mathbf{Q})(\mathbf{I} - \mathbf{Q})^{-2}\mathbf{1} - \left(\xi(\mathbf{I} - \mathbf{Q})^{-1}\mathbf{1} \right)^2 \quad (\text{A5.76})$$

$$\text{CFAR}_{1-of-1(U)} = (p_{8C} | G = F) \quad (\text{see A5.45})$$

where $\mathbf{Q} = \mathbf{Q}_{1-of-1(U)}^{\text{Con}(2 \times 2)}$ is the conditional essential transition probability matrix, conditioned on $\mathbf{Z} = (X_{(c:m)})$.

The unconditional run-length distribution, unconditional run-length distribution characteristics and $UFAR$ are obtained by averaging the conditional distributions given in A5.38, A5.40, A5.41 and A5.45 over all possible values of the order statistic estimated from the Phase I reference sample.

The unconditional run-length distribution, unconditional run-length distribution characteristics and $UFAR$ are given by:

$$P(N_{1-of-1(U)} = j) = \int_0^1 P_C(N_{1-of-1(U)} = j) f_c(\kappa) d\kappa = \int_0^1 \xi(\mathbf{Q})^{j-1} (\mathbf{I} - \mathbf{Q}) \mathbf{1} f_c(\kappa) d\kappa \quad (\text{A5.77})$$

$$ARL_{1-of-1(U)} = \int_0^1 CARL_{1-of-1(U)} f_c(\kappa) d\kappa = \int_0^1 \xi(\mathbf{I} - \mathbf{Q})^{-1} \mathbf{1} f_c(\kappa) d\kappa \quad (\text{A5.78})$$

$$\begin{aligned} VRL_{1-of-1(U)} &= \int_0^1 CVRL_{1-of-1(U)} f_c(\kappa) d\kappa + \int_0^1 (CARL_{1-of-1(U)})^2 f_c(\kappa) d\kappa - \left(\int_0^1 CARL_{1-of-1(U)} f_c(\kappa) d\kappa \right)^2 \\ &= \int_0^1 \xi(\mathbf{I} + \mathbf{Q})(\mathbf{I} - \mathbf{Q})^{-2} \mathbf{1} - (\xi(\mathbf{I} - \mathbf{Q})^{-1} \mathbf{1})^2 f_c(\kappa) d\kappa \\ &\quad + \int_0^1 (\xi(\mathbf{I} - \mathbf{Q})^{-1} \mathbf{1})^2 f_c(\kappa) d\kappa - \left(\int_0^1 \xi(\mathbf{I} - \mathbf{Q})^{-1} \mathbf{1} f_c(\kappa) d\kappa \right)^2 \end{aligned} \quad (\text{A5.79})$$

$$FAR_{1-of-1(U)} = \int_0^1 CFAR_{1-of-1(U)} f_c(\kappa) d\kappa = \int_0^1 (p_{8C} | G = F) f_c(\kappa) d\kappa \quad (\text{A5.80})$$

where $\mathbf{Q} = \mathbf{Q}_{1-of-1(U)}^{Con(2 \times 2)}$ (see A5.23)

$f_c(\kappa)$: is the density of the $u_{(c:m)}$ order statistic (see AR5.8)

$CARL_{1-of-1(U)}$: is given in A5.75 where $\mathbf{Q} = \mathbf{Q}_{1-of-1(U)}^{Con(2 \times 2)}$

$CVRL_{1-of-1(U)}$: is given in A5.76 where $\mathbf{Q} = \mathbf{Q}_{1-of-1(U)}^{Con(2 \times 2)}$

$CFAR_{1-of-1(U)}$ is given in A5.45.

$$\xi = \xi_{1 \times 2} = (1, 0)$$

$$\mathbf{1} = \mathbf{1}_{2 \times 1} = (1, 1)^T$$

$$\mathbf{I} = \mathbf{I}_{2 \times 2}$$

The unconditional distribution, unconditional characteristics of the distribution and *UFAR* are obtained by averaging the conditional distribution, the characteristics of the conditional distribution and *CFAR* given in A5.38, A5.40, A5.41 and A5.45 over the distribution of $\mathbf{Z} = (X_{(cm)})$.

The same approach is used to find the unconditional run-length distribution, unconditional run-length distribution characteristics and *UFAR* for the other charts namely the lower *1-of-1*, two-sided *1-of-1*, upper *2-of-2*, lower *2-of-2*, two-sided *2-of-2*, upper *2-of-3*, lower *2-of-3*, two-sided *2-of-3*, upper *improved 2-of-2*, lower *improved 2-of-2*, two-sided *improved 2-of-2*, upper *improved 2-of-3*, lower *improved 2-of-3* and two-sided *improved 2-of-3*. Note that in the calculations involving the integrals the order statistics $u_{(a:m)}$, $u_{(b:m)}$, $u_{(c:m)}$ and $u_{(d:m)}$ are reduced to integral constants. The order statistics $u_{(a:m)}$, $u_{(b:m)}$, $u_{(c:m)}$ and $u_{(d:m)}$ are replaced by θ , ι , κ and λ respectively in the integrals for notational simplicity.

The derivation of the unconditional run-length distribution, unconditional run-length distribution characteristics and *UFAR* for the different control charts differ slightly since not all the charts condition on the same and same number of Phase I estimated control limits.

Expressions are provided for the unconditional run-length distribution, unconditional run-length distribution characteristics and *UFAR* for the different control charts:

The lower $1\text{-of-}1$ precedence chart

$$P(N_{1\text{-of-}1(L)} = j) = \int_0^1 P_C(N_{1\text{-of-}1(L)} = j) f_b(t) dt = \int_0^1 \xi(\mathbf{Q})^{j-1} (\mathbf{I} - \mathbf{Q}) \mathbf{1} f_b(t) dt \quad (\text{A5.81})$$

$$ARL_{1\text{-of-}1(L)} = \int_0^1 CARL_{1\text{-of-}1(L)} f_b(t) dt = \int_0^1 \xi(\mathbf{I} - \mathbf{Q})^{-1} \mathbf{1} f_b(t) dt \quad (\text{A5.82})$$

$$\begin{aligned} VRL_{1\text{-of-}1(L)} &= \int_0^1 CVRL_{1\text{-of-}1(L)} f_b(t) dt + \int_0^1 (CARL_{1\text{-of-}1(L)})^2 f_b(t) dt - \left(\int_0^1 CARL_{1\text{-of-}1(L)} f_b(t) dt \right)^2 \\ &= \int_0^1 \left(\xi(\mathbf{I} + \mathbf{Q})(\mathbf{I} - \mathbf{Q})^{-2} \mathbf{1} - (\xi(\mathbf{I} - \mathbf{Q})^{-1} \mathbf{1})^2 \right) f_b(t) dt \\ &\quad + \int_0^1 \left(\xi(\mathbf{I} - \mathbf{Q})^{-1} \mathbf{1} \right)^2 f_b(t) dt - \left(\int_0^1 \xi(\mathbf{I} - \mathbf{Q})^{-1} \mathbf{1} f_b(t) dt \right)^2 \end{aligned} \quad (\text{A5.83})$$

$$FAR_{1\text{-of-}1(L)} = \int_0^1 CFAR_{1\text{-of-}1(L)} f_b(t) d\kappa = \int_0^1 (p_{9C} | G = F) f_b(t) d\kappa \quad (\text{A5.84})$$

where $\mathbf{Q} = \mathbf{Q}_{1\text{-of-}1(L)}^{Con(2 \times 2)}$ (see A5.24)

$f_b(t)$: is the density of the $u_{(b,m)}$ order statistic (see AR5.8)

$CARL_{1\text{-of-}1(L)}$: is given in A5.75 where $\mathbf{Q} = \mathbf{Q}_{1\text{-of-}1(L)}^{Con(2 \times 2)}$

$CVRL_{1\text{-of-}1(L)}$: is given in A5.76 where $\mathbf{Q} = \mathbf{Q}_{1\text{-of-}1(L)}^{Con(2 \times 2)}$

$CFAR_{1\text{-of-}1(L)}$: is given in A5.46.

$$\xi = \xi_{1 \times 2} = (1, 0)$$

$$\mathbf{1} = \mathbf{1}_{2 \times 1} = (1, 1)^T$$

$$\mathbf{I} = \mathbf{I}_{2 \times 2}$$

The unconditional distribution, unconditional characteristics of the distribution and $UFAR$ are obtained by averaging the conditional distribution, the characteristics of the conditional distribution and $CFAR$ given in A5.38, A5.40, A5.41 and A5.46 over the distribution of $\mathbf{Z} = (X_{(b,m)})$.

The two-sided I -of- I precedence chart

$$P(N_{1-of-1(T)} = j) = \int_0^1 \int_0^\kappa P_C(N_{1-of-1(T)} = j) f_{bc}(t, \kappa) dt d\kappa = \int_0^1 \int_0^\kappa \xi(\mathbf{Q})^{j-1} (\mathbf{I} - \mathbf{Q}) \mathbf{1} f_{bc}(t, \kappa) dt d\kappa \quad (\text{A5.85})$$

$$ARL_{1-of-1(T)} = \int_0^1 \int_0^\kappa CARL_{1-of-1(T)} f_{bc}(t, \kappa) dt d\kappa = \int_0^1 \int_0^\kappa \xi(\mathbf{I} - \mathbf{Q})^{-1} \mathbf{1} f_{bc}(t, \kappa) dt d\kappa \quad (\text{A5.86})$$

$$\begin{aligned} VRL_{1-of-1(T)} &= \int_0^1 \int_0^\kappa CVRL_{1-of-1(T)} f_{bc}(t, \kappa) dt d\kappa + \int_0^1 \int_0^\kappa (CARL_{1-of-1(T)})^2 f_{bc}(t, \kappa) dt d\kappa \\ &\quad - \left(\int_0^1 \int_0^\kappa CARL_{1-of-1(T)} f_{bc}(t, \kappa) dt d\kappa \right)^2 \\ &= \int_0^1 \int_0^\kappa \left(\xi(\mathbf{I} + \mathbf{Q})(\mathbf{I} - \mathbf{Q})^{-2} \mathbf{1} - (\xi(\mathbf{I} - \mathbf{Q})^{-1} \mathbf{1})^2 \right) f_{bc}(t, \kappa) dt d\kappa \\ &\quad + \int_0^1 \int_0^\kappa (\xi(\mathbf{I} - \mathbf{Q})^{-1} \mathbf{1})^2 f_{bc}(t, \kappa) dt d\kappa - \left(\int_0^1 \int_0^\kappa \xi(\mathbf{I} - \mathbf{Q})^{-1} \mathbf{1} f_{bc}(t, \kappa) dt d\kappa \right)^2 \end{aligned} \quad (\text{A5.87})$$

$$FAR_{1-of-1(T)} = \int_0^1 \int_0^\kappa UFAR_{1-of-1(T)} f_{bc}(t, \kappa) dt d\kappa = \int_0^1 \int_0^\kappa (p_{8C} + p_{9C} | G = F) f_{bc}(t, \kappa) dt d\kappa \quad (\text{A5.88})$$

where $\mathbf{Q} = \mathbf{Q}_{1-of-1(T)}^{Con(2 \times 2)}$ (see A5.25)

$f_{bc}(t, \kappa)$: is the joint density of the order statistics $u_{(b:m)}$ and $u_{(c:m)}$ (see AR5.9)

$CARL_{1-of-1(T)}$: is given in A5.75 where $\mathbf{Q} = \mathbf{Q}_{1-of-1(T)}^{Con(2 \times 2)}$

$CVRL_{1-of-1(T)}$: is given in A5.76 where $\mathbf{Q} = \mathbf{Q}_{1-of-1(T)}^{Con(2 \times 2)}$

$UFAR_{1-of-1(T)}$: is given in A5.47.

$$\xi = \xi_{1 \times 2} = (1, 0)$$

$$\mathbf{1} = \mathbf{1}_{2 \times 1} = (1, 1)^T$$

$$\mathbf{I} = \mathbf{I}_{2 \times 2}$$

The unconditional distribution, the unconditional characteristics of the distribution and *UFAR* are obtained by averaging the conditional distribution, conditional characteristics and *CFAR* given in A5.38, A5.40, A5.41 and A5.47 over the distribution of $\mathbf{Z} = (X_{(b:m)}, X_{(c:m)})$.

The upper one-sided 2-of-2 precedence chart

$$P(N_{2\text{-of-}2(U)} = j) = \int_0^1 P_C(N_{2\text{-of-}2(U)} = j) f_c(\kappa) d\kappa = \int_0^1 \xi(\mathbf{Q})^{j-1} (\mathbf{I} - \mathbf{Q}) \mathbf{1} f_c(\kappa) d\kappa \quad (\text{A5.89})$$

$$ARL_{2\text{-of-}2(U)} = \int_0^1 CARL_{2\text{-of-}2(U)} f_c(\kappa) d\kappa = \int_0^1 \xi(\mathbf{I} - \mathbf{Q})^{-1} \mathbf{1} f_c(\kappa) d\kappa \quad (\text{A5.90})$$

$$\begin{aligned} VRL_{2\text{-of-}2(U)} &= \int_0^1 CVRL_{2\text{-of-}2(U)} f_c(\kappa) d\kappa + \int_0^1 (CARL_{2\text{-of-}2(U)})^2 f_c(\kappa) d\kappa - \left(\int_0^1 CARL_{2\text{-of-}2(U)} f_c(\kappa) d\kappa \right)^2 \\ &= \int_0^1 \left(\xi(\mathbf{I} + \mathbf{Q})(\mathbf{I} - \mathbf{Q})^{-2} \mathbf{1} - (\xi(\mathbf{I} - \mathbf{Q})^{-1} \mathbf{1})^2 \right) f_c(\kappa) d\kappa \\ &\quad + \int_0^1 \left(\xi(\mathbf{I} - \mathbf{Q})^{-1} \mathbf{1} \right)^2 f_c(\kappa) d\kappa - \left(\int_0^1 \xi(\mathbf{I} - \mathbf{Q})^{-1} \mathbf{1} f_c(\kappa) d\kappa \right)^2 \end{aligned} \quad (\text{A5.91})$$

$$FAR_{2\text{-of-}2(U)} = \int_0^1 CFAR_{2\text{-of-}2(U)} f_c(\kappa) d\kappa = \int_0^1 \left((p_{8C})^2 \mid G = F \right) f_c(\kappa) d\kappa \quad (\text{A5.92})$$

where $\mathbf{Q} = \mathbf{Q}_{2\text{-of-}2(U)}^{Con(3 \times 3)}$ (see A5.26)

$f_c(\kappa)$: is the density of the $u_{(c:m)}$ order statistic (see AR5.8)

$CARL_{2\text{-of-}2(U)}$: is given in A5.75 where $\mathbf{Q} = \mathbf{Q}_{2\text{-of-}2(U)}^{Con(2 \times 2)}$

$CVRL_{2\text{-of-}2(U)}$: is given in A5.76 where $\mathbf{Q} = \mathbf{Q}_{2\text{-of-}2(U)}^{Con(2 \times 2)}$

$CFAR_{2\text{-of-}2(U)}$: is given in A5.48.

$$\xi = \xi_{1 \times 3} = (1, 0, 0)$$

$$\mathbf{1} = \mathbf{1}_{3 \times 1} = (1, 1, 1)^T$$

$$\mathbf{I} = \mathbf{I}_{3 \times 3}$$

The unconditional distribution, the unconditional characteristics of the distribution and *UFAR* are obtained by averaging the conditional distribution, characteristics of the conditional distribution and *CFAR* given in A5.38, A5.40, A5.41 and A5.48 over the distribution of $\mathbf{Z} = (X_{(cm)})$.

The lower one-sided 2-of-2 precedence chart

$$P(N_{2\text{-of-}2(L)} = j) = \int_0^1 P_C(N_{2\text{-of-}2(L)} = j) f_b(t) dt = \int_0^1 \xi(\mathbf{Q})^{j-1} (\mathbf{I} - \mathbf{Q}) \mathbf{1} f_b(t) dt \quad (\text{A5.93})$$

$$ARL_{2\text{-of-}2(L)} = \int_0^1 CARL_{2\text{-of-}2(L)} f_b(t) dt = \int_0^1 \xi(\mathbf{I} - \mathbf{Q})^{-1} \mathbf{1} f_b(t) dt \quad (\text{A5.94})$$

$$\begin{aligned} VRL_{2\text{-of-}2(L)} &= \int_0^1 CVRL_{2\text{-of-}2(L)} f_b(t) dt + \int_0^1 (CARL_{2\text{-of-}2(L)})^2 f_b(t) dt - \left(\int_0^1 CARL_{2\text{-of-}2(L)} f_b(t) dt \right)^2 \\ &= \int_0^1 \left(\xi(\mathbf{I} + \mathbf{Q})(\mathbf{I} - \mathbf{Q})^{-2} \mathbf{1} - (\xi(\mathbf{I} - \mathbf{Q})^{-1} \mathbf{1})^2 \right) f_b(t) dt \\ &\quad + \int_0^1 (\xi(\mathbf{I} - \mathbf{Q})^{-1} \mathbf{1})^2 f_b(t) dt - \left(\int_0^1 \xi(\mathbf{I} - \mathbf{Q})^{-1} \mathbf{1} f_b(t) dt \right)^2 \end{aligned} \quad (\text{A5.95})$$

$$FAR_{2\text{-of-}2(L)} = \int_0^1 CFAR_{2\text{-of-}2(L)} f_b(t) dt = \int_0^1 ((p_{9C})^2 | G = F) f_b(t) dt \quad (\text{A5.96})$$

where $\mathbf{Q} = \mathbf{Q}_{2\text{-of-}2(L)}^{Con(3 \times 3)}$ (see A5.27)

$f_b(t)$: is the density of the $u_{(b;m)}$ order statistic (see AR5.8)

$CARL_{2\text{-of-}2(L)}$: is given in A5.75 where $\mathbf{Q} = \mathbf{Q}_{2\text{-of-}2(L)}^{Con(3 \times 3)}$

$CVRL_{2\text{-of-}2(L)}$: is given in A5.76 where $\mathbf{Q} = \mathbf{Q}_{2\text{-of-}2(L)}^{Con(3 \times 3)}$

$CFAR_{2\text{-of-}2(L)}$: is given in A5.49.

$$\xi = \xi_{1 \times 3} = (1, 0, 0)$$

$$\mathbf{1} = \mathbf{1}_{3 \times 1} = (1, 1, 1)^T$$

$$\mathbf{I} = \mathbf{I}_{3 \times 3}$$

The unconditional distribution, unconditional characteristics of the distribution and *UFAR* are obtained by averaging the conditional distribution, the characteristics of the conditional distribution and *CFAR* given in A5.38, A5.40, A5.41 and A5.49 over the distribution of $\mathbf{Z} = (X_{(b:m)})$.

The two-sided 2-of-2 precedence chart

$$P(N_{2\text{-of-}2(T)} = j) = \int_0^1 \int_0^\kappa P_C(N_{2\text{-of-}2(T)} = j) f_{bc}(t, \kappa) dt d\kappa = \int_0^1 \int_0^\kappa \xi(\mathbf{Q})^{j-1} (\mathbf{I} - \mathbf{Q}) \mathbf{1} f_{bc}(t, \kappa) dt d\kappa \quad (\text{A5.97})$$

$$ARL_{2\text{-of-}2(T)} = \int_0^1 \int_0^\kappa CARL_{2\text{-of-}2(T)} f_{bc}(t, \kappa) dt d\kappa = \int_0^1 \int_0^\kappa \xi(\mathbf{I} - \mathbf{Q})^{-1} \mathbf{1} f_{bc}(t, \kappa) dt d\kappa \quad (\text{A5.98})$$

$$\begin{aligned} VRL_{2\text{-of-}2(T)} &= \int_0^1 \int_0^\kappa CVRL_{2\text{-of-}2(T)} f_{bc}(t, \kappa) dt d\kappa + \int_0^1 \int_0^\kappa (CARL_{2\text{-of-}2(T)})^2 f_{bc}(t, \kappa) dt d\kappa \\ &\quad - \left(\int_0^1 \int_0^\kappa CARL_{2\text{-of-}2(T)} f_{bc}(t, \kappa) dt d\kappa \right)^2 \\ &= \int_0^1 \int_0^\kappa \left(\xi(\mathbf{I} + \mathbf{Q})(\mathbf{I} - \mathbf{Q})^{-2} \mathbf{1} - (\xi(\mathbf{I} - \mathbf{Q})^{-1} \mathbf{1})^2 \right) f_{bc}(t, \kappa) dt d\kappa \\ &\quad + \int_0^1 \int_0^\kappa (\xi(\mathbf{I} - \mathbf{Q})^{-1} \mathbf{1})^2 f_{bc}(t, \kappa) dt d\kappa - \left(\int_0^1 \int_0^\kappa \xi(\mathbf{I} - \mathbf{Q})^{-1} \mathbf{1} f_{bc}(t, \kappa) dt d\kappa \right)^2 \end{aligned} \quad (\text{A5.99})$$

$$FAR_{2\text{-of-}2(T)} = \int_0^1 \int_0^\kappa CFAR_{2\text{-of-}2(T)} f_{bc}(t, \kappa) dt d\kappa = \int_0^1 \int_0^\kappa \left((p_{8C})^2 + (p_{9C})^2 \mid G = F \right) f_{bc}(t, \kappa) dt d\kappa \quad (\text{A5.100})$$

where $\mathbf{Q} = \mathbf{Q}_{2\text{-of-}2(T)}^{Con(4 \times 4)}$ (see A5.28)

$f_{bc}(t, \kappa)$: is the joint density of the order statistics $u_{(b:m)}$ and $u_{(c:m)}$ (see AR5.9)

$CARL_{2\text{-of-}2(T)}$: is given in A5.75 where $\mathbf{Q} = \mathbf{Q}_{2\text{-of-}2(T)}^{Con(4 \times 4)}$

$CVRL_{2\text{-of-}2(T)}$: is given in A5.76 where $\mathbf{Q} = \mathbf{Q}_{2\text{-of-}2(T)}^{Con(4 \times 4)}$

$CFAR_{2\text{-of-}2(T)}$: is given in A5.50.

$$\xi = \xi_{1 \times 4} = (1, \dots, 0)$$

$$\mathbf{1} = \mathbf{1}_{4 \times 1} = (1, \dots, 1)^T$$

$$\mathbf{I} = \mathbf{I}_{4 \times 4}$$

The unconditional distribution, the unconditional characteristics of the distribution and *UFAR* are obtained by averaging the conditional distribution, the characteristics of the conditional distribution and *CFAR* given in A5.38, A5.40, A5.41 and A5.50 over the distribution of $\mathbf{Z} = (X_{(b,m)}, X_{(c,m)})$.

The upper one-sided 2-of-3 precedence chart

$$P(N_{2\text{-of-}3(U)} = j) = \int_0^1 P_C(N_{2\text{-of-}3(U)} = j) f_c(\kappa) d\kappa = \int_0^1 \xi(\mathbf{Q})^{j-1} (\mathbf{I} - \mathbf{Q}) \mathbf{1} f_c(\kappa) d\kappa \quad (\text{A5.101})$$

$$ARL_{2\text{-of-}3(U)} = \int_0^1 CARL_{2\text{-of-}3(U)} f_c(\kappa) d\kappa = \int_0^1 \xi(\mathbf{I} - \mathbf{Q})^{-1} \mathbf{1} f_c(\kappa) d\kappa \quad (\text{A5.102})$$

$$\begin{aligned} VRL_{2\text{-of-}3(U)} &= \int_0^1 CVRL_{2\text{-of-}3(U)} f_c(\kappa) d\kappa + \int_0^1 (CARL_{2\text{-of-}3(U)})^2 f_c(\kappa) d\kappa - \left(\int_0^1 CARL_{2\text{-of-}3(U)} f_c(\kappa) d\kappa \right)^2 \\ &= \int_0^1 \left(\xi(\mathbf{I} + \mathbf{Q})(\mathbf{I} - \mathbf{Q})^{-2} \mathbf{1} - (\xi(\mathbf{I} - \mathbf{Q})^{-1} \mathbf{1})^2 \right) f_c(\kappa) d\kappa \\ &\quad + \int_0^1 \left(\xi(\mathbf{I} - \mathbf{Q})^{-1} \mathbf{1} \right)^2 f_c(\kappa) d\kappa - \left(\int_0^1 \xi(\mathbf{I} - \mathbf{Q})^{-1} \mathbf{1} f_c(\kappa) d\kappa \right)^2 \end{aligned} \quad (\text{A5.103})$$

$$FAR_{2\text{-of-}3(U)} = \int_0^1 CFAR_{2\text{-of-}3(U)} f_c(\kappa) d\kappa \quad (\text{A5.104})$$

where $\mathbf{Q} = \mathbf{Q}_{2\text{-of-}3(U)}^{Con(5 \times 5)}$ (see A5.29)

$f_c(\kappa)$: is the density of the $u_{(c,m)}$ order statistic (see AR5.8)

$CARL_{2\text{-of-}3(U)}$: is given in A5.75 where $\mathbf{Q} = \mathbf{Q}_{2\text{-of-}3(U)}^{Con(5 \times 5)}$

$CVRL_{2\text{-of-}3(U)}$: is given in A5.76 where $\mathbf{Q} = \mathbf{Q}_{2\text{-of-}3(U)}^{Con(5 \times 5)}$

$CFAR_{2\text{-of-}3(U)}$: is given in A5.51 and A5.52.

$$\xi = \xi_{1 \times 5} = (1, \dots, 0)$$

$$\mathbf{1} = \mathbf{1}_{5 \times 1} = (1, \dots, 1)^T$$

$$\mathbf{I} = \mathbf{I}_{5 \times 5}$$

The unconditional distribution, unconditional characteristics of the distribution and *UFAR* are obtained by averaging the conditional distribution, the characteristics of the conditional distribution and *CFAR* given in A5.38, A5.40, A5.41, A5.51 and A5.52 over the distribution of $\mathbf{Z} = (X_{(c:m)})$.

The lower one-sided 2-of-3 precedence chart

$$P(N_{2\text{-of-}3(L)} = j) = \int_0^1 P_C(N_{2\text{-of-}3(L)} = j) f_b(t) dt = \int_0^1 \xi(\mathbf{Q})^{j-1} (\mathbf{I} - \mathbf{Q}) \mathbf{1} f_b(t) dt \quad (\text{A5.105})$$

$$ARL_{2\text{-of-}3(L)} = \int_0^1 CARL_{2\text{-of-}3(L)} f_b(t) dt = \int_0^1 \xi(\mathbf{I} - \mathbf{Q})^{-1} \mathbf{1} f_b(t) dt \quad (\text{A5.106})$$

$$\begin{aligned} VRL_{2\text{-of-}3(L)} &= \int_0^1 CVRL_{2\text{-of-}3(L)} f_b(t) dt + \int_0^1 (CARL_{2\text{-of-}3(L)})^2 f_b(t) dt - \left(\int_0^1 CARL_{2\text{-of-}3(L)} f_b(t) dt \right)^2 \\ &= \int_0^1 \left(\xi(\mathbf{I} + \mathbf{Q})(\mathbf{I} - \mathbf{Q})^{-2} \mathbf{1} - (\xi(\mathbf{I} - \mathbf{Q})^{-1} \mathbf{1})^2 \right) f_b(t) dt \\ &\quad + \int_0^1 \left(\xi(\mathbf{I} - \mathbf{Q})^{-1} \mathbf{1} \right)^2 f_b(t) dt - \left(\int_0^1 \xi(\mathbf{I} - \mathbf{Q})^{-1} \mathbf{1} f_b(t) dt \right)^2 \end{aligned} \quad (\text{A5.107})$$

$$FAR_{2\text{-of-}3(L)} = \int_0^1 CFAR_{2\text{-of-}3(L)} f_b(t) dt \quad (\text{A5.108})$$

where $\mathbf{Q} = \mathbf{Q}_{2\text{-of-}3(L)}^{Con(5 \times 5)}$ (see A5.30)

$f_b(t)$: is the density of the $u_{(b:m)}$ order statistic (see AR5.8)

$CARL_{2\text{-of-}3(L)}$: is given in A5.75 where $\mathbf{Q} = \mathbf{Q}_{2\text{-of-}3(L)}^{Con(5 \times 5)}$

$CVRL_{2\text{-of-}3(L)}$: is given in A5.76 where $\mathbf{Q} = \mathbf{Q}_{2\text{-of-}3(L)}^{Con(5 \times 5)}$

$CFAR_{2\text{-of-}3(L)}$: is given in A5.53 and A5.54.

$$\xi = \xi_{1 \times 5} = (1, \dots, 0)$$

$$\mathbf{1} = \mathbf{1}_{5 \times 1} = (1, \dots, 1)^T$$

$$\mathbf{I} = \mathbf{I}_{5 \times 5}$$

The unconditional distribution, the unconditional characteristics of the distribution and *UFAR* are obtained by averaging the conditional distribution, the characteristics of the conditional distribution and *CFAR* given in A5.38, A5.40, A5.41, A5.53 and A5.54 over the distribution of $\mathbf{Z} = (X_{(b:m)})$.

The two-sided 2-of-3 precedence chart

$$P(N_{2\text{-of-}3(T)} = j) = \int_0^1 \int_0^\kappa P_C(N_{2\text{-of-}3(T)} = j) f_{bc}(t, \kappa) dtd\kappa = \int_0^1 \int_0^\kappa \xi(\mathbf{Q})^{j-1} (\mathbf{I} - \mathbf{Q}) \mathbf{1} f_{bc}(t, \kappa) dtd\kappa \quad (\text{A5.109})$$

$$ARL_{2\text{-of-}3(T)} = \int_0^1 \int_0^\kappa CARL_{2\text{-of-}3(T)} f_{bc}(t, \kappa) dtd\kappa = \int_0^1 \int_0^\kappa \xi(\mathbf{I} - \mathbf{Q})^{-1} \mathbf{1} f_{bc}(t, \kappa) dtd\kappa \quad (\text{A5.110})$$

$$\begin{aligned} VRL_{2\text{-of-}3(T)} &= \int_0^1 \int_0^\kappa CVRL_{2\text{-of-}3(T)} f_{bc}(t, \kappa) dtd\kappa + \int_0^1 \int_0^\kappa (CARL_{2\text{-of-}3(T)})^2 f_{bc}(t, \kappa) dtd\kappa \\ &\quad - \left(\int_0^1 \int_0^\kappa CARL_{2\text{-of-}3(T)} f_{bc}(t, \kappa) dtd\kappa \right)^2 \\ &= \int_0^1 \int_0^\kappa \left(\xi(\mathbf{I} + \mathbf{Q})(\mathbf{I} - \mathbf{Q})^{-2} \mathbf{1} - (\xi(\mathbf{I} - \mathbf{Q})^{-1} \mathbf{1})^2 \right) f_{bc}(t, \kappa) dtd\kappa \\ &\quad + \int_0^1 \int_0^\kappa (\xi(\mathbf{I} - \mathbf{Q})^{-1} \mathbf{1})^2 f_{bc}(t, \kappa) dtd\kappa - \left(\int_0^1 \int_0^\kappa \xi(\mathbf{I} - \mathbf{Q})^{-1} \mathbf{1} f_{bc}(t, \kappa) dtd\kappa \right)^2 \end{aligned} \quad (\text{A5.111})$$

$$FAR_{2\text{-of-}3(T)} = \int_0^1 \int_0^\kappa CFAR_{2\text{-of-}3(T)} f_{bc}(t, \kappa) dtd\kappa \quad (\text{A5.112})$$

where $\mathbf{Q} = \mathbf{Q}_{2\text{-of-}3(T)}^{Con(8 \times 8)}$ (see A5.31)

$f_{bc}(t, \kappa)$: is the joint density of the order statistics $u_{(b:m)}$ and $u_{(c:m)}$ (see AR5.9)

$CARL_{2\text{-of-}3(T)}$: is given in A5.75 where $\mathbf{Q} = \mathbf{Q}_{2\text{-of-}3(T)}^{Con(8 \times 8)}$

$CVRL_{2\text{-of-}3(T)}$: is given in A5.76 where $\mathbf{Q} = \mathbf{Q}_{2\text{-of-}3(T)}^{Con(8 \times 8)}$

$CFAR_{2\text{-of-}3(T)}$: is given in A5.55 and A5.56.

$$\xi = \xi_{1 \times 8} = (1, \dots, 0)$$

$$\mathbf{1} = \mathbf{1}_{8 \times 1} = (1, \dots, 1)^T$$

$$\mathbf{I} = \mathbf{I}_{8 \times 8}$$

The unconditional distribution, the unconditional characteristics of the distribution and *UFAR* are obtained by averaging the conditional distribution, characteristics of the conditional distribution and *CFAR* given in A5.38, A5.40, A5.41, A5.55 and A5.56 over the distribution of $\mathbf{Z} = (X_{(b:m)}, X_{(c:m)})$.

The upper one-sided *improved 2-of-2* precedence chart

$$P(N_{12\text{-of-}2(U)} = j) = \int_0^1 \int_0^\lambda P_C(N_{12\text{-of-}2(U)} = j) f_{cd}(\kappa, \lambda) d\kappa d\lambda = \int_0^1 \int_0^\lambda \xi(\mathbf{Q})^{j-1} (\mathbf{I} - \mathbf{Q}) \mathbf{1} f_{cd}(\kappa, \lambda) d\kappa d\lambda \quad (\text{A5.113})$$

$$ARL_{12\text{-of-}2(U)} = \int_0^1 \int_0^\lambda CARL_{12\text{-of-}2(U)} f_{cd}(\kappa, \lambda) d\kappa d\lambda = \int_0^1 \int_0^\lambda \xi(\mathbf{I} - \mathbf{Q})^{-1} \mathbf{1} f_{cd}(\kappa, \lambda) d\kappa d\lambda \quad (\text{A5.114})$$

$$\begin{aligned} VRL_{12\text{-of-}2(U)} &= \int_0^1 \int_0^\lambda CVRL_{12\text{-of-}2(U)} f_{cd}(\kappa, \lambda) d\kappa d\lambda + \int_0^1 \int_0^\lambda (CARL_{12\text{-of-}2(U)})^2 f_{cd}(\kappa, \lambda) d\kappa d\lambda \\ &\quad - \left(\int_0^1 \int_0^\lambda CARL_{12\text{-of-}2(U)} f_{cd}(\kappa, \lambda) d\kappa d\lambda \right)^2 \\ &= \int_0^1 \int_0^\lambda \left(\xi(\mathbf{I} + \mathbf{Q})(\mathbf{I} - \mathbf{Q})^{-2} \mathbf{1} - (\xi(\mathbf{I} - \mathbf{Q})^{-1} \mathbf{1})^2 \right) f_{cd}(\kappa, \lambda) d\kappa d\lambda \\ &\quad + \int_0^1 \int_0^\lambda \left(\xi(\mathbf{I} - \mathbf{Q})^{-1} \mathbf{1} \right)^2 f_{cd}(\kappa, \lambda) d\kappa d\lambda - \left(\int_0^1 \int_0^\lambda \xi(\mathbf{I} - \mathbf{Q})^{-1} \mathbf{1} f_{cd}(\kappa, \lambda) d\kappa d\lambda \right)^2 \end{aligned} \quad (\text{A5.115})$$

$$FAR_{12\text{-of-}2(U)} = \int_0^1 \int_0^\lambda CFAR_{12\text{-of-}2(U)} f_{cd}(\kappa, \lambda) d\kappa d\lambda \quad (\text{A5.116})$$

where $\mathbf{Q} = \mathbf{Q}_{12\text{-of-}2(U)}^{\text{Con}(3 \times 3)}$ (see A5.32)

$f_{cd}(\kappa, \lambda)$: is the joint density of the order statistics $u_{(c:m)}$ $u_{(d:m)}$ (see AR5.9)

$CARL_{12\text{-of-}2(U)}$: is given in A5.75 where $\mathbf{Q} = \mathbf{Q}_{12\text{-of-}2(U)}^{\text{Con}(3 \times 3)}$

$CVRL_{12\text{-of-}2(U)}$: is given in A5.76 where $\mathbf{Q} = \mathbf{Q}_{12\text{-of-}2(U)}^{\text{Con}(3 \times 3)}$

$CFAR_{12\text{-of-}2(U)}$: is given in A5.57 and A5.58.

$$\xi = \xi_{1 \times 3} = (1,0,0)$$

$$\mathbf{1} = \mathbf{1}_{3 \times 1} = (1,1,1)^T$$

$$\mathbf{I} = \mathbf{I}_{3 \times 3}$$

The unconditional distribution, the characteristics of the unconditional distribution and $UFAR$ are obtained by averaging the conditional distribution, the characteristics of the conditional distribution and $CFAR$ given in A5.38, A5.40, A5.41, A5.57 and A5.58 over the distribution of $\mathbf{Z} = (X_{(c:m)}, X_{(d:m)})$.

The lower one-sided *improved 2-of-2* precedence chart

$$P(N_{12\text{-of-}2(L)} = j) = \int_0^1 \int_0^t P_C(N_{12\text{-of-}2(L)} = j) f_{ab}(\theta, t) d\theta dt = \int_0^1 \int_0^t \xi(\mathbf{Q})^{j-1} (\mathbf{I} - \mathbf{Q}) \mathbf{1} f_{ab}(\theta, t) d\theta dt \quad (\text{A5.117})$$

$$ARL_{12\text{-of-}2(L)} = \int_0^1 \int_0^t CARL_{12\text{-of-}2(L)} f_{ab}(\theta, t) d\theta dt = \int_0^1 \int_0^t \xi(\mathbf{I} - \mathbf{Q})^{-1} \mathbf{1} f_{ab}(\theta, t) d\theta dt \quad (\text{A5.118})$$

$$\begin{aligned} VRL_{12\text{-of-}2(L)} &= \int_0^1 \int_0^t CVRL_{12\text{-of-}2(L)} f_{ab}(\theta, t) d\theta dt + \int_0^1 \int_0^t (CARL_{12\text{-of-}2(L)})^2 f_{ab}(\theta, t) d\theta dt \\ &\quad - \left(\int_0^1 \int_0^t CARL_{12\text{-of-}2(L)} f_{ab}(\theta, t) d\theta dt \right)^2 \\ &= \int_0^1 \int_0^t \left(\xi(\mathbf{I} + \mathbf{Q})(\mathbf{I} - \mathbf{Q})^{-2} \mathbf{1} - (\xi(\mathbf{I} - \mathbf{Q})^{-1} \mathbf{1})^2 \right) f_{ab}(\theta, t) d\theta dt \\ &\quad + \int_0^1 \int_0^t (\xi(\mathbf{I} - \mathbf{Q})^{-1} \mathbf{1})^2 f_{ab}(\theta, t) d\theta dt - \left(\int_0^1 \int_0^t \xi(\mathbf{I} - \mathbf{Q})^{-1} \mathbf{1} f_{ab}(\theta, t) d\theta dt \right)^2 \end{aligned} \quad (\text{A5.119})$$

$$FAR_{12\text{-of-}2(L)} = \int_0^1 \int_0^t CFAR_{12\text{-of-}2(L)} f_{ab}(\theta, t) d\theta dt \quad (\text{A5.120})$$

where $\mathbf{Q} = \mathbf{Q}_{12\text{-of-}2(L)}^{Con(3 \times 3)}$ (see A5.33)

$f_{ab}(\theta, t)$: is the joint density of the order statistics $u_{(a:m)}$ $u_{(b:m)}$ (see AR5.9)

$CARL_{12\text{-of-}2(L)}$: is given in A5.75 where $\mathbf{Q} = \mathbf{Q}_{12\text{-of-}2(L)}^{Con(3 \times 3)}$

$CVRL_{12\text{-of-}2(L)}$: is given in A5.76 where $\mathbf{Q} = \mathbf{Q}_{12\text{-of-}2(L)}^{Con(3 \times 3)}$

$CFAR_{I2-of-2(L)}$: is given in A5.59 and A5.60.

$$\xi = \xi_{1 \times 3} = (1, 0, 0)$$

$$\mathbf{1} = \mathbf{1}_{3 \times 1} = (1, 1, 1)^T$$

$$\mathbf{I} = \mathbf{I}_{3 \times 3}$$

The unconditional distribution, the unconditional characteristics of the distribution and $UFAR$ are obtained by averaging the conditional distribution, the characteristics of the conditional distribution and $CFAR$ given in A5.38, A5.40, A5.41, A5.59 and A5.60 over the distribution of $\mathbf{Z} = (X_{(a:m)}, X_{(b:m)})$.

The two-sided *improved 2-of-2* precedence chart

$$\begin{aligned} P(N_{I2-of-2(T)} = j) &= \int_0^1 \int_0^\lambda \int_0^\kappa \int_0^t P_C(N_{I2-of-2(T)} = j) f_{abcd}(\theta, \iota, \kappa, \lambda) d\theta d\iota d\kappa d\lambda \\ &= \int_0^1 \int_0^\lambda \int_0^\kappa \int_0^t \xi(\mathbf{Q})^{j-1} (\mathbf{I} - \mathbf{Q}) \mathbf{1} f_{abcd}(\theta, \iota, \kappa, \lambda) d\theta d\iota d\kappa d\lambda \end{aligned} \quad (\text{A5.121})$$

$$\begin{aligned} ARL_{I2-of-2(T)} &= \int_0^1 \int_0^\lambda \int_0^\kappa \int_0^t CARL_{I2-of-2(T)} f_{abcd}(\theta, \iota, \kappa, \lambda) d\theta d\iota d\kappa d\lambda \\ &= \int_0^1 \int_0^\lambda \int_0^\kappa \int_0^t \xi(\mathbf{I} - \mathbf{Q})^{-1} \mathbf{1} f_{abcd}(\theta, \iota, \kappa, \lambda) d\theta d\iota d\kappa d\lambda \end{aligned} \quad (\text{A5.122})$$

$$\begin{aligned} VRL_{I2-of-2(T)} &= \int_0^1 \int_0^\lambda \int_0^\kappa \int_0^t CVRL_{I2-of-2(T)} f_{abcd}(\theta, \iota, \kappa, \lambda) d\theta d\iota d\kappa d\lambda \\ &\quad + \int_0^1 \int_0^\lambda \int_0^\kappa \int_0^t (CARL_{I2-of-2(T)})^2 f_{abcd}(\theta, \iota, \kappa, \lambda) d\theta d\iota d\kappa d\lambda \\ &\quad - \left(\int_0^1 \int_0^\lambda \int_0^\kappa \int_0^t CARL_{I2-of-2(T)} f_{abcd}(\theta, \iota, \kappa, \lambda) d\theta d\iota d\kappa d\lambda \right)^2 \\ &= \int_0^1 \int_0^\lambda \int_0^\kappa \int_0^t \left(\xi(\mathbf{I} + \mathbf{Q})(\mathbf{I} - \mathbf{Q})^{-2} \mathbf{1} - (\xi(\mathbf{I} - \mathbf{Q})^{-1} \mathbf{1})^2 \right) f_{abcd}(\theta, \iota, \kappa, \lambda) d\theta d\iota d\kappa d\lambda \\ &\quad + \int_0^1 \int_0^\lambda \int_0^\kappa \int_0^t (\xi(\mathbf{I} - \mathbf{Q})^{-1} \mathbf{1})^2 f_{abcd}(\theta, \iota, \kappa, \lambda) d\theta d\iota d\kappa d\lambda \\ &\quad - \left(\int_0^1 \int_0^\lambda \int_0^\kappa \int_0^t \xi(\mathbf{I} - \mathbf{Q})^{-1} \mathbf{1} f_{abcd}(\theta, \iota, \kappa, \lambda) d\theta d\iota d\kappa d\lambda \right)^2 \end{aligned} \quad (\text{A5.123})$$

$$FAR_{12\text{-of-}2(T)} = \int_0^1 \int_0^\lambda \int_0^\kappa \int_0^\iota CFAR_{12\text{-of-}2(T)} f_{abcd}(\theta, \iota, \kappa, \lambda) d\theta d\iota d\kappa d\lambda \quad (\text{A5.124})$$

where $\mathbf{Q} = \mathbf{Q}_{12\text{-of-}2(T)}^{Con(4 \times 4)}$ (see A5.34)

$f_{abcd}(\theta, \iota, \kappa, \lambda)$: is the joint density of the order statistics $u_{(a:m)}$, $u_{(b:m)}$, $u_{(c:m)}$ and $u_{(d:m)}$ (see AR5.10)

$CARL_{12\text{-of-}2(T)}$: is given in A5.75 where $\mathbf{Q} = \mathbf{Q}_{12\text{-of-}2(T)}^{Con(4 \times 4)}$

$CVRL_{12\text{-of-}2(T)}$: is given in A5.76 where $\mathbf{Q} = \mathbf{Q}_{12\text{-of-}2(T)}^{Con(4 \times 4)}$

$CFAR_{12\text{-of-}2(T)}$: is given in A5.61 and A5.62.

$$\xi = \xi_{1 \times 4} = (1, 0, 0, 0)$$

$$\mathbf{1} = \mathbf{1}_{4 \times 1} = (1, 1, 1, 1)^T$$

$$\mathbf{I} = \mathbf{I}_{4 \times 4}$$

The unconditional distribution, the unconditional characteristics of the distribution and $UFAR$ are obtained by averaging the conditional distribution, the characteristics of the conditional distribution and $CFAR$ given in A5.38, A5.40, A5.41, A5.61 and A5.62 over the distribution of $\mathbf{Z} = (X_{(a:m)}, X_{(b:m)}, X_{(c:m)}, X_{(d:m)})$.

The upper one-sided *improved 2-of-3* precedence chart

$$P(N_{12\text{-of-}3(U)} = j) = \int_0^1 \int_0^\lambda P_C(N_{12\text{-of-}3(U)} = j) f_{cd}(\kappa, \lambda) d\kappa d\lambda = \int_0^1 \int_0^\lambda \xi(\mathbf{Q})^{j-1} (\mathbf{I} - \mathbf{Q}) \mathbf{1} f_{cd}(\kappa, \lambda) d\kappa d\lambda \quad (\text{A5.125})$$

$$ARL_{12\text{-of-}3(U)} = \int_0^1 \int_0^\lambda CARL_{12\text{-of-}3(U)} f_{cd}(\kappa, \lambda) d\kappa d\lambda = \int_0^1 \int_0^\lambda \xi(\mathbf{I} - \mathbf{Q})^{-1} \mathbf{1} f_{cd}(\kappa, \lambda) d\kappa d\lambda \quad (\text{A5.126})$$

$$VRL_{12\text{-of-}3(U)} = \int_0^1 \int_0^\lambda CVRL_{12\text{-of-}3(U)} f_{cd}(\kappa, \lambda) d\kappa d\lambda + \int_0^1 \int_0^\lambda (CARL_{12\text{-of-}3(U)})^2 f_{cd}(\kappa, \lambda) d\kappa d\lambda - \left(\int_0^1 \int_0^\lambda CARL_{12\text{-of-}3(U)} f_{cd}(\kappa, \lambda) d\kappa d\lambda \right)^2$$

$$\begin{aligned}
 &= \int_0^1 \int_0^\lambda \left(\xi(\mathbf{I} + \mathbf{Q})(\mathbf{I} - \mathbf{Q})^{-2} \mathbf{1} - (\xi(\mathbf{I} - \mathbf{Q})^{-1} \mathbf{1})^2 \right) f_{cd}(\kappa, \lambda) d\kappa d\lambda \\
 &\quad + \int_0^1 \int_0^\lambda (\xi(\mathbf{I} - \mathbf{Q})^{-1} \mathbf{1})^2 f_{cd}(\kappa, \lambda) d\kappa d\lambda - \left(\int_0^1 \int_0^\lambda \xi(\mathbf{I} - \mathbf{Q})^{-1} \mathbf{1} f_{cd}(\kappa, \lambda) d\kappa d\lambda \right)^2
 \end{aligned} \tag{A5.127}$$

$$FAR_{12\text{-of-}3(U)} = \int_0^1 \int_0^\lambda CFAR_{12\text{-of-}3(U)} f_{cd}(\kappa, \lambda) d\kappa d\lambda = \int_0^1 \int_0^\lambda \xi(\mathbf{Q})^{j-1} (\mathbf{I} - \mathbf{Q}) \mathbf{1} f_{cd}(\kappa, \lambda) d\kappa d\lambda \tag{A5.128}$$

where $\mathbf{Q} = \mathbf{Q}_{12\text{-of-}3(U)}^{Con(5 \times 5)}$ (see A5.35)

$f_{cd}(\kappa, \lambda)$: is the joint density of the order statistics $u_{(cm)}$ $u_{(dm)}$ (see AR5.9)

$CARL_{12\text{-of-}3(U)}$: is given in A5.75 where $\mathbf{Q} = \mathbf{Q}_{12\text{-of-}3(U)}^{Con(5 \times 5)}$

$CVRL_{12\text{-of-}3(U)}$: is given in A5.76 where $\mathbf{Q} = \mathbf{Q}_{12\text{-of-}3(U)}^{Con(5 \times 5)}$

$CFAR_{12\text{-of-}3(U)}$: is given in A5.63, A5.64 and A5.65.

$$\xi = \xi_{1 \times 5} = (1, \dots, 0)$$

$$\mathbf{1} = \mathbf{1}_{5 \times 1} = (1, \dots, 1)^T$$

$$\mathbf{I} = \mathbf{I}_{5 \times 5}$$

The unconditional distribution, the unconditional characteristics of the distribution and $UFAR$ are obtained by averaging the conditional distribution, the characteristics of the conditional distribution and $CFAR$ given in A5.38, A5.40, A5.41, A5.63, A5.64 and A5.65 over the distribution of $\mathbf{Z} = (X_{(cm)}, X_{(dm)})$.

The lower one-sided *improved 2-of-3* precedence chart

$$P(N_{12\text{-of-}3(L)} = j) = \int_0^1 \int_0^t P_C(N_{12\text{-of-}3(L)} = j) f_{ab}(\theta, t) d\theta dt = \int_0^1 \int_0^t \xi(\mathbf{Q})^{j-1} (\mathbf{I} - \mathbf{Q}) \mathbf{1} f_{ab}(\theta, t) d\theta dt \tag{A5.129}$$

$$ARL_{12\text{-of-}3(L)} = \int_0^1 \int_0^t CARL_{12\text{-of-}3(L)} f_{ab}(\theta, t) d\theta dt = \int_0^1 \int_0^t \xi(\mathbf{I} - \mathbf{Q})^{-1} \mathbf{1} f_{ab}(\theta, t) d\theta dt \tag{A5.130}$$

$$\begin{aligned}
 VRL_{12\text{-of-}3(L)} &= \int_0^1 \int_0^t CVRL_{12\text{-of-}3(L)} f_{ab}(\theta, t) d\theta dt + \int_0^1 \int_0^t \left(CARL_{12\text{-of-}3(L)} \right)^2 f_{ab}(\theta, t) d\theta dt \\
 &\quad - \left(\int_0^1 \int_0^t CARL_{12\text{-of-}3(L)} f_{ab}(\theta, t) d\theta dt \right)^2 \\
 &= \int_0^1 \int_0^t \left(\xi(\mathbf{I} + \mathbf{Q})(\mathbf{I} - \mathbf{Q})^{-2} \mathbf{1} - \left(\xi(\mathbf{I} - \mathbf{Q})^{-1} \mathbf{1} \right)^2 \right) f_{ab}(\theta, t) d\theta dt \\
 &\quad + \int_0^1 \int_0^t \left(\xi(\mathbf{I} - \mathbf{Q})^{-1} \mathbf{1} \right)^2 f_{ab}(\theta, t) d\theta dt - \left(\int_0^1 \int_0^t \xi(\mathbf{I} - \mathbf{Q})^{-1} \mathbf{1} f_{ab}(\theta, t) d\theta dt \right)^2
 \end{aligned} \tag{A5.131}$$

$$FAR_{12\text{-of-}3(L)} = \int_0^1 \int_0^t CFAR_{12\text{-of-}3(L)} f_{ab}(\theta, t) d\theta dt \tag{A5.132}$$

where $\mathbf{Q} = \mathbf{Q}_{12\text{-of-}3(L)}^{Con(5 \times 5)}$ (see A5.36)

$f_{ab}(\theta, t)$: is the joint density of the order statistics $u_{(a:m)}$ $u_{(b:m)}$ (see AR5.9)

$CARL_{12\text{-of-}3(L)}$: is given in A5.75 where $\mathbf{Q} = \mathbf{Q}_{12\text{-of-}3(L)}^{Con(5 \times 5)}$

$CVRL_{12\text{-of-}3(L)}$: is given in A5.76 where $\mathbf{Q} = \mathbf{Q}_{12\text{-of-}3(L)}^{Con(5 \times 5)}$

$CFAR_{12\text{-of-}3(L)}$: is given in A5.66, A5.67 and A5.68.

$$\xi = \xi_{1 \times 5} = (1, \dots, 0)$$

$$\mathbf{1} = \mathbf{1}_{5 \times 1} = (1, \dots, 1)^T$$

$$\mathbf{I} = \mathbf{I}_{5 \times 5}$$

The unconditional distribution, the unconditional characteristics of the distribution and $UFAR$ are obtained by averaging the conditional distribution, the characteristics of the conditional distribution and $CFAR$ given in A5.38, A5.40, A5.41, A5.66, A5.67 and A5.68 over the distribution of $\mathbf{Z} = (X_{(a:m)}, X_{(b:m)})$.

The two-sided *improved 2-of-3* precedence chart

$$\begin{aligned}
 P(N_{12\text{-of-}3(T)} = j) &= \int_0^1 \int_0^\lambda \int_0^\kappa \int_0^t P_C(N_{12\text{-of-}3(T)} = j) f_{abcd}(\theta, \iota, \kappa, \lambda) d\theta d\iota d\kappa d\lambda \\
 &= \int_0^1 \int_0^\lambda \int_0^\kappa \int_0^t \xi(\mathbf{Q})^{j-1} (\mathbf{I} - \mathbf{Q}) \mathbf{1} f_{abcd}(\theta, \iota, \kappa, \lambda) d\theta d\iota d\kappa d\lambda
 \end{aligned} \tag{A5.133}$$

$$\begin{aligned}
 ARL_{12\text{-of-}3(T)} &= \int_0^1 \int_0^\lambda \int_0^\kappa \int_0^t CARL_{12\text{-of-}3(T)} f_{abcd}(\theta, \iota, \kappa, \lambda) d\theta d\iota d\kappa d\lambda \\
 &= \int_0^1 \int_0^\lambda \int_0^\kappa \int_0^t \xi(\mathbf{I} - \mathbf{Q})^{-1} \mathbf{1} f_{abcd}(\theta, \iota, \kappa, \lambda) d\theta d\iota d\kappa d\lambda
 \end{aligned} \tag{A5.134}$$

$$\begin{aligned}
 VRL_{12\text{-of-}3(T)} &= \int_0^1 \int_0^\lambda \int_0^\kappa \int_0^t CVRL_{12\text{-of-}3(T)} f_{abcd}(\theta, \iota, \kappa, \lambda) d\theta d\iota d\kappa d\lambda \\
 &\quad + \int_0^1 \int_0^\lambda \int_0^\kappa \int_0^t (CARL_{12\text{-of-}3(T)})^2 f_{abcd}(\theta, \iota, \kappa, \lambda) d\theta d\iota d\kappa d\lambda \\
 &\quad - \left(\int_0^1 \int_0^\lambda \int_0^\kappa \int_0^t CARL_{12\text{-of-}3(T)} f_{abcd}(\theta, \iota, \kappa, \lambda) d\theta d\iota d\kappa d\lambda \right)^2 \\
 &= \int_0^1 \int_0^\lambda \int_0^\kappa \int_0^t \left(\xi(\mathbf{I} + \mathbf{Q})(\mathbf{I} - \mathbf{Q})^{-2} \mathbf{1} - (\xi(\mathbf{I} - \mathbf{Q})^{-1} \mathbf{1})^2 \right) f_{abcd}(\theta, \iota, \kappa, \lambda) d\theta d\iota d\kappa d\lambda \\
 &\quad + \int_0^1 \int_0^\lambda \int_0^\kappa \int_0^t (\xi(\mathbf{I} - \mathbf{Q})^{-1} \mathbf{1})^2 f_{abcd}(\theta, \iota, \kappa, \lambda) d\theta d\iota d\kappa d\lambda \\
 &\quad - \left(\int_0^1 \int_0^\lambda \int_0^\kappa \int_0^t \xi(\mathbf{I} - \mathbf{Q})^{-1} \mathbf{1} f_{abcd}(\theta, \iota, \kappa, \lambda) d\theta d\iota d\kappa d\lambda \right)^2
 \end{aligned} \tag{A5.135}$$

$$FAR_{12\text{-of-}3(T)} = \int_0^1 \int_0^\lambda \int_0^\kappa \int_0^t CFAR_{12\text{-of-}3(T)} f_{abcd}(\theta, \iota, \kappa, \lambda) d\theta d\iota d\kappa d\lambda \tag{A5.136}$$

where $\mathbf{Q} = \mathbf{Q}_{12\text{-of-}3(T)}^{Con(8 \times 8)}$ (see A5.37)

$f_{abcd}(\theta, \iota, \kappa, \lambda)$: is the joint density of the order statistics $u_{(a:m)}$, $u_{(b:m)}$, $u_{(c:m)}$ and $u_{(d:m)}$ (see AR5.10)

$CARL_{12\text{-of-}3(T)}$: is given in A5.75 where $\mathbf{Q} = \mathbf{Q}_{12\text{-of-}3(T)}^{Con(8 \times 8)}$

$CVRL_{12\text{-of-}3(T)}$: is given in A5.76 where $\mathbf{Q} = \mathbf{Q}_{12\text{-of-}3(T)}^{Con(8 \times 8)}$

$CFAR_{12\text{-of-}3(T)}$: is given in A5.69, A5.70 and A5.71.

$$\boldsymbol{\xi} = \boldsymbol{\xi}_{1 \times 8} = (1, \dots, 0)$$

$$\mathbf{1} = \mathbf{1}_{8 \times 1} = (1, \dots, 1)^T$$

$$\mathbf{I} = \mathbf{I}_{8 \times 8}$$

The unconditional distribution, the unconditional characteristics of the distribution and *UFAR* are obtained by averaging the conditional distribution, the characteristics of the conditional distribution and *CFAR* given in A5.38, A5.40, A5.41, A5.69, A5.70 and A5.71 over the distribution of $\mathbf{Z} = (X_{(a:m)}, X_{(b:m)}, X_{(c:m)}, X_{(d:m)})$.

Appendix: Computer programs

Introduction

The computer programs appendix provides a reference to SAS[®]9.2 and Mathcad[®]14.0 programs. These programs are used to populate the charting constant Tables and performance comparison Tables in Chapters 4 and 5.

SAS Program 1

SAS Program 1 is a program that is used to calculate the IC performance of the sign control charts. This program is used to populate all the IC (charting constant) Tables in Chapter 4.

The SAS Program 1 is written in a general form. The program has sections of code that is enclosed by stars and forward slashes; this is referred to as a block of code. Whenever a block of code appears in the program, the user has to read the caption of the block of code to determine if that block of code needs to be submitted, in order to obtain the desired results. When all the appropriate sections of code are identified and selected, the user may then submit the code to obtain the desired results.

`Proc Iml;`

```
      n = 10;          /*Sample Size*/
      UCLB = 10;       /*Outer Upper Control Limit*/
      UCLA = 8;        /*Inner Upper Control Limit*/
      LCLA = n-UCLA;   /*Inner Lower Control Limit*/
      LCLB = n-UCLB;   /*Outer Lower Control Limit*/

      Info = J(1,12,0);
      med = J(n,1,0);  /*Median Matrix*/
```

```
print n  LCLB LCLA UCLA UCLB;
```

```

/* Transition Probabilities that is used to construct */
/* the essential Transition Probability Matrix */
p0 = 0.5;
p_1 = 1-(CDF('BINOMIAL',UCLB-1,p0,n));
p_2 = (CDF('BINOMIAL',UCLB-1,p0,n))-(CDF('BINOMIAL',UCLA-1,p0,n));
p_3 = (CDF('BINOMIAL',UCLA-1,p0,n))-(CDF('BINOMIAL',LCLA,p0,n));
p_4 = (CDF('BINOMIAL',LCLA,p0,n))-(CDF('BINOMIAL',LCLB,p0,n));
p_5 = (CDF('BINOMIAL',LCLB,p0,n));
p_6 = 1-(CDF('BINOMIAL',LCLA,p0,n));
p_7 = (CDF('BINOMIAL',UCLA-1,p0,n));
p_8 = 1-(CDF('BINOMIAL',UCLA-1,p0,n));
p_9 = CDF('BINOMIAL',LCLA,p0,n);

/**/*****
/**/*****
/**/
/**/      For the Upper One-Sided Improved 2-of-2 sign chart the      /**/
/**/      following block of code needs to be submitted                /**/
/**/
/**/*****
/**/*****
/**/
/**/      * Calculates the FAR ;                                         /**/
/**/      FAR_Exact_1 = (p_1);                                           /**/
/**/      FAR_Exact_234 = (p_2**2)+(p_1);                                /**/
/**/
/**/      Q = J(3,3,0);                                                  /**/
/**/      z = {1 0 0};                                                  /**/
/**/      e = {1 1 1};                                                  /**/
/**/
/**/      /*Populate the essential transition probability matrix*/      /**/
/**/      Q[1,1] = 0; Q[1,2] = p_7; Q[1,3] = p_2;                       /**/
/**/      Q[2,1] = 0; Q[2,2] = p_7; Q[2,3] = p_2;                       /**/
/**/      Q[3,1] = 0; Q[3,2] = p_7; Q[3,3] = 0;                         /**/
/**/
/**/*****
/**/*****

```

```

/**/*****
/**/*****
/**/
/**/      For the Lower One-Sided Improved 2-of-2 sign chart the      /**/
/**/      following block of code needs to be submitted                /**/
/**/
/**/*****
/**/*****
/**/
/**/      * Calculates the FAR ;
/**/      FAR_Exact_1   = (p_5);
/**/      FAR_Exact_234 = (p_4**2)+(p_5);
/**/
/**/      Q = J(3,3,0);
/**/      z = {1 0 0};
/**/      e = {1 1 1};
/**/
/**/      /*Populate the essential transition probability matrix*/
/**/      Q[1,1] = 0; Q[1,2] = p_6; Q[1,3] = p_4;
/**/      Q[2,1] = 0; Q[2,2] = p_6; Q[2,3] = p_4;
/**/      Q[3,1] = 0; Q[3,2] = p_6; Q[3,3] = 0;
/**/
/**/*****
/**/*****

```

```

/**/*****
/**/*****
/**/
/**/      For the Two-Sided Improved 2-of-2 sign chart the      /**/
/**/      following block of code needs to be submitted                /**/
/**/
/**/*****
/**/*****
/**/
/**/      * Calculates the FAR ;
/**/      FAR_Exact_1   = (p_1)+(P_5);
/**/      FAR_Exact_234 = (p_2**2)+(p_1)+(p_4**2)+(p_5);
/**/
/**/      Q = J(4,4,0);
/**/      z = {1 0 0 0};
/**/      e = {1 1 1 1};
/**/
/**/      /*Populate the essential transition probability matrix*/
/**/      Q[1,1] = 0; Q[1,2] = p_3; Q[1,3] = p_2; Q[1,4] = p_4;
/**/      Q[2,1] = 0; Q[2,2] = p_3; Q[2,3] = p_2; Q[2,4] = p_4;
/**/      Q[3,1] = 0; Q[3,2] = p_3; Q[3,3] = 0;   Q[3,4] = p_4;
/**/      Q[4,1] = 0; Q[4,2] = p_3; Q[4,3] = p_2; Q[4,4] = 0;
/**/
/**/*****
/**/*****

```



```

/**/*****
/**/*****
/**/
/**/      For the Upper One-Sided Improved 2-of-3 sign chart the      /**/
/**/      following block of code needs to be submitted                /**/
/**/
/**/*****
/**/*****
/**/
/**/      * Calculates the FAR ;
/**/      FAR_Exact_1 = (p_1);
/**/      FAR_Exact_2 = (p_1)+(p_2*p_2);
/**/      FAR_Exact_345 = (p_1)+(2*(p_7*p_2*p_2));
/**/
/**/      Q = J(5,5,0);
/**/      z = {1 0 0 0 0};
/**/      e = {1 1 1 1 1};
/**/
/**/      /*Populate the essential transition probability matrix*/
/**/      Q[1,1] = 0; Q[1,2] = p_7; Q[1,3] = p_2; Q[1,4] = 0;   Q[1,5] = 0;
/**/      Q[2,1] = 0; Q[2,2] = p_7; Q[2,3] = 0;   Q[2,4] = p_2; Q[2,5] = 0;
/**/      Q[3,1] = 0; Q[3,2] = 0;   Q[3,3] = 0;   Q[3,4] = 0;   Q[3,5] = p_7;
/**/      Q[4,1] = 0; Q[4,2] = 0;   Q[4,3] = 0;   Q[4,4] = 0;   Q[4,5] = p_7;
/**/      Q[5,1] = 0; Q[5,2] = p_7; Q[5,3] = 0;   Q[5,4] = 0;   Q[5,5] = 0;
/**/
/**/*****
/**/*****

```

```

/**/*****
/**/*****
/**/
/**/      For the Lower One-Sided Improved 2-of-3 sign chart the      /**/
/**/      following block of code needs to be submitted                /**/
/**/
/**/*****
/**/*****
/**/
/**/      * Calculates the FAR ;
/**/      FAR_Exact_1 = (p_5);
/**/      FAR_Exact_2 = (p_5)+(p_4*p_4);
/**/      FAR_Exact_345 = (p_5)+(2*(p_6*p_4*p_4));
/**/
/**/      Q = J(5,5,0);
/**/      z = {1 0 0 0 0};
/**/      e = {1 1 1 1 1};
/**/
/**/      /*Populate the essential transition probability matrix*/
/**/      Q[1,1] = 0; Q[1,2] = p_6; Q[1,3] = p_4; Q[1,4] = 0;   Q[1,5] = 0;
/**/      Q[2,1] = 0; Q[2,2] = p_6; Q[2,3] = 0;   Q[2,4] = p_4; Q[2,5] = 0;
/**/      Q[3,1] = 0; Q[3,2] = 0;   Q[3,3] = 0;   Q[3,4] = 0;   Q[3,5] = p_6;
/**/      Q[4,1] = 0; Q[4,2] = 0;   Q[4,3] = 0;   Q[4,4] = 0;   Q[4,5] = p_6;
/**/      Q[5,1] = 0; Q[5,2] = p_6; Q[5,3] = 0;   Q[5,4] = 0;   Q[5,5] = 0;
/**/
/**/*****
/**/*****

```

```

/**/*****
/**/*****
/**/
/**/      For the Two-Sided Improved 2-of-3 sign chart the
/**/      following block of code needs to be submitted
/**/
/**/*****
/**/*****
/**/
/**/      * Calculates the FAR ;
/**/      FAR_Exact_1 = (p_1)+(p_5);
/**/      FAR_Exact_2 = (p_1)+(p_5)+(p_2**2)+(p_4**2);
/**/      FAR_Exact_345 = (p_1)+(p_5)+(2*p_3*(p_2**2))+(2*p_3*(p_4**2))+
/**/                      (p_4*(p_2**2))+(p_2*(p_4**2));
/**/
/**/      Q = J(8,8,0);
/**/      z = {1 0 0 0 0 0 0 0};
/**/      e = {1 1 1 1 1 1 1 1};
/**/
/**/      /*Populate the essential transition probability matrix*/
/**/      Q[1,1] = 0;   Q[1,2] = p_3; Q[1,3] = p_2; Q[1,4] = 0;
/**/      Q[1,5] = 0;   Q[1,6] = p_4; Q[1,7] = 0;   Q[1,8] = 0;
/**/
/**/      Q[2,1] = 0;   Q[2,2] = p_3; Q[2,3] = 0;   Q[2,4] = p_2;
/**/      Q[2,5] = 0;   Q[2,6] = 0;   Q[2,7] = p_4; Q[2,8] = 0;
/**/
/**/      Q[3,1] = 0;   Q[3,2] = 0;   Q[3,3] = 0;   Q[3,4] = 0;
/**/      Q[3,5] = p_3; Q[3,6] = p_4; Q[3,7] = 0;   Q[3,8] = 0;
/**/
/**/      Q[4,1] = 0;   Q[4,2] = 0;   Q[4,3] = 0;   Q[4,4] = 0;
/**/      Q[4,5] = p_3; Q[4,6] = p_4; Q[4,7] = 0;   Q[4,8] = 0;
/**/
/**/      Q[5,1] = 0;   Q[5,2] = p_3; Q[5,3] = 0;   Q[5,4] = 0;
/**/      Q[5,5] = 0;   Q[5,6] = 0;   Q[5,7] = p_4; Q[5,8] = 0;
/**/
/**/      Q[6,1] = 0;   Q[6,2] = 0;   Q[6,3] = p_2; Q[6,4] = 0;
/**/      Q[6,5] = 0;   Q[6,6] = 0;   Q[6,7] = 0;   Q[6,8] = p_3;
/**/
/**/      Q[7,1] = 0;   Q[7,2] = 0;   Q[7,3] = p_2; Q[7,4] = 0;
/**/      Q[7,5] = 0;   Q[7,6] = 0;   Q[7,7] = 0;   Q[7,8] = p_3;
/**/
/**/      Q[8,1] = 0;   Q[8,2] = p_3; Q[8,3] = 0;   Q[8,4] = p_2;
/**/      Q[8,5] = 0;   Q[8,6] = 0;   Q[8,7] = 0;   Q[8,8] = 0;
/**/
/**/*****
/**/*****

```

```

/* Calculates the number of rows in the          */
/* essential transition probability matrix        */
nr = nrow(Q);

/*Calculates the ARL VARL and SDRL*/
  ARL_Exact = z*inv(I(nr)-Q)*e`;
  VARL_Exact = z*(I(nr)+Q)*inv(I(nr)-Q)*inv(I(nr)-Q)*e`-ARL_Exact**2;
  SDRL_Exact = sqrt(VARL_Exact);

/* The following do loop calculates the          */
/* 25th percentile of the run-length distribution */
cumulativeprob = 0;
  j = 0;
  signal = 0;
  do until (signal=1);
    j = j + 1;
    cumulativeprob = cumulativeprob + z*(Q**(j-1))*(I(nr)-Q)*e`;

    if cumulativeprob>=0.25 then do; Q1RLD_Exact=j; signal=1; end;

  end;

/* The following do loop calculates the          */
/* 50th percentile of the run-length distribution */
cumulativeprob = 0;
  j = 0;
  signal = 0;
  do until (signal=1);
    j = j + 1;
    cumulativeprob = cumulativeprob + z*(Q**(j-1))*(I(nr)-Q)*e`;

    if cumulativeprob>=0.50 then do; Q2RLD_Exact=j; signal=1; end;

  end;

/* The following do loop calculates the          */
/* 75th percentile of the run-length distribution */
cumulativeprob = 0;
  j = 0;
  signal = 0;
  do until (signal=1);
    j = j + 1;
    cumulativeprob = cumulativeprob + z*(Q**(j-1))*(I(nr)-Q)*e`;

    if cumulativeprob>=0.75 then do; Q3RLD_Exact=j; signal=1; end;

  end;

```

```

/**/*****
/**/*****
/**/
/**/ For the Upper One-Sided Improved 2-of-2 sign chart the
/**/ following block of code needs to be submitted to obtain
/**/ the sample size, control limits, False Alarm Rate and the
/**/ characteristics of the control chart
/**/
/**/*****
/**/*****
/**/
/**/
/**/ Print n UCLB UCLA FAR_Exact_1 FAR_Exact_234;
/**/ Print ARL_Exact VARL_Exact SDRL_Exact Q1RLD_Exact;
/**/ Print Q2RLD_Exact Q3RLD_Exact;
/**/
/**/*****
/**/*****

```

```

/**/*****
/**/*****
/**/
/**/ For the Lower One-Sided Improved 2-of-2 sign chart the
/**/ following block of code needs to be submitted to obtain
/**/ the sample size, control limits, False Alarm Rate and the
/**/ characteristics of the control chart
/**/
/**/*****
/**/*****
/**/
/**/
/**/ Print n LCLA LCLB FAR_Exact_1 FAR_Exact_234;
/**/ Print ARL_Exact VARL_Exact SDRL_Exact Q1RLD_Exact;
/**/ Print Q2RLD_Exact Q3RLD_Exact;
/**/
/**/*****
/**/*****

```

```

/**/*****
/**/*****
/**/
/**/ For the Two-Sided Improved 2-of-2 sign chart the
/**/ following block of code needs to be submitted to obtain
/**/ the sample size, control limits, False Alarm Rate and the
/**/ characteristics of the control chart
/**/
/**/*****
/**/*****
/**/
/**/
/**/ Print n UCLB UCLA LCLA LCLB FAR_Exact_1 FAR_Exact_234;
/**/ Print ARL_Exact VARL_Exact SDRL_Exact;
/**/ Print Q1RLD_Exact Q2RLD_Exact Q3RLD_Exact;
/**/
/**/*****
/**/*****

```

```

/**/*****
/**/*****
/**/
/**/ For the Upper One-Sided Improved 2-of-3 sign chart the
/**/ following block of code needs to be submitted to obtain
/**/ the sample size, control limits, False Alarm Rate and the
/**/ characteristics of the control chart
/**/
/**/*****
/**/*****
/**/
/**/          *;
/**/ Print n UCLB UCLA FAR_Exact_1 FAR_Exact_2 FAR_Exact_345;
/**/ Print ARL_Exact VARL_Exact SDRL_Exact Q1RLD_Exact;
/**/ Print Q2RLD_Exact Q3RLD_Exact;
/**/
/**/*****
/**/*****

```

```

/**/*****
/**/*****
/**/
/**/ For the Lower One-Sided Improved 2-of-3 sign chart the
/**/ following block of code needs to be submitted to obtain
/**/ the sample size, control limits, False Alarm Rate and the
/**/ characteristics of the control chart
/**/
/**/*****
/**/*****
/**/
/**/          *;
/**/ Print n LCLA LCLB FAR_Exact_1 FAR_Exact_2 FAR_Exact_345;
/**/ Print ARL_Exact VARL_Exact SDRL_Exact Q1RLD_Exact;
/**/ Print Q2RLD_Exact Q3RLD_Exact;
/**/
/**/*****
/**/*****

```

```

/**/*****
/**/*****
/**/
/**/ For the Two-Sided Improved 2-of-3 sign chart the
/**/ following block of code needs to be submitted to obtain
/**/ the sample size, control limits, False Alarm Rate and the
/**/ characteristics of the control chart
/**/
/**/*****
/**/*****
/**/
/**/          *;
/**/ Print n UCLB UCLA LCLA LCLB FAR_Exact_1 FAR_Exact_2;
/**/ Print FAR_Exact_345 ARL_Exact VARL_Exact SDRL_Exact;
/**/ Print Q1RLD_Exact Q2RLD_Exact Q3RLD_Exact;
/**/
/**/*****
/**/*****

```

SAS Program 2

SAS Program 2 is a program that is used to calculate the OOC performance comparisons between the run-rules and *improved* runs-rules sign charts. This program is used to populate all the OOC (performance comparison) Tables in Chapter 4.

The SAS Program 2 is written in a general form. The program has sections of code that is enclosed by stars and forward slashes; this is referred to as a block of code. Whenever a block of code appears in the program, the user has to read the caption of the block of code to determine if that block of code needs to be submitted, in order to obtain the desired results. When all the appropriate sections of code are identified and selected, the user may then submit the code to obtain the desired results.

Proc Iml;

```

      n = 20;          /*Sample Size*/
      UCLB = 19;      /*Outer Upper Control Limit*/
      UCLA = 14;      /*Inner Upper Control Limit*/
      LCLA = n-UCLA;  /*Inner Lower Control Limit*/
      LCLB = n-UCLB;  /*Outer Lower Control Limit*/
      shift = -0.2;   /*In standard deviation units*/

/**/*****
/**/*****
/**/
/**/      When the underlying process distribution is Exp(1),
/**/      the following block of code needs to be submitted
/**/
/**/*****
/**/*****
/**/
/**/      * median of the Exp(1) distribution ;
/**/      median = -log(0.5);
/**/
/**/      * the sign statistic follows a Bin(n,p0) distribution ;
/**/      p0 = 1-CDF('EXPONENTIAL',median-shift,1);
/**/
/**/*****
/**/*****

```

```

/**/*****
/**/*****
/**/
/**/      When the underlying process distribution is N(0,1),
/**/      the following block of code needs to be submitted
/**/
/**/*****
/**/*****
/**/
/**/      * median of the N(0,1) distribution ;
/**/      median = 0;
/**/
/**/      * the sign statistic follows a Bin(n,p0) distribution ;
/**/      p0 = 1-CDF('NORMAL',median-shift);
/**/
/**/*****
/**/*****

```

```

/**/*****
/**/*****
/**/
/**/      When the underlying process distribution is T(4),
/**/      the following block of code needs to be submitted
/**/
/**/*****
/**/*****
/**/
/**/      * median of the T(4) distribution ;
/**/      median = 0;
/**/
/**/      * the sign statistic follows a Bin(n,p0) distribution ;
/**/      p0 = 1-CDF('T',median-sqrt(2)*shift,4);
/**/
/**/*****
/**/*****

```

```

/* Transition Probabilities that is used to construct */
/* the essential Transition Probability Matrix */;
p_1 = 1-(CDF('BINOMIAL',UCLB-1,p0,n));
p_2 = (CDF('BINOMIAL',UCLB-1,p0,n))-(CDF('BINOMIAL',UCLA-1,p0,n));
p_3 = (CDF('BINOMIAL',UCLA-1,p0,n))-(CDF('BINOMIAL',LCLA,p0,n));
p_4 = (CDF('BINOMIAL',LCLA,p0,n))-(CDF('BINOMIAL',LCLB,p0,n));
p_5 = (CDF('BINOMIAL',LCLB,p0,n));
p_6 = 1-(CDF('BINOMIAL',LCLA,p0,n));
p_7 = (CDF('BINOMIAL',UCLA-1,p0,n));
p_8 = 1-(CDF('BINOMIAL',UCLA-1,p0,n));
p_9 = CDF('BINOMIAL',LCLA,p0,n);

```

```

/**/*****
/**/*****
/**/
/**/          For the Upper One-Sided 2-of-2 sign chart the          /**/
/**/          following block of code needs to be submitted          /**/
/**/
/**/*****
/**/*****
/**/
/**/          * Calculates the FAR ;          /**/
/**/          FAR_Exact_1 = 0;          /**/
/**/          FAR_Exact_234 = p_8*p_8;          /**/
/**/
/**/          Q = J(3,3,0);          /**/
/**/          z = {1 0 0};          /**/
/**/          e = {1 1 1};          /**/
/**/
/**/          /*Populate the essential transition probability matrix*/          /**/
/**/          Q[1,1] = 0; Q[1,2] = p_7; Q[1,3] = p_8;          /**/
/**/          Q[2,1] = 0; Q[2,2] = p_7; Q[2,3] = p_8;          /**/
/**/          Q[3,1] = 0; Q[3,2] = p_7; Q[3,3] = 0;          /**/
/**/
/**/*****
/**/*****

```

```

/**/*****
/**/*****
/**/
/**/          For the Lower One-Sided 2-of-2 sign chart the          /**/
/**/          following block of code needs to be submitted          /**/
/**/
/**/*****
/**/*****
/**/
/**/          * Calculates the FAR ;          /**/
/**/          FAR_Exact_1 = 0;          /**/
/**/          FAR_Exact_234 = p_9*p_9;          /**/
/**/
/**/          Q = J(3,3,0);          /**/
/**/          z = {1 0 0};          /**/
/**/          e = {1 1 1};          /**/
/**/
/**/          /*Populate the essential transition probability matrix*/          /**/
/**/          Q[1,1] = 0; Q[1,2] = p_6; Q[1,3] = p_9;          /**/
/**/          Q[2,1] = 0; Q[2,2] = p_6; Q[2,3] = p_9;          /**/
/**/          Q[3,1] = 0; Q[3,2] = p_6; Q[3,3] = 0;          /**/
/**/
/**/*****
/**/*****

```



```

/**/*****
/**/*****
/**/
/**/          For the Two-Sided 2-of-2 sign chart the          /**/
/**/          following block of code needs to be submitted      /**/
/**/
/**/*****
/**/*****
/**/
/**/          * Calculates the FAR ;                               /**/
/**/          FAR_Exact_1    = 0;                                /**/
/**/          FAR_Exact_234 = (p_8*p_8)+(p_9*p_9);              /**/
/**/
/**/          Q = J(4,4,0);                                       /**/
/**/          z = {1 0 0 0};                                       /**/
/**/          e = {1 1 1 1};                                       /**/
/**/
/**/          /*Populate the essential transition probability matrix*/ /**/
/**/          Q[1,1] = 0; Q[1,2] = p_3; Q[1,3] = p_8; Q[1,4] = p_9;  /**/
/**/          Q[2,1] = 0; Q[2,2] = p_3; Q[2,3] = p_8; Q[2,4] = p_9;  /**/
/**/          Q[3,1] = 0; Q[3,2] = p_3; Q[3,3] = 0;   Q[3,4] = p_9;  /**/
/**/          Q[4,1] = 0; Q[4,2] = p_3; Q[4,3] = p_8; Q[4,4] = 0;  /**/
/**/
/**/*****
/**/*****

```

```

/**/*****
/**/*****
/**/
/**/          For the Upper One-Sided 2-of-3 sign chart the      /**/
/**/          following block of code needs to be submitted      /**/
/**/
/**/*****
/**/*****
/**/
/**/          * Calculates the FAR ;                               /**/
/**/          FAR_Exact_1 = 0;                                    /**/
/**/          FAR_Exact_2 = p_8*p_8;                             /**/
/**/          FAR_Exact_345 = 2*p_7*p_8*p_8;                    /**/
/**/
/**/          Q = J(5,5,0);                                       /**/
/**/          z = {1 0 0 0 0};                                       /**/
/**/          e = {1 1 1 1 1};                                       /**/
/**/
/**/          /*Populate the essential transition probability matrix*/ /**/
/**/          Q[1,1] = 0; Q[1,2] = p_7; Q[1,3] = p_8; Q[1,4] = 0;   Q[1,5] = 0;  /**/
/**/          Q[2,1] = 0; Q[2,2] = p_7; Q[2,3] = 0;   Q[2,4] = p_8; Q[2,5] = 0;  /**/
/**/          Q[3,1] = 0; Q[3,2] = 0;   Q[3,3] = 0;   Q[3,4] = 0;   Q[3,5] = p_7;  /**/
/**/          Q[4,1] = 0; Q[4,2] = 0;   Q[4,3] = 0;   Q[4,4] = 0;   Q[4,5] = p_7;  /**/
/**/          Q[5,1] = 0; Q[5,2] = p_7; Q[5,3] = 0;   Q[5,4] = 0;   Q[5,5] = 0;  /**/
/**/
/**/*****
/**/*****

```

```

/**/*****/**/
/**/*****/**/
/**/
/**/          For the Lower One-Sided 2-of-3 sign chart the          /**/
/**/          following block of code needs to be submitted          /**/
/**/
/**/*****/**/
/**/*****/**/
/**/
/**/      * Calculates the FAR ;          /**/
/**/      FAR_Exact_1 = 0;          /**/
/**/      FAR_Exact_2 = p_9*p_9;          /**/
/**/      FAR_Exact_345 = 2*p_6*(p_9*p_9);          /**/
/**/
/**/      Q = J(5,5,0);          /**/
/**/      z = {1 0 0 0 0};          /**/
/**/      e = {1 1 1 1 1};          /**/
/**/
/**/      /*Populate the essential transition probability matrix*/          /**/
/**/      Q[1,1] = 0; Q[1,2] = p_6; Q[1,3] = p_9; Q[1,4] = 0;   Q[1,5] = 0;          /**/
/**/      Q[2,1] = 0; Q[2,2] = p_6; Q[2,3] = 0;   Q[2,4] = p_9; Q[2,5] = 0;          /**/
/**/      Q[3,1] = 0; Q[3,2] = 0;   Q[3,3] = 0;   Q[3,4] = 0;   Q[3,5] = p_6;          /**/
/**/      Q[4,1] = 0; Q[4,2] = 0;   Q[4,3] = 0;   Q[4,4] = 0;   Q[4,5] = p_6;          /**/
/**/      Q[5,1] = 0; Q[5,2] = p_6; Q[5,3] = 0;   Q[5,4] = 0;   Q[5,5] = 0;          /**/
/**/
/**/*****/**/
/**/*****/**/

```

```

/**/*****
/**/*****
/**/
/**/
/**/      For the Two-Sided 2-of-3 sign chart the
/**/      following block of code needs to be submitted
/**/
/**/*****
/**/*****
/**/
/**/      * Calculates the FAR ;
/**/      FAR_Exact_1 = 0;
/**/      FAR_Exact_2 = (p_8*p_8)+(p_9*p_9);
/**/      FAR_Exact_345 = (2*p_3*p_8*p_8)+(2*p_3*p_9*p_9)+
/**/      (p_8*p_9*p_9)+(p_9*p_8*p_8);
/**/
/**/      Q = J(8,8,0);
/**/      z = {1 0 0 0 0 0 0 0};
/**/      e = {1 1 1 1 1 1 1 1};
/**/
/**/      /*Populate the essential transition probability matrix*/
/**/      Q[1,1] = 0;   Q[1,2] = p_3; Q[1,3] = p_8; Q[1,4] = p_9;
/**/      Q[1,5] = 0;   Q[1,6] = 0;   Q[1,7] = 0;   Q[1,8] = 0;
/**/
/**/      Q[2,1] = 0;   Q[2,2] = p_3; Q[2,3] = 0;   Q[2,4] = 0;
/**/      Q[2,5] = p_8; Q[2,6] = p_9; Q[2,7] = 0;   Q[2,8] = 0;
/**/
/**/      Q[3,1] = 0;   Q[3,2] = 0;   Q[3,3] = 0;   Q[3,4] = p_9;
/**/      Q[3,5] = 0;   Q[3,6] = 0;   Q[3,7] = p_3; Q[3,8] = 0;
/**/
/**/      Q[4,1] = 0;   Q[4,2] = 0;   Q[4,3] = p_8; Q[4,4] = 0;
/**/      Q[4,5] = 0;   Q[4,6] = 0;   Q[4,7] = 0;   Q[4,8] = p_3;
/**/
/**/      Q[5,1] = 0;   Q[5,2] = 0;   Q[5,3] = 0;   Q[5,4] = p_9;
/**/      Q[5,5] = 0;   Q[5,6] = 0;   Q[5,7] = p_3; Q[5,8] = 0;
/**/
/**/      Q[6,1] = 0;   Q[6,2] = 0;   Q[6,3] = p_8; Q[6,4] = 0;
/**/      Q[6,5] = 0;   Q[6,6] = 0;   Q[6,7] = 0;   Q[6,8] = p_3;
/**/
/**/      Q[7,1] = 0;   Q[7,2] = p_3; Q[7,3] = 0;   Q[7,4] = 0;
/**/      Q[7,5] = 0;   Q[7,6] = p_9; Q[7,7] = 0;   Q[7,8] = 0;
/**/
/**/      Q[8,1] = 0;   Q[8,2] = p_3; Q[8,3] = 0;   Q[8,4] = 0;
/**/      Q[8,5] = p_8; Q[8,6] = 0;   Q[8,7] = 0;   Q[8,8] = 0;
/**/
/**/*****
/**/*****

```

```

/**/*****
/**/*****
/**/
/**/      For the Upper One-Sided Improved 2-of-2 sign chart the      /**/
/**/      following block of code needs to be submitted                /**/
/**/
/**/*****
/**/*****
/**/
/**/      * Calculates the FAR ;
/**/      FAR_Exact_1   = (p_1);
/**/      FAR_Exact_234 = (p_2**2)+(p_1);
/**/
/**/      Q = J(3,3,0);
/**/      z = {1 0 0};
/**/      e = {1 1 1};
/**/
/**/      /*Populate the essential transition probability matrix*/
/**/      Q[1,1] = 0; Q[1,2] = p_7; Q[1,3] = p_2;
/**/      Q[2,1] = 0; Q[2,2] = p_7; Q[2,3] = p_2;
/**/      Q[3,1] = 0; Q[3,2] = p_7; Q[3,3] = 0;
/**/
/**/*****
/**/*****

```

```

/**/*****
/**/*****
/**/
/**/      For the Lower One-Sided Improved 2-of-2 sign chart the      /**/
/**/      following block of code needs to be submitted                /**/
/**/
/**/*****
/**/*****
/**/
/**/      * Calculates the FAR ;
/**/      FAR_Exact_1   = (p_5);
/**/      FAR_Exact_234 = (p_4**2)+(p_5);
/**/
/**/      Q = J(3,3,0);
/**/      z = {1 0 0};
/**/      e = {1 1 1};
/**/
/**/      /*Populate the essential transition probability matrix*/
/**/      Q[1,1] = 0; Q[1,2] = p_6; Q[1,3] = p_4;
/**/      Q[2,1] = 0; Q[2,2] = p_6; Q[2,3] = p_4;
/**/      Q[3,1] = 0; Q[3,2] = p_6; Q[3,3] = 0;
/**/
/**/*****
/**/*****

```

```

/**/*****
/**/*****
/**/
/**/      For the Two-Sided Improved 2-of-2 sign chart the      /**/
/**/      following block of code needs to be submitted          /**/
/**/
/**/*****
/**/*****
/**/
/**/      * Calculates the FAR ;
/**/      FAR_Exact_1   = (p_1)+(P_5);
/**/      FAR_Exact_234 = (p_2**2)+(p_1)+(p_4**2)+(p_5);
/**/
/**/      Q = J(4,4,0);
/**/      z = {1 0 0 0};
/**/      e = {1 1 1 1};
/**/
/**/      /*Populate the essential transition probability matrix*/
/**/      Q[1,1] = 0; Q[1,2] = p_3; Q[1,3] = p_2; Q[1,4] = p_4;
/**/      Q[2,1] = 0; Q[2,2] = p_3; Q[2,3] = p_2; Q[2,4] = p_4;
/**/      Q[3,1] = 0; Q[3,2] = p_3; Q[3,3] = 0;   Q[3,4] = p_4;
/**/      Q[4,1] = 0; Q[4,2] = p_3; Q[4,3] = p_2; Q[4,4] = 0;
/**/
/**/*****
/**/*****

```

```

/**/*****
/**/*****
/**/
/**/      For the Upper One-Sided Improved 2-of-3 sign chart the  /**/
/**/      following block of code needs to be submitted          /**/
/**/
/**/*****
/**/*****
/**/
/**/      * Calculates the FAR ;
/**/      FAR_Exact_1 = (p_1);
/**/      FAR_Exact_2 = (p_1)+(p_2*p_2);
/**/      FAR_Exact_345 = (p_1)+(2*(p_7*p_2*p_2));
/**/
/**/      Q = J(5,5,0);
/**/      z = {1 0 0 0 0};
/**/      e = {1 1 1 1 1};
/**/
/**/      /*Populate the essential transition probability matrix*/
/**/      Q[1,1] = 0; Q[1,2] = p_7; Q[1,3] = p_2; Q[1,4] = 0;   Q[1,5] = 0;
/**/      Q[2,1] = 0; Q[2,2] = p_7; Q[2,3] = 0;   Q[2,4] = p_2; Q[2,5] = 0;
/**/      Q[3,1] = 0; Q[3,2] = 0;   Q[3,3] = 0;   Q[3,4] = 0;   Q[3,5] = p_7;
/**/      Q[4,1] = 0; Q[4,2] = 0;   Q[4,3] = 0;   Q[4,4] = 0;   Q[4,5] = p_7;
/**/      Q[5,1] = 0; Q[5,2] = p_7; Q[5,3] = 0;   Q[5,4] = 0;   Q[5,5] = 0;
/**/
/**/*****
/**/*****

```

```

/**/*****/**/
/**/*****/**/
/**/
/**/      For the Lower One-Sided Improved 2-of-3 sign chart the      /**/
/**/      following block of code needs to be submitted                /**/
/**/
/**/*****/**/
/**/*****/**/
/**/
/**/      * Calculates the FAR ;
/**/      FAR_Exact_1 = (p_5);
/**/      FAR_Exact_2 = (p_5)+(p_4*p_4);
/**/      FAR_Exact_345 = (p_5)+(2*(p_6*p_4*p_4));
/**/
/**/      Q = J(5,5,0);
/**/      z = {1 0 0 0 0};
/**/      e = {1 1 1 1 1};
/**/
/**/      /*Populate the essential transition probability matrix*/
/**/      Q[1,1] = 0; Q[1,2] = p_6; Q[1,3] = p_4; Q[1,4] = 0;   Q[1,5] = 0;
/**/      Q[2,1] = 0; Q[2,2] = p_6; Q[2,3] = 0;   Q[2,4] = p_4; Q[2,5] = 0;
/**/      Q[3,1] = 0; Q[3,2] = 0;   Q[3,3] = 0;   Q[3,4] = 0;   Q[3,5] = p_6;
/**/      Q[4,1] = 0; Q[4,2] = 0;   Q[4,3] = 0;   Q[4,4] = 0;   Q[4,5] = p_6;
/**/      Q[5,1] = 0; Q[5,2] = p_6; Q[5,3] = 0;   Q[5,4] = 0;   Q[5,5] = 0;
/**/
/**/*****/**/
/**/*****/**/

```

```

/**/*****
/**/*****
/**/
/**/      For the Two-Sided Improved 2-of-3 sign chart the
/**/      following block of code needs to be submitted
/**/
/**/*****
/**/*****
/**/
/**/      * Calculates the FAR ;
/**/      FAR_Exact_1 = (p_1)+(p_5);
/**/      FAR_Exact_2 = (p_1)+(p_5)+(p_2**2)+(p_4**2);
/**/      FAR_Exact_345 = (p_1)+(p_5)+(2*p_3*(p_2**2))+(2*p_3*(p_4**2))+
/**/                      (p_4*(p_2**2))+(p_2*(p_4**2));
/**/
/**/      Q = J(8,8,0);
/**/      z = {1 0 0 0 0 0 0 0};
/**/      e = {1 1 1 1 1 1 1 1};
/**/
/**/      /*Populate the essential transition probability matrix*/
/**/      Q[1,1] = 0;   Q[1,2] = p_3; Q[1,3] = p_2; Q[1,4] = 0;
/**/      Q[1,5] = 0;   Q[1,6] = p_4; Q[1,7] = 0;   Q[1,8] = 0;
/**/
/**/      Q[2,1] = 0;   Q[2,2] = p_3; Q[2,3] = 0;   Q[2,4] = p_2;
/**/      Q[2,5] = 0;   Q[2,6] = 0;   Q[2,7] = p_4; Q[2,8] = 0;
/**/
/**/      Q[3,1] = 0;   Q[3,2] = 0;   Q[3,3] = 0;   Q[3,4] = 0;
/**/      Q[3,5] = p_3; Q[3,6] = p_4; Q[3,7] = 0;   Q[3,8] = 0;
/**/
/**/      Q[4,1] = 0;   Q[4,2] = 0;   Q[4,3] = 0;   Q[4,4] = 0;
/**/      Q[4,5] = p_3; Q[4,6] = p_4; Q[4,7] = 0;   Q[4,8] = 0;
/**/
/**/      Q[5,1] = 0;   Q[5,2] = p_3; Q[5,3] = 0;   Q[5,4] = 0;
/**/      Q[5,5] = 0;   Q[5,6] = 0;   Q[5,7] = p_4; Q[5,8] = 0;
/**/
/**/      Q[6,1] = 0;   Q[6,2] = 0;   Q[6,3] = p_2; Q[6,4] = 0;
/**/      Q[6,5] = 0;   Q[6,6] = 0;   Q[6,7] = 0;   Q[6,8] = p_3;
/**/
/**/      Q[7,1] = 0;   Q[7,2] = 0;   Q[7,3] = p_2; Q[7,4] = 0;
/**/      Q[7,5] = 0;   Q[7,6] = 0;   Q[7,7] = 0;   Q[7,8] = p_3;
/**/
/**/      Q[8,1] = 0;   Q[8,2] = p_3; Q[8,3] = 0;   Q[8,4] = p_2;
/**/      Q[8,5] = 0;   Q[8,6] = 0;   Q[8,7] = 0;   Q[8,8] = 0;
/**/
/**/*****
/**/*****

```

```

/* Calculates the number of rows in the          */
/* essential transition probability matrix      */
nr = nrow(Q);

/*Calculates the ARL VARL and SDRL*/
  ARL_Exact = z*inv(I(nr)-Q)*e`;
  VARL_Exact = z*(I(nr)+Q)*inv(I(nr)-Q)*inv(I(nr)-Q)*e`-ARL_Exact**2;
  SDRL_Exact = sqrt(VARL_Exact);

/* The following do loop calculates the          */
/* 5th percentile of the run-length distribution */
cumulativeprob = 0;
  j = 0;
  signal = 0;
  do until (signal=1);
    j = j + 1;
    cumulativeprob = cumulativeprob + z*(Q**(j-1))*(I(nr)-Q)*e`;

    if cumulativeprob>=0.05 then do; P05RLD_Exact=j; signal=1; end;

  end;

/* The following do loop calculates the          */
/* 25th percentile of the run-length distribution */
cumulativeprob = 0;
  j = 0;
  signal = 0;
  do until (signal=1);
    j = j + 1;
    cumulativeprob = cumulativeprob + z*(Q**(j-1))*(I(nr)-Q)*e`;

    if cumulativeprob>=0.25 then do; Q1RLD_Exact=j; signal=1; end;

  end;

/* The following do loop calculates the          */
/* 50th percentile of the run-length distribution */
cumulativeprob = 0;
  j = 0;
  signal = 0;
  do until (signal=1);
    j = j + 1;
    cumulativeprob = cumulativeprob + z*(Q**(j-1))*(I(nr)-Q)*e`;

    if cumulativeprob>=0.50 then do; Q2RLD_Exact=j; signal=1; end;

  end;

```



```

/* The following do loop calculates the          */
/* 75th percentile of the run-length distribution */
cumelativeprob = 0;
    j = 0;
    signal = 0;
do until (signal=1);
    j = j + 1;
    cumelativeprob = cumelativeprob + z*(Q**(j-1))*(I(nr)-Q)*e`;

if cumelativeprob>=0.75 then do; Q3RLD_Exact=j; signal=1; end;
end;

/* The following do loop calculates the          */
/* 95th percentile of the run-length distribution */
cumelativeprob = 0;
    j = 0;
    signal = 0;
do until (signal=1);
    j = j + 1;
    cumelativeprob = cumelativeprob + z*(Q**(j-1))*(I(nr)-Q)*e`;

if cumelativeprob>=0.95 then do; P95RLD_Exact=j; signal=1; end;
end;

/**/*****
/**/*****
/**/
/**/ For the Upper One-Sided 2-of-2 sign chart the following block of
/**/ code needs to be submitted to obtain the sample size,
/**/ control limits, shift, False Alarm Rate and characteristics
/**/ of the control chart
/**/
/**/*****
/**/*****
/**/
/**/ *;
/**/ Print n UCLA shift FAR_Exact_1 FAR_Exact_234 ARL_Exact;
/**/ Print VARL_Exact SDRL_Exact P05RLD_Exact Q1RLD_Exact;
/**/ Print Q2RLD_Exact Q3RLD_Exact P95RLD_Exact;
/**/
/**/*****
/**/*****

```

```

/**/*****
/**/*****
/**/
/**/ For the Lower One-Sided 2-of-2 sign chart the following block of
/**/ code needs to be submitted to obtain the sample size,
/**/ control limits, shift, False Alarm Rate and characteristics
/**/ of the control chart
/**/
/**/*****
/**/*****
/**/
/**/      *;
/**/ Print n LCLA shift FAR_Exact_1 FAR_Exact_234 ARL_Exact VARL_Exact;
/**/ Print SDRL_Exact P05RLD_Exact Q1RLD_Exact;
/**/ Print Q2RLD_Exact Q3RLD_Exact P95RLD_Exact;
/**/
/**/*****
/**/*****

```

```

/**/*****
/**/*****
/**/
/**/ For the Two-Sided 2-of-2 sign chart the following block of
/**/ code needs to be submitted to obtain the sample size,
/**/ control limits, shift, False Alarm Rate and characteristics
/**/ of the control chart
/**/
/**/*****
/**/*****
/**/
/**/      *;
/**/ Print n UCLA LCLA shift FAR_Exact_1 FAR_Exact_234 ARL_Exact;
/**/ Print VARL_Exact SDRL_Exact P05RLD_Exact Q1RLD_Exact;
/**/ Print Q2RLD_Exact Q3RLD_Exact P95RLD_Exact;
/**/
/**/*****
/**/*****

```

```

/**/*****
/**/*****
/**/
/**/ For the Upper One-Sided 2-of-3 sign chart the following block of
/**/ code needs to be submitted to obtain the sample size,
/**/ control limits, shift, False Alarm Rate and characteristics
/**/ of the control chart
/**/
/**/*****
/**/*****
/**/
/**/      *;
/**/ Print n UCLA shift FAR_Exact_1 FAR_Exact_2 FAR_Exact_345;
/**/ Print ARL_Exact VARL_Exact SDRL_Exact P05RLD_Exact Q1RLD_Exact;
/**/ Print Q2RLD_Exact Q3RLD_Exact P95RLD_Exact;
/**/
/**/*****
/**/*****

```

```

/**/*****
/**/*****
/**/
/**/ For the Lower One-Sided 2-of-3 sign chart the following block of
/**/ code needs to be submitted to obtain the sample size,
/**/ control limits, shift, False Alarm Rate and characteristics
/**/ of the control chart
/**/
/**/*****
/**/*****
/**/
/**/
/**/ Print n LCLA shift FAR_Exact_1 FAR_Exact_2 FAR_Exact_345;
/**/ Print ARL_Exact VARL_Exact SDRL_Exact P05RLD_Exact Q1RLD_Exact;
/**/ Print Q2RLD_Exact Q3RLD_Exact P95RLD_Exact;
/**/
/**/*****
/**/*****

/**/*****
/**/*****
/**/
/**/ For the Two-Sided 2-of-3 sign chart the following block of
/**/ code needs to be submitted to obtain the sample size,
/**/ control limits, shift, False Alarm Rate and characteristics
/**/ of the control chart
/**/
/**/*****
/**/*****
/**/
/**/
/**/ Print n UCLA LCLA shift FAR_Exact_1 FAR_Exact_2 FAR_Exact_345;
/**/ Print ARL_Exact VARL_Exact SDRL_Exact P05RLD_Exact Q1RLD_Exact;
/**/ Print Q2RLD_Exact Q3RLD_Exact P95RLD_Exact;
/**/
/**/*****
/**/*****

/**/*****
/**/*****
/**/
/**/ For the Upper One-Sided Improved 2-of-2 sign chart the following
/**/ block of code needs to be submitted to obtain the sample size,
/**/ control limits, shift, False Alarm Rate and characteristics
/**/ of the control chart
/**/
/**/*****
/**/*****
/**/
/**/
/**/ Print n UCLB UCLA shift FAR_Exact_1 FAR_Exact_234 ARL_Exact;
/**/ Print VARL_Exact SDRL_Exact P05RLD_Exact Q1RLD_Exact;
/**/ Print Q2RLD_Exact Q3RLD_Exact P95RLD_Exact;
/**/
/**/*****
/**/*****

```

```

/**/*****
/**/*****
/**/
/**/ For the Lower One-Sided Improved 2-of-2 sign chart the following
/**/ block of code needs to be submitted to obtain the sample size,
/**/ control limits, shift, False Alarm Rate and characteristics
/**/ of the control chart
/**/
/**/*****
/**/*****
/**/
/**/      *;
/**/ Print n LCLA LCLB shift FAR_Exact_1 FAR_Exact_234 ARL_Exact;
/**/ Print VARL_Exact SDRL_Exact P05RLD_Exact Q1RLD_Exact;
/**/ Print Q2RLD_Exact Q3RLD_Exact P95RLD_Exact;
/**/
/**/*****
/**/*****

```

```

/**/*****
/**/*****
/**/
/**/ For the Two-Sided Improved 2-of-2 sign chart the following
/**/ block of code needs to be submitted to obtain the sample size,
/**/ control limits, shift, False Alarm Rate and characteristics
/**/ of the control chart
/**/
/**/*****
/**/*****
/**/
/**/      *;
/**/ Print n UCLB UCLA LCLA LCLB shift FAR_Exact_1 FAR_Exact_234;
/**/ Print ARL_Exact VARL_Exact SDRL_Exact P05RLD_Exact Q1RLD_Exact;
/**/ Print Q2RLD_Exact Q3RLD_Exact P95RLD_Exact;
/**/
/**/*****
/**/*****

```

```

/**/*****
/**/*****
/**/
/**/ For the Upper One-Sided Improved 2-of-3 sign chart the following
/**/ block of code needs to be submitted to obtain the sample size,
/**/ control limits, shift, False Alarm Rate and characteristics
/**/ of the control chart
/**/
/**/*****
/**/*****
/**/
/**/      *;
/**/ Print n UCLB UCLA shift FAR_Exact_1 FAR_Exact_2 FAR_Exact_345;
/**/ Print ARL_Exact VARL_Exact SDRL_Exact P05RLD_Exact Q1RLD_Exact;
/**/ Print Q2RLD_Exact Q3RLD_Exact P95RLD_Exact;
/**/
/**/*****
/**/*****

```

```

/**/*****//
/**/*****//
/**/
/**/ For the Lower One-Sided Improved 2-of-3 sign chart the following //
/**/ block of code needs to be submitted to obtain the sample size, //
/**/ control limits, shift, False Alarm Rate and characteristics //
/**/ of the control chart //
/**/ //
/**/*****//
/**/*****//
/**/
/**/ *; //
/**/ Print n LCLA LCLB shift FAR_Exact_1 FAR_Exact_2 FAR_Exact_345; //
/**/ Print ARL_Exact VARL_Exact SDRL_Exact P05RLD_Exact Q1RLD_Exact; //
/**/ Print Q2RLD_Exact Q3RLD_Exact P95RLD_Exact; //
/**/ //
/**/*****//
/**/*****//

```

```

/**/*****//
/**/*****//
/**/
/**/ For the Two-Sided Improved 2-of-3 sign chart the following //
/**/ block of code needs to be submitted to obtain the sample size, //
/**/ control limits, shift, False Alarm Rate and characteristics //
/**/ of the control chart //
/**/ //
/**/*****//
/**/*****//
/**/
/**/ *; //
/**/ Print n UCLB UCLA LCLA LCLB shift FAR_Exact_1 FAR_Exact_2; //
/**/ Print FAR_Exact_345 ARL_Exact VARL_Exact SDRL_Exact P05RLD_Exact; //
/**/ Print Q1RLD_Exact Q2RLD_Exact Q3RLD_Exact P95RLD_Exact; //
/**/ //
/**/*****//
/**/*****//

```

SAS Program 3

SAS Program 3 is a program that is used to calculate the OOC performance comparisons between the run-rules and *improved* runs-rules precedence charts. This program is used to populate all the OOC (performance comparison) Tables in Chapter 5.

The SAS Program 3 is written in a general form. The program has sections of code that is enclosed by stars and forward slashes; this is referred to as a block of code. Whenever a block of code appears in the program, the user has to read the caption of the block of code to determine if that block of code needs to be submitted, in order to obtain the desired results. When all the appropriate sections of code are identified and selected, the user may then submit the code to obtain the desired results.

Proc Iml;

```

nsim = 100;      /* Number of simulations */

  m = 500;      /* Reference sample size */
  n = 7;       /* Test sample size */
  j = (n+1)/2; /* Number of the order statistic from the test sample
                that is used as the plotting statistic */

shift = -0.05;  /* In standard deviation units */

  d = 385;      /* Number of the order statistic from the reference sample
                that is used as the UCLB */
  c = 382;      /* Number of the order statistic from the reference sample
                that is used as the UCLA */
  b = m-c+1;    /* Number of the order statistic from the reference sample
                that is used as the LCLA */
  a = m-d+1;    /* Number of the order statistic from the reference sample
                that is used as the LCLB */

/* Creating a row vector that contains the number of simulations, test
   and reference sample size, control limits (order statistics) and the
   size of the shift */
InfoM = nsim||m||n||j||d||c||b||a||shift;

/* Creating a dataset Info from the InfoM row vector */
create Info from InfoM[colname={'nsim' , 'm' , 'n' , 'j' , 'd' , 'c' , 'b' , 'a' ,
'shift'}}];
append from InfoM;

```



```

/**/*****
/**/*****
/**/
/**/      When the underlying process distribution is Exp(1),
/**/      the following block of code needs to be submitted
/**/
/**/*****
/**/*****
/**/      * populate the y vector (test sample) with EXP(1) random values;
/**/              call randgen(y,'EXPO');
/**/
/**/*****
/**/*****

```

```

/**/*****
/**/*****
/**/
/**/      When the underlying process distribution is N(0,1),
/**/      the following block of code needs to be submitted
/**/
/**/*****
/**/*****
/**/      * populate the y vector (test sample) with N(0,1) random values;
/**/              call randgen(y,'NORMAL');
/**/
/**/*****
/**/*****

```

```

/**/*****
/**/*****
/**/
/**/      When the underlying process distribution is T(4),
/**/      the following block of code needs to be submitted
/**/
/**/*****
/**/*****
/**/      * populate the y vector (test sample) with T(4) random values ;
/**/              call randgen(y,'T',4);
/**/
/**/*****
/**/*****

```

```

/* Populate the shiftM vector */
shiftM = J(n,1,shift);

/* Adding a shift to the the test sample */
y = y + shiftM;

/* Sort the test sample */
call sort(y,1);

```

```

/**/*****
/**/*****
/**/
/**/      For the Upper One-Sided 2-of-2 sign chart the      /**/
/**/      following block of code needs to be submitted      /**/
/**/
/**/*****
/**/*****
/**/
/**/          *;
/**/      Ti    = y[j,1];
/**/
/**/
/**/      if ((Ti >= UCLA) & (Ti_1 >= UCLA)) then do; signal=1; end;
/**/
/**/      Ti_1 = Ti;
/**/
/**/*****
/**/*****

```

```

/**/*****
/**/*****
/**/
/**/      For the Upper One-Sided 2-of-3 sign chart the      /**/
/**/      following block of code needs to be submitted      /**/
/**/
/**/*****
/**/*****
/**/
/**/          *;
/**/      Ti    = y[j,];
/**/
/**/
/**/      /*1*/ if (Ti_1 >= UCLA) & (Ti >= UCLA) then do; signal=1; end;
/**/
/**/      /*2*/ if (Ti_2 < UCLA) & (Ti_1 >= UCLA) & (Ti >= UCLA)
/**/      then do; signal=1; end;
/**/
/**/      /*3*/ if (Ti_2 >= UCLA) & (Ti_1 < UCLA) & (Ti >= UCLA)
/**/      then do; signal=1; end;
/**/
/**/
/**/      Ti_2 = Ti_1;
/**/      Ti_1 = Ti;
/**/
/**/*****
/**/*****

```

```

/**/*****
/**/*****
/**/
/**/      For the Upper One-Sided Improved 2-of-2 sign chart the      /**/
/**/      following block of code needs to be submitted                /**/
/**/
/**/*****
/**/*****
/**/
/**/      *;
/**/
/**/      Ti = y[j,1];
/**/
/**/      if (Ti >= UCLB) then do; signal=1; end;
/**/
/**/      if ((Ti >= UCLA) & (Ti < UCLB)) &
/**/      ((Ti_1 >= UCLA) & (Ti_1 < UCLB)) then do; signal=1; end;
/**/
/**/      Ti_1 = Ti;
/**/
/**/
/**/*****
/**/*****

```

```

/**/*****
/**/*****
/**/
/**/      For the Upper One-Sided Improved 2-of-3 sign chart the      /**/
/**/      following block of code needs to be submitted                /**/
/**/
/**/*****
/**/*****
/**/
/**/      *;
/**/
/**/      Ti = y[j,1];
/**/
/**/      /*1*/ if (Ti >= UCLB) then do; signal=1; end;
/**/
/**/      /*2*/ if ((Ti_1 >= UCLA) & (Ti_1 < UCLB)) &
/**/      ((Ti >= UCLA) & (Ti < UCLB)) then do; signal=1; end;
/**/
/**/      /*3*/ if (Ti_2 < UCLA) & ((Ti_1 >= UCLA) & (Ti_1 < UCLB)) &
/**/      ((Ti >= UCLA) & (Ti < UCLB)) then do; signal=1; end;
/**/
/**/      /*4*/ if ((Ti_2 >= UCLA) & (Ti_2 < UCLB)) & (Ti_1 < UCLA) &
/**/      ((Ti >= UCLA) & (Ti < UCLB)) then do; signal=1; end;
/**/
/**/
/**/      Ti_2 = Ti_1;
/**/      Ti_1 = Ti;
/**/
/**/
/**/
/**/*****
/**/*****

```



```
/* Printing the dataset Final, containing the number of simulations,  
   test and reference sample size, control limits,  
   the size of the shift and the characteristics of the control chart */
```

```
Proc Print data = Final;  
run;
```

Mathcad Program 1

Mathcad Program 1 is a program that is used to calculate the IC performance of the upper one-sided *improved 2-of-2* precedence control charts. This program is used to populate the IC (charting constant) Table for the upper one-sided *improved 2-of-2* precedence chart in Chapter 5.

Note that in the program below FAR_o represents False Alarm Rate one i.e. the FAR at the first point in time and FAR_{ttf} represents False Alarm Rate two three four i.e. the FAR after the first point in time.

$$c := 382 \quad d := 465 \quad m := 500 \quad n := 7 \quad j := 4$$

$$fcd(ucm, udm) := \left(\frac{m!}{(c-1)!(d-c-1)!(m-d)!} \right) \cdot ucm^{c-1} \cdot (udm - ucm)^{d-c-1} \cdot (1 - udm)^{m-d}$$

$$p1c(udm) := 1 - \left(\frac{n!}{(j-1)!(n-j)!} \cdot \int_0^{udm} w^{j-1} \cdot (1-w)^{n-j} dw \right)$$

$$p2c(ucm, udm) := \frac{n!}{(j-1)!(n-j)!} \cdot \left(\int_0^{udm} w^{j-1} \cdot (1-w)^{n-j} dw - \int_0^{ucm} w^{j-1} \cdot (1-w)^{n-j} dw \right)$$

$$p7c(ucm) := \frac{n!}{(j-1)!(n-j)!} \cdot \int_0^{ucm} w^{j-1} \cdot (1-w)^{n-j} dw$$

$$Qc(ucm, udm) := \begin{pmatrix} 0 & p7c(ucm) & p2c(ucm, udm) \\ 0 & p7c(ucm) & p2c(ucm, udm) \\ 0 & p7c(ucm) & 0 \end{pmatrix} \quad one := \begin{pmatrix} 1 \\ 1 \\ 1 \end{pmatrix}$$

$$Id := \begin{pmatrix} 1 & 0 & 0 \\ 0 & 1 & 0 \\ 0 & 0 & 1 \end{pmatrix} \quad \xi := (1 \ 0 \ 0)$$

$$ARL := \int_0^1 \int_0^{udm} \xi \cdot (Id - Qc(ucm, udm))^{-1} \cdot one \cdot fcd(ucm, udm) ducm dudm$$

$$FAR_o := \int_0^1 \int_0^{udm} p1c(udm) \cdot fcd(ucm, udm) ducm dudm$$

$$FAR_{ttf} := \int_0^1 \int_0^{udm} (p1c(udm) + (p2c(ucm, udm))^2) \cdot fcd(ucm, udm) ducm dudm$$

$$ARL = \quad FAR_o = \quad FAR_{ttf} =$$

Mathcad Program 2

Mathcad Program 2 is a program that is used to calculate the IC performance of the upper one-sided *improved 2-of-3* precedence control charts. This program is used to populate the IC (charting constant) Table for the upper one-sided *improved 2-of-3* precedence chart in Chapter 5.

Note that in the program below *FARo* represents False Alarm Rate one i.e. the *FAR* at the first point in time. *FARt* represents False Alarm Rate two i.e. the *FAR* at the second point in time and *FARtff* represents False Alarm Rate three four five i.e the *FAR* after the second point in time.

$$c := 393 \quad d := 495 \quad m := 500 \quad n := 7 \quad j := 4$$

$$fcd(ucm, udm) := \left(\frac{m!}{(c-1)!(d-c-1)!(m-d)!} \right) \cdot ucm^{c-1} \cdot (udm - ucm)^{d-c-1} \cdot (1 - udm)^{m-d}$$

$$p1c(udm) := 1 - \left(\frac{n!}{(j-1)!(n-j)!} \cdot \int_0^{udm} w^{j-1} \cdot (1-w)^{n-j} dw \right)$$

$$p2c(ucm, udm) := \frac{n!}{(j-1)!(n-j)!} \cdot \left(\int_0^{udm} w^{j-1} \cdot (1-w)^{n-j} dw - \int_0^{ucm} w^{j-1} \cdot (1-w)^{n-j} dw \right)$$

$$p7c(ucm) := \frac{n!}{(j-1)!(n-j)!} \cdot \int_0^{ucm} w^{j-1} \cdot (1-w)^{n-j} dw$$

$$Qc(ucm, udm) := \begin{pmatrix} 0 & p7c(ucm) & p2c(ucm, udm) & 0 & 0 \\ 0 & p7c(ucm) & 0 & p2c(ucm, udm) & 0 \\ 0 & 0 & 0 & 0 & p7c(ucm) \\ 0 & 0 & 0 & 0 & p7c(ucm) \\ 0 & p7c(ucm) & 0 & 0 & 0 \end{pmatrix} \quad one := \begin{pmatrix} 1 \\ 1 \\ 1 \\ 1 \\ 1 \end{pmatrix}$$

$$Id := \begin{pmatrix} 1 & 0 & 0 & 0 & 0 \\ 0 & 1 & 0 & 0 & 0 \\ 0 & 0 & 1 & 0 & 0 \\ 0 & 0 & 0 & 1 & 0 \\ 0 & 0 & 0 & 0 & 1 \end{pmatrix} \quad \xi := (1 \ 0 \ 0 \ 0 \ 0)$$

$$ARL := \int_0^1 \int_0^{udm} \xi \cdot (Id - Qc(ucm, udm))^{-1} \cdot one \cdot fcd(ucm, udm) ducm dudm$$

$$FARo := \int_0^1 \int_0^{udm} p1c(udm) \cdot fcd(ucm, udm) ducm dudm$$

$$FARt := \int_0^1 \int_0^{udm} (p1c(udm) + (p2c(ucm, udm))^2) \cdot fcd(ucm, udm) ducm dudm$$

$$FARtff := \int_0^1 \int_0^{udm} (p1c(udm) + 2 \cdot p7c(ucm) \cdot (p2c(ucm, udm))^2) \cdot fcd(ucm, udm) ducm dudm$$

ARL =

FARo =

FARt =

FARtff =

References

- Amin, R.W., Reynolds, M.R. Jr., Bakir, S. (1995). “Nonparametric quality control charts based on the sign statistic”. *Communications in Statistics - Theory and Methods*, 24(6):1597-1623.
- Bain, L.J., Engelhardt, M. (1992). *Introduction to probability and mathematical statistics*, 2nd edition, Duxbury Press.
- Bissell, A.F. (1978). “An Attempt to Unify the Theory of Quality Control Procedures”. *Bulletin in Applied Statistics*, 5:113-128.
- Borror, C.M., Champ, C.W. (2001). “Phase I control charts for independent Bernoulli data”. *Quality and Reliability Engineering International*, 17(5):391-396.
- Borror, C.M., Montgomery, D.C. and Runger, G.C. (1999). “Robustness of the EWMA control chart to non-normality”. *Journal of Quality Technology*, 31(3):309-316.
- Brook, D., Evans, D.A. (1972). “An approach to the probability distribution of cusum run length”. *Biometrika*, 59(3):539-549.
- Chakraborti, S. (2000). “Run length, average run length and false alarm rate of Shewhart X-bar chart: Exact derivations by conditioning”. *Communications in Statistics - Simulation and Computation*, 29(1):61-81.
- Chakraborti, S., Van der Laan, P., Bakir, S.T. (2001). “Nonparametric control charts: An overview and some results”. *Journal of Quality Technology*, 33(3):304-315.
- Chakraborti, S., Van der Laan, P., Van de Wiel, M.A. (2004). “A class of distribution-free control charts”. *Journal of the Royal Statistical Society. Series C: Applied Statistics*, 53(3):443-462.
- Chakraborti, S. (2007). “Run length distribution and percentiles: The Shewhart \bar{X} chart with unknown parameters”. *Quality Engineering*, 19(2):119-127.
- Chakraborti, S. and Graham, M.A. (2007). “Nonparametric control charts.” *Encyclopedia of Statistics in Quality and Reliability*, 1:415 – 429, New York: John Wiley.

- Chakraborti, S., Eryilmaz, S., Human S.W. (2009a). “A phase II nonparametric control chart based on precedence statistics with runs-type signaling rules”. *Computational Statistics and Data Analysis* 53(4):1054-1065.
- Chakraborti, S., Human, S.W., Graham, M.A. (2009b). “Phase I statistical process control charts: An overview and some results”. *Quality Engineering*, 21(1):52-62.
- Chakraborti, S., Human, S.W. and Graham, M.A. (2010). “Nonparametric (distribution-free) quality control charts.” In Handbook of *Methods and Applications of Statistics: Engineering, Quality Control, and Physical Sciences*. N. Balakrishnan, Ed., 298-329, John Wiley & Sons, New York.
- Champ,C.W., Woodall,W.H. (1987). “Exact Results for Shewhart Control Charts With Supplementary Runs Rules”. *Technometrics*, 29(4):393-399.
- Crosier, R.B. (1986). “A New Two-Sided Cumulative Sum Quality Control Scheme”. *Technometrics*, 28(3):187-194.
- Crowder, S.V. (1987). “A Simple Method for Studying Run-Length Distributions of Exponentially Weighted Moving Average Charts”. *Technometrics*, 29(4):401-407.
- Crowder, S.V. (1989). “Design of Exponentially Weighted Moving Average Schemes”. *Journal of Quality Technology*, 21(3):155-162.
- Derman, C., Ross, S.M. (1997). *Statistical aspects of quality control*, San Diego: Academic Press.
- De Vargas, V.d C.C., Lopes, L.F.D., Souza, A.M. (2004). “Comparative study of the performance of the CUSUM and EWMA control charts”. *Computers & Industrial Engineering*, 46(4):707-724.
- Farnum, N.R. (1994). *Modern statistical quality control and improvement*, Duxbury.
- Fu, J.C., Lou, W.Y.W. (2003). *Distribution theory of runs and patterns and its applications: a finite Markov chain imbedding approach*, World Scientific Publishing Co. Pte. Ltd.
- Fu, J.C., Spiring, F.A. and Xie, H. (2002). “On the average run lengths of quality control schemes using a Markov chain approach.” *Statistics and Probability Letters*, **56**, 369-380.

Graham, M.A., Human, S.W. and Chakraborti, S. (2009). “A nonparametric EWMA control chart based on the sign statistic.” Technical report, 09/04, Department of Statistics, University of Pretoria.

Graham, M.A., Chakraborti, S. and Human, S.W. (2011). (*Accepted*) “A nonparametric EWMA sign chart for location for individual measurements.” *Quality Engineering*.

Gibbons, J.D., Chakraborti, S. (2003). *Nonparametric statistical inference*, 4th edition, New York: Marcel Dekker.

Hawkins, D.M., Olwell, D.H. (1998). *Cumulative sum charts and charting for quality improvement*, Springer-Verlag, New York.

Human, S.W., Graham, M.A. (2007). “Average run lengths and operating characteristic curves”. *Encyclopedia of Quality and Reliability*, 1:159-168, New York: John Wiley.

Human, S.W., Chakraborti, S., Smit, C.F. (2009). “Nonparametric Shewhart-type control charts with runs-type signalling rules”, Technical Report, 09/02, Department of Statistics, University of Pretoria.

Human, S.W., Chakraborti, S., Smit, C.F. (2010). “Nonparametric Shewhart-type sign control charts based on runs”. *Communications in Statistics-Theory and Methods*, 39(11):2046-2062.

Human, S.W., Kritzing, P., Chakraborti, S. “Robustness of the EWMA control chart for individual observations”. *Journal of Applied Statistics*, First published on 24 January 2011.

Jones, L.A., Champ, C.W., Rigdon, S.E. (2001). “The Performance of Exponentially Weighted Moving Average Charts With Estimated Parameters”. *Technometrics*, 43(2):156-167.

Jones, L.A., Champ, C.W., Rigdon, S.E. (2004). “The run length distribution of the CUSUM with estimated parameters”. *Journal of Quality Technology*, 36(1):95-108.

Khoo, M.B.C. (2003). “Design of Runs Rules Schemes”. *Quality Engineering*, 16(1):27-43.

Khoo, M.B.C. (2005). “A Control Chart Based on Sample Median for the Detection of a Permanent Shift in the Process Mean”. *Quality Engineering*, 17(2):243-257.

Khoo, M.B.C., Ariffin, K.N. (2006). “Two Improved Runs Rules for the Shewhart \bar{X} Control Chart” *Quality Engineering*, 18:173-178.

- Klein, M. (2000). "Two alternatives to the Shewhart \bar{X} control chart". *Journal of Quality Technology*, 32(4):427-431.
- Kotz, S., Balakrishnan, N., Read, C.B., Vidakovic, B., Johnson, N.L. (2006). *Encyclopedia of statistical sciences* 2nd edition, John Wiley.
- Lucas, J.M., Saccucci, M.S. (1990). "Exponentially weighted moving average control schemes: properties and enhancements". *Technometrics*, 32(1):1-29.
- Montgomery, D.C. (2005). *Introduction to statistical quality control*, 5th edition, John Wiley.
- Montgomery, D.C., Runger, G.C. (2003). *Applied Statistics and Probability for Engineers*, 3rd ed., Wiley, New York.
- Page, E.S. (1954). "Continuous Inspection Schemes". *Biometrics*, 41(1):100-115.
- Page, E.S. (1955). "Control Charts with Warning Lines". *Biometrics*, 42:243-257.
- Page, E.S. (1962). "A Modified Control Chart with Warning Lines". *Biometrika*, 49:171-176.
- Quesenberry, C.P. (1991a). "SPC Q -charts for Start-Up Processes and Short or Long Runs". *Journal of Quality Technology*, 23(3):213-224
- Quesenberry, C.P. (1991b). "SPC Q -charts for a Binomial Parameter p : Short or Long Runs". *Journal of Quality Technology*, 23(3):239-246
- Quesenberry, C.P. (1991c). "SPC Q -charts for a Poisson Parameter λ : Short or Long Runs". *Journal of Quality Technology*, 23(4):296-303
- Quesenberry, C.P. (1995a). "On properties of Q -charts for variables". *Journal of Quality Technology*, 27(3):184-203
- Quesenberry, C.P. (1995b). "On properties of Binomial Q -charts for Attributes". *Journal of Quality Technology*, 27(3):204-213
- Quesenberry, C.P. (1995c). "Geometric Q -charts for High Quality Processes". *Journal of Quality Technology*, 27(4):304-315

- Quesenberry, C.P. (1995d). “On properties of Poisson Q -charts for attributes”. *Journal of Quality Technology*, 27(4):293-303
- Roberts, S.W. (1958). “Properties of Control Chart Zone Tests”. *The Bell System Technical Journal*, 37:83-114.
- Roberts, S.W. (1959). “Control chart tests based on geometric moving averages”. *Technometrics*, 1(3):239-250.
- Ross, S.M. (1997). Introduction to Probability Models, 6th edition, Academic Press.
- Saccucci, M.S. and Lucas, J.M. (1990). “Average Run Lengths for Exponentially Weighted Moving Average Control Schemes Using the Markov Chain Approach”. *Journal of Quality Technology*, 22(2):154-157.
- SAS[®]9.2 SAS Institute, Inc.
- Wheeler, D.J. (1983). “Detecting a Shift in Process Average: Tables of the Power Function for X Charts”. *Journal of Quality Technology*, 15:155-170.
- Weindling, J.I., Littauer, S.B., De Oliveira, J.T. (1970). “Mean Action Time of the \bar{X} Control Chart with Warning Limits”. *Journal of Quality Technology*, 2(2):79-85.
- Western Electric Company (1956), *Statistical Quality Control Handbook*, Western Electric Corporation, Indianapolis, IN.
- Woodall, W.H. (1984). “On the Markov Chain Approach to the Two-Sided CUSUM Procedure” *Technometrics*, 26(1):41-46
- Woodall, W.H. (2000). “Controversies and contradictions in statistical process control” *Journal of Quality Technology*, 32(4):341-350.
- Woodall, W.H., Spitzner, D.J., Montgomery, D.C., Gupta, S. (2004). “Using Control Charts to Monitor Process and Product Quality Profiles”. *Journal of Quality Technology*, 36(3):309-320.